

**A PHYTOCHEMICAL INVESTIGATION
OF *ACRIDOCARPUS NATALITIUS*
AND *TYPHA CAPENSIS***

By Abdul Samad Mahomed

**Submitted in partial fulfillment of the
requirements for the degree of Master of Science
in the Department of Chemistry, University of
Durban-Westville, Durban**

4000




PREFACE

The experimental work described in this dissertation was carried out in Department of Chemistry, University of Durban-Westville, Durban, from February 1999 to September 2000 under the supervision of Dr. F. O. Shode.

This study represents original work by the author and has not been submitted in any other form to another university. Where use was made of the work of others, it has been duly acknowledged in the text.

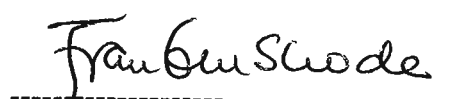
Signed:



A. S. Mahomed

I hereby certify that the above statement is correct.

Signed:



Dr. F. O. Shode

ACNOWLEDGEMENTS

I thank *Almighty God* for the privilege of an education, for the knowledge he has bestowed on me and for his guidance.

I also wish to express my sincere gratitude to:

Dr. F.O. Shode for his continuous support, his guidance, constructive criticism and encouraging enthusiasm during this study. His friendship and loyalty, his willingness to help with the most trivial of problems and his patience has been invaluable. A great deal of the knowledge that I have acquired during this work was due to his unselfish need to let others learn, for this I am truly grateful.

Professor C.B. Rogers for his assistance, advice, his patience amidst my continuous interruptions and for guiding me whenever I went astray.

Dr. Neil Crouch for collection of plant material, for the slides and for his assistance in the literature survey of *Acridocarpus natalitius*. Mr. P. Poorun for his assistance in collection and identification of plant material.

Mr. D. Jagjivan of the University of Natal for kindly recording NMR spectra, for his advice and for his friendship.

Dr. P. Boshoff at the Cape Technikon for the running of high-resolution mass spectra and Dr. D. Pienaar for running mass spectra at the University of Durban-Westville.

Mr. S. Singh for his friendship, guidance and assistance during my stay at this university. Mr. L. Naidoo, Mrs. M. Padayachee, Mr. S. Sewsanker, Mr. M. Nundkumar, Mrs. S. Sooklall, Mr. S. Naidoo, Mrs. P. Govender, Mr. A. Bissessur and Miss R. Singh for their help and friendship. Miss I. Toplan, for her assistance in correcting this manuscript, chemicals and apparatus, and her invaluable friendship.

To all my friends past and present, especially Mr. J. Chetty, Miss. A. Hariram, Mr. L. Qwabe, Mr. S. Sarabjeet, Miss P. Gengan, Mr. V. Chunilall and Mr S. Ntlahla.

My parents, for all the years of sacrifice, guidance, good advice, patience, love and good example.

My family and relatives for their moral support and finally Sasol and the University of Durban-Westville for financial assistance.

ABSTRACT

In the present study, a phytochemical investigation of two medicinal plants, namely, *Acridocarpus natalitius* and *Typha capensis* is presented.

The roots of *A. natalitius* afforded a variety of pentacyclic triterpenoids, namely, friedelin [41], *epi*-friedelinol [42], lupeol [43] and oleanolic acid [44], including stigmasterol [45] from the hexane extract, whilst the methanolic extract produced a flavonoid, (-)-epicatechin [4] and carbohydrates which included glucose [64] and sucrose [65].

Two new bibenzyls were isolated from the hexane extract of the rhizomes of *T. capensis*, namely, typharin [47] and typhaphthalide [48]. β -Sitosterol [49] was also isolated. The acetone extract afforded several flavan-3-ols which were isolated in their free phenolic form. These include, afzelechin [10], epiafzelechin [23], (+)-catechin [11] and (-)-epicatechin [4]. A biological survey was carried out on the crude methanolic extract in an independent survey and a brief discussion is presented here.

All the compounds were isolated using a series of chromatographic techniques and structures were elucidated by means of NMR spectroscopy, infrared spectroscopy and mass spectrometry.

LIST OF ABBREVIATIONS

^{13}C NMR	- carbon-13 magnetic resonance spectroscopy
^1H NMR	- proton magnetic resonance spectroscopy
A	- acetone
Ac-MVA	- acetate mevalonic acid
ADEPT	- distortionless enhancement by polarisation transfer
B	- benzene
brs	- broad singlet
CDCl_3	- deuterated chloroform
CoA	- coenzyme A
COSY	- correlation nuclear magnetic resonance spectroscopy
d	- doublet
D_2O	- deuterated water
dd	- doublet of doublets
DMAPP	- dimethylallyl diphosphate
2,4-DNPH	- 2,4 dinitrophenyl hydrazine
EA	- ethyl acetate
FPP	- farnesyl pyrophosphate
GGPP	- geranylgeranyl pyrophosphate
GFPP	- geranylfarnesyl pyrophosphate
GPP	- geranyl pyrophosphate
H	- hexane
HETCOR	- heteronuclear shift correlation nuclear magnetic resonance
Hz	- hertz
IPP	- inosine pyrophosphate/isopentenyl diphosphate
IR	- infrared spectroscopy
M / MeOH	- methanol
m	- multiplet
MEP	- 2-C-methyl erythritol 4-phosphate
MP	- melting point
MS	- mass spectrometry

NADH	- nicotinamide adenine dinucleotide
NADPH	- nicotinamide adenine dinucleotide phosphate
NOESY	- nuclear overhauser effect spectroscopy
PE	- petroleum ether
PLC	- preparative layer chromatography
ppm	- parts per million
q	- quartet
qq	- quartet of quartets
s	- singlet
t	- triplet
TLC	- thin layer chromatography
UV	- ultra violet

LIST OF FIGURES

<u>Chapter Four</u>	<u>Page</u>
Figure 4.1: Bark	46
Figure 4.2: Flowers	46
Figure 4.3: Fruits resembling 'moths'	46
Figure 4.4: Leaves (broad, lanceolate)	47
Figure 4.5: Roots in their natural habitat	47
} of <i>A. natalitius</i>	
Figure 4.6: Expansion of EF-1 showing H-3 doublet of <i>epi</i> -friedelinol	59
Figure 4.7: Stereochemistry of friedelin A-ring	59
<u>Chapter Five</u>	
Figure 5.1: Distribution of <i>T. capensis</i> in Southern Africa	61
Figure 5.2: Flowering and fruiting stalks of <i>T. capensis</i>	62
Figure 5.3: Rhizomes as they are sold for medicinal use	62
Figure 5.4: Typhasterol	63
Figure 5.5: Fragment A	67
Figure 5.6: Fragment B	68
Figure 5.7: Fragment C	69
} Structure elucidation of typharin	
Figure 5.8: Expansion of H-3 quartet	70
Figure 5.9: Fragment D	70
Figure 5.10: Fragment E	71
Figure 5.11: Fragment F	71
Figure 5.12: Fragment G	72
} Structure elucidation of typharin	
Figure 5.13: (<i>E</i>)- propenylbenzene	72
Figure 5.14: [47] showing long range coupling	73
Figure 5.15: 3-D structures of [47]	73
Figure 5.16: Fragments A and B	77
Figure 5.17: Fragment C	78
} Structure elucidation of typhaphthalide	
Figure 5.18: 3-D structures of [48]	79

Chapter Six

Figure 6.1: Set-up for flash column chromatography

89

LIST OF TABLES

<u>Chapter Two</u>	<u>Page</u>
Table 2.1: Suggested names for naturally occurring Flavan-3-ols	11
Table 2.2: ^{13}C chemical-shift ranges for various carbon types encountered in flavonoids	17
Table 2.3: List of enzymes leading to various flavonoid classes	21
<u>Chapter Three</u>	
Table 3.1: Chemical shifts of the different species of carbons in pentacyclic triterpenoids	34
Table 3.2: Effect of 3-oxo group on C-23 of selected friedelanes	36
Table 3.3: Effect of 3-OH group on C-23 of selected friedelanes	36
<u>Chapter Five</u>	
Table 5.1: Comparative ^{13}C NMR (ppm) data of (<i>E</i>)-propenylbenzene and fragment G of typharin	72
Table 5.2: ^{13}C NMR data (ppm) of [47] and [57] (selected carbons)	75
Table 5.3: Comparative ^1H NMR data (ppm) of [47] and [58]	76
Table 5.4: NMR data of selected atoms [60], [61] and [48]	80
<u>Chapter Seven</u>	
Table 7.1: Summary of fractions of hexane extract of <i>A. natalitius</i>	94
Table 7.2: Summary of fractions of methanol extract of <i>A. natalitius</i>	99
<u>Chapter Eight</u>	
Table 8.1: Summary of fractions of hexane extract of <i>T. capensis</i>	103
Table 8.2: Summary of fractions of acetone extract of <i>T. capensis</i>	106

LIST OF SCHEMES

<u>Chapter Two</u>	<u>Page</u>
Scheme 2.1: Structures of monomeric flavonoids	7
Scheme 2.2: Structures of natural flavan-3-ols (2R,3S configuration)	12
Scheme 2.3: Structures of basic skeletons of the Flavanoids	15
Scheme 2.4: Biosynthetic pathways to major flavonoid classes	22
<u>Chapter Three</u>	
Scheme 3.1: Common terpenoid skeleta	26
Scheme 3.2: Pentacyclic triterpenoid skeleta	28
Scheme 3.3: Terpenoid skeleta (to C ₂₅) derived from the MAP	38
Scheme 3.4: Formation of squalene	40
Scheme 3.5: Formation of the protosteryl cation (tetracyclic precursor)	41
Scheme 3.6: Formation of the dammarenyl cation (pentacyclic precursor)	42
Scheme 3.7: Formation of the lupenyl and oleanyl cations	43
Scheme 3.8: "Friedo" rearrangement	44
<u>Appendix</u>	
Scheme M1: Fragmentation of Typhaphthalide [48]	161
Scheme M2: Fragmentation of Afzelechin tetraacetate [54] and Epiafzelechin tetraacetate [55]	164

STRUCTURE LIST OF COMPOUNDS ISOLATED

<u>Compound</u>	<u>Page</u>
i) Friedelin [41]	49
ii) <i>Epi</i> -Friedelinol [42]	51
iii) Lupeol [43]	52
iv) Oleanolic Acid [44]	53
v) Stigmasterol [45]	54
vi) (-)-Epicatechin [4]	55
vii) (-)-Epicatechin pentaacetate [46]	55
viii) Glucose [64]	56
ix) Sucrose [65]	57
x) Typhaphthalide [48]	64
xi) Typharin [47]	65
xii) β -Sitosterol [49]	66
xiii) Afzelechin [10]	81
xiv) Afzelechin tetraacetate [54]	81
xv) Epiafzelechin [23]	82
xvi) Epiafzelechin tetraacetate [55]	82
xvii) (+)-Catechin [11]	84
xviii) (+)-Catechin pentaacetate [56]	84

TABLE OF CONTENTS

Preface	I
Acknowledgements	II
Abstract	IV
List of Abbreviations	V
List of Figures	VII
List of Tables	IX
List of Schemes	X
Structure list of compounds isolated	XI

PART A

Chapter One: Introduction	1
Chapter Two: The flavonoids	
2.1 Introduction	4
2.2 The flavan-3-ols	8
2.3 Structure elucidation of the flavonoids	13
2.4 Biosynthesis of the flavonoids	19
Chapter Three: The Triterpenoids	
3.1 Introduction to the terpenoids	23
3.2 The pentacyclic triterpenoids	27
3.3 Structure elucidation of the pentacyclic triterpenoids	33
3.4 Biosynthesis of the terpenoids	37

PART B

Results/Discussion

Chapter Four: Extractives from *A. natalitius*

4.1 Introduction	45
4.2 Pentacyclic triterpenoids and stigmasterol	48
4.3 (-)-Epicatechin and carbohydrates	55
4.4 Attempted synthesis of <i>epi</i> -friedelinol	58

Chapter Five: Extractives from *T. capensis*

5.1 Introduction	61
5.2 Bibenzyls and β -Sitosterol	64
5.3 Structure elucidation of typharin	67
5.4 Structure elucidation of typhaphthalide	76
5.5 Flavan-3-ols	81
5.6 Spray Colours	86
5.7 Biological Activity	86

PART C

Experimental

Chapter Six: Standard experimental procedure

6.1 Chromatographic Methods	88
6.2 Spectroscopic Methods	91
6.3 Chemical Methods	92

Chapter Seven: Isolation of extractives from *Acridocarpus natalitius*

7.1	Extraction of root	93
7.2	Separation	93
7.2.1	Hexane extract	93
7.2.2	Methanol extract	98
7.3	Attempted synthesis of <i>epi</i> -friedelinol	100

Chapter Eight: Isolation of compounds from *Typha capensis*

8.1	Extraction of root	102
8.2	Separation	102
8.2.1	Hexane Extract	102
8.2.2	Acetone Extract	106
8.3	Spray reagents	109
8.4	Biological Activity	109

PART D

Appendix

9.	1D-NMR spectroscopy	
9.1	¹ H NMR	111
9.2	¹³ C NMR	131
9.3	ADEPT	131
10.	2D-NMR spectroscopy	
11.1	COSY	147
11.2	HETCOR	147
11.3	NOESY	147

11. IR spectroscopy	154
12. Mass spectrometry	154
13. NMR data tables	165
References	176

PART A

**INTRODUCTION AND
LITERATURE SURVEY**

CHAPTER ONE

INTRODUCTION

Biodiversity is a term commonly used to denote the variety of species and the multiplicity of forms of life. But this variety is deeper than is generally imagined. In addition to the process of primary metabolism that involve essentially the same chemistry across great swathes of life, there are a myriad of secondary metabolites-natural products - usually confined to a particular group of organisms, or to a single species, or even to a single strain growing under certain conditions. In most cases we do not really know what biological role these compounds play, except that they represent a treasure trove of chemistry that can be of both interest and benefit to us. Tens of thousands of natural products have been described, but in a world where we are not even close to documenting all the extant species, there are almost certainly many more thousands of compounds waiting to be discovered¹.

Many scientists would echo this sentiment and this is the driving force behind any study of this kind. In addition, we are fortunate that here in South Africa we have a wide cultural diversity amongst the many different race groups; many of whom have chosen to carry on the traditions of their forefathers. Hence a huge library of knowledge has been established with regards to how the different ethnic groups use plants for a wide variety of applications, which include medicinal, cosmetic and even spiritual.

It has become common practice for many people the world over, to resort to alternative medicine rather than take the conventional path. This behavior of obtaining 'remedies' from nature is an age-old tradition especially amongst the indigenous people from all the continents. From the rain forests of the Amazon to the deserts of Asia, plants have proved a rich source of therapeutic substances.

In the past, studies of medicinal plants were governed by their uses by the native people. Although this was a limiting approach, it proved very successful in the light of numerous drugs being identified from such plants. However, the impact of modern

diseases like Aids for example, has encouraged scientists to look at plants that were not considered significant as medicinal plants.

The excitement of the discovery of novel compounds is heightened when such compounds show biological activity. It must be remembered however, that although certain compounds may not show immediate activity in their standard form, a mere modification or functionalisation of the compound might render it a potent drug or biologically active. Hence, the work of a natural product chemist does not end at the isolation and identification stage, but continues until all avenues of scientific and/or biological research are exhausted. A monotonous and time consuming process indeed but, one that pays dividends for both the discoverer as well as those who will benefit from its therapeutic properties.

Taking into account the vast number of plant species that still remain hidden from the onslaught of modern natural chemistry, it was the aim of this work to study the chemistry of two plants that fell on opposite sides of the spectrum in terms of what is a medicinal plant and what is not. The first is a plant that as tradition would have it, is used for a variety of different medicinal applications, while the second is used mainly as a 'charm' plant, the use of which is invoked by the deep spiritual needs of the indigenous people.

The approach was to study the same part of both plants, gain an understanding of their chemistry and finally draw conclusions with reference to their use. The methodology was simple and involved some mechanical means to crush the plant parts used and chemical means to extract and isolate the compounds of interest. Finally, various instrumental analytical techniques were used to identify as many of the compounds as possible. By no means does this imply that the chemical study of these plants is exhausted, quite the contrary, as many minor components need to be searched out and identified. Another point of note is the fact that certain compounds or metabolites occur at different stages of growth in plants; therefore, depending at which stage of development the particular part of the plant was harvested, this could have severe implications as to the type of compounds isolated and the relative composition of these metabolites. As a result, different samples of each plant were studied and comparisons drawn therefrom.

The study proved fruitful in the light of the fact that these plants were studied for the first time. As a result valuable information regarding their phytochemistry was established.

CHAPTER TWO

THE FLAVONOIDS

2.1 INTRODUCTION

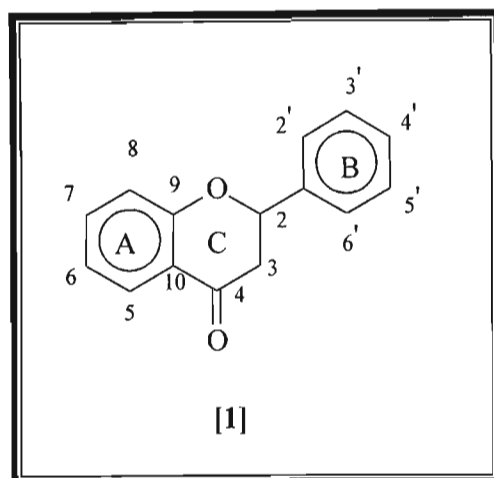
The flavonoids, which are one of the most diverse and widespread groups of natural constituents, have invoked a great deal of interest due to their many properties and applications. The attractive colours of flowers, leaves and fruit are mainly due to the water soluble anthocyanins, tannins and flavones. Some flavonoids have commercial importance and play a role in the tanning of leather, the manufacture of cocoa, the flavouring qualities of foodstuffs and many adhesive applications in the wood industry².

The near ubiquitous distribution of flavonoids in green plants, their relative chemical stability and the ease with which most can be identified have made them particularly useful as taxonomic markers in plant classification.

Flavonoids occur in a wide variety of structural forms (Scheme 2.1). They all contain fifteen carbon atoms in their parent nucleus and share the common structural feature of two phenyl rings linked by a three-carbon chain, i.e. diphenyl propane derivatives. The three-carbon chain may be formed into a third, five- or six- member ring through oxygen on one of these phenyl rings generating a tricyclic system. The tricyclic ring compounds possessing a five-member heterocyclic ring are referred to as auronoids, whereas those possessing a six-member heterocyclic ring are designated flavonoids. Similar tricyclic compounds derived from 1,2-diphenylpropane systems are known as isoflavonoids, 3-phenylcoumarins and pterocarpan, while those derived from 1,1-diphenylpropane are called neoflavonoids³.

In tricyclic compounds of the flavonoid, auronoid and isoflavonoid types; rings are labeled A, B and C, and the individual carbon atoms are referred to by a numbering

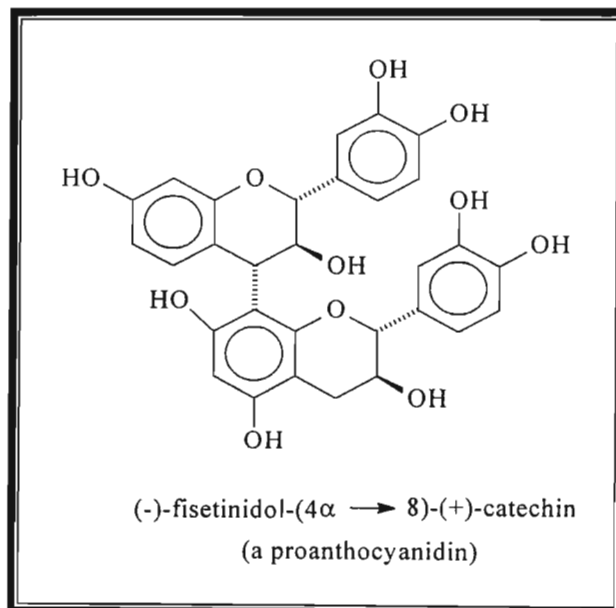
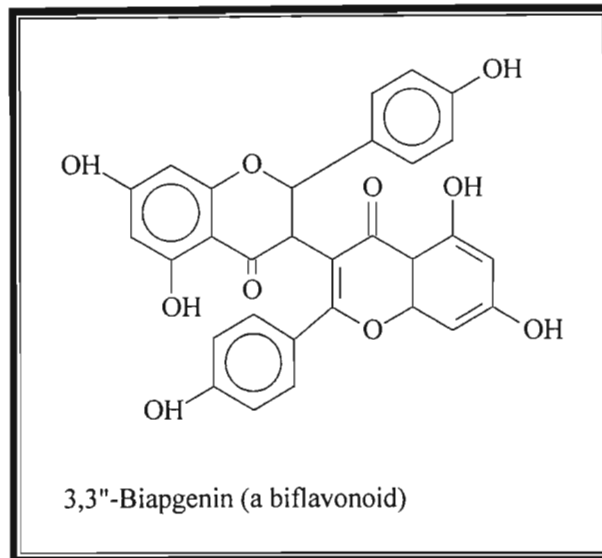
system which utilizes ordinary numerals for the A- and C-rings and 'primed' numerals for the B-ring [1].

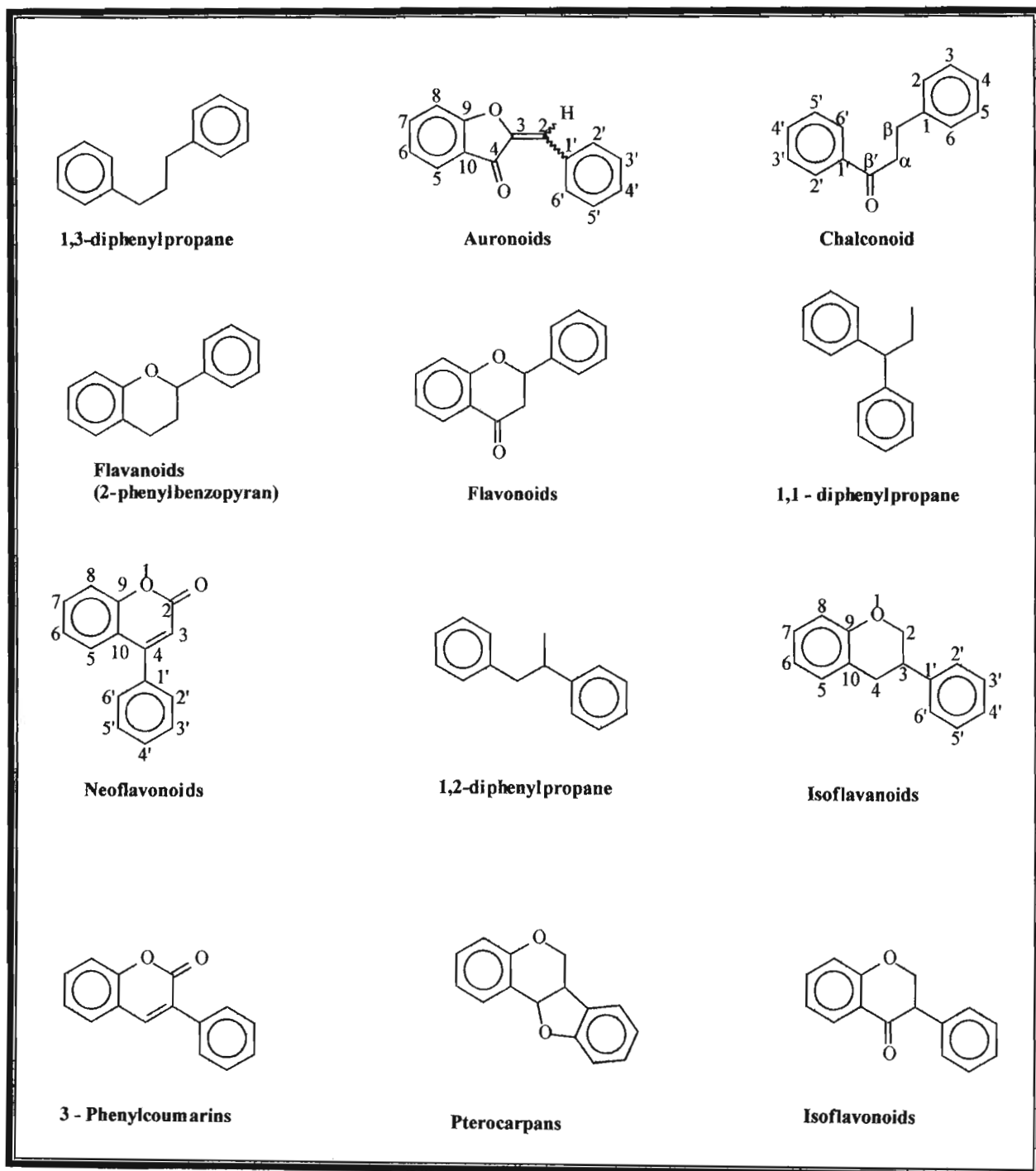


Natural flavonoids and isoflavonoids are usually oxygenated and bear hydroxyl and/or methoxyl substituents. The structure and numbering of the common naturally occurring classes of monomeric flavonoids are illustrated in Scheme 2.1³.

A large number of flavonoids occur as O-glycosides in which one or more of the hydroxyl groups of the flavonoid are bound to a sugar or sugars via an acid labile acetal bond. In flavonoid C-glycosides, the sugar is C-linked and this linkage is acid resistant. The effect of glycosylation is to render the flavonoid less reactive and more water-soluble.

Flavonoids also occur as dimers. These may be linked by a C-C or an - O - linkage and are termed biflavonoids, e.g. 3,3"-biapgenin⁴. When the monomeric units are flavan-3-ols, the C-C linked dimeric flavonoids are referred to as condensed proanthocyanins, e.g. (-)-fisetinidol- (4 → 8)-(+)-catechin⁴.





Scheme 2.1: Structures of monomeric flavonoids

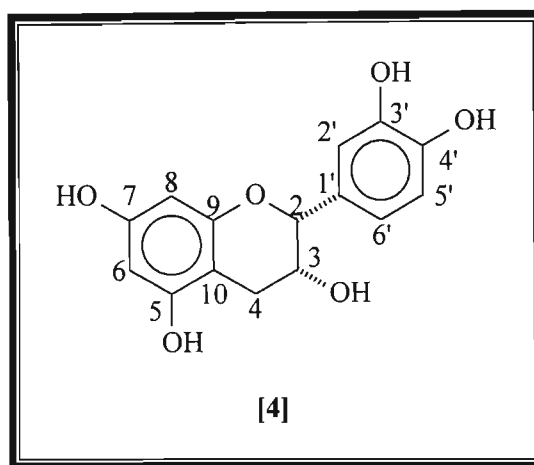
2.2 THE FLAVAN-3-OLS

2.2.1 Nomenclature

The flavan-3-ols are also known as the catechins or flavanoids. For the purpose of this work, the name flavan-3-ol will be used.

A list of the naturally occurring flavan-3-ols with the 2R,3S configuration is given in Table 2.1⁴. Those compounds with the 2R,3R configuration are prefixed with 'epi', e.g. epicatechin [4].

The numbering system is adopted from the flavone skeleton [1], as shown for epicatechin [4].



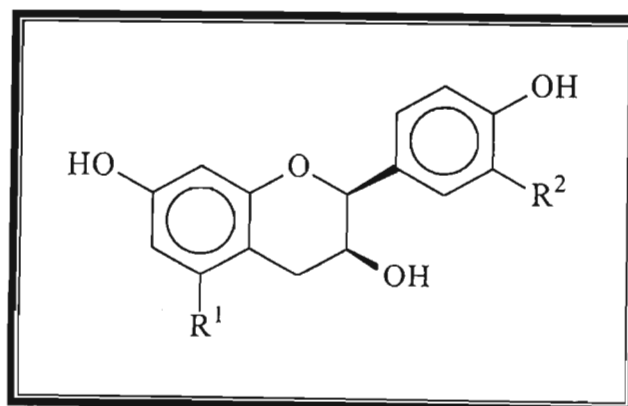
2.2.2 Occurrence

The most widely distributed members of this class of phenolic flavan-3-ols in nature are the diastereomeric pair, (+)-catechin [11] and (-)-epicatechin [4]. The structures and absolute configuration of other naturally occurring flavan-3-ols are shown in Table 2.1

and Scheme 2.2⁴, while the plant sources for most are given in a comprehensive list in various texts^{5,6,7}.

A list of modified flavan-3-ols, for example, glycosides together with their sources is given by Porter⁷. Undoubtedly, the most important addition to this group was the discovery of flavan-3-ols with the (+)-epi-configuration in nature. Marini-Bettolo *et al*⁸, isolated (+)-epiafzelechin [20] and (+)-epicatechin [21] from several *Palmae* species. Drewes and Roux⁹ showed the presence of (+)-epifisitinidol [22] in *Colophospermum mopane* heartwood. These have the 2S,3S-configuration.

Afzelechin [10] was first isolated from *Eucalyptus calophylla* by Hillis and Carle¹⁰. Other sources include *Nothofagus fusca*¹¹, *Saxifraga ligulata* root¹², *Desmoncus plicanthus* leaf¹³, *Juniperus communis* fruit¹⁴, *Prunus persica*¹⁵, *Kardelia candel* bark¹⁶ and *Cassia abbreviata* bark¹⁷.



[20] $R^1=OH, R^2=H$

[21] $R^1=R^2=OH$

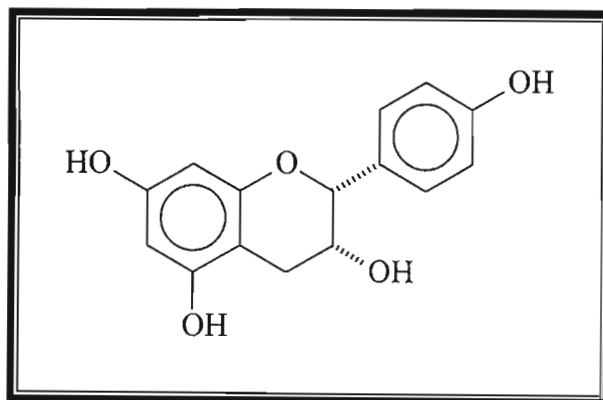
[22] $R^1=H, R^2=OH$

Table 2.1 Suggested names for naturally occurring Flavan-3-ols

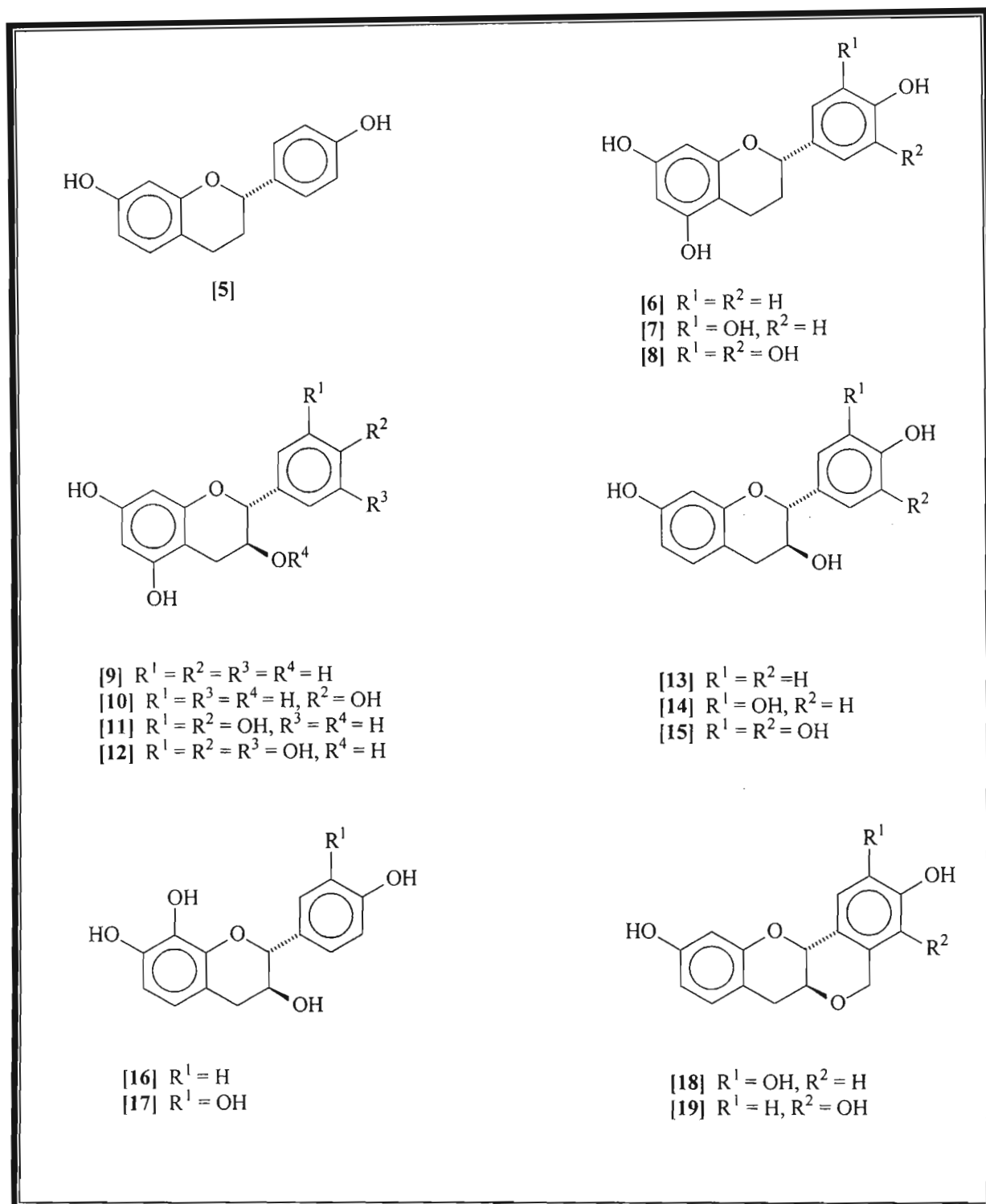
COMPOUND	SUBSTITUTION PATTERN						
	3	5	7	8	3'	4'	5'
Cassiaflavan [5]	H	H	OH	H	H	OH	H
Apigeniniflavan [6]	H	OH	OH	H	H	OH	H
Luteoflavan [7]	H	OH	OH	H	OH	OH	H
Tricetiniflavan [8]	H	OH	OH	H	OH	OH	OH
Distenin [9]	OH	OH	OH	H	H	H	H
Afzelechin [10]	OH	OH	OH	H	H	OH	H
Catechin [11]	OH	OH	OH	H	OH	OH	H
Gallocatechin [12]	OH	OH	OH	H	OH	OH	OH
Guibourtinidol [13]	OH	H	OH	H	H	OH	H
Fisetinidol [14]	OH	H	OH	H	OH	OH	H
Robinetinidol [15]	OH	H	OH	H	OH	OH	OH
Oritin [16]	OH	H	OH	OH	H	OH	H
Mesquitol [17]	OH	H	OH	OH	OH	OH	H
Peltogynane [18]	OCH ₂ -6'	H	OH	H	OH	OH	H
Mopane [19]	OCH ₂ -6'	H	OH	H	H	OH	OH

Epiafzelechin [23] was isolated from *Afzelea* species and characterised by chemical means by King and co-workers¹⁸. The compound was also isolated from *Cassia siebrana*¹⁹, *Cassia fistula*²⁰, *Cassia abbreviata*¹⁷, *Larix* species²¹, *Juniperis communis* fruit¹⁴ and *Ephedra* species²².

(+)-Catechin [11] was first isolated from *Uncaria gambir*²³ while (-)-epicatechin [4] was isolated from *Acacia catechu*²⁴. Both now show a very wide distribution in both the Monocotyledoneae and the Dicotyledoneae.



[23]



Scheme 2.2: Structures of natural Flavan-3-ols (2R,3S configuration)

2.3 STRUCTURE ELUCIDATION OF THE FLAVONOIDS

2.3.1 Proton Magnetic Resonance (¹H NMR)

2.3.1.1 The Aromatic Protons²⁵

The coupling patterns for the flavonoid aromatic protons are typical for the benzenoid system with combinations of ABX, AB, AX and AA'BB'. The chemical shifts of these protons occur from 6.0 ppm to 8.0ppm, with J-values of 8-, 2- and 1,0 Hz for the ortho, meta and para coupled protons respectively.

In 5,7-dihydroxy flavonoids, for example, epicatechin [4] the protons at C-6 and C-8 appear separately as doublets (meta-coupled, J~2Hz), with the H-6 doublet occurring at higher field than the H-8 doublet. When a 7-hydroxyflavonoid (ABX system) has a C-4 keto group, the C-5 proton is deshielded and appears as a doublet due to ortho coupling (J~8Hz) with H-6. In 4' oxygenated flavonoids, for example, afzelechin [10], the H-3', H-5' doublet appears upfield from the H-2', H-6' doublet due to the deshielding effect of the oxygens of the C-ring functions on H-2' and H-6'.

In 3', 4', 5' -oxygenated flavonoids, for example, galocatechin [12], H-2' and H-6' appear as a two-proton singlet because of magnetic equivalence. O-Methylation of the 3' or 5' hydroxyl may lead to non-equivalence of H-2' and H-6' resulting in a distinct doublet (J = 2 Hz).

2.3.1.2 Methoxyl and Acetoxyl protons

Methoxyl proton signals appear in the range 3.5-4.1 ppm while aromatic acetoxyl proton signals occur in the range 2.25-2.50 ppm²⁶. Protons ortho and para to acetoxyl groups are shifted downfield by about 0.3 ppm to 0.5 ppm respectively while meta protons are shifted very slightly. The C-ring acetoxyl protons resonate between 1.6-2.0ppm.

2.3.1.3 Heterocyclic Ring Protons²⁵

The chemical shifts (ppm) and coupling constants of the heterocyclic (C-ring) protons of the flavonoids may be summarised as follows:

- | | |
|--|--|
| a) Flavones ²⁷ | H-3: 6.3 (s) |
| b) Isoflavones ²⁸ | H-2: 7.6 – 7.9 (s) |
| c) Flavanones ²⁹ (e.g. [1]) | H-2: 5.0 – 5.5 (q, $J = 11_{\text{trans}}$ Hz, 5_{cis} Hz)
H-3: 2.8 (qq, $J = 17$ Hz) |
| d) Dihydroflavonols ³⁰ | H-2: 4.8 – 5.0 (d, $J = 11$ Hz)
H-3: 4.1 – 4.3 (d, $J = 11$ Hz) |
| e) Flavan-3-ol (e.g. [4]) | H-2: 4.2 – 6.0 (d, $J = 8$ Hz)
H-3: 3.5 – 4.3 (m)
H-4eq: 2.3 - 3.4 (dd, $J = 6$ Hz and 16Hz)
H-4ax: 2.3 – 3.4 (dd, $J = 9$ Hz and 16Hz) |
| f) Flavan-4-ols (Scheme 2.3) | H-2: 4.2 – 6.0 (dd, $J = \text{ca. } 11.5$ Hz)
H-3: 1.8 – 2.3 (m)
H-4: 4.2 – 6.0 (t, $J = 5.5$ Hz) |

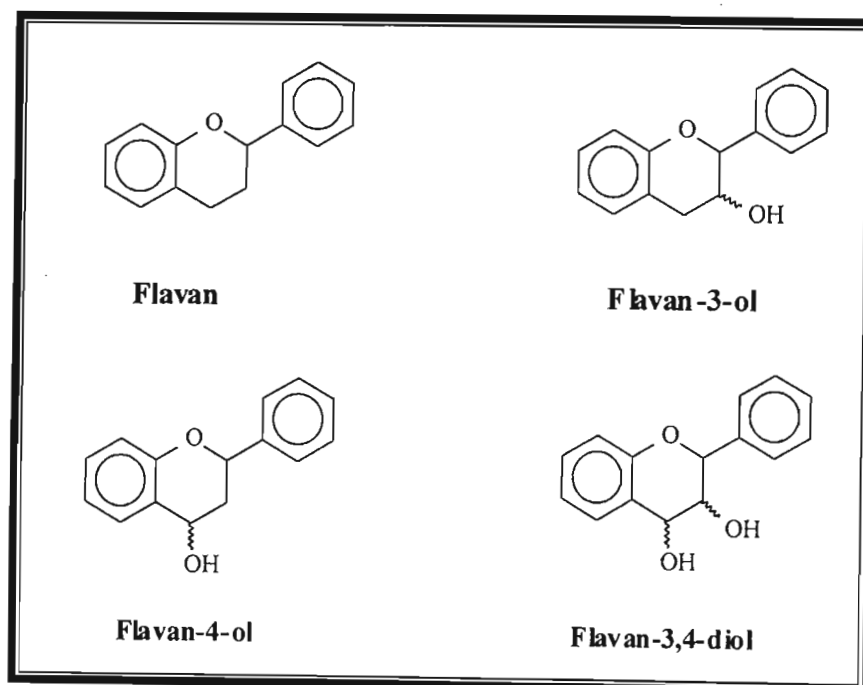
2.3.2 Carbon-13 Magnetic Resonance Spectroscopy (¹³C NMR)³

Carbon-13 NMR spectrum of an unknown flavonoid permits ready differentiation between 4-keto flavonoids, flavonoids which lack a keto group, 2,3-unsaturated flavonoids and 2,3-saturated flavonoids. The 4-keto flavonoids possess a carbonyl carbon resonance in the range 170-205 ppm, which is not present in flavanoids which lack the 4-keto function. All fifteen signals due to the flavonoid nucleus resonate in the region 90-210 ppm in the case of 2,3-unsaturated flavonoids and isoflavonoids. 2,3-Saturated flavonoids and isoflavonoids however, possess only thirteen signals in

this region, the two additional signals resonating at higher field. The flavans and their derivatives, together with pterocarpanoids and chalcones possess three aliphatic resonances and twelve aromatic resonances in above mentioned chemical shift range. The presence of many signals in the 60-80 ppm region is generally indicative of glycosidic carbons. Compilations of ^{13}C NMR data of the monomeric flavanoids seem to be scattered through the literature. However, Agrawal *et al*³, have compiled an extant ^{13}C NMR literature and discussed its utility for structural and stereochemical elucidation of the various classes of flavan derivatives.

The ^{13}C NMR chemical shifts of the compounds shown in Scheme 2.3 may generally be divided into three groups:

- 1) Those of carbons 2,3 and 4 in the heterocyclic ring, occurring normally in the region 19-85 ppm.
- 2) Those of the remaining carbons, on the A- and B- rings, which are aromatic carbons, occur in the region 95-160ppm.
- 3) Those arising from non-flavanoid co-metabolites, which may be substituents (either O or C) such as O-glycosides, O-gallates and O-cinnamate derivatives.



Scheme 2.3: The structures of the basic skeletons of the Flavanoids

2.3.2.1 Flavan-3-ols

This group contains the most commonly occurring natural products in this class: catechin [11] and epicatechin [4], and will thus be discussed in more detail. A detailed discussion of the ^{13}C NMR chemical shifts of the other groups in this class including the proanthocyanidins is given by Agrawal *et al*³.

By analogy with studies on cyclohexane³¹ the chemical shifts for the C-ring carbons will be dependent on both the electronegativity of the substituents and the relative stereochemistry of these substituents. In the case of catechin and epicatechin these chemical shifts will be controlled by the orientation of the 3-hydroxyl group. However, it can be mentioned that among the oxymethine signals for C-2 and C-3, the C-2 signal resonates 12-15 ppm downfield from C-3 and therefore the signal assignments are straightforward. Thus, resonances due to C-2, C-3 and C-4 appear at 76.7-82.3, 65.1-69.5 and 24.0-32.6 ppm respectively.

The three quaternary carbons C-1', C-9 and C-10 show relatively constant shifts among the different flavanoids of 129-133 ppm, 155-158 ppm and 99-102 ppm respectively.

The carbons of the aromatic A- and B-rings show shifts, which depends on the substitution pattern of each. The A- ring oxygenated carbons are found in the region 155-158 ppm and non-oxygenated carbons, 90-100 ppm. The B-ring oxygenated carbons resonate at around 140-150 ppm and non-oxygenated carbons at about 110-120 ppm.

Acetylation of the 3-hydroxy group usually causes an upfield shift of the C-2, C-3 and C-4 carbons with shifts of 2-5 ppm, 0.2-0.5 ppm and 3-5 ppm respectively. Acetylation of the aromatic OH groups usually causes an upfield shift of the oxygenated carbons by 6.6-15.6 ppm and a downfield shift of the non-oxygenated carbons with ortho- signals moving downfield by 4.1-12.1 ppm and para-carbon signals by 2-7.9 ppm. C-1' and C-10 are also drastically affected, with C-1' experiencing a downfield shift by approximately 5-6ppm and C-10 by as much as 10

ppm. Carbon-9 shows a shift of about 1.5-2ppm upfield as compared to the fully hydroxylated compounds.

Methylation of free phenolic hydroxyl groups generally produces smaller, opposite and rather variable effects. The resonance of the carbon attached to the oxygen function shifts downfield by 3-4 ppm, and the ortho-related carbons on the A- or B-ring are shifted upfield by 2-3 ppm.

Table 2.2 ^{13}C chemical-shift ranges for various carbon types encountered in flavonoids³

<u>Carbon type</u>	<u>Approximate shift range (ppm)</u>
Carbonyl (4-keto, acyl)	210-170
Oxyaryl carbon (without <i>ortho</i> or <i>para</i> oxygenation)	168-155
Flavone (C-2)	
Isoflavone (C-2)	
Anthocyanidin (C-2)	
Flavonol (C-2)	158-136
Chalcone (C- β)	
Anthocyanidin (C-3)	
Flavonol (C-3)	144-135
Anthocyanidin	
3-Methoxyflavone	
Oxyaryl (with <i>ortho</i> or <i>para</i> oxygenation)	150-130
Non-oxygenated aromatic carbons	135-90

Flavone (C-3)	
Isoflavone (C-3)	
Chalcone (C- α)	
Flavanone (C-2)	89-65
Flavanol (C-2, C-3)	
Flavan-3-ol (C-2, C-3)	
Flavan-3,4-diol (C-2, C-3, C-4)	
Sugar (<u>C</u> H ₂ OH, <u>C</u> HOH)	78-56
C-glycoside (C-1)	
Flavan-4-ol (C-4; with 5-O-substituent)	
3-Methoxyflavone (3-O <u>C</u> H ₃)	59-58
Aromatic OCH ₃ (<i>ortho</i> -disubstituted)	63-59
Flavanone (C-3)	52-40
Flavan-4-ol (C-3)	40-34
Flavan-3-ol (C-4)	33-25
Flavan (C-3)	
Acetoxy-CH ₃	26-19
Flavan (C-4)	
Aromatic C-CH ₃	ca. 20
Aliphatic C-CH ₃	ca. 17

2.4 BIOSYNTHESIS OF THE FLAVONOIDS

In the last two decades, considerable progress has been made in elucidating the biosynthesis of flavonoids. In particular, knowledge of enzymology has developed rapidly.

From these studies, it became fully established that all classes of flavonoids derive their carbon skeleton from compounds of intermediary cell metabolism through the action of two consecutive pathways. The first is called, General Polypropanoid metabolism, and the second, which is the major part, deals with the reactions of the various flavonoid pathways⁴.

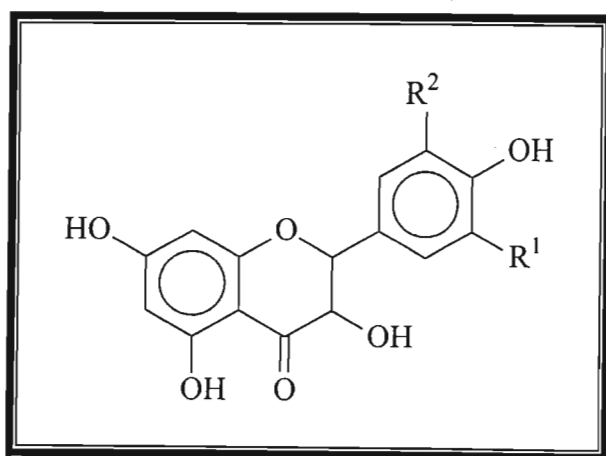
Information on the subject is now included in various texts^{4, 5, 32, 33, 34} and reviews⁵, hence a detailed discussion is unnecessary, however, the biosynthesis of the flavan-3-ols will be given little more attention. A general overview incorporating both pathways is given in Scheme 2.4⁴. Ring B and part of the heterocyclic ring of the flavonoid skeleton are provided by a suitable hydroxy-cinnamic acid-CoA ester, while the A-ring originates from three acetate units via malonyl-CoA. Both precursors are derived from carbohydrates. The scheme shows the synthesis being initiated by the amino acid phenylalanine which is itself synthesized via the shikimate/arogenate pathway and leading to the formation via enzyme catalysed reactions to the various flavonoid products. Table 2.3 gives the list of the enzymes involved⁴.

2.4.1 The Flavan-3-ols

Generally, the flavan-3-ols are formed directly from the leucocyanidins. For example, the formation of catechin [11] was first demonstrated by Stafford and Lester³⁵, with a crude extract from *Pseudotsuga* cell suspension cultures using 2,3-*trans*-3,4-*cis*-leucocyanidins as substrate and NADPH. The enzyme catalysing this reaction was called Leucocyanidin-4-reductase or flavan-3,4-*cis* diol 4-reductase. The leucocyanidin is derived from dihydroflavanols. Kristiansen³⁶ demonstrated the dependence of flavan-3-

ol formation on NADPH while the leucocyanidin could form with NADH. The final products depend on the A- and B-ring substitution pattern of the precursors. For example, afzelechin [10] is derived from dihydrokempferol [24] while catechin [11] and gallocatechin [12] are derived from dihydroquercetin [25] and dihydromyricetin [26] respectively.

The hydroxylation pattern of the B-ring was found not to start from the polypropanoid pathway but was due to modifications of the flavone precursor by enzymes specific for this purpose. Enzymatic studies revealed that hydroxylation in position 3' and 5' for example, is achieved by specific enzymes acting at the C₁₅ level. Two enzymes were identified as, flavonoid-3'-hydroxylase (F3'H) and flavonoid-3', 5'-hydroxylase (F3', 5'H). The A-ring hydroxylation however, remains less defined. The 5 and/or 7 position is hydroxylated during the synthesis of the flavonoid skeleton. Additional hydroxyl groups are found in positions 6 and 8. Attempts to hydroxylate the A-ring in these positions *in vitro* have not been achieved⁴.



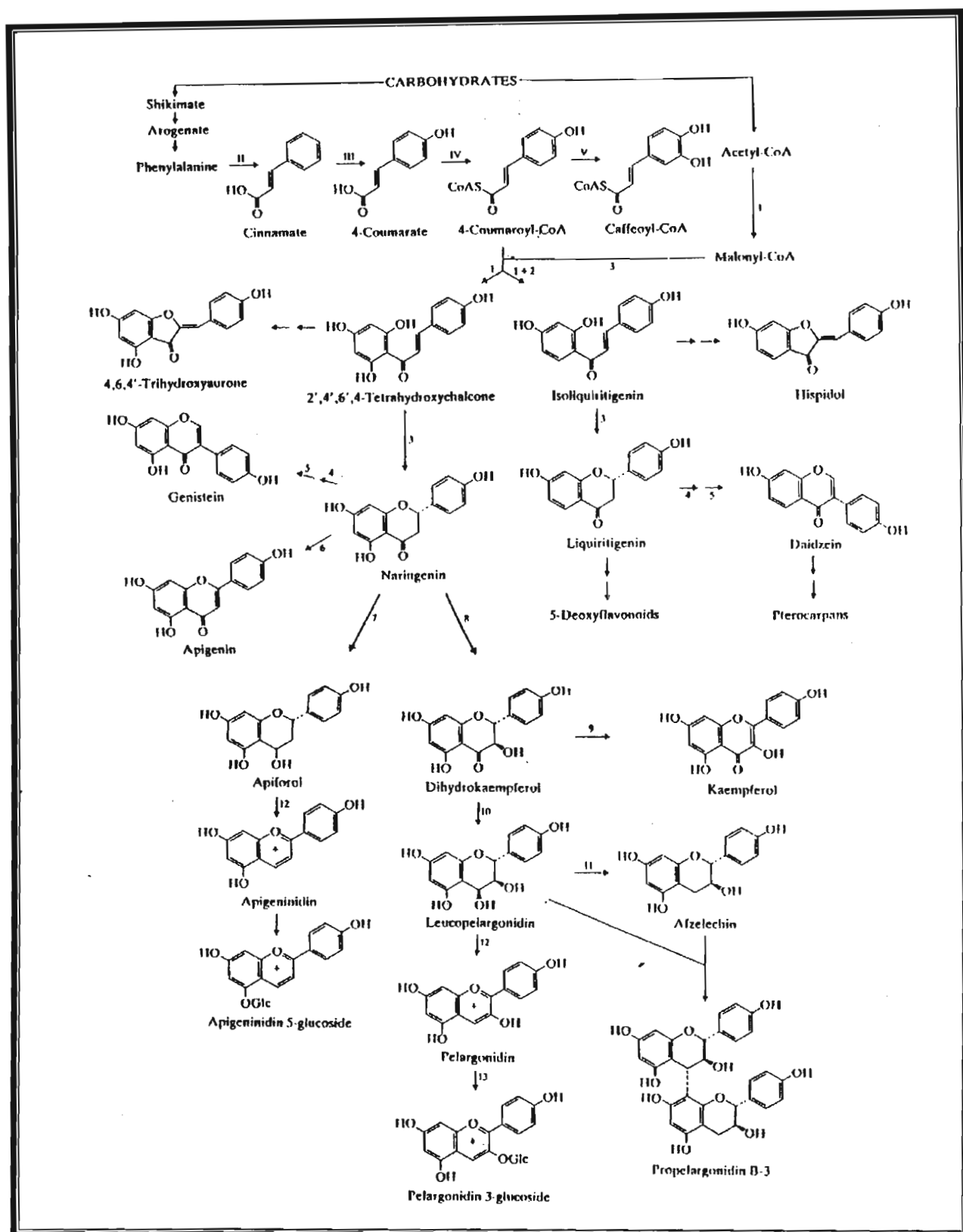
[24] R¹=R²=H

[25] R¹=OH, R²=H

[26] R¹=R²=OH

Table 2.3 List of enzymes leading to various flavonoid classes

ENZYME	ACRONYM
NON-FLAVONOID PRECURSORS	
I Acetyl-CoA carboxylate	ACC
II Phenylalanine ammonia-lyase	PAL
III Cinnamate 4-hydroxylase	C4H
IV 4-Coumarate:CoA ligase	4CL
V 4-Coumaryl-CoA 3-hydroxylase	CC3H
FLAVONOID CLASSES	
1 Chalcone synthase	CHS
2 Polyketide reductase	PKR
3 Chalcone isomerase	CHI
4 2-Hydroxyisoflavanone synthase	IFS
5 2-Hydroxyisoflavanone dehydratase	IFD
6 Flavone synthase I Flavone synthase II	FNS I FNS II
7 Flavanone 4-reductase	FNR
8 Flavanone 3-hydroxylase	FHT
9 Flavonol synthase	FLS
10 Dihydroflavonol 4-reductase	DFR
11 Leucoanthocyanidin 4-reductase (flavan-3,4-cis-diol 4-reductase)	LAR
12 Anthocyanidin synthase	ANS
13 Flavonoid (Anthocyanidin/Flavonol) 3-O-glucosyltransferase	FGT

Scheme 2.4: Biosynthetic pathways to major flavonoid classes⁴

CHAPTER THREE

3.1 INTRODUCTION TO THE TERPENOIDS

The terpenoids are amongst the most widespread and chemically interesting groups of natural products. They can be defined as a group of natural products whose structure may be divided into C_5 isoprene units. This immediately leads to a rational classification of the terpenoids depending upon the number of such isoprene units³⁷.

Monoterpenoids – C_{10}

Sesquiterpenoids – C_{15}

Diterpenoids - C_{20}

Sesterterpenoids - C_{25}

Triterpenoids - C_{30}

Carotenoids - C_{40}

Rubber - $(C_5)_n$

In practice, it is possible to discern a further subdivision of the terpenoids. The terpenoids up to C_{25} contain isoprene units linked in a head-to-tail fashion. The triterpenoids and carotenoids are made up of two C_{15} and C_{20} units respectively linked in a tail-to-tail fashion³⁷.

The utility of the terpenoids spans the centuries of civilization. Essential oils, particularly, oil of turpentine, were known to the Ancient Egyptians. Astringent and toxic properties of sesquiterpenoids and diterpenoid bitter principles figure in many folk medicines. Camphor was introduced to Europe from the East by the Arabs and is recorded in several eleventh-century manuscripts³⁷.

It is no surprise then, that the chemical study of the terpenoids also started at an early stage with analysis of oil of turpentine recorded in 1818 by J.J. Houton de la Billardiere who showed that the carbon-hydrogen ratio was 5 to 8. Physical and chemical data on

many oils were recorded from 1830 onwards. Structure elucidation began in earnest in the late nineteenth century but it was not until the advent of spectroscopic techniques by the mid twentieth century that an immense explosion in terpenoid chemistry, if not all natural product chemistry, was stimulated.

Terpenoids have also been shown to be responsible for the biological activity of various systems. A number of antibiotics have been developed based on sesqui- and diterpenoids. The insect juvenile hormones appear to be derived from sesquiterpenoids, whilst gibberellin plant growth hormones are diterpenoids. Several sesquiterpenoids have been found to be active against experimental tumours³⁷. The biological activities of triterpenoids are discussed in more detail in section 3.2.

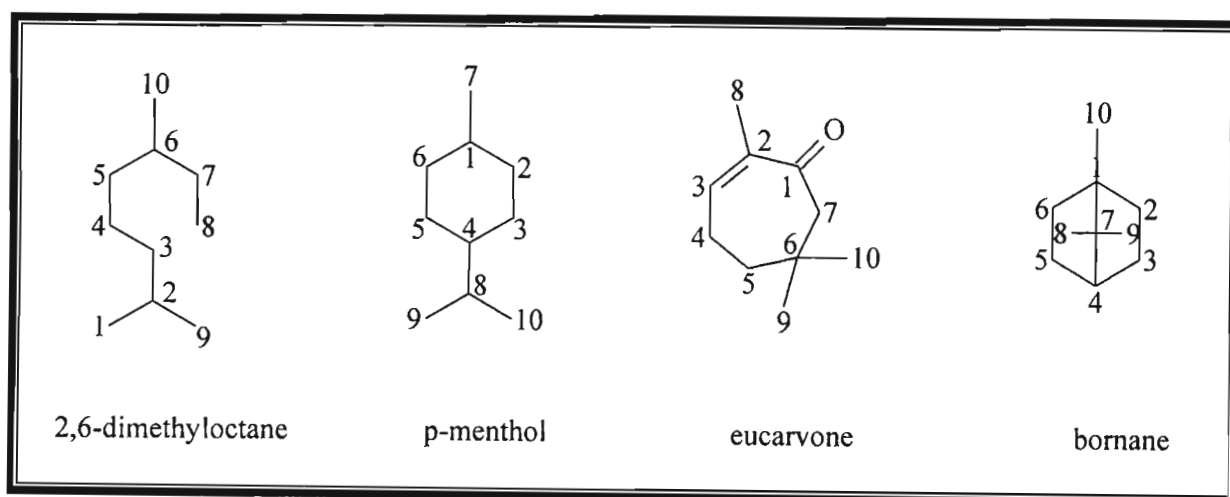
3.1.1 Nomenclature

The nomenclature of the terpenoids has been dealt with by numerous authors in quite some detail, including discussion of each of the different groups³⁷. In practice however, trivial names have been given to most of the terpenoids, often because they were isolated and described in literature long before their structure was known. As with many natural products, the rules for nomenclature are constantly under revision. The common skeletal and numbering system for some typical terpenoids are set out in Scheme 3.1³⁷.

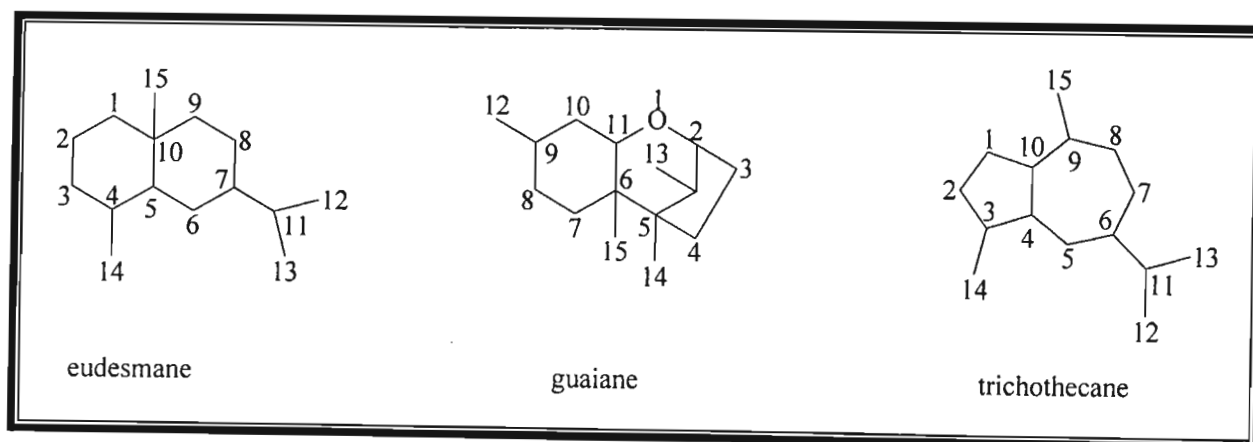
3.1.2 The Triterpenoids³⁸

The triterpenoids constitute by far the largest terpenoid class. They have been known and investigated for over 140 years but it is only within the latter half of the twentieth century that serious progress has been made towards the elucidation of their structures. They are widely distributed in nature, for the most part, in the vegetable kingdom. They may occur as esters, glycosides or in their free state. The sugar moieties in the glycoside include pentoses, such as arabinose, xylose and rhamnose and hexoses such as glucose, fructose and galactose.

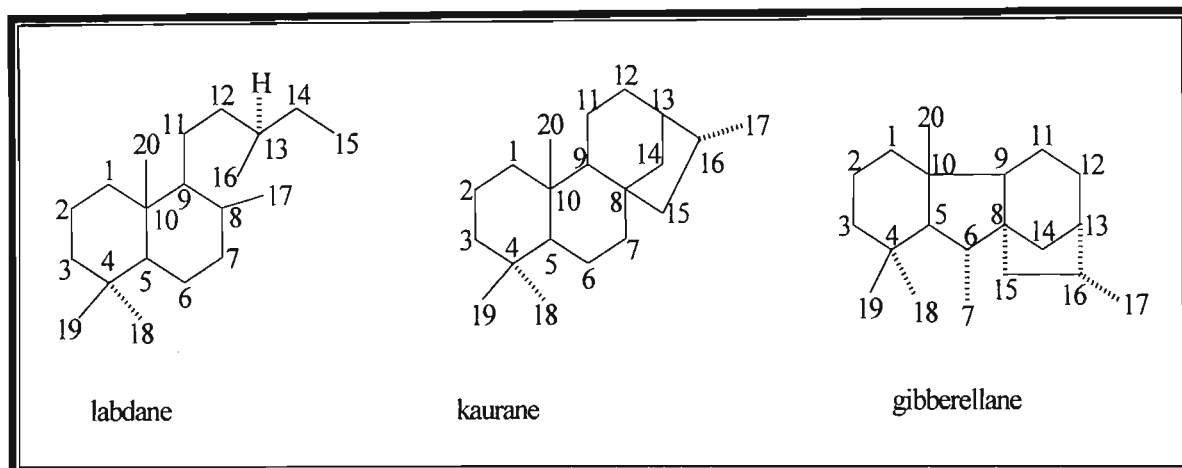
Historically, the triterpenoids were classified into three groups as follows: (a) ambrein and squalene, (b) the tetracyclic triterpenoids and (c) the pentacyclic triterpenoids. The last group, being the largest of the three, was further subdivided into three groups. These were, the α -amyrin, β -amyrin and lupeol groups. This division was somewhat arbitrary. It arose when full structures were not known and substances were related to the simplest alcohol with the same skeleton. Since then, the full structures and still more recently conversion from one group into another have been accomplished. Section 3.2 discusses the various pentacyclic triterpenoids, while section 3.4 gives a brief description of their biosynthesis.



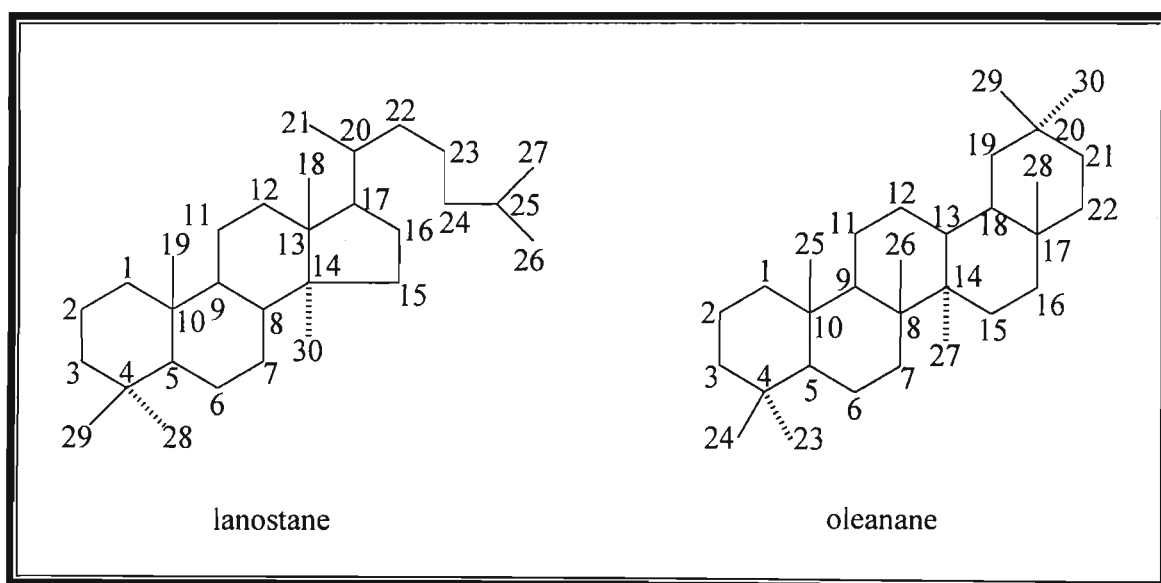
Typical monoterpenoid skeleta



Sesquiterpenoid skeleta



Diterpenoid Skeleta



Typical triterpenoid skeleta

Scheme 3.1 Common terpenoid skeleta

3.2 THE PENTACYCLIC TRITERPENOIDS

The pentacyclic triterpenoids are the dominant constituents of the triterpenoid class. They are derived from squalene via squalene epoxide, as discussed in section 3.4, and show a variety of structural forms. The nomenclature as mentioned in section 3.1 is usually based on the source of isolation, or modification based on the parent skeleton.

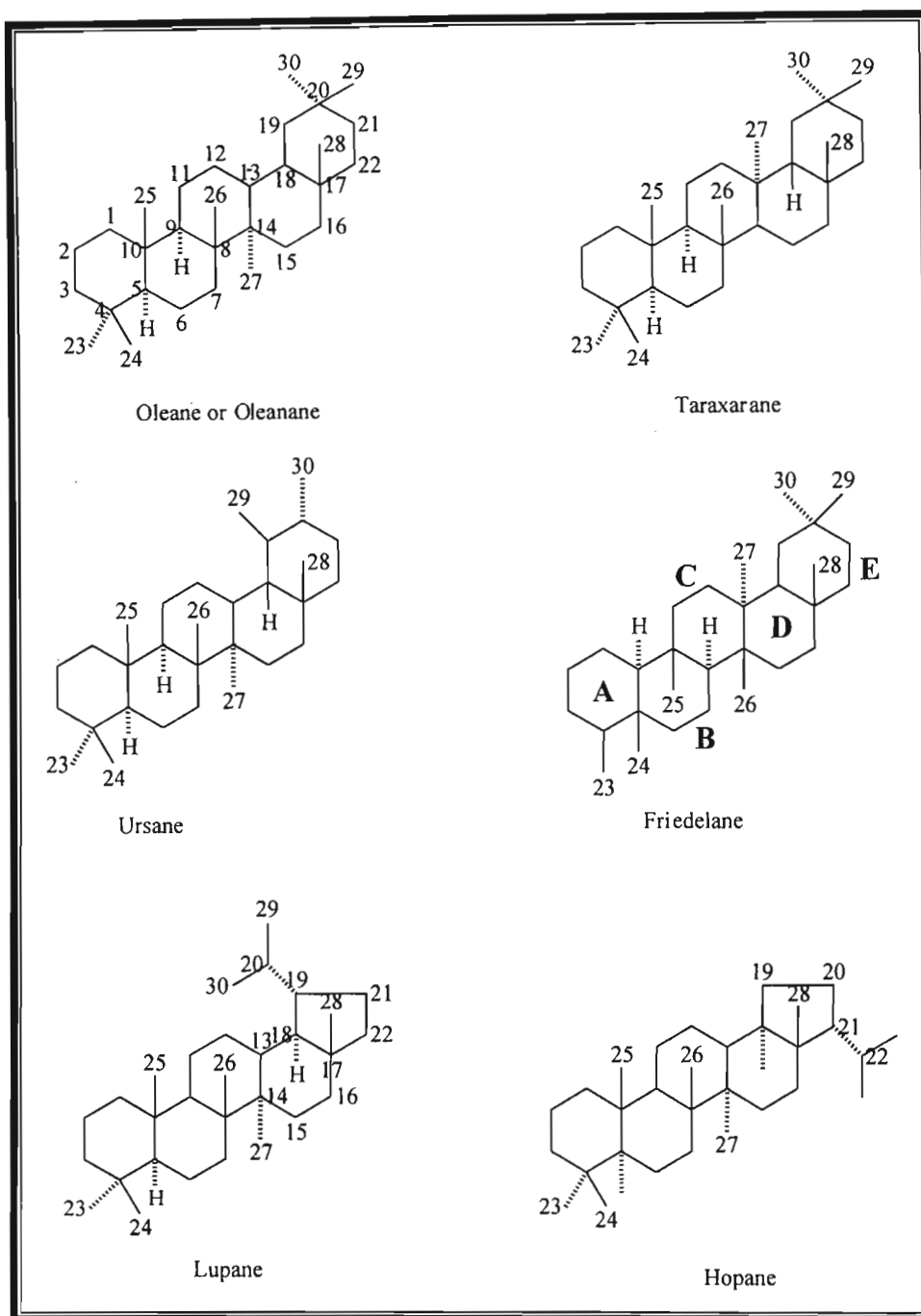
Despite the remarkable diversity that is already known to exist among the carbon skeletons of the pentacyclic triterpenoids, new variants continue to emerge. Several review articles have covered this subject^{39, 40}, however, for the purpose of this work a general scheme showing the typical skeletons is presented (Scheme 3.2), with their numbering. In their review of the triterpenoids, Mahato *et al*⁴⁰ have also presented new carbon skeletons.

3.2.1 Oleanes or Oleananes

This forms perhaps the largest group amongst the pentacyclic triterpenoids. The most notable of the group is β -amyirin [27]. The typical features are gemdimethyls at C-4 and C-20. Modifications to the oleanane skeleton include double bonds in the 12:13, 13(18), 11:12, 9(11), and 5:6 positions. The most common functional group is the 3β -OH which is a remnant from the squalene precursor. Hydroxyl groups may also be found in other positions but usually in positions C-2, C-16, C-22, C-23 and C-28. Other functional groups include aldehydes, epoxides, carboxylic acid esters, ketones and carboxylic acids e.g. oleanolic acid [44], which is an ubiquitous example of the β -amyirin group.

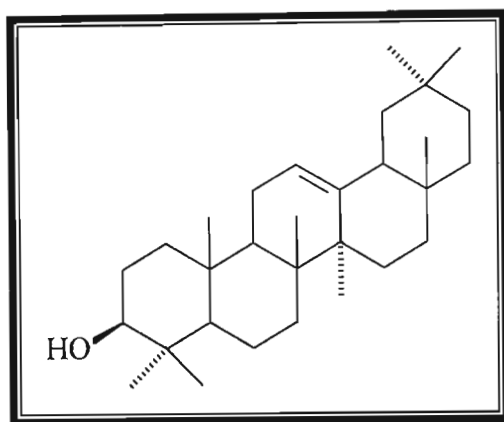
3.2.2 The Ursanes

This group is second only to the oleanes in terms of numbers. Its most famous member being α -amyirin [29].

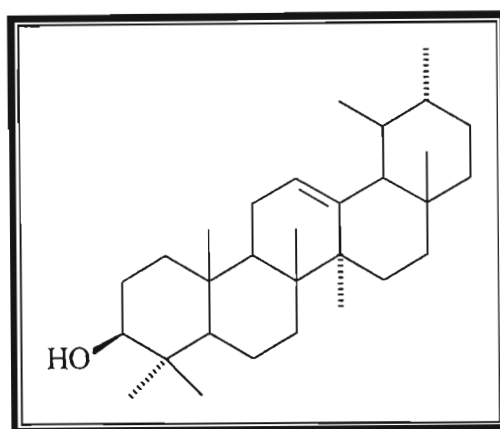


Scheme 3.2 Pentacyclic triterpenoid skeleta

Like the oleanes, it possesses a gemdimethyl at C-4 but not at C-20, rather, two methyl groups are found at C-19 and C-20 respectively. Modifications of the skeleton are similar to the oleanes.



[27]



[29]

3.2.3 The Taxaranes

The group is almost identical, structurally speaking, to the oleanes, except that the C-27 methyl group is found at C-13 instead of at C-14. The usual skeletal modifications apply.

3.2.4 The Lupanes

This group is differentiated from the others in that the gemdimethyl groups (C-29 and C-30), of ring E, form an isopropyl side chain with C-20 resulting in ring E conforming to a cyclopentane ring rather than the typical cyclohexane system. The most notable modification being a 20(29) terminal double bond in the isopropyl moiety, for example, lupeol [43].

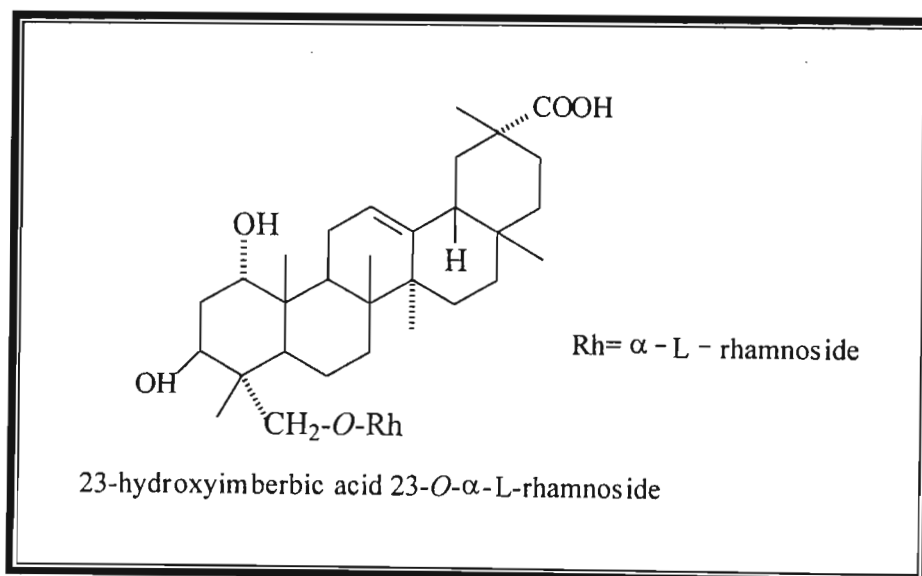
3.2.5 The Hopanes

The hopanes are similar to the lupanes except that the isopropyl group is now attached at C-21, with C-22 incorporated in the side chain. Also, C-28 is at C-18, not at the usual C-17 position.

3.2.6 The Friedelanes

This group possesses the typical pentacyclic structure having five cyclohexane ring systems. However, it is the arrangement of the methyl groups that make this group unique. A dramatic shift in the methyl groups as discussed in Section 3.4, results in the structure shown. The C-29, C-30 gemdimethyl groups are retained, but the C-23 and C-24 groups are found at C-4 and C-5 respectively. C-25, C-26 and C-27 are also subsequently affected. Modifications of the skeleton as for the other groups allow for a myriad of different compounds. An example of note in this group is friedelin [41].

Brief mention should also be made of glycoside triterpenoids. Here the usual functional groups are replaced by sugars e.g. glucose, rhamnose, etc. The glycoside units usually occur as monomers. A typical example is shown in 23-hydroxyimberbic acid 23-O- α -L-rhamnoside⁴¹.



3.2.7 **Biological Activity**

The occurrence and structural diversity of this group of natural products has certainly attracted attention for evaluation of their biological activity. Although applications of these secondary metabolites as successful therapeutic agents is very limited, extensive exploratory activities in this area have been underway in recent years⁴⁰.

3.2.7.1 **Antitumor and anticancer activity**

The relation between chemical structure and anticancer activity of some pentacyclic and tetracyclic triterpenoids was studied by Ling *et al*⁴². The anticancer effects were tested against several human cancer cell lines. Several of the terpenoids studied showed cytotoxic activity. A detailed explanation is given by Mahato *et al*⁴⁰.

3.2.7.2 **Action on Metabolism**

Several studies have shown the effects of terpenoids on both human and animal metabolism. Tests have shown positive effects on the rat renal system⁴³, prostaglandin E2 release into gastric juice was examined in peptic ulcer patients under the influence of carbenoxolone which resulted in a decrease in acidity⁴⁴, and another triterpenoid, glycyrrhetic acid⁴⁵ induced a decrease in blood cholesterol in rats.

3.2.7.3 **Anti-inflammatory activity**

The anti-inflammatory action of some triterpenoid derivatives of the oleanane series was examined on arachidonic acid induced ear edema in mice⁴⁶. Several of the compounds examined showed a strong inhibition of ear edema on both topical and oral administration.

The presence of 12-oleane derivatives isolated from *Maesa chisis* var. *angustifolia* showed anti-inflammatory, analgesic and antipyretic activities in various pharmacological tests in experimental animals⁴⁷.

3.2.7.4 **Miscellaneous**

Oleanolic acid was effective in the prevention of experimental liver injury induced by injection of CCl₄ in rats⁴⁸. Carbenoxolone was shown to provide a protective effect to experimentally induced lower urinary tract infections in the rabbit model⁴⁹. The antitussive and expectorant activities of glycyrrhetic acid choline were evaluated in guinea pigs and mice⁵⁰. The antiviral activity of some dammar resin triterpenoids was investigated by Poehland *et al*⁵¹. The circulatory effects of oleanolic acid sodium hydrogen succinate (OSS), an analogue of the anti-ulcer drug carbenoxolone, were investigated by Filczewski *et al*⁵².

3.3 STRUCTURE ELUCIDATION OF THE PENTACYCLIC TRITERPENOIDS

The application of spectroscopic techniques has tremendously eased the problem of structure elucidation of natural products, which, in most cases, is now successfully achieved without resorting to the conventional chemical degradative procedures. It was the development of NMR spectroscopy that catapulted the enhancement of structural elucidation of the terpenoids.

^1H NMR alone is not satisfactory for structure elucidation because of inadequate dispersion in the upfield region of the spectrum. ^{13}C NMR however, is now frequently employed for the structural analysis of triterpenoids using various methods of signal assignment e.g. attached proton transfer (APT), insensitive nucleus enhancement by polarisation transfer (DEPT), 2-D spectroscopy and single frequency off-resonance decoupling³⁹.

Carbon-13 NMR data of a large number of pentacyclic triterpenoids have been published^{53, 54, 55, 56, 57}. A compilation of selected varieties of naturally occurring pentacyclic triterpenoids is given by Mahato and Kundu³⁹.

3.3.1 Proton Magnetic Resonance (^1H NMR)

The bulk of the proton signals are found in the region 0.8ppm to 2.0 ppm.

Methyl groups are usually found between 0.8 – 1.0 ppm. An obvious downfield shift is observed if they are attached to electron-withdrawing groups. The methylenes are located in the region 1.5 – 2.0 ppm.

If a proton is substituted by a hydroxyl group, the α -proton experiences a downfield shift to between 3.5 – 4.0 ppm. The β -protons are affected to a lesser extent. Carbonyl functionalities cause a shift of α -protons to between 2.0 – 2.5 ppm. Alpha methyls resonate between 1.95 – 2.2 ppm. Olefinic protons occur in the 4.0 – 6.0 ppm range. Hydroxyl groups are variable; aldehydic protons are found in a relatively

small range of 9.5 – 10.0 ppm, while the acids are found very much downfield between 10.0 – 13.0 ppm.

3.3.2 Carbon-13 Magnetic Resonance Spectroscopy (^{13}C NMR)

This is much more useful than ^1H NMR. Table 3.1 below gives the approximate shifts of the different species of carbons encountered in the pentacyclic triterpenoids⁵⁸.

Table 3.1 Chemical shifts of the different species of carbons in pentacyclic triterpenoids

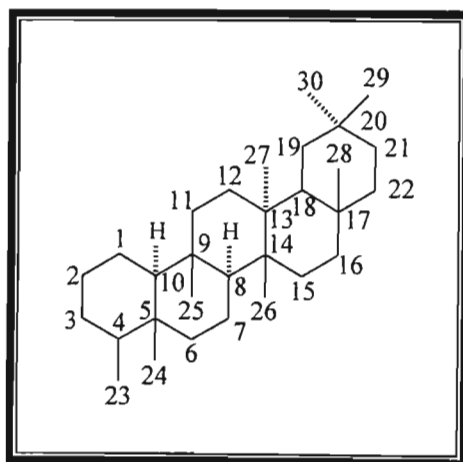
SPECIES	APPROXIMATE SHIFT (ppm)
C-CH ₃	12-24
-CH ₂	20-41
-C-H	35-57
C (quaternary)	27-43
-C-OH	65-91
-C=C-	119-172
$\begin{array}{c} \text{O} \\ \\ \text{C} \\ / \quad \backslash \end{array}$	177-220

Introduction of OH groups results in downfield shifts of 34.0 – 50.0 ppm for α -carbons, 2.0 – 10.0 ppm for β -carbons; and upfield shifts of 0 – 9.0 ppm for γ -carbons. A detailed discussion on the location and configurational determination of hydroxyl groups is given by Mahato and Kundu³⁹.

The carbonyl resonances are variable. The ketones resonate between 215-220 ppm. Aldehydic carbonyls resonate at 205-207 ppm, while the carbonyl of acids is found at around 180 ppm. Hence, the position of these signals distinguishes the different carbonyl functional groups present. Olefinic carbons show chemical shifts in the range 120-145 ppm, with the quaternary carbons resonating more downfield than the methine groups. The C-23 and C-24 gemdimethyl groups occur most often at C-4 in

most of the triterpenoid classes except the friedelanes. They resonate at about 34 and 22 ppm respectively with no C-3 substituents. A C-3-OH group causes an upfield shift of these groups of about 4-6 and 6 ppm respectively. A C-3 carbonyl with no other substituents in the vicinity has the same effect, causing C-23 to resonate at 26.5 ppm and C-24 at 21.5 ppm. The C-29 and C-30 show characteristic shifts of 33.2 and 23.6 ppm respectively with no E-ring substitution.

Because of the rearrangement of the skeleton in the friedelanes, some unique chemical shifts are observed which deserve some attention.



- [30] 3-oxo, 15 α -OH
- [31] 3-oxo, 16 β -OH
- [32] 3-oxo, 28-OH
- [33] 3-oxo, 17 α -OH, 28-nor
- [34] 3-oxo, 29-OH
- [35] 3-oxo, 27 \rightarrow 15 α olide
- [36] 3 β -OH, 27-COOH
- [37] 3 β -OH, 26-nor, \triangle ¹⁴
- [38] 3 β -OH, 7-oxo
- [39] 2 α , 3 α -OH

A carbonyl at C-3 causes the C-23 methyl to resonate upfield at about 6.8 ppm. This is demonstrated with the ¹³C NMR data of compounds [30-35]³⁹ (Table 3.2).

Table 3.2 Effect of 3-oxo group on C-23 of selected friedelanes

COMPOUND	C-23 (ppm)
30	6.8
31	6.8
32	6.7
33	6.8
34	6.8
35	6.8

However, if the carbonyl group is replaced by an OH group, this causes the C-23 methyl to move downfield. The shift however, is dependent on the orientation of the OH group. If the OH group is beta (axial) the shift is about 4.8 ppm and hence resonates at 11.6 or 11.7 ppm. If it is alpha (equatorial), then the C-23 methyl resonates between 9.5 and 10.0 ppm, a downfield shift of about 3 ppm. Compounds [36-38]³⁹ (Table 3.3) support this argument. This information was useful in the structure elucidation of *epi*-friedelinol [42]. The C-24 methyl also shows an upfield shift resonating between 14.5 and 14.7 ppm.

Table 3.3 Effect of 3-OH group on C-23 of selected friedelanes

COMPOUND	C-3 (PPM)	C-23 (ppm)
36	72.7	11.6
37	72.7	11.6
38	72.0	11.6
39	73,2	9.6
<i>epi</i> -friedelinol	72,76	11.62

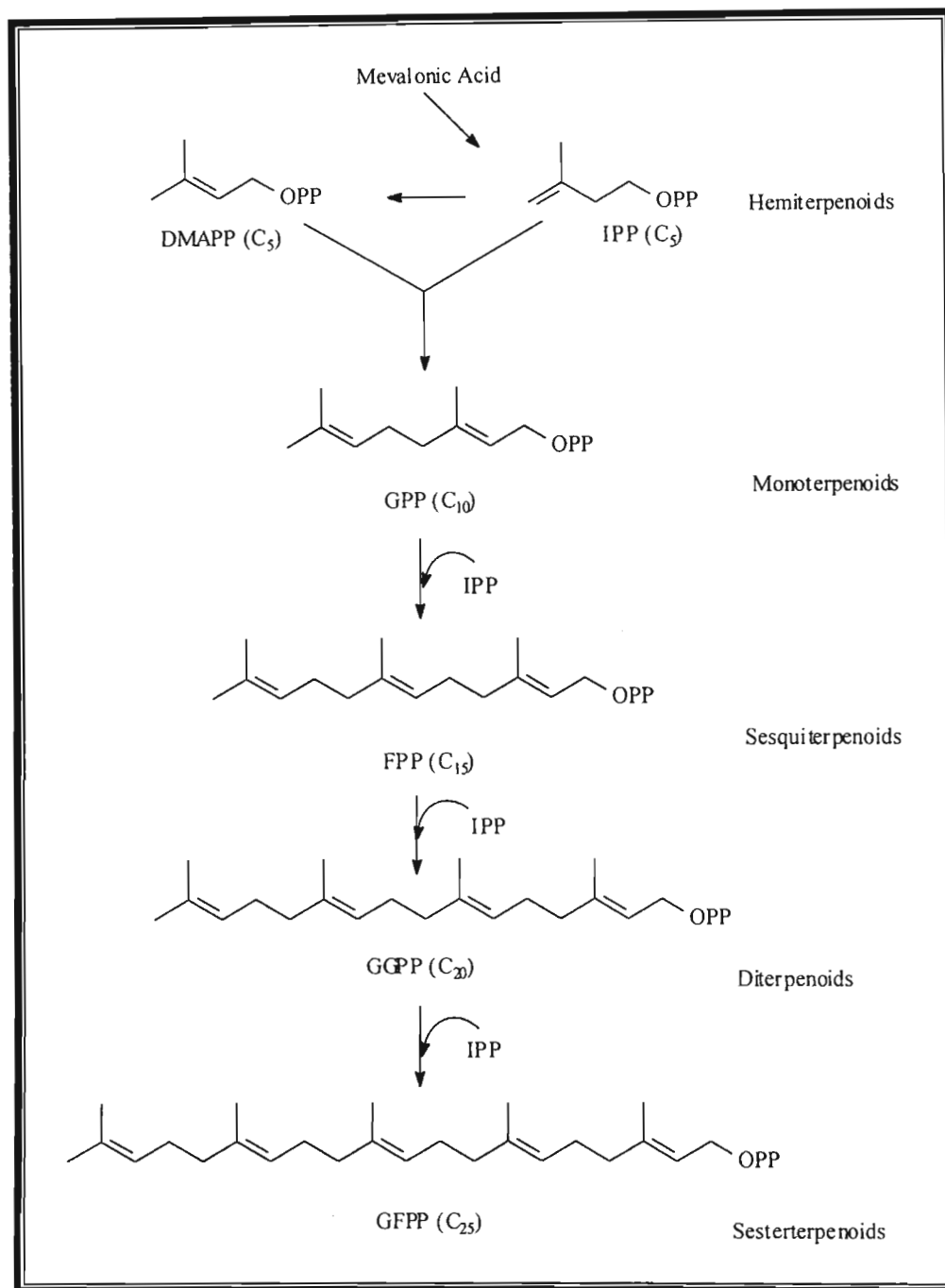
3.4 BIOSYNTHESIS OF THE TERPENOIDS

Recent studies have now shed new light on the biosynthesis of terpenoids. The research has presented a new pathway for the synthesis of the C₅ (isoprene) building blocks namely, the 2-C-methyl erythritol 4-phosphate (MEP) pathway, completely distinct from the acetate-mevalonate (Ac-MVA) pathway. This new route begins with the condensation of glyceraldehyde phosphate and pyruvate to form 1-deoxyxylulose 5-phosphate. In plants, the MEP pathway appears to be localized in the plastids and is the likely source of substrate for plastid-associated terpenoids, such as phytol and carotenoids. In contrast, the mevalonate pathway seems restricted to the cytosol/endoplasmic reticulum because all known pathway genes are targeted to this compartment⁵⁹.

However, an accompanying study drew critical questions that have led to the idea of the co-existence of the two pathways. A model, based on the medicinal plant *Marrubium vulgare*, was used to study the regulatory aspects of both pathways. Shoot cultures were shown to produce sterols built via the Ac-MVA pathway, and furanic labdane diterpenoids which were shown to be built via the new pathway^{60, 61}. Hence, the Ac-MVA pathway cannot be discounted, since from the above study, it is clear that at this stage, either pathway cannot be considered independent of each other. As a result, the general biosynthetic scheme shown, (Scheme 3.3), which offers a brief explanation as to the steps leading up to the different terpenoids is based on the Ac-MVA pathway, considering the limited information available on the MEP pathway.

The studies above have also made major advances in the study of terpenoid enzymology, including structure determination and reaction mechanisms.

With the myriad of texts⁶² and reviews⁶² on the biosynthesis of the terpenoids currently available, it seemed inappropriate to rewrite the text on the subject. However, attention was paid to the triterpenoid biosynthesis, especially the pentacyclic triterpenoids, in the hope of showing a biogenetic link between the various forms in this class with reference to the compounds isolated.



Scheme 3.3: Terpenoid skeleta (to C₂₅) derived from the Mevalonic Acid Pathway

The scheme shows the initiation of the sequence, after the initial primer formation, with the C₁₀ monoterpene units formed by the combination of dimethylallyl pyrophosphate (DMAPP) and isopentenyl pyrophosphate (IPP) to yield geranyl pyrophosphate (GPP).

Modest changes of this precursor lead to a range of linear and cyclic products. Addition of a further IPP unit to GPP leads to the fundamental sesquiterpenoid precursor farnesyl pyrophosphate (FPP). The diterpenoid and sesquiterpenoid precursors are formed by a similar chain extension mechanism, where IPP adds to FPP to form geranylgeranyl pyrophosphate (GGPP) for diterpenoids and IPP adds to GGPP to yield geranylgeranyl pyrophosphate (GFPP), the sesquiterpenoid precursor.

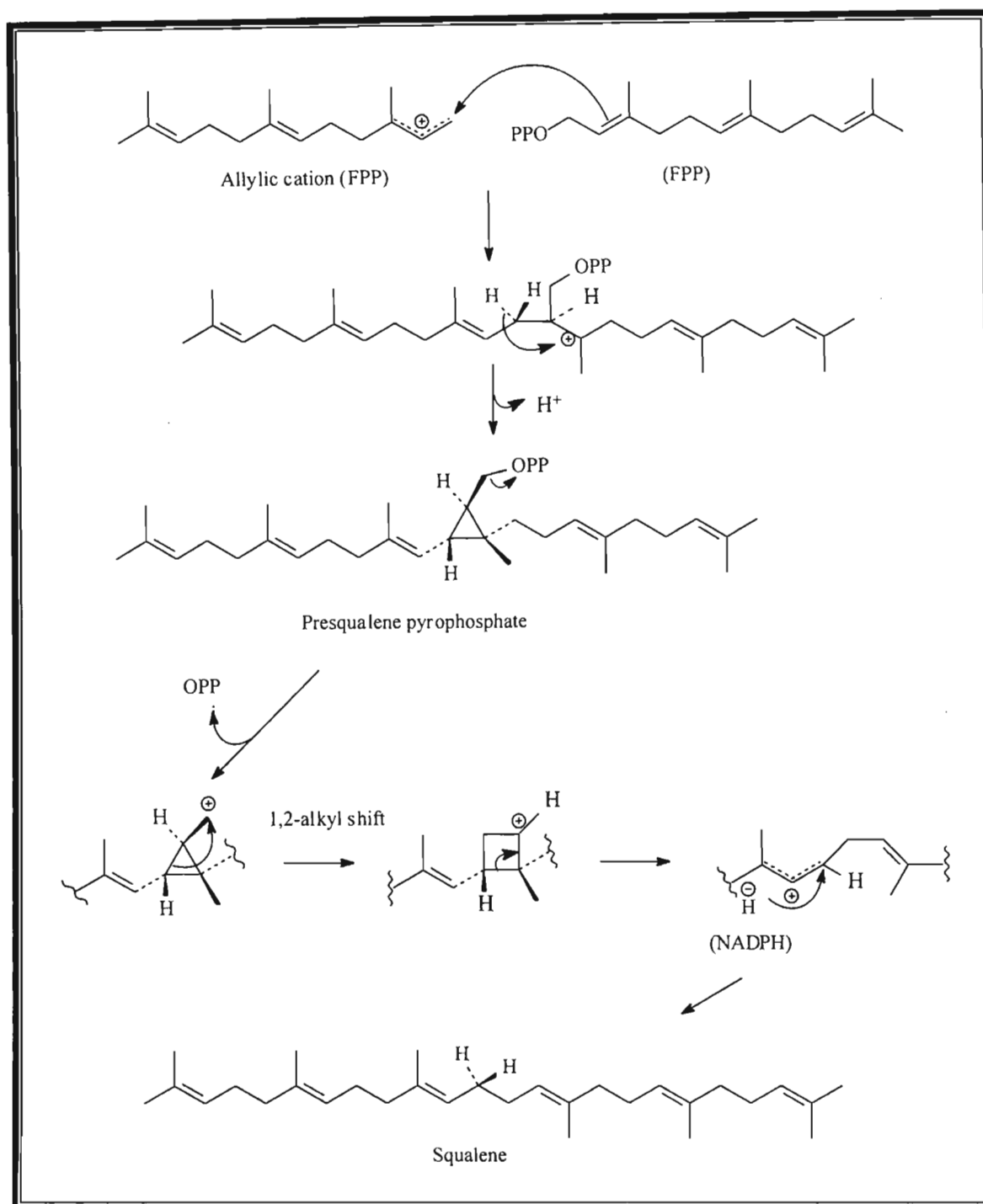
3.4.1 Triterpenoids

The triterpenoids are not formed by an extension of the familiar process of adding IPP to the growing chain. Instead, two molecules of FPP are joined tail-to-tail to yield the hydrocarbon squalene. Scheme 3.4 shows the formation of squalene from two molecules of FPP to first yield an intermediate called presqualene pyrophosphate, which is formed when the tertiary carbocation cyclises to form the cyclopropane ring. Loss of the diphosphate gives a primary cation which being not very stable, induces a 1,2-alkyl shift (Wagner-Meerwein rearrangement) to generate a more favourable secondary cation and less strained cyclobutane ring. Bond cleavage leads to the formation of an allylic cation, and the generation of squalene is completed by supply of hydride from NADPH.

The tetracyclic triterpenoids are formed when squalene cyclises via the intermediate squalene-2,3-oxide. Following this, an intermediate protosteryl cation is formed by cyclisation of the squalene oxide. For the formation of this cation the squalene oxide must be in the chair-boat-chair-boat conformation (Scheme 3.5). The cyclisation is followed by a series of Wagner-Meerwein migrations of methyls and hydrides in two different ways to give lanosterol in animals and cycloartenol in plants⁶².

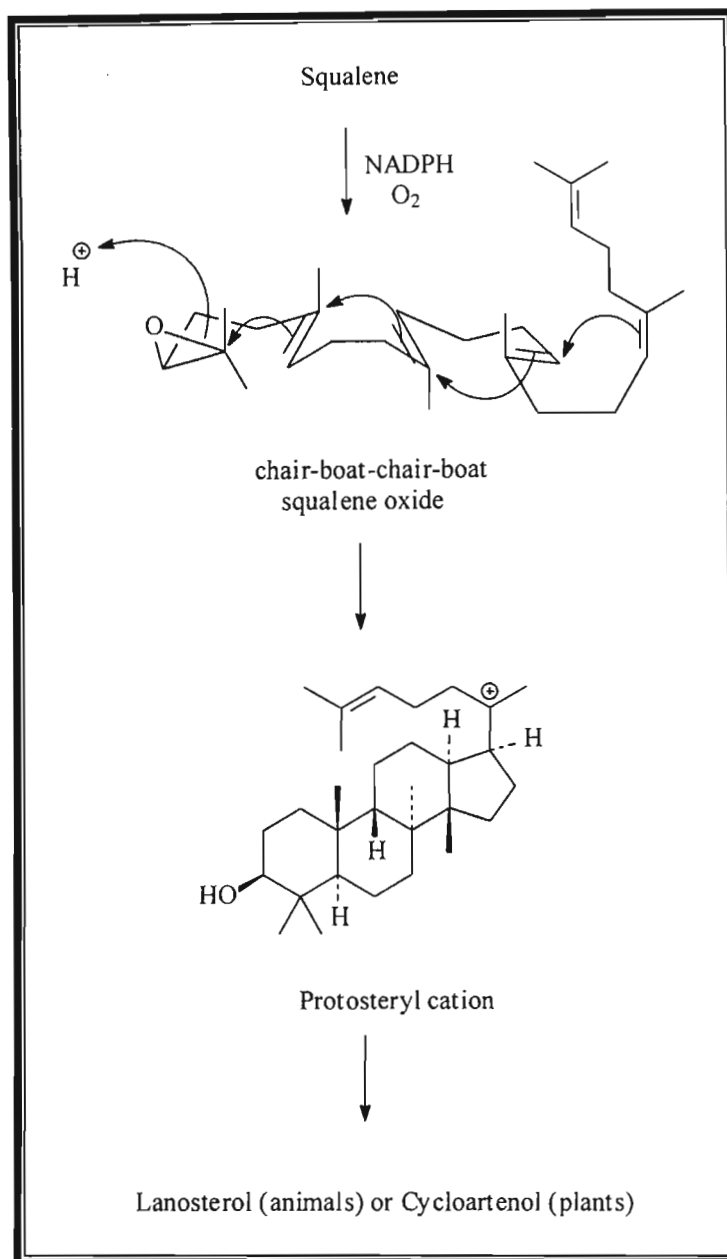
3.4.2 The pentacyclic triterpenoids⁶²

When squalene oxide is in the chair-chair-chair-boat conformation, the damaryl cation (Scheme 3.6) is formed which undergoes a 1,2-alkyl shift to produce a secondary



Scheme 3.4: Formation of squalene

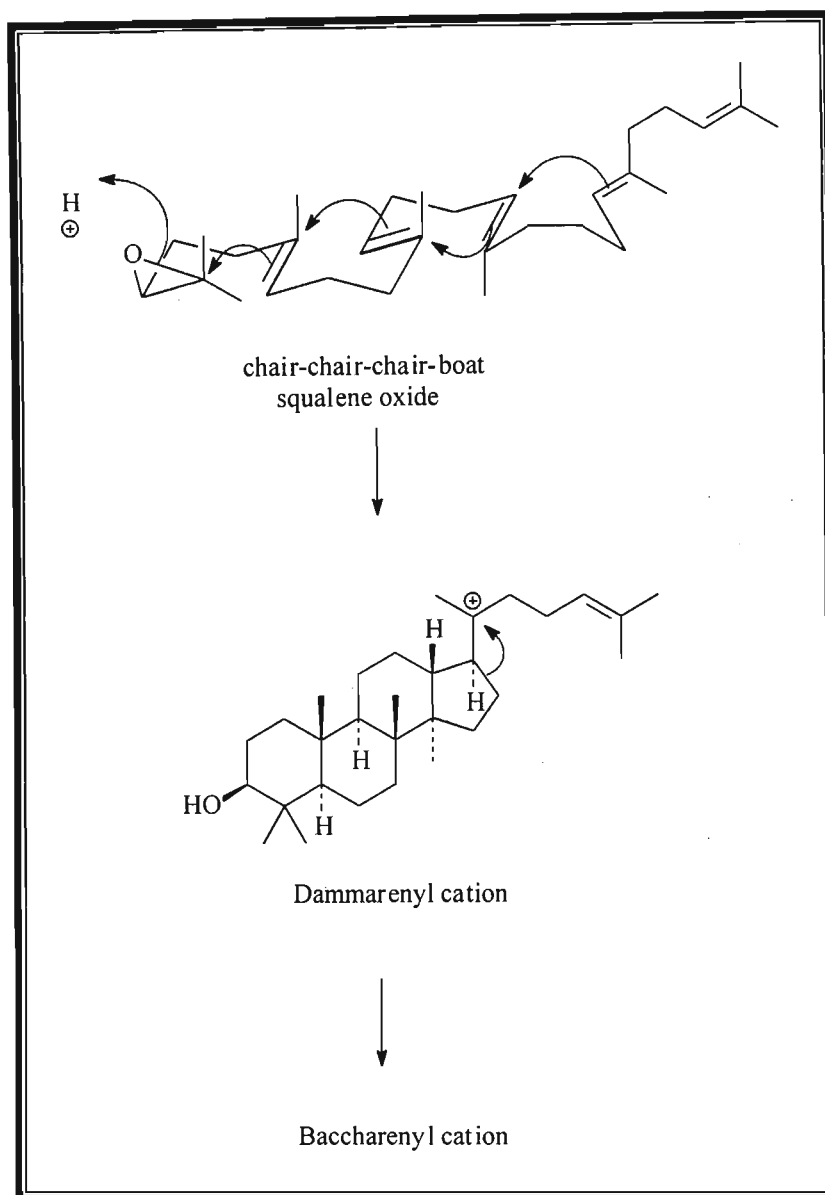
carbocation called a baccharenyl cation (Scheme 3.7). A pentacyclic ring system can now be formed by cyclisation on to the double bond, giving a new five-member ring and a tertiary lupenyl cation. Loss of proton from the lupenyl cation gives lupeol.



Scheme 3.5: Formation of the protosteryl cation (tetracyclic precursor)

Ring expansion in the lupenyl cation by bond migration gives the oleanyl system, from which the widely distributed β -amyirin is derived. Formation of the isomeric α -amyirin involves first the migration of a methyl in the oleanyl cation then discharge of the new taraxasteryl cation by three hydride migrations and loss of a proton (Scheme 3.7).

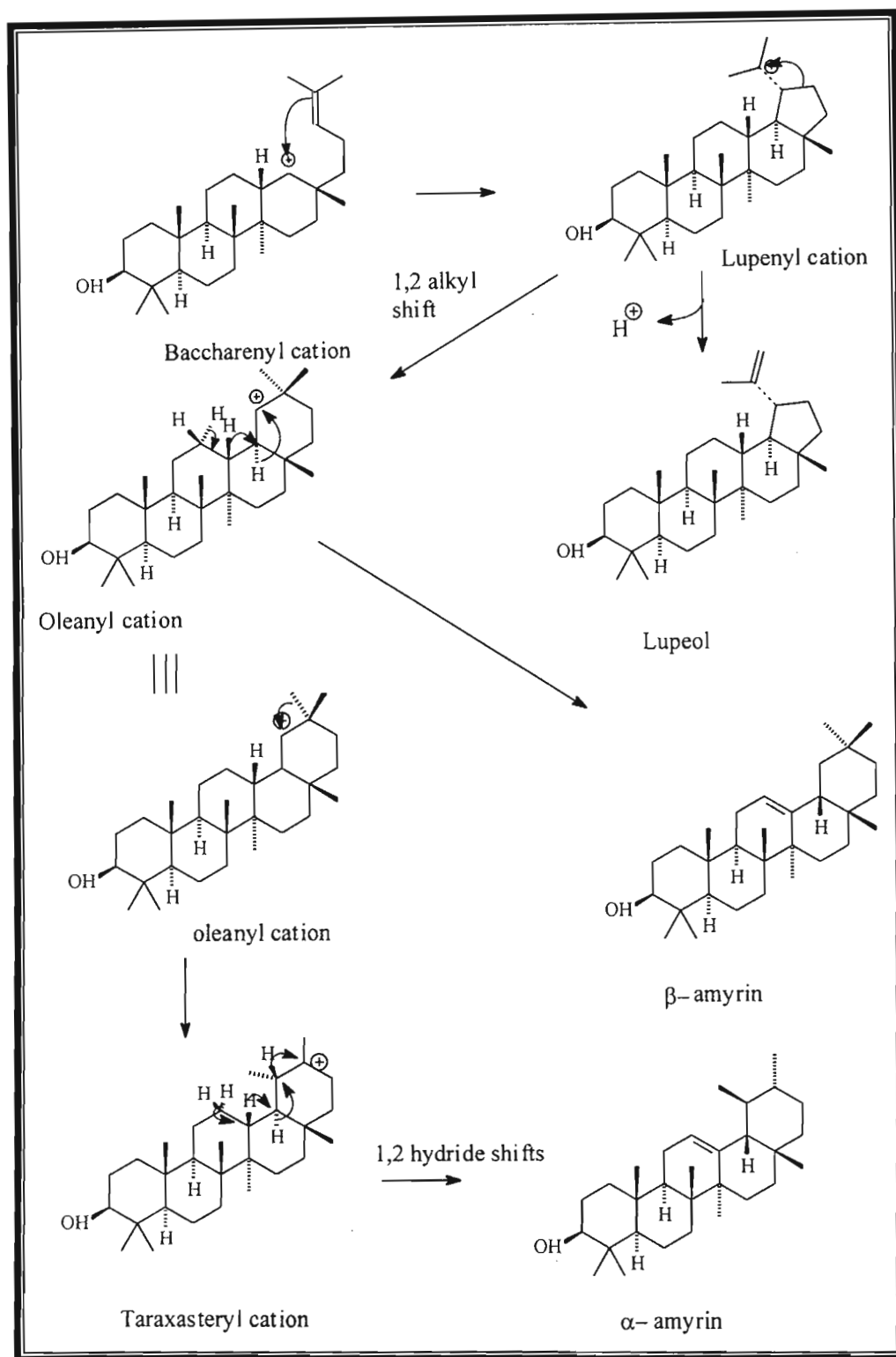
The formation of α - and β -amyrin from the oleanyl cation involves basically rings C, D and E. With the friedelanes however, a dramatic hydride/methyl shift occurs involving all five rings.



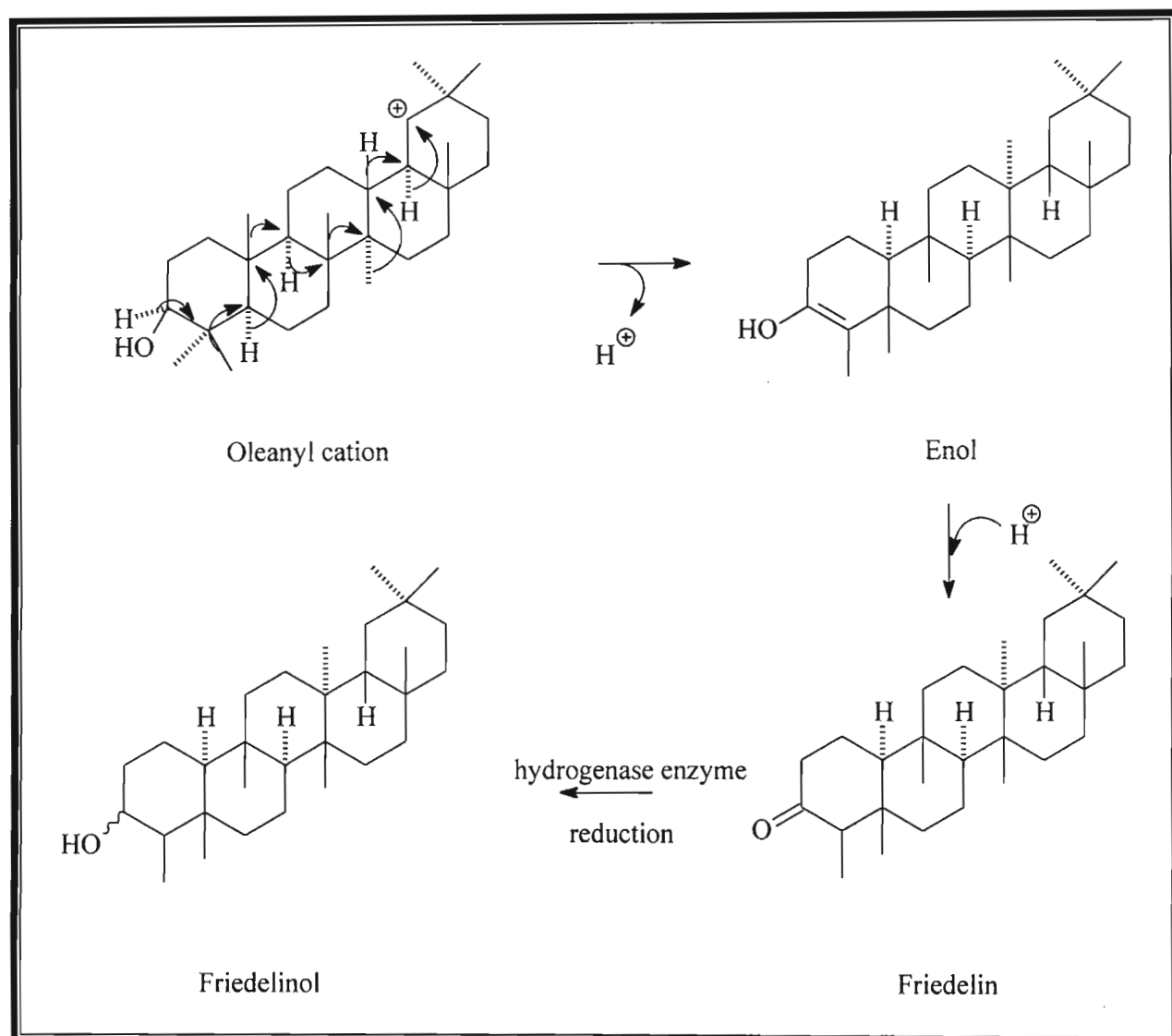
Scheme 3.6: Formation of the dammerenyl cation (pentacyclic precursor)

Instead of the 12,13-double bond formation by loss of a proton, hydride/methyl shifts continue until the enol of friedelin is formed. Friedelin being formed by subsequent reduction of the enol. This rearrangement is termed "friedo" rearrangement. The

formation of friedelinol is likely to involve enzymatic reduction by a hydrogenase enzyme (Scheme 3.8).



Scheme 3.7: Formation of the lupenyl and oleanyl cations



Scheme 3.8: "Friedo" rearrangement

PART B

RESULTS AND DISCUSSION

CHAPTER FOUR

EXTRACTIVES FROM *ACRIDOCARPUS NATALITIUS*

4.1 INTRODUCTION

Acridocarpus natalitius Adr. Juss. (Malpighiaceae) is one of many traditional medicinal plants used as charm plants by the native people. African doctors (sangomas) use them in the preparation of an ointment, which is believed to safeguard warriors in battle. Both Pondos and Zulus believe that the leaves have the power to prevent a person from performing some undesirable deed, from uttering undesirable words or passing on secret information⁶³.

The plant root is claimed to possess gentle laxative properties and produce a natural movement of the bowels. It is either ingested in raw powdered form, a teaspoon at a time or made into an infusion and drunk like a tea. Half a cup is prescribed twice a day to relieve constipation⁶⁴.

Two subspecies of *Acridocarpus* exist in Natal namely, *A. natalitius* Juss var. *linearifolius* Launert and *A. natalitius* Juss. var. *natalitius*. The second type was used in the present study. The plant is described as a shrub with a marked tendency to scramble, sometimes reaching the forest canopy, but sometimes develops into a small tree up to 5m in height. The bark is grey (fig. 4.1) with the tips of the branches often twining and the leaves are alternate, simple, oblong to linear-lanceolate and leathery (fig. 4.4). The flowers are deep yellow, about 3cm in diameter, produced in sturdy, pyramidal spikes (fig. 4.2). Fruits are twin nutlets, each with a broad membranous wing (fig 4.3). The two wings together resembling a dark reddish-brown moth, hence the common name, Moth-fruit tree. The roots are longitudinal, with a soft outer covering and a hard, woody core (fig. 4.5)⁶³.



Fig. 4.2 Flowers



Fig. 4.3 Fruits resembling 'moths'

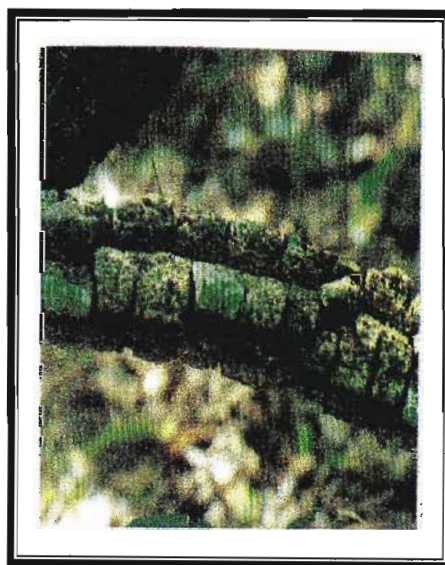


Fig. 4.1 Bark



Fig. 4.4 Leaves (broad, lanceolate)
(courtesy: Dr. N. Crouch, Natal Herbarium)



Fig. 4.5 Roots in their natural habitat
(courtesy: Dr. N. Crouch, Natal Herbarium)

Classification⁶³:

Family: Malpighiaceae

Genus: *Acridocarpus*

Species: *natalitius*

The present study of the roots of *A. natalitius* has revealed the presence of several pentacyclic triterpenoids and stigmasterol from the hexane extract. The methanol extract produced (-)-epicatechin [4] as the major metabolite, together with glucose and sucrose.

- a) Friedelin [41]
- b) *epi*-Friedelinol [42]
- c) Lupeol [43]
- d) Oleanolic acid [44]
- e) Stigmasterol [45]
- f) (-)-Epicatechin [4]
- g) Glucose [64]
- h) Sucrose [65]

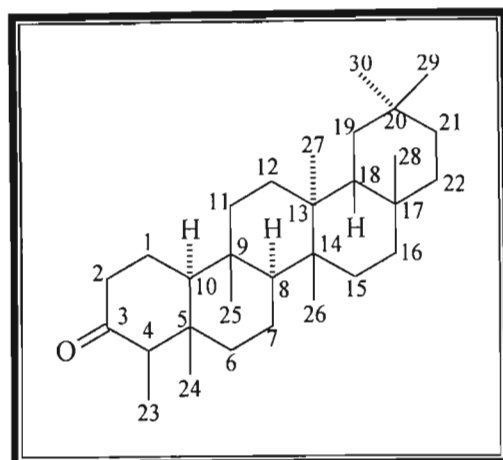
All the above compounds have previously been isolated and identified from other plant species^{24, 65}. This is the first time that these compounds have been reported in this plant.

4.2 PENTACYCLIC TRITERPENOID AND STIGMASTEROL

4.2.1 Friedelan-3-one [41]

[Friedelin 41]

Friedelin [41] was obtained as colourless crystals as described in 7.2.1.1.



[41]

The ^1H NMR [plate H-1] of friedelin [41] showed eight conspicuous methyl resonances in the upfield region of the spectrum. This information coupled with the thirty-carbon figure from the ^{13}C NMR data [plate C-1, Table A1], led to the conclusion that the compound was a triterpenoid. The compound showed properties of lacking any polar constituents due to its behaviour during TLC analysis.

Inspection of the ^{13}C NMR showed a resonance at 213.26 ppm from which the presence of a carbonyl functionality was suspected. This was confirmed from the IR data [plate I-1], which showed a strong peak at 1718.79cm^{-1} . The compound also gave a positive test to 2,4-DNPH. As no aldehydic protons were present, a ketone functionality was concluded. The carbonyls of aldehydes usually resonate at about 207 ppm. Also, the aldehyde proton would be present in the ^1H NMR spectrum, resonating between 9-11 ppm.

The pentacyclic nature of the compound was arrived at from the study of tetracyclic triterpenoids. Structurally, all tetracyclic triterpenoids contain a side chain attached at C-17 that is comprised of 8 to 10 carbon atoms. The side chain can be saturated or have at least one double bond.

The isopropyl methyl protons (C-26, C-27) appear at roughly 0.87ppm as doublets ($J=5.4\text{Hz}$), due to them coupling to the C-25 proton. With a 24, 25-double bond, two

broadened three-proton singlets occur at 1.7 and 1.6 ppm. The C-21 methyl also appears as a doublet ($J=6\text{Hz}$), because of coupling with H-20.

Friedelin [41] however, showed three methyl resonances at 0.70, 0.84 and 0.86 ppm, the most upfield of the methyl resonances. All appeared as three proton singlets. Further evidence was furnished from the ^{13}C NMR data, which negated the presence of a side chain. Thus, the only way to accommodate thirty carbons without a side chain is the formation of an additional ring, suggesting a pentacyclic triterpenoid.

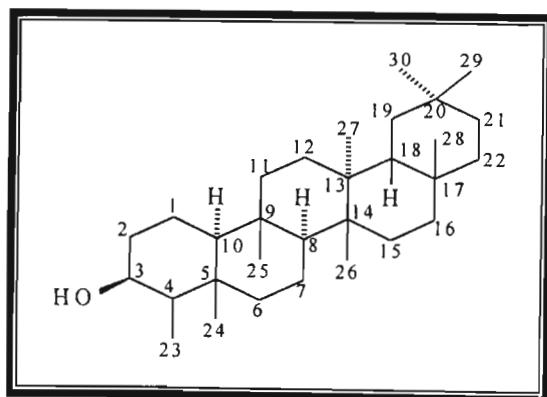
A study of a compilation of ^{13}C NMR data of pentacyclic triterpenoids was used as the basis for the final structure elucidation of friedelin [41]. A conspicuous methyl signal found considerably upfield in the ^{13}C NMR of friedelin (6.8 ppm) was used as a fingerprint to compare and verify the structure from the reported data. A detailed explanation of structure elucidation of pentacyclic triterpenoids is given in section 3.3.

4.2.2 Friedelan-3 β -ol [42]

[*epi*-Friedelinol 42]

epi-Friedelinol [42] was isolated as plate-like crystals as described in section 7.2.1.2.

As for friedelin, characteristic signals in the ^1H NMR [plate H-2] and atomic number from the ^{13}C NMR data [plate C-2, Table A1], *epi*-friedelinol [42] was concluded to have a pentacyclic structure.



[42]

A broad doublet at 3.72 ppm ($J=1.8$ Hz) was indicative of an alcoholic α -proton. Further evidence of an OH group was given by the ^{13}C NMR, which showed a peak resonating at 72.76 ppm. Inspection and comparison of the ^{13}C NMR data with that of friedelin revealed many similarities. Thus, the absence of the carbonyl group and the presence of an OH functionality led to the proposal that the compound was the reduced form of friedelin. An argument given in section 3.3 about the effect of substituting the carbonyl group with an OH group further established the above proposal. Information gained from the melting point again strengthened this conclusion, since the α -isomer melts at 300°C whilst the β -isomer melts between $283.5^{\circ} - 285^{\circ}\text{C}$ ⁶⁵.

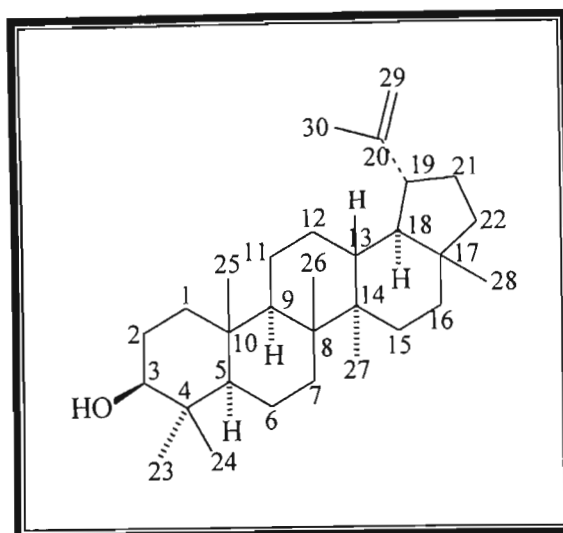
The reduction of friedelin [41] as discussed in section 7.3⁶⁶ did not go to completion even after several attempts. However, TLC analysis showed that a product of the reduction had the same characteristics as *epi*-friedelinol [42], but was in too small a quantity for isolation purposes. The ^1H NMR of the reduction mixture shows unreacted friedelin [41] as the major compound; however, expansion of the spectrum clearly shows the one proton doublet ($J=1.8$ Hz) that is characteristic in the proton spectrum of *epi*-friedelinol [42].

From the data accumulated and the results of the reduction of friedelin [41] (see section 4.4). It was concluded that the compound was *epi*-friedelinol [42] having an axial OH group at C-3.

4.2.3 3 β -Hydroxylup-20(29)-ene [43]

[Lupeol 43]

Lupeol [43] was isolated as colourless crystals as described in section 7.2.1.3.



[43]

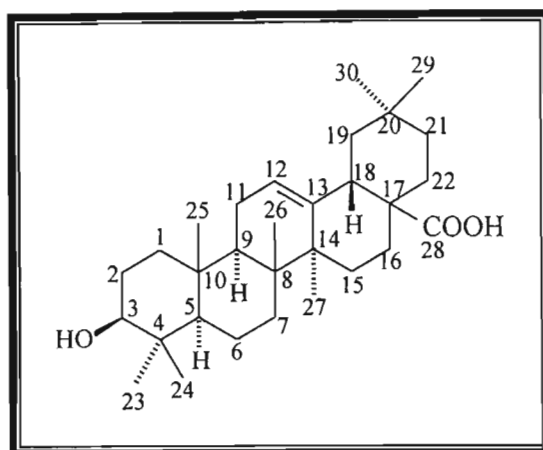
The spectral data of lupeol [43] was not very dissimilar to the ^1H NMR and ^{13}C NMR spectra of the previous two terpenoids, revealing characteristics that allowed a pentacyclic triterpenoid structure to be arrived at.

The ^1H NMR [plate H-3] spectrum showed a multiplet at 2.35 ppm that was due to the geminal protons at C-2 coupling with H-1a, H-1b and H-3. A doublet of doublets at 3.17 ppm due to H-3 suggested an alcoholic α -proton. The region of resonance was indicative of this. Further evidence of the OH group was provided by the ^{13}C NMR, which showed a resonance at 79.02 ppm. An AB coupled doublet at 4.6 ppm was indicative of olefinic geminal protons. Also the ^{13}C NMR showed shifts in the region appropriate for olefinic carbons (109.33 and 150.99 ppm), their positions however, were suggestive of only one of them being protonated.

Mahato and Kundu³⁹, from their compilation of ^{13}C NMR data, showed that the lupanes contained a side chain isopropylidene group. The hopanes (Scheme 3.2), another class of pentacyclic triterpenoids, may also possess a very similar skeleton to the lupanes, however the position of C-28 is found at C-18 rather than at C-17. The effect of this is that the C-27 is deshielded in the hopanes in comparison to the lupanes, due to the loss of the γ -effect from C-18 and the gain of δ -effect from C-28³⁹.

4.2.4 3 β -Hydroxy-12-oleanen-28-oic acid [44]**[Oleanolic Acid 44]**

The acid [44] was isolated as a white powder from the hexane extract as discussed in section 7.2.1.5.



[44]

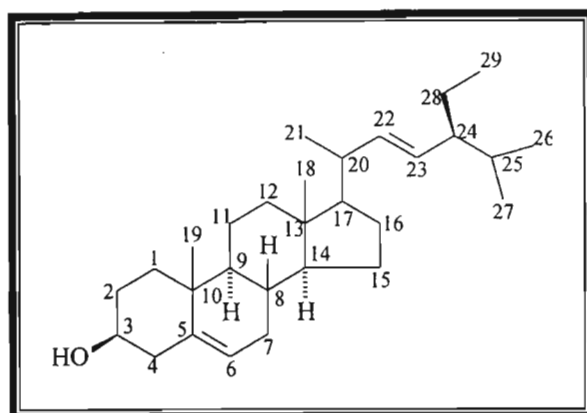
The proton spectrum of oleanolic acid [44] [plate H-4] showed only seven methyl resonances in the appropriate region. A multiplet at 3.21 ppm was indicative of proton alpha to an alcohol functionality showing coupling to H-1a and H-1b and H-2a and H-2b. The doublet of doublets at 2.8 ppm is due to H-2a and H-2b coupling to H-3. Signals at 143.4 and 122.1 ppm in the ^{13}C NMR spectrum [plate C-4, Table A1] were indicative of olefinic carbons. However, since only one proton signal (integral) was observed in the olefinic region in the ^1H NMR (brs, 5.26 ppm), this suggested that the double bond was located at the ring junction. The presence of an acid was first suspected from the TLC characteristics (low mobility in solvent system) together with a distinct resonance in the ^{13}C NMR spectrum at 184 ppm. The one methyl deficit in the ^1H NMR led to the conclusion that the acid was in a position previously occupied by the methyl substituent. A study of the literature showed that the methyl shifts in oleanolic acid were very similar to those compounds that contained the oleanane skeleton (Scheme 3.2). Hence, the

structure of oleanolic acid was arrived at by comparison of spectral data and the fact that it co-migrated with an authentic specimen.

4.2.5 24 β -Ethylcholest-5,22-dien-3 β -ol [45]

[Stigmasterol 45]

The isolation of stigmasterol [45] is described in section 7.2.1.4.



[45]

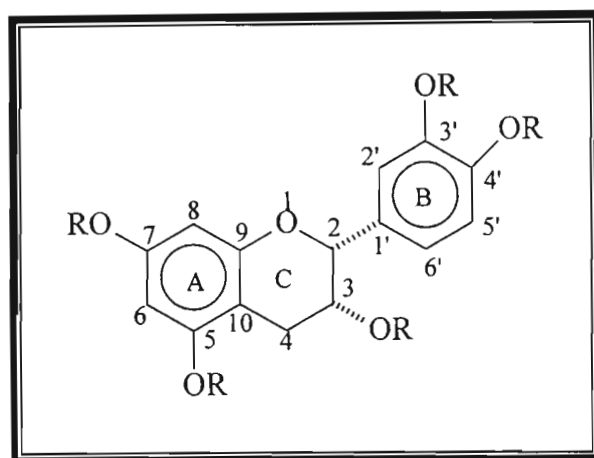
The ^1H NMR [plate H-5] and ^{13}C NMR [plate C-5, Table A1] data of stigmasterol [45] is well established. The characteristic signals were easily identified thus establishing the identity of stigmasterol by comparison with published data⁵⁷. Confirmation was also obtained from TLC analysis with an authentic sample. Due to the widespread distribution of stigmasterol, it proved insignificant to pursue any further investigations pertaining to this compound.

4.3 (-)-EPICATECHIN AND CARBOHYDRATES

4.3.1 (2R,3R)-2,3-cis-Flavan-3,3',4',5,7-pentol [4]

[(-)-Epicatechin 4]

(-)-Epicatechin [4] was obtained as a brown amorphous, non-crystalline compound by subjecting the methanol extract to different chromatographic techniques as discussed in section 7.2.2.



[4] R = H

[46] R = Ac

Two meta-coupled doublets at 5.94 and 6.04 ppm ($J=2.4$ Hz) due to H-6 and H-8 were evident in the ^1H NMR spectrum [Plate H-6]. An ABX system defined the B-ring substitution pattern. H-2' was seen as a meta coupled doublet at 7.07 ppm ($J=2.1$ Hz). H-5' occurred as a doublet at 6.81 ppm (ortho coupled, $J=8.1$ Hz). H-6' appeared as a doublet of doublets at 6.86 ppm ($J=2.1$ and 8.1 Hz) due to ortho coupling with H-5' and meta coupling with H-2'. A one-proton singlet at 4.90 ppm and a one-proton multiplet at 3.66 ppm indicated the *cis* orientation of H-2 and H-3 respectively. Finally, the geminal protons of H-4 were seen as a doublet of doublets for each. H-4_{ax} resonating at 2.76 ppm and H-4_{eq} at 2.89 ppm.

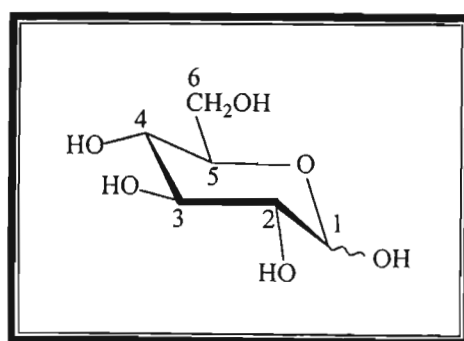
The phenolic carbons of rings A and B were clearly distinguished in the ^{13}C NMR [plate C-6]. Those of ring-A resonating at 156.5 and 156.4 ppm while those of ring-B showed resonances at 144.1 and 144.3 ppm. The comparatively lower field positions of ring-A phenolic carbons were due to the deshielding effect of the electron withdrawing aliphatic ring. The aliphatic carbon signals are also clearly indicative of the flavan-3-ol aliphatic ring system. Signals at 78.3, 65.8 and 27.9 ppm were due to C-2, C-3 and C-4 respectively.

Analysis of the ^1H NMR [plate H-7] and ^{13}C NMR [plate C-7] of the acetylated derivative unambiguously indicated structural allocation and substitution pattern for [46] in congruence with, and thereby confirming that obtained for epicatechin [4]. The structure was finally verified by comparison with published data³ and TLC with an authentic sample.

4.3.2 α -D-, β -D-Glucopyranoside [64]

[Glucose 64]

Glucose [64] was isolated as an amorphous brown solid from the methanol extract as described in section 7.2.2.3



[64]

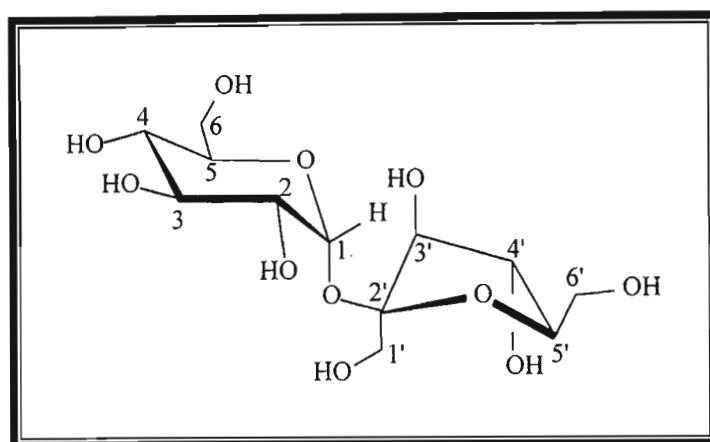
Examination of the ^1H NMR [plate H-8] spectrum of glucose showed that it was a mixture of the α - and β -anomers. The signal at 5.24 ppm (d, 3,9 Hz) is due to the anomeric proton of the α -anomer, whilst the anomeric proton of the β -anomer is

represented by a doublet ($J = 7.8$ Hz) at 4.66 ppm. The compound was verified by comparison of ^1H NMR data and migration on TLC plate with an authentic, pure sample.

4.3.3 β -D-Fructofuranosyl α -D-glucopyranoside [65]

[Sucrose 65]⁶⁷

Sucrose [65] was isolated as colourless crystals from the same extract that gave glucose as described in section 7.2.2.4.



[65]

The compound was found to be readily soluble in water. From this information, together with the characteristic green colour observed during TLC analysis, a sugar was suspected. The ^1H NMR spectrum [plate H-9] contained several multiplets in the region 3.4-3.9 ppm, which is indicative of a typical sugar. The compound was suggested to be sucrose [65] by comparison of TLC results and the ^1H NMR spectrum of an authentic sample.

The doublet at 5.41 ppm ($J = 3.9$ Hz) was ascribed to the anomeric proton of the glucosyl moiety. Further doublets at 4.21 ($J = 8.7$ Hz) and 3.82 ppm ($J = 2.1$ Hz) were due to H-3' and H-6,-6' respectively. Triplets at 4.05 ($J = 8.4$ Hz), 3.46 ($J = 9.3$ Hz) and 3.76 ($J = 9.6$ Hz) were ascribed to H-4', H-4 and H-3 respectively. H-1' was seen as a broad singlet at 3.67 ppm.

4.4 ATTEMPTED SYNTHESIS OF *EPI*-FRIEDELINOL [42]

TLC analysis of the product obtained revealed two spots co-migrating with friedelin and *epi*-friedelinol. However, the spot co-migrating with friedelin [41] was darker when compared to the second spot. Thus, it was concluded that friedelin [41] was reduced only to a small extent. Repetition of the experiment showed no improvement in the yield. The amount of *epi*-friedelinol [42] present was too small to isolate and analyse and so the entire mixture, designated EF-1, was analysed.

The ^1H NMR spectrum of EF-1 [plate H-10] revealed the presence of a doublet at 3.72ppm($J=1.8\text{Hz}$). The expansion of this doublet is seen in fig. 4.6. The ^1H NMR of *epi*-friedelinol [42] [plate H-2] also displays this doublet at 3.72 ppm ($J= 1.8$ Hz).

Figure 4.7 gives a partial structure of friedelin [41] [A] showing the stereochemistry of the cyclohexanone A-ring. Cherest and Felkin^{68, 69, 70} considered the stereochemistry of organometallic compound addition to cyclohexanones to be influenced by two factors: (1) steric interaction of the incoming group with the 1,5 axial substituents and (2) the torsional strain of the incoming group with the 2,4-axial substituents. Torsional strain implies bond repulsion between the forming C-R bond and the 2,4-axial hydrogen bonds. The methyl group at position C-3 is axial, and will hence influence steric interaction between itself and the forming OH group, [B] and [C], depending on the orientation of the OH group.

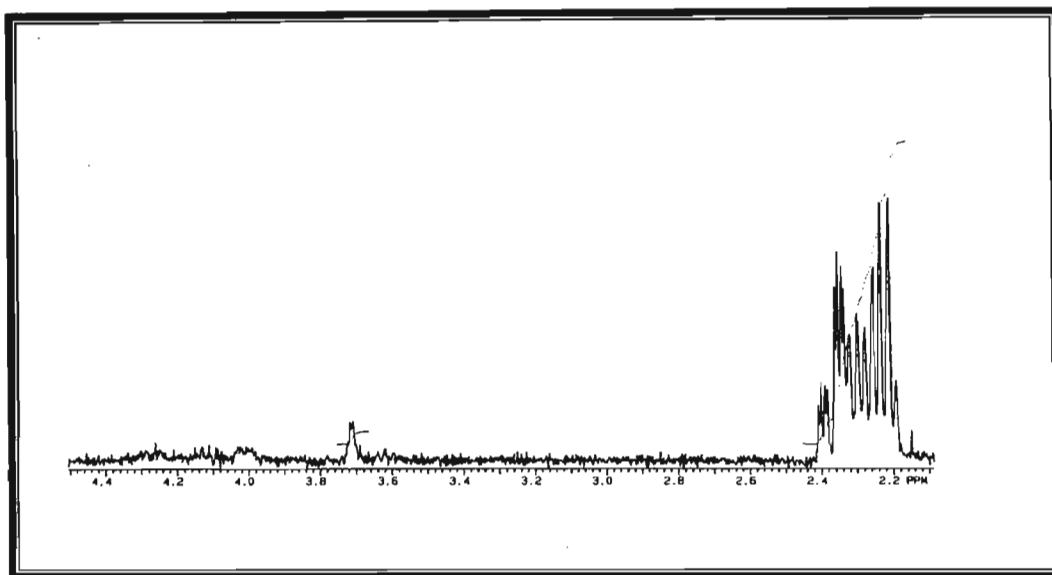


Fig. 4.6 Expansion of EF-1 showing H-3 doublet of *epi*-friedelinol [42]

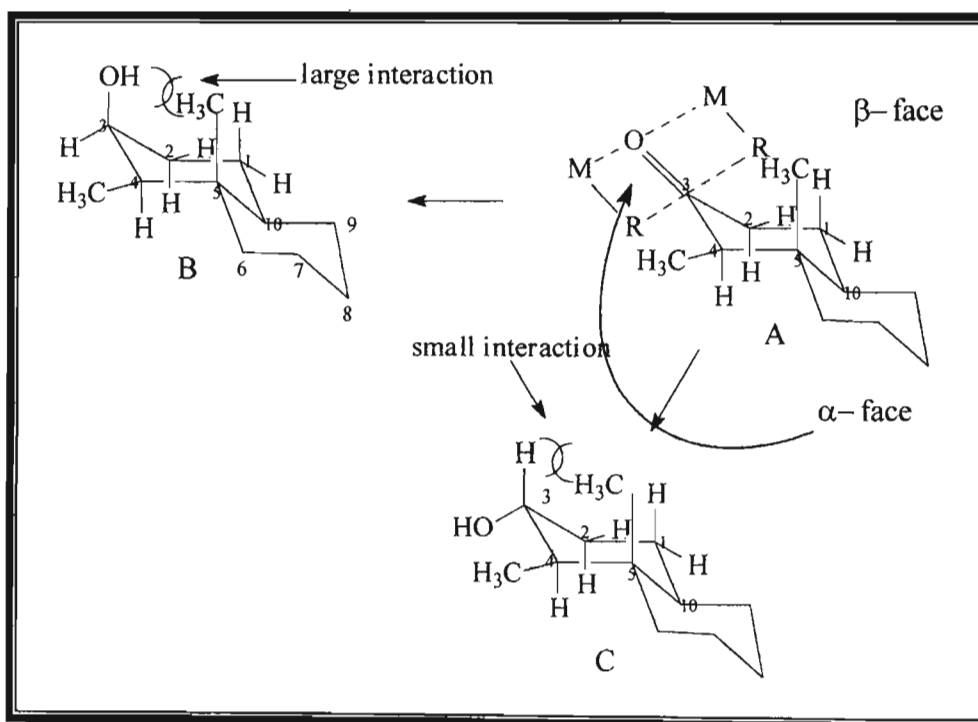


Fig.4.7 Stereochemistry of friedelin A-ring

Since reduction of a keto group is perpendicular to the plane of the carbonyl and the least hindered side is favoured, this implies that for friedelin [41] the α -face is favoured (see figure 4.7, p59). This results in a 3β -OH (axial) and a C-3 α H (equatorial). Even though friedelinol [C] looks the more favourable product, its formation is thermodynamically less favourable.

CHAPTER FIVE

EXTRACTIVES FROM *TYPHA CAPENSIS*

5.1 INTRODUCTION

Typha capensis (Rohrb.) N.E.Br (Typhaceae) is also known as ibuma (Zulu), bulrush (English) and papkuil (Afrikaans). The plant is very common in South Africa, found in all parts, but sparse in the North Western Cape region. It is usually found in wet or seasonally wet places⁷¹.

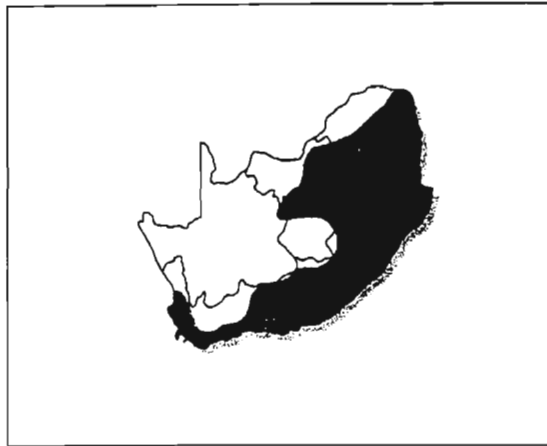


Fig. 5.1 Distribution of *T. capensis* in Southern Africa

The plant is described as a robust, reed-like plant of up to three metres in height (fig. 5.2). The rhizomes are thick, fleshy and spongy and creep horizontally (fig 5.3). Erect stems protrude from the rhizomes to end in thick, strappy, hairless leaves. The characteristic flower stalk has minute male flowers towards the tip with the female flowers packed below the male part in a thick brown mass (fig 5.2). The bulrush 'flower' is formed when the male flowers fall off⁷¹.

Medicinal uses of the rhizomes include prescription during pregnancy to ensure easy delivery, for venereal diseases, dysmenorrhoea, diarrhoea, dysentery and to enhance the

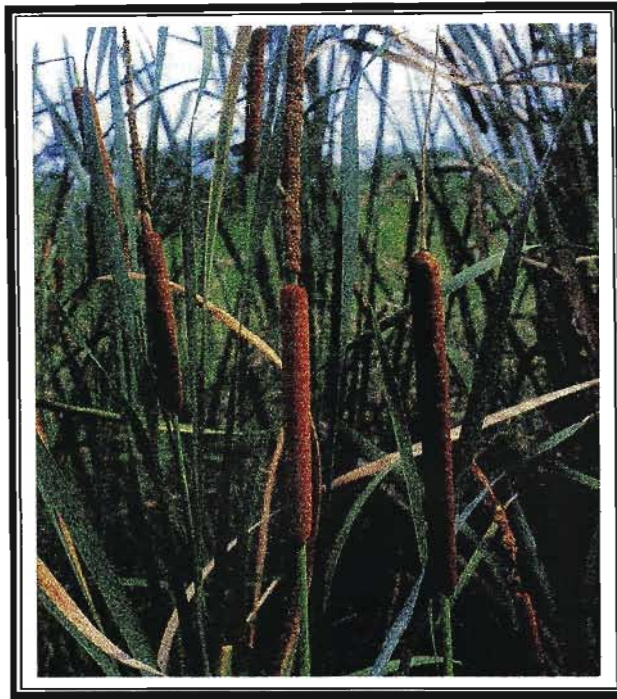


Fig. 5.2 Flowering and fruiting stalks of *T. capensis*

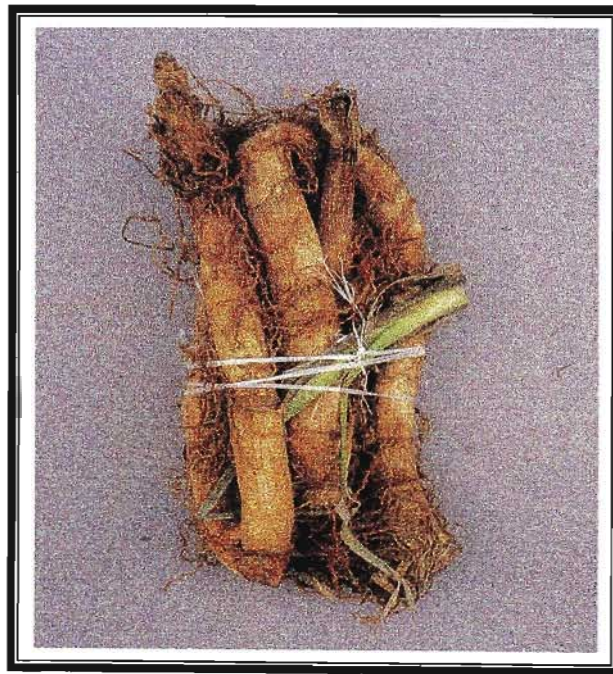


Fig. 5.3 Rhizomes as they are sold for medicinal use

male potency and libido. Other uses include treatment of genital problems, promotion of fertility in women and to improve blood circulation. Its use in childbirth stems from the claim that it strengthens uterine contractions and promotes expulsion of the placenta^{72, 73}. The patient is prescribed one or two cups of a decoction of the roots in boiling water, which is taken daily for a week⁷⁴.

The phytochemistry of several species of *Typha* have been documented⁷⁵. Several flavones and other phenolic compounds, long chain hydrocarbons as well as various triterpenoids with a steroidal skeleton e.g. typhasterol (fig 5.4) have been isolated⁷⁶.

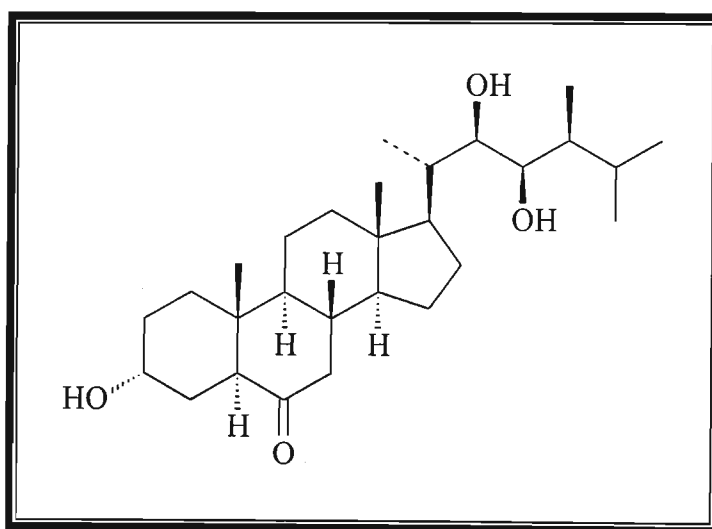


Fig. 5.4 Typhasterol

The plant is classified⁷¹ as:

Family: Typhaceae

Genus: *Typha*

Species: *capensis*

No triterpenoid like steroids were detected in the present study, however, the hexane extract has revealed two new phenolic compounds, namely, i) typharin [47] and ii) typhaphthalide [48], including iii) β -sitosterol [49].

The acetone extract has also produced several known flavan-3-ols, which were isolated as mixtures in their free phenolic form; these include, i) afzelechin [10], ii) epiafzelechin [23], iii) (+)-catechin [11], and iv) (-)-epicatechin [4].

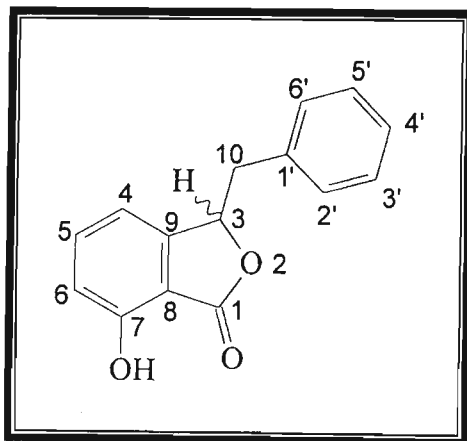
All the above compounds except [47] and [48] have been previously isolated from other plant species.

5.2 BIBENZYLs AND β -SITOSTEROL

5.2.1 7-Hydroxy-3-benzylphthalide [48]

[Typhaphthalide 48]

Compound [48] was isolated as fine, white crystals as described in section 8.2.1.1.



[48]

The ^1H NMR [plate H-11] and ^{13}C NMR [plate C-8] revealed the following properties of compound [48];

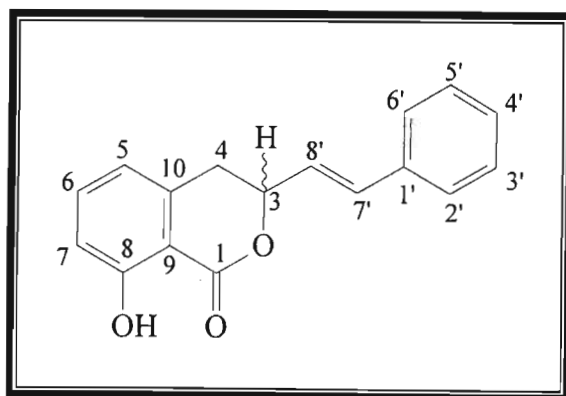
- The compound had two aromatic rings,
- A carbonyl functionality, confirmed from the IR [plate I-2] and NMR data.
- A hydroxyl group; confirmed by deuterium exchange,
- A CH_2 group attached to an aromatic ring (from mass spectrum and NMR data)

The complete structural analysis is discussed in section 5.3.

5.2.2 8-Hydroxy-3-[2-(phenyl)ethenyl]dihydroisocoumarin [47]

[Typharin 47]

Typharin [47] was isolated as a non-crystalline, yellow compound as described in section 8.2.1.2



[47]

The aromatic nature of [47] was determined from the ^1H NMR [plate H-12] which showed signals in the region from 6.0 to 7.5 ppm. The ^1H NMR spectrum also displayed olefinic signals between 4 and 6 ppm and from the coupling constants, a *trans* orientation was deduced. The ^{13}C NMR revealed the presence of a carbonyl functionality and a hydroxyl group. The presence of the hydroxyl group was established by deuterium

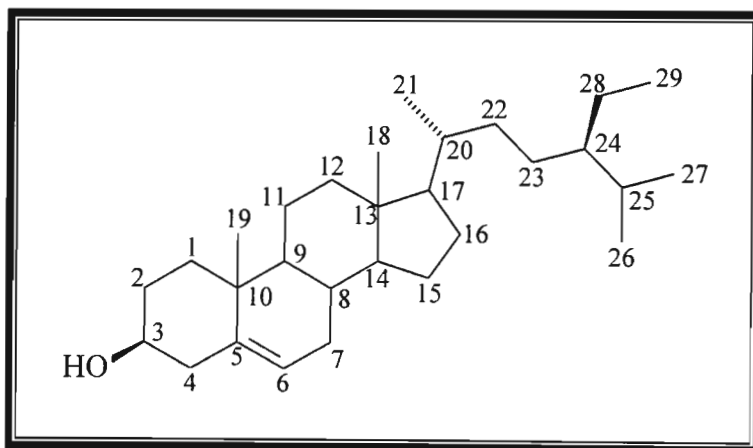
exchange experiments. The detailed analytical discussion of the structural elucidation is given in section 5.4.

5.2.3 24 α -Ethylcholest-5-en-3 β -ol [49]

β -sitosterol [49]

β -sitosterol [49], as discussed in section 8.2.1.3, was isolated as opaque, needle-like crystals from the roots of *T. capensis*.

Like stigmasterol, the spectral data of β -sitosterol is well recognized and the ^1H NMR [plate H-13] displays characteristic peaks, which easily distinguishes β -sitosterol from stigmasterol. The compound was verified from TLC results and NMR data of an authentic sample. No further investigations or analyses of [49] were pursued.



[49]

5.3 STRUCTURE ELUCIDATION OF [47]

5.3.1 The aromatic fragments

The ^1H NMR of [47] showed a multitude of signals between 6 and 7.5 ppm, which integrated for 10 protons, assuming the smallest integral to be one. The multiplet between 7.2 and 7.5 ppm is characteristic of a mono-substituted ring. This provided a good point for structure modelling and was designated fragment A.

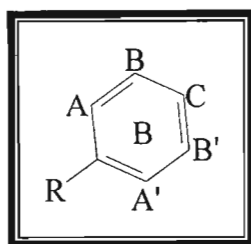


Fig.5.5 Fragment A

Further evidence came from the ^{13}C NMR [plate C-9], which showed magnetically equivalent carbons at 128.73 and 126.79 ppm, which showed a 2:1 integration with the other methine carbons. A peak at 128.53 ppm that integrated for one carbon, was shown from the ADEPT [plate AD-2] analysis to be a methine group. The HETCOR [plate HE-2] and COSY [plate CO-2] plots showed a direct correlation of this proton with the ones previously mentioned. Hence, it was deduced that these five protons formed an AA'BB'C system as shown in fragment A. However, the signals between 7.2 and 7.5 ppm integrated for six protons. Since five of these were accommodated for in fragment A, it was deduced that the sixth proton was from another aromatic system.

Inspection of the HH-COSY revealed a single proton (7.42 ppm) coupling to two other protons at 6.90 (d, $J = 8.4\text{Hz}$) and 6.72 ppm (d, $J = 8.1\text{Hz}$). The lone proton at 7.42 ppm was considered a fused doublet of doublets ($J = 8.0$ and 8.1 Hz). Two further protons at 6.78 and 6.30 ppm were discounted as being aromatic by virtue of their coupling constants and also because they showed no direct correlation to the latter mentioned

aromatic protons. From these results and in the absence of any further aromatic groups, it was concluded that the second aromatic system was tri-substituted and designated fragment B.

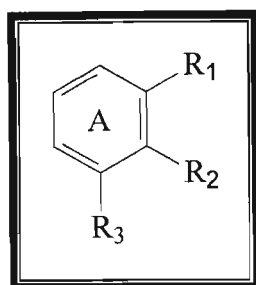


Fig.5.6 Fragment B

5.3.2 The aliphatic fragments

The two protons at 6.78 and 6.30 ppm had a coupling constant of 16Hz and by virtue of their position were considered olefinic with a *trans* orientation. The proton at 6.30 ppm also showed strong coupling to another methine proton at 5.23 ppm. This explained why it was split into a doublet of doublets. Further analysis of the HH-COSY showed that this proton was also coupled to a methylene group found at 3.12 ppm with a somewhat strange splitting pattern, a doublet and a singlet. Fragment C (fig. 5.7) was arrived at from this coupling pattern.

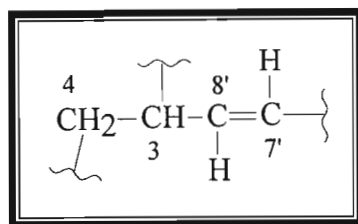


Fig.5.7 Fragment C

At first glance, H-3 was considered as olefinic, but, this notion was negated due to it resonating at 5.23 ppm which is too upfield for an olefinic proton. The splitting pattern of this proton on expansion (fig. 5.8) showed that it was actually a multiplet although the spectrum shows the resonance as a quartet. The NOESY [plate NO-2] shows long range coupling with H-7' (see fig. 5.14, p.73) which would account for the splitting. Due to the splitting pattern of H-4a and H-4b which did not show distinct geminal protons, an AA' system was assumed rather than an AB system. Since H-3 was not olefinic, its downfield position could be explained by it being connected to a heteroatom or a carbonyl group. Inspection of the ^{13}C NMR revealed a carbonyl group at 169.49 ppm, confirmed from the IR spectrum [plate I-3], which showed a strong carbonyl stretching at 1689.6 cm^{-1} . However a methine group attached to a carbonyl group resonates at higher field than that shown⁷⁷. If the carbon was attached directly to a nitrogen, the range is 60-70 ppm⁷⁷, however, if it was attached directly to an oxygen atom then a shift of 82 ppm was possible⁷⁷. Hence, fragment C was modified to yield fragment D (fig. 5.9).

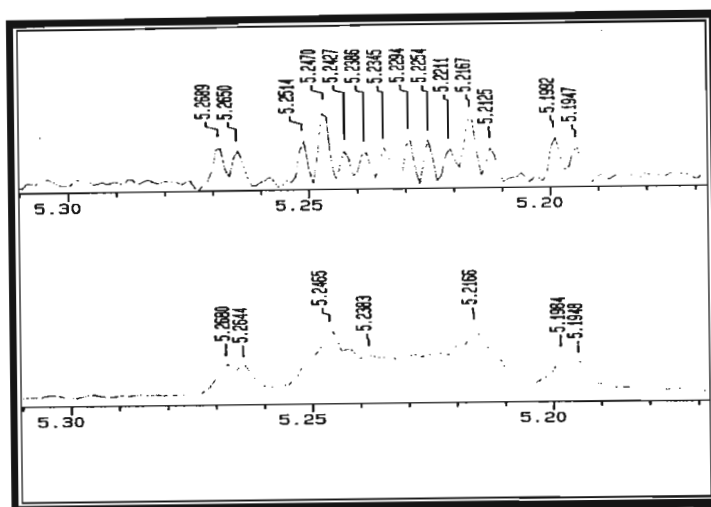


Fig. 5.8 Expansion of H-3 quartet

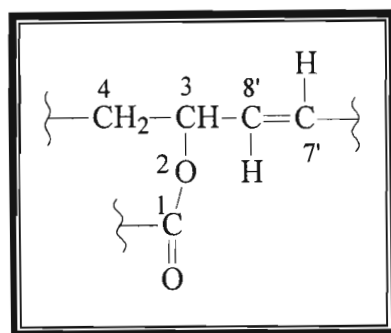


Fig.5.9 Fragment D

5.3.3 Construction of compound

A sharp singlet at 10.97 ppm represented an OH functionality due to its suppression by deuterium exchange. A signal at 162.26 ppm in the ^{13}C NMR was indicative of a phenolic carbon. This had to be found on fragment B as shown in fragment E (fig. 5.10). At this stage, all atoms were accounted for.

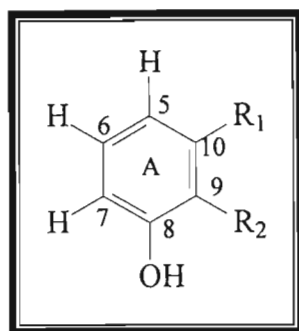


Fig.5.10 Fragment E

The connectivity of the methylene carbon (C-4) was determined by its relative downfield shift and confirmed by the NOESY, which showed long range coupling between H-4 and H-5 (see frag. F). Since no coupling was seen between H-4 and the OH group the substitution seen in fragment E was assumed correct. This result led to the conclusion that the carbonyl group had to be connected to the ring in the absence of any further carbons giving fragment F (fig. 5.11).

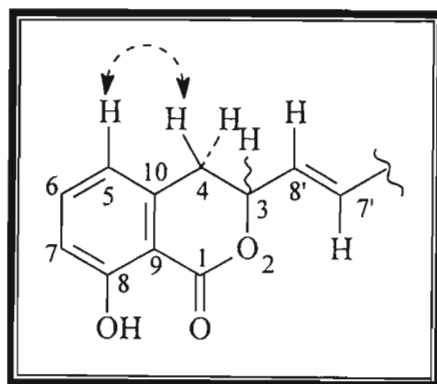


Fig.5.11 Fragment F

The connectivity of H-7' and H-8' to fragment A (see fig. 5.12, fragment G) was evident from the NOESY (long range coupling of H-2' and H-7', see fig. 5.14). Comparison of the ^{13}C NMR data with that of (*E*)-propenylbenzene (fig. 5.13, Table 5.1) gives further evidence for this argument.

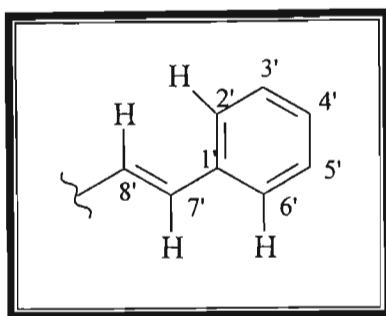


Fig. 5.12 Fragment G

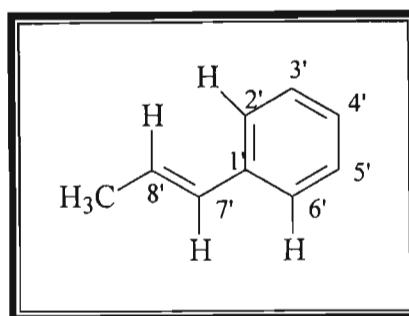
Fig. 5.13 (*E*)-propenylbenzene

Table 5.1 Comparative ^{13}C NMR (ppm) data of (*E*)-propenylbenzene and Fragment G

Carbon No.	(<i>E</i>)-propenylbenzene	Fragment G
1'	138.0	138.89
2'	126.8	126.79
3'	128.5	128.73
4'	125.9	128.53
5'	128.5	128.73
6'	126.8	126.79
7'	131.2	133.96
8'	125.4	125.145

With all connectivities now deduced, the structure of [47] was derived, as shown.

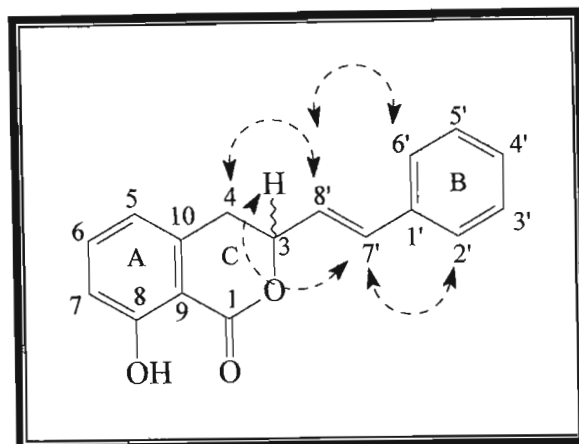


Fig. 5.14 [47] (----- = long range coupling)

The orientation of H-3 is yet to be determined. A 3-D model based on bond angles and bond lengths is shown in fig. 5.15.

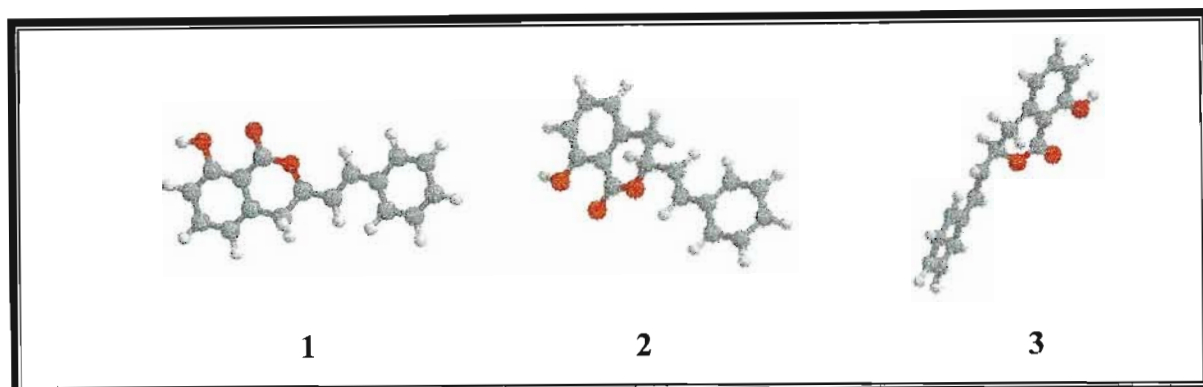
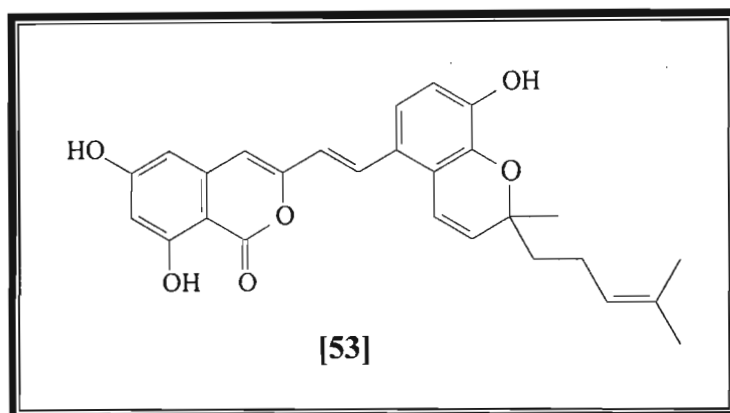
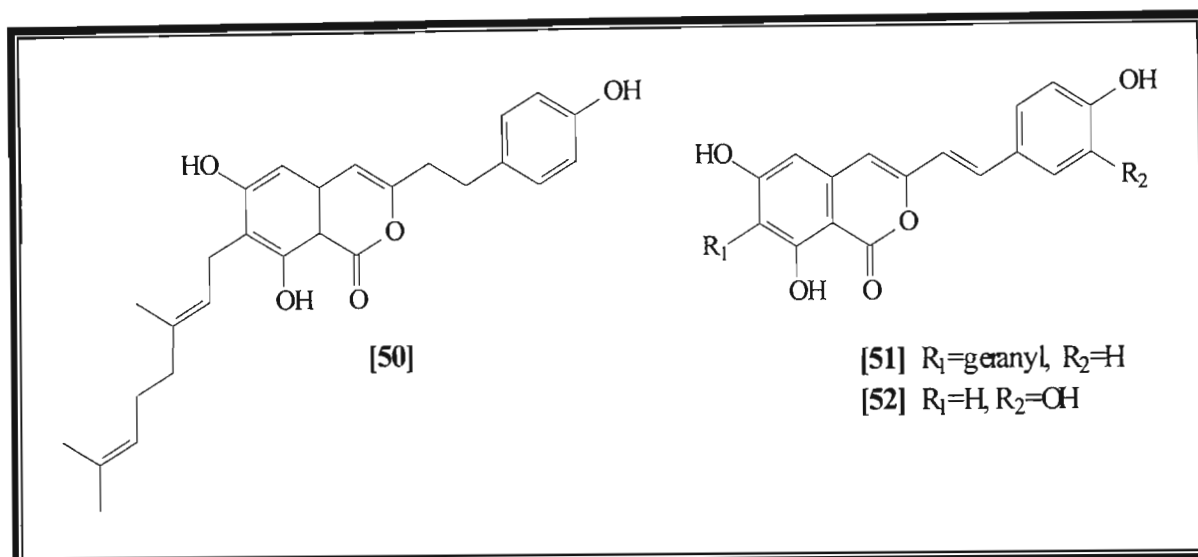


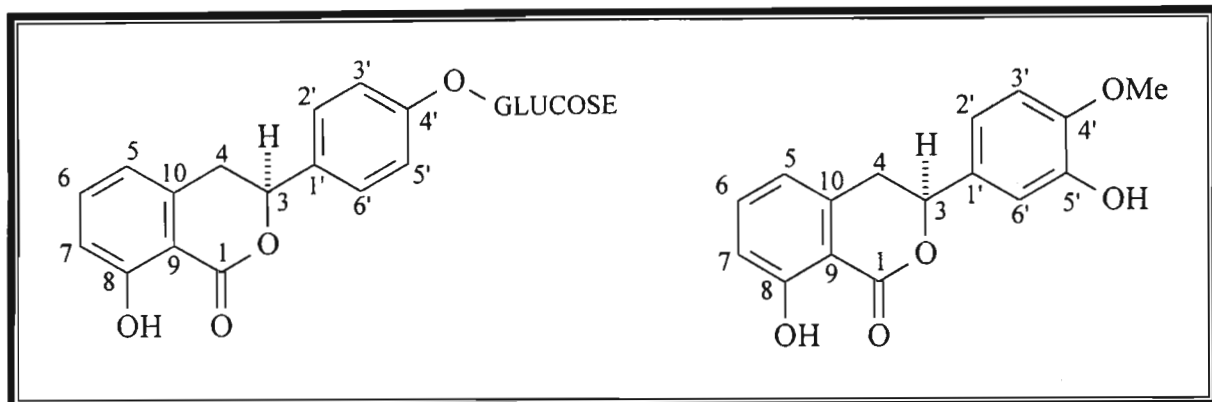
Fig. 5.15 3-D structures of [47]

5.3.4 Literature survey

A survey of the phytochemical literature revealed several compounds with a closely related structure. Mizuno *et al*⁷⁸ isolated several isocoumarins from *Achlys triphylla* which were called achlisocoumarin-I [50], -II [51], -III [52] and -IV [53].



Mizuno *et al*⁷⁸ declared that the skeleton was novel and according to the source used for the literature survey, no further compounds with the same skeleton have been identified. Thus, [47] is believed to be a new compound according to the references sourced⁷⁵. Due to the different substituents and substitution pattern of compounds [50] to [53], few similarities were seen in the chemical shifts between them and [47]. Two further compounds were sourced to verify the connectivities of rings A and C; namely, hydrangenol 4'-O-glucoside [57]⁷⁹ and phyllodulcin [58]⁸⁰.



[57]

[58]

Table 5.2 shows ^{13}C NMR data (ppm) of selected carbons of [57] and [47] and Table 5.3 shows comparative ^1H NMR data (ppm) of [47] and [58].

Table 5.2 ^{13}C NMR data (ppm) of [47] and [57] (selected carbons)

Carbon no.	[47]	[57]
1	169.49	169.3
3	79.65	80.2
4	33.48	33.6
5	118.05	118.5
6	136.32	136.5
7	116.46	115.6
8	162.26	161.0
9	109.31	108.5
10	138.89	140.6

Table 5.3 Comparative ¹H NMR data (ppm) of [47] and [58]

Proton no.	[47]	[58]
3	5.23 (q, J= 6.2, 14.3 Hz)	5.56 (q, J= 5, 11 Hz)
4	3.12 (m)	3.13 (m)
8-OH (phenolic)	10.97	10.48

5.4 STRUCTURE DETERMINATION OF [48]

5.4.1 Preliminary data

A constituent of the hexane extract of *T. capensis*, [48] showed a somewhat low melting point (70°-75°C), and supported a molecular formula of C₁₅H₁₂O₃ (m/z 240.0786). Oxygenation suggested hydroxyl and/or carbonyl functionalities. This contention was supported by the IR spectrum [plate I-2] of [48] which showed a characteristic carbonyl stretching at 1713 cm⁻¹ while bands at 3436 and 3543cm⁻¹ could be attributed to a phenyl moiety's O-H stretching vibration. Further evidence was given by the ¹³C NMR data (plate C-8), which showed signals at 171.93 and 156.49 ppm, indicative of a carbonyl group and a hydroxyl group, respectively.

The aromatic nature of the compound was deduced from NMR data. The ¹H NMR (plate H-11) revealed approximately eight protons (integral) in the region between 6.5 to 7.5 ppm, indicative of aromatic protons. The ¹³C NMR data also showed signals in the aromatic region (see table A4). From the number of protons and the double bond equivalence calculations two rings were suspected.

A low field methine signal (82.59 ppm) was believed to be connected to a heteroatom, in this case, oxygen. This would account for the third oxygen atom considering the presence of one hydroxyl and one carbonyl group. Finally, from the HH COSY (long range coupling, plate CO-1) a methylene at 40.69 ppm was shown to be attached to an

unsubstituted aromatic ring as well as the fact that the mass spectrum showed a fragment with a mass of 91.055, which indicated a molecular formula of C_7H_7 . The base peak at m/z 149.024 is the difference obtained between the molecular mass of [48] and the C_7H_7 fragment. The next step involved the connectivities of the atoms.

5.4.2 The aromatic fragments

Fragment A (fig. 5.16) was known from the mass spectral data and NMR data. Hence, the substitution pattern of the second ring system needed to be determined. With the knowledge that the system was phenolic, an inspection of the HH-COSY showed a triplet ($J=8.0$ and 7.6 Hz) coupled directly to two doublets ($J=8.0$ and 7.2 Hz). Thus, fragment B was deduced (fig. 5.16)

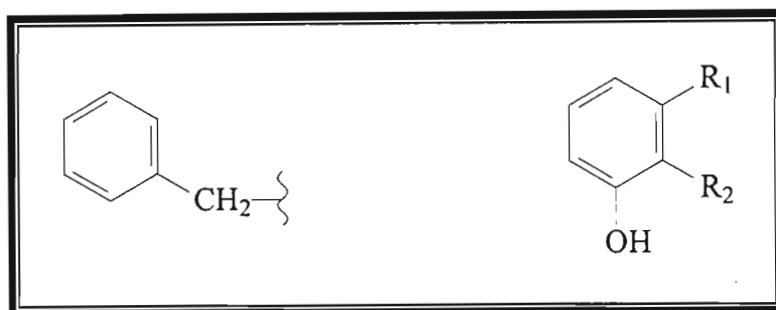


Fig. 5.16

Fragment A

Fragment B

5.4.3 The aliphatic fragment

An AB system due to geminal protons was seen as two doublet of doublets at 3.14 ppm ($J=6.2$ and 14.1 Hz) and 3.25 ppm ($J=6.7$ and 14.1 Hz). These protons showed direct coupling to a deshielded methine proton at 5.68 ppm (t, $J=6.5$ and 6.3 Hz). From the preliminary study it was known that the carbon was directly bonded to oxygen. The carbonyl stretching for cyclic ketones in the IR spectrum would be expected between 1740 - 1780cm^{-1} . Since the observed stretching vibration was lower, a lactone was suspected. Asakawa *et al*⁸¹ showed that for phthalides, the IR absorption bands of a non-

OH bonded CO is found between $1754\text{--}1764\text{ cm}^{-1}$, while OH bonded CO is found between $1734\text{--}1738\text{ cm}^{-1}$. Thus, although the signal was lower than expected the IR provided two clues, 1) the two oxygens formed a lactone ring and 2) the OH showed hydrogen bonding with the carbonyl group. This led to fragment B being modified to give fragment C (fig. 5.17).

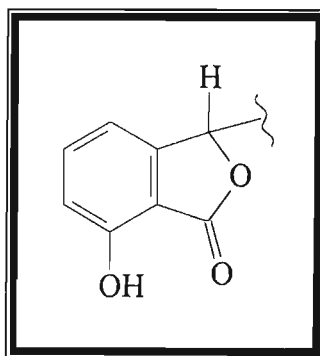
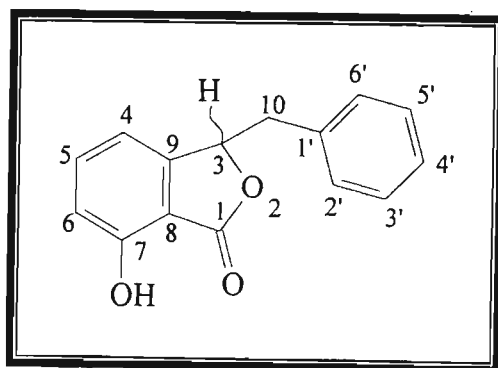


Fig. 5.17 Fragment C

The fragment was supported by the mass spectral data, which showed a peak for m/z 149 (100%).

5.4.4 Construction of [48]

Knowing the connectivities of the methylene and methine groups, fragments A and C were combined to give [48].



[48]

Like [47] the stereochemistry at the epimeric carbon (C-3) is uncertain. The most probable stereochemical arrangement is given in the 3-D structures below (fig. 5.18).

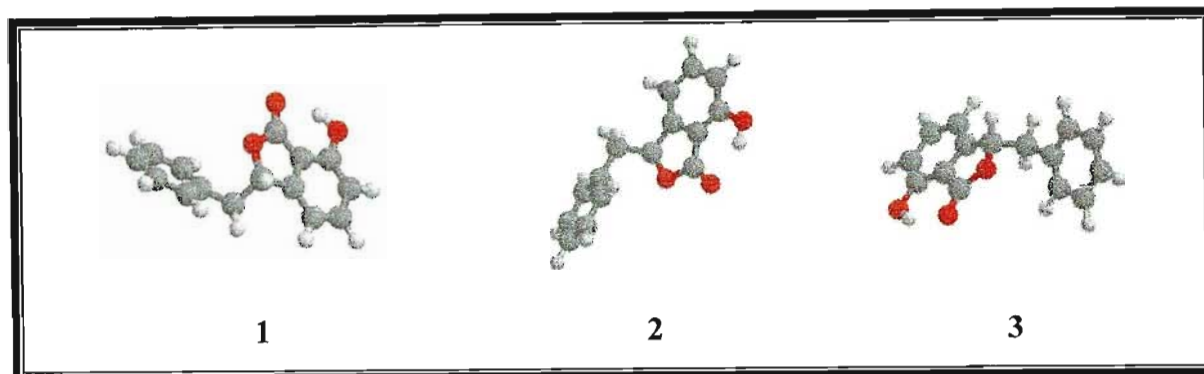
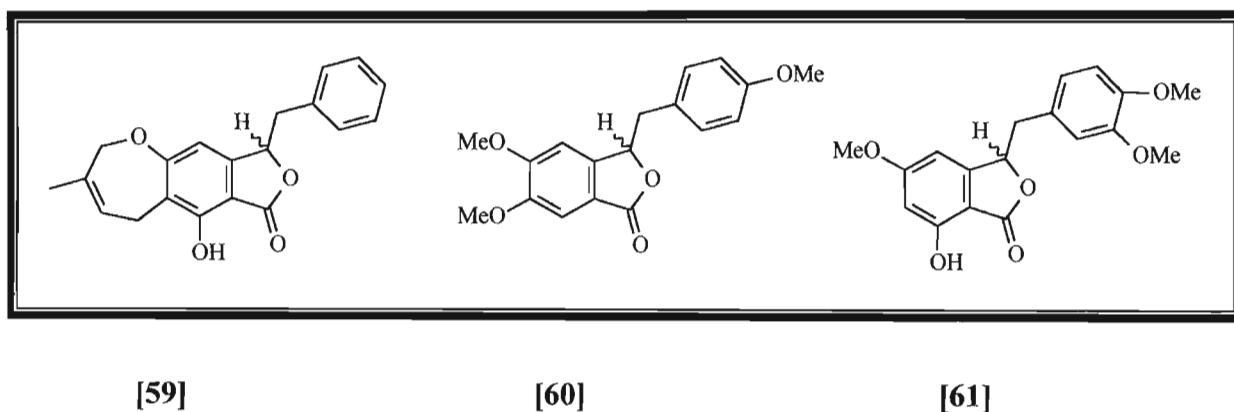


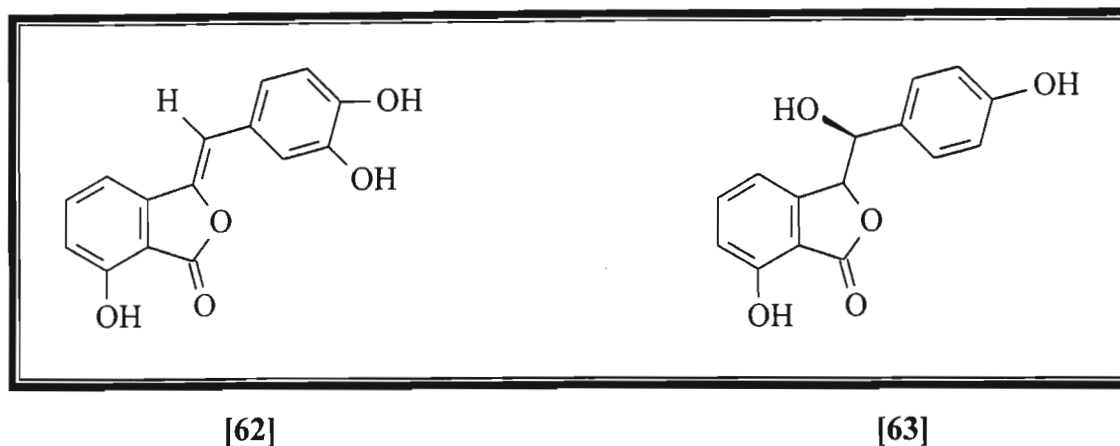
Fig. 5.18 3-D structures of [48]

5.4.5 Literature Survey

Several compounds with a similar skeleton as [48] were found in literature. Asakawa *et al*⁸¹, isolated a novel compound from *Radula complanata* called redulanolide [59]. From *Frullania falciloba*⁸² they isolated [60] and, compound [61] from *Balantiopsis rosea*⁸³.



Yoshikawa *et al*⁸⁴ showed the presence of thunberginol F [62] and hydramacrophyllol A [63] in *Hydrangea dulcis folium*.



A comparison of the NMR data of selected atoms of [60], [61] and [48] is given in Table 5.4.

Table 5.4 NMR data of selected atoms of [60], [61] and [48]

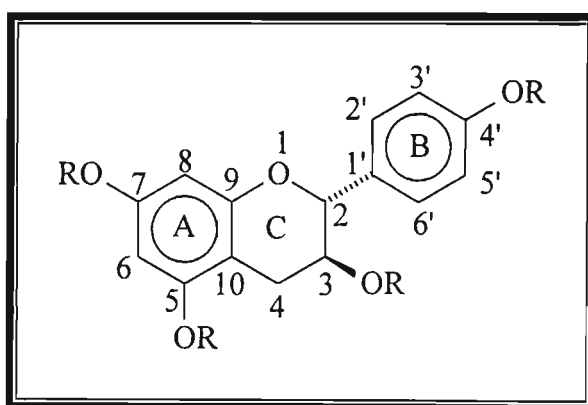
No.	[60]		[61]		[48]	
	¹ H NMR	¹³ C	¹ H	¹³ C	¹ H	¹³ C
1		174.4		168.2		171.93
3	5.59 (t, 6.2)	82.3	5.35 (t, 6.2)	80.1	5,68 (t, 6.4)	82.59
10a	3.09 (dd, 13.7, 6.2)	40.2	2.97 (dd, 14.3, 6.2)	40.0	3.14 (dd, 14.1, 6.2)	40.69
10b	3.20 (dd, 13.7, 6.2)		3.04 (dd, 14.3, 6.2)		3.26 (dd, 14.1, 6.7)	

5.5 FLAVAN-3-OLS

5.5.1 (2R,3S)-2,3-trans-Flavan-3,4',5,7-tetraacetate [54]

[Afzelechin tetraacetate 54]¹⁷

Afzelechin tetraacetate was obtained as an amorphous solid as described in sections 8.2.2.1 and 8.2.2.2. In the free phenolic form, afzelechin [10] was isolated as a mixture with epiafzelechin [23].



[10] R= H

[54] R= Ac

Ring A

H-6 and H-8 were seen as meta-coupled doublets at 6.56 and 6.64 ppm respectively ($J=2,1$ Hz) in the ^1H NMR of the acetate derivative [plate H-16].

Ring B

A doublet for H-2',6' ($J=8.4$ Hz) was seen at 7.33 ppm while the H-3',5' doublet ($J=8.7$ Hz) resonated at 7.07 ppm. This AA'BB' system was concluded from the integration of the ^1H NMR.

Ring C

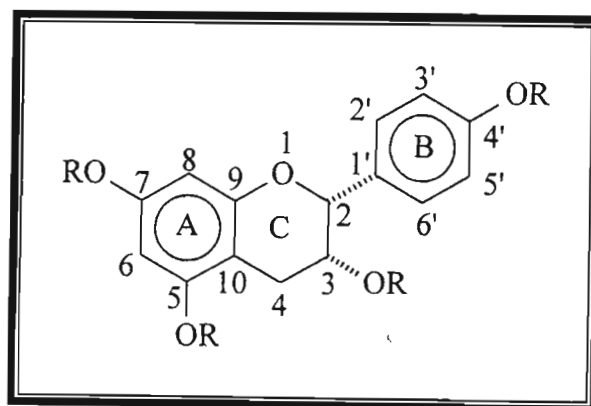
A one-proton doublet at 5.15 ppm ($J=6.0$ Hz) and a one-proton multiplet at 5.26 ppm indicated the *trans*-orientated H-2 and H-3 respectively. H-4_{ax} and H-4_{eq} were seen as doublet of doublets for each at 2.64 ppm ($J=6.0$ and 16.9 Hz) and 2.81 ppm ($J=5.1$ and 16.8 Hz) respectively.

On consideration of the above allocations, the three acetate singlets (2.25, 2.26, 2.27 and 1.96 ppm) were attributed to 5-OAc, 7-OAc, 4'-OAc and 3-OAc.

5.5.2 (2R,3R)-2,3-cis-Flavan-3,4',5,7-tetraacetate [55]

[Epiafzelechin tetraacetate 55]¹⁷

The acetylated derivative of epiafzelechin [23] was obtained as a light brown, non-crystalline solid from the isomeric mixture of afzelechin [10] and epiafzelechin [23] as described in sections 8.2.2.1 and 8.2.2.3. Epiafzelechin [23] was isolated as a mixture with [10].



[23] R= H

[55] R= Ac

A-ring

The H-6 and H-8 doublets were found at 6.55 ppm ($J=2.1$ Hz) and 6.65 ppm ($J=2.4$ Hz) respectively; a downfield shift for H-8 and an upfield shift for H-6 as compared to H-8 and H-6 of afzelechin tetraacetate.

B-ring

An AA'BB' system (7.43 ppm, d, $J=8.4$ Hz, H-2',6') and (7.10 ppm, d, $J=8.7$ Hz, H-3',5') defined the B-ring substitution pattern.

C-ring

H-2, unlike H-2 of afzelechin, resonated as a broad singlet at 5.10 ppm whilst the H-3 multiplet showed a downfield shift to 5.37 ppm indicating the *cis*-configuration of the two protons. The H-4 protons also displayed downfield shifts in comparison to afzelechin, with the H-4ax doublet of doublets at 2.84 ppm ($J=2.0$ and 18.0 Hz) and the H-4eq signal at 2.97 ppm ($J=4.5$ and 18.0 Hz). The acetate groups of rings A and B showed resonances at 2.26 (s), 2.28 (s) and 2.29 (s) ppm, while the three-proton aliphatic singlet was found at 1.89 ppm.

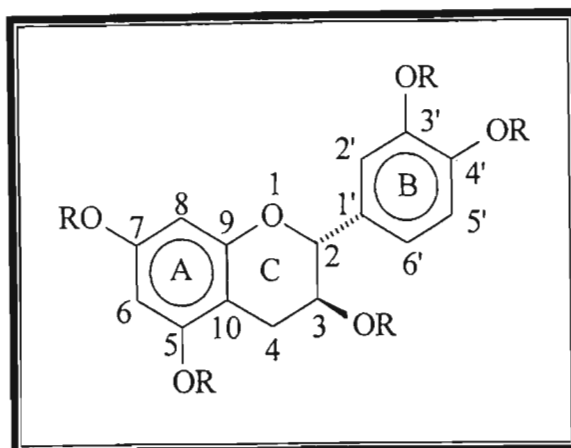
5.5.3 (2R,3S)-2,3-trans-Flavan-3,3',4',5,7-pentaacetate [56]

[Catechin pentaacetate 56]

The isolation of catechin pentaacetate [56] is described in sections 8.2.2.4 and 8.2.2.5.

Ring-A

The meta-coupled doublets of ring-A representing H-6 and H-8 were found at 6.57 ppm ($J=2.1$ Hz) and 6.63 ppm ($J=2.1$ Hz) respectively.



[11] R= H

[56] R= Ac

Ring-B

An ABX system defined the B-ring with H-2', H-5' and H-6' represented by signals at 7.22, 7.18 and 7.15 ppm respectively.

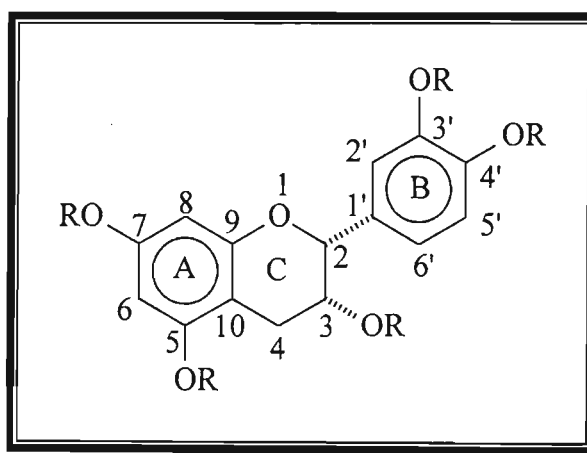
Ring-C

The aliphatic C-ring was defined by an ABMX system with a doublet ($J=6.3$ Hz) at 5.12 ppm and a multiplet at 5.23 ppm being attributed to H-2 and H-3 respectively. The splitting pattern was reminiscent of a trans-configuration. H-4_{ax} and H-4_{eq} were seen at 2.608 ppm (dd, $J=6.6$ and 16.8 Hz) and 2.84 ppm (dd, $J=5.1$ and 16.8 Hz) respectively.

The signals between 2.25 and 2.26 ppm integrated for four methyl groups, which were attributed to the four aromatic acetate groups while the signal at 1.98 ppm was indicative of an aliphatic acetate group.

5.5.4 (2R,3R)-2,3-cis-Flavan-3,3',4',5,7-pentaacetate [46][Epicatechin pentaacetate 46]

Epicatechin pentaacetate [46] was obtained by acetylation and subsequent PLC separation of the same fraction that afforded catechin pentaacetate [56] as described in sections 8.2.2.4 and 8.2.2.6. Epicatechin [4] was isolated as a mixture with catechin [11].



[4] R= H

[46] R= Ac

A-ring

The substitution pattern continues in [46] with H-6 and H-8 resonating at 6.55 and 6.65 ppm respectively (d, J=1.8 Hz) [plate H-7].

B-ring

The ^1H NMR exhibited an ABX system for ring-B with H-2' at 7.33 ppm. H-6' and H-5' were seen as doublets at 7.26 and 7.17 ppm respectively.

C-ring

A broad singlet at 5.09 ppm attributed to H-2 and a one-proton multiplet at 5.36 ppm attributed to H-3 defined a 2,3-*cis* relative configuration. A doublet of doublets at 2.96 ppm ($J=4.5$ and 17 Hz) and another at 2.74 ppm ($J=1.5$ and 17 Hz) attributed to H-4_{eq} and H-4_{ax} respectively completed definition of an ABMX pattern.

5.6 SPRAY COLOURS

On spraying (standard experimental section 6.1.5) of the TLC plates with the anisaldehyde reagent, the flavan-3-ols displayed a brown to reddish-brown colour, and the dihydroisocoumarin a colour light purple to grey. Typhaphthalide [48] was unreactive to anisaldehyde spray reagent but showed a brown colour with Dragendorff reagent.

5.7 BIOLOGICAL ACTIVITY⁸⁵

5.7.1 Antibacterial activity

The crude methanolic extract of *T. capensis* showed inhibition of growth of some of the bacteria, which are believed to be pathogenically responsible for the conditions, which this plant is used to treat. The micro-organisms against which the extract was found to be active include;

Staphylococcus aureus

Enterobacter aerogenes

Klebsiella pneumonia

Citobacter freundii

5.7.2 Antifungal activity

No anti-fungal activity was displayed by the extract. This confirms observations of fungal growth on an aqueous preparation of the crude extract when left at room temperature for seven days in an open vessel.

5.7.3 Cytotoxic activity

The results of cytotoxic testing shows that the extract had negligible activity. Since the plant is used as an aid during child birth, the results are appropriate in light of this.

5.7.4 Uterotonic activity

A consistent finding was that in the presence of the plant extract, irrespective of concentration and of the concentration of acetylcholine, the muscle did not recover to resting length, that is, the muscle remained in a partially contracted state. It was therefore apparent that application of the extract on its own is not a smooth muscle stimulant, but that it augments the action of a stimulant such as acetylcholine. The result of this test is in agreement with the claim that the plant root strengthens uterine contractions in woman.

PART C

EXPERIMENTAL

CHAPTER SIX

STANDARD EXPERIMENTAL PROCEDURE

6.1 CHROMATOGRAPHIC METHODS

6.1.1 Column Chromatography

Various sizes of glass columns were used, with variable dimensions.

- a) 30mm x 1000mm
- b) 20mm x 500mm
- c) standard 50 ml burette
- d) pasteur pipette 150 mm

6.1.1.1 Silica gel as absorbent

Depending on whether the column was of the open , flash or pipette type, different mesh sizes of silica were used. Merck Kieselgel (Art. 7734, 170-230 mesh) was used for the open column, which was packed by adding a slurry to the column. The slurry was prepared by using the same solvent as used for the eluent. The solvent was run through the column several times to ensure a tight packing as well as to remove any air bubbles. The ratio of material to be separated to silica gel was in the ratio 1 : 30. Fractions were collected in test tubes of different sizes.

6.1.1.2 Flash column

The silica was prepared and packed as described above except that Merck Kieselgel (Art. 7773.333) was used as the stationery phase. The column was then flushed with eluting solvent under applied pressure. Fig. 6.1 shows the flash set up. Samples were applied as for the open column. The separation was carried out under pressure at an elution rate

dependent on column and fraction size. Compressed air proved satisfactory for this purpose; ideally, nitrogen should be used, however it is expensive.

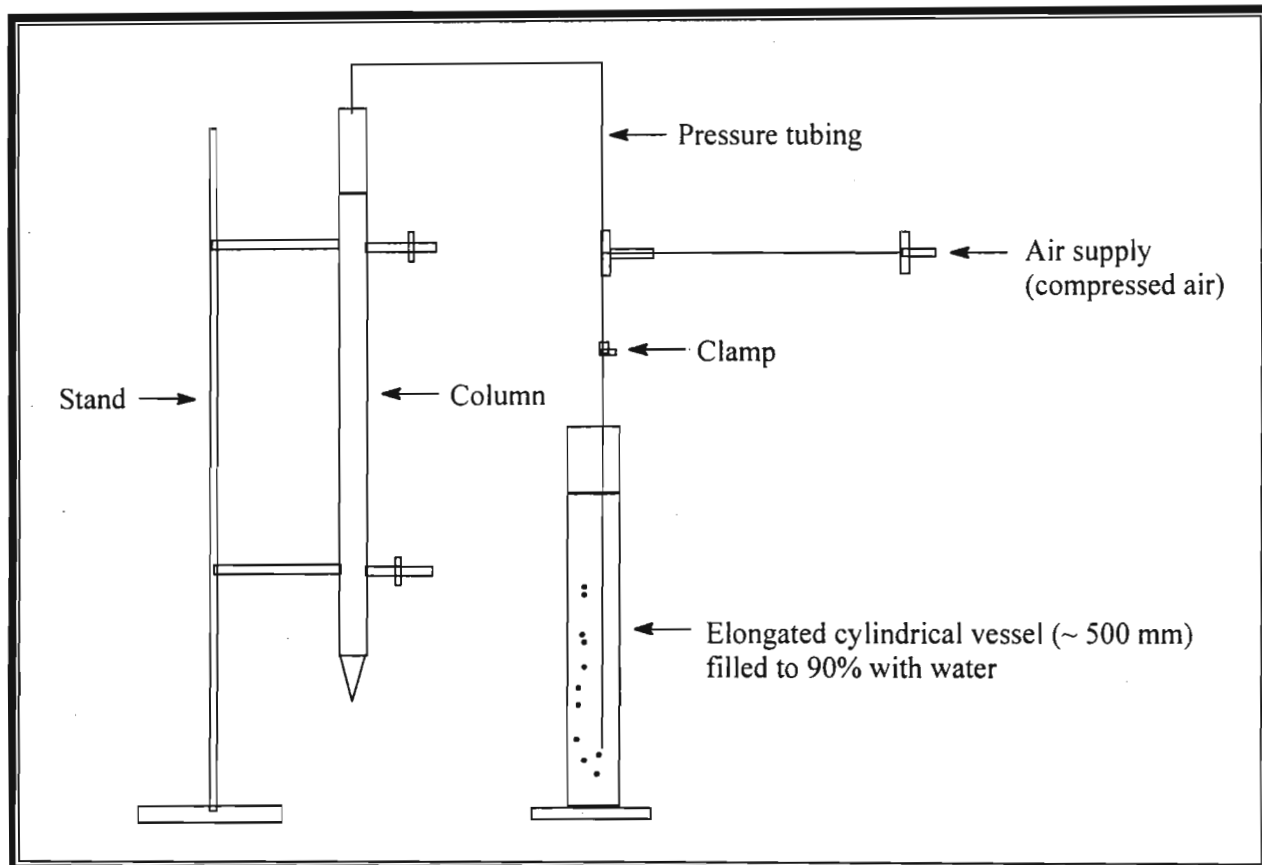


Fig. 6.1 Set-up for flash column chromatography⁸⁶

6.1.2 Thin Layer Chromatography (TLC)

Commercially obtained TLC plates were used for isolation (Merck Art. 5554). Between 5 and 10 mg of sample was applied. After development in an appropriate solvent system, the plates were air dried and viewed under UV light. The relevant bands were then marked and scraped off. The silica was extracted thereafter with an appropriate solvent. The sample was finally isolated by removing the solvent under vacuum.

6.1.3 Preparative Layer Chromatography (PLC)

PLC plates were prepared by using Merck Kieselgel (Art 7747) on 200mm x 200mm glass plates. The slurry was made by adding 450ml of water to 200g of silica. The slurry was swirled for approximately 20min and thereafter uniformly spread over the plates using a spreader. Plates of 1,5mm and 2mm thickness were prepared. The plates were air dried in a draft free environment for 24 hours and then activated at 120° C for one hour. Sample sizes varied from 10mg to 25mg per plate. Compounds of interest were isolated and recovered as for TLC above.

6.1.4 Pasteur Pipettes

Silica used for PLC was also packed into pasteur pipettes for final purification. The silica was first added dry to a height of about 60%. This was then removed and mixed with the eluting solvent into a slurry. A cotton wool plug was placed at the tapered end of the pipette and a little purified sand was added. The slurry was then loaded using another pasteur pipette. Elution of the mobile phases was carried out under gravity. Sample sizes varied from 10 to 40mg. Fraction sizes were approximately 1ml.

6.1.5 Spray reagents

6.1.5.1 Anisaldehyde / H₂SO₄

Chromatograms were sprayed lightly with the above, mixed as follows:

para-anisaldehyde 5%	}	Solution A
absolute ethanol or methanol 45%		

H ₂ SO ₄ 5%	}	Solution B
absolute ethanol or methanol 45%		

Solutions **A** and **B** were mixed in the ratio 1:1. After spraying, the plates were heated at 120° C until maximum colour was developed. It was observed that H₂SO₄ that contained abnormally high concentration of SO₂ caused the spray reagent to become discolored in a short period of time. Fresh concentrated H₂SO₄ proved very satisfactory maintaining the colourless status of the solution. Solutions **A** and **B** were kept in the freezer. Once mixed, in small aliquots, the solution could be kept in the refrigerator until desired.

6.1.5.2 Dragendorff reagent

This solution was prepared as follows:

17 g bismuth subnitrate and 200 g tartaric acid in 800 ml water: Solution **A**

160 g potassium iodide in 400 ml water: Solution **B**

A + **B** = stock solution (1:1)

Spray reagent : 50 ml stock solution + 500 ml water + 100 g tartaric acid

The chromatograms were sprayed lightly with the reagent, and spots evaluated in visible light. The spots appeared orange/brown against a light yellow background.

6.2 SPECTROSCOPIC METHODS

6.2.1 Nuclear magnetic resonance spectroscopy

¹H NMR spectra were recorded on a Varian 300 (300 MHz). ¹³C NMR spectra were recorded at 75 MHz. All spectra were recorded at room temperature. Chemical shifts are given on the delta (δ) scale and coupling constants (J) in hertz (Hz).

6.2.2 Mass spectrometry

High resolution mass spectra were recorded on a Kratos 9/50 HRMS instrument by Dr. P. Boshoff at Cape Technikon. Low resolution spectra were recorded on MAT Finnigin GCQ spectrometer.

6.2.3 Infrared Spectroscopy

A Nicolet Impact 420 spectrophotometer was used to record FTIR spectra in KBr.

6.2.4 Optical Rotation

Optical rotation was measured at ambient temperature in chloroform using an Optical Activity AA-5 Polarimeter together with a Series A-2 stainless steel (4x200mm) unjacketed flow tube. Concentration was quoted in g/100ml.

6.3 CHEMICAL METHODS

6.3.1 Preparation of acetate derivatives⁸⁷

The sample or dried extract was dissolved in a minimum of pyridine and an excess of acetic anhydride was added. The solution was then heated at 70°C for 8 hrs and the acetate derivative isolated by addition of crushed ice to the mixture. The precipitate was filtered and washed free of excess pyridine and acetic anhydride, with ice water.

CHAPTER SEVEN

ISOLATION OF EXTRACTIVES FROM *ACRIDOCARPUS NATALITIUS*

The roots were kindly supplied by Dr. Neil Crouch of the Natal Herbarium, Durban (Voucher No., Crouch 810, NH). They were collected from Nagome Forest, KwaZulu-Natal.

7.1 EXTRACTION OF ROOTS

The root was composed of a soft, corky outer covering with a woody inner core. The soft covering was removed and each part was treated separately. Both the inner and outer parts of the roots were air dried to give the following masses:

Outer root (500g) [A]

Inner root (300g) [B]

After drying, both **A** and **B** were extracted with hexane for 72 hours. The solvent was recovered under vacuum to yield a waxy residue; 2g for **A** and 1g for **B**. TLC analysis showed that both **A** and **B** had very similar fingerprints except that the major compounds were more pronounced in **A** than in **B**. The inner root was then extracted with methanol for 48 hours. Removal of the solvent produced a dark brown, resin-like residue (25g).

7.2 SEPARATION

7.2.1 Hexane Extract

The extract obtained from **A** was then separated using column chromatography (Silica gel Merck-7734). Eluents of about 20ml were collected in test tubes with hexane, petroleum ether, and petroleum ether/EtOAc as follows:

100% Hex - 2000ml

100% Pet ether - 500ml

PE/EA: (97:3)-500ml

(95:5)-2000ml

(94:6)-500ml

(93:7)-1000ml

(90:10)-1500ml

(80:20)-1500ml

The fractions were monitored by TLC and combinations were made to give enriched fractions as summarised in Table 7.1.

Table 7.1 Summary of fractions

FRACTION NO.	TEST TUBES
1	1-40
2	41-161
3	162-167
4	168-179
5	180-190
6	191-262
7	263-300
8	301-335
9	336-420
10	421-500

Fractions 1, 3 and 4 produced fatty acids, which were identified by their characteristic green colour with anisaldehyde/H₂SO₄, as well as by their ¹H NMR results [plate H-19].

7.2.1.1 Friedelan-3-one [41]

[Friedelin 41]

Friedelin [41] (25mg) was isolated pure without further purification from fraction 2.

M.P. 259°C-261°C [lit. 262°C –263°C]⁶⁵

Rf: 0.6 (H:EA 9:1 v/v), Mass Spec.: [Plate MS-1]

I.R. plate I-1 ν_{\max} (cm⁻¹): 2932 (bulk CH₂), 1719 (C = O stretching)

¹H NMR: δ [CDCl₃, 300MHz, 298K, plate H-1]

¹³C NMR: δ [CDCl₃, 75MHz, 298K, plate C-1, Table A1]

UV activity: none

Spray reagent: anisaldehyde-[purple/blue]

7.2.1.2 Friedelan-3 β -ol [42]

[*epi*-Friedelinol 42]

epi-Friedelinol [42] (12mg) was obtained as colourless plate like crystals after solvent recovery and recrystallisation with ether, from fraction 5.

M.P. 279°C –282°C [lit. 283.5°C –285°C]⁶⁵

Rf: 0.42 (H:EA 9:1 v/v), Mass Spec.: [Plate MS-2]

^1H NMR: δ [CDCl_3 , 300MHz, 298K, plate H-2]

^{13}C NMR: δ [CDCl_3 , 75MHz, 298K, plate C-2, Table A1]

UV activity: none

Spray reagent: anisaldehyde- [purple]

7.2.1.3 3 β -Hydroxylup-20(29)-ene [43]

[Lupeol 43]

Fraction 6 deposited colourless crystals in a yellow coloured waxy residue. TLC showed lupeol [43] as a major component with several minor impurities. The fraction was purified by using a 150mm pasteur pipette and flash silica gel to give lupeol, as colourless crystals (10.2 mg).

M.P. 215°C-218°C [lit. 215°C-216°C]⁶⁵

Rf: 0.32 (H:EA 9:1 v/v)

^1H NMR: δ [CDCl_3 , 300MHz, 298K, plateH-3, Table A8]

^{13}C NMR: δ [CDCl_3 , 75MHz, 298K, plate C-3, Table A1]

UV activity: none

Spray reagent: anisaldehyde- [light blue after few minutes]

7.2.1.4 24 α -Ethylcholest-5,22-dien-3 β -ol [45]**[Stigmasterol 45]**

The test tubes of fraction 8 showed a large concentration of white longitudinal crystals on its walls. Hence combination and removal of solvent gave stigmasterol [45] (12 mg).

M.P. 172°C-174°C [lit. 170°C]⁷⁵

Rf: 0.39 (H:EA 8:2 v/v)

¹H NMR: δ [CDCl₃, 300MHz, 298K, plate H-5, Table A7]

¹³C NMR: δ [CDCl₃, 75MHz, 298K, plate C-5, Table A1]

UV activity: none

Spray reagent: anisaldehyde- [blue]

7.2.1.5 3 β -Hydroxy-12-oleanen-28-oic acid [44]**[Oleanolic acid 44]**

Oleanolic acid [44] was observed as a white powdery substance on the sides of the test tubes. Subsequent combinations gave fraction 10. The minor impurities were removed by washing the solid with a minimum of hexane, repeatedly, until the product was relatively pure by TLC (6.8 mg)

Rf: 0.29 (H:EA 8:2 v/v)

¹H NMR: δ [CDCl₃, 300MHz, 298K, plate H-4, Table A10]

^{13}C NMR: δ [CDCl_3 , 75MHz, 298K, plate C-4, Table A1]

UV activity: none

Spray reagent: anisaldehyde- [blue]

7.2.2 Methanol Extract

Two grams of the methanol extract was loaded on a flash column and eluted with ethyl acetate until TLC analysis of the fractions showed epicatechin as a single brown spot with anisaldehyde/ H_2SO_4 spray reagent.

7.2.2.1 (2R,3R)-2,3-cis-Flavan-3,3',4',5,7-pentol [4]

[(-)-Epicatechin 4]

(-)-Epicatechin [4] was isolated as a brown, amorphous solid (12mg) as described above.

^1H NMR: δ [Acetone- d_6 , 300MHz, 298K, plate H-6, Table A12]

^{13}C NMR: δ [Acetone- d_6 , 75MHz, 298K, plateC-6, Table A11]

Spray reagent: anisaldehyde- [mustard brown]

7.2.2.2 (2R,3R)-2,3-cis-Flavan-3,3',4',5,7-pentaacetate [46]

[(-)-Epicatechin pentaacetate 46]

Acetylation of epicatechin [4] (standard experimental section 6.3.1) produced 15mg of the acetate [46], also as a brown amorphous solid.

^1H NMR: δ [CDCl_3 , 300MHz, 298K, plate H-7, Table A3]

^{13}C NMR: δ [CDCl_3 , 75MHz, 298K, plate C-7, Table A13]

The column was then eluted with ethyl acetate:methanol:water mixtures as follows:

EA:M:H₂O - 35:15:1

35:17:1

35:17:2

These gave fractions, which were pooled as shown in Table 7.2

Table 7.2 Summary of factions

Fraction No	Test tubes
1	1-6
2	7-9
3	10-14
4	15-100

7.2.2.3 α -D- and β -D-Glucopyranoside [64]

[Glucose 64]

Fraction 1 gave glucose [64] as a brown, gummy residue (5.4 mg).

^1H NMR: δ [D_2O , 300MHz, 298K, plate H-8]

UV activity: none

Spray reagent: anisaldehyde- [green]

7.2.2.4 β -D-Fructofuranosyl- α -D-glucopyranoside [65]

[Sucrose 65]

Sucrose [65] was isolated as crystals from fraction 2 (10mg).

$^1\text{H NMR}$: δ [D₂O, 300MHz, 298K, plate H-9, Table A9]

UV activity: none

Spray reagent: anisaldehyde- [green]

Fractions 3 and 4 produced mixtures having the same characteristic colours as the previous carbohydrates with anisaldehyde spray reagent.

7.3 ATTEMPTED SYNTHESIS OF *EPI*-FRIEDELINOL⁶⁶

All apparatus were thoroughly dried in a hot (>120°C) oven before use. The LiAlH₄ (50mg) was weighed into a 25ml round bottomed flask as rapidly as possible, and covered with 5ml of sodium-dried ether. The flask was set up for reflux. Friedelin [41] (12mg) was weighed in a 10ml Erlenmeyer flask, and dissolved in approx. 2ml of sodium dried ether (ultra-sonic bath) and this solution was added dropwise by pipette down the condenser at such a rate that the stirred mixture refluxed gently. The contents of the Erlenmeyer flask were rinsed out with a small amount of dry ether, and this was added to the mixture as well. The mixture was gently refluxed for 18-hours and then allowed to cool. During the reflux-period, some wet ether was prepared by shaking 10ml of ether with an equal volume of water in a separatory funnel for 5min. The upper organic layer

T030125



was retained. About 3ml of the wet ether was added to the cooled reaction mixture, while shaking the solution to decompose excess hydride.

After addition of wet ether, the mixture was refluxed for a further 10 min. to complete decomposition of the hydride. After cooling, the mixture was transferred to a separatory funnel and approx. 1,5ml of 5% H₂SO₄ was added, followed by thorough shaking to decompose the aluminium complex. The organic phase was retained while the aqueous phase was re-extracted with a further 2ml of ether. The solution was dried over MgSO₄, filtered and the solvent removed on the rotary evaporator. This gave a colourless, crystalline solid, which was recrystallised from ether (10mg).

The solid was dissolved in CHCl₃ and subjected to TLC analysis together with pure friedelin [41] and *epi*-friedelinol [42].

CHAPTER EIGHT

ISOLATION OF COMPOUNDS FROM *TYPHA CAPENSIS*

Samples were obtained from the Muti-Market (Durban) and Pinetown. Samples were verified by Mr. Praveen Poorun at the Herbarium, Department of Botany, UDW.

8.1 EXTRACTION OF ROOTS

The air-dried roots, which were chopped and crushed (300g), were first extracted with hexane for 48 hours and this was followed by extraction with acetone for a further 48 hours. The solvents were removed under vacuum to yield a light yellow waxy residue (1g) for the hexane extract and a brown friable solid for the acetone extract (12,5g).

8.2 SEPARATION

8.2.1 Hexane extract

The extract on standing for several days produced a white crystalline solid. The residue was washed repeatedly with hexane. The solid was isolated pure by filtration (6.8 mg). The washings were combined and after removal of the hexane, were subjected to flash chromatography.

The column was eluted consecutively with H : EA mixtures of 95:5 (500 ml) and 9:1 (1000ml) and the fractions collected in test tubes as shown in Table 8.1.

Table 8.1 Summary of fractions

FRACTION	TEST TUBES
1	1-20
2	21-30
3	31-35
4	36-40
5	41-43
6	45-55

8.2.1.1 7-Hydroxy-3-benzylphthalide [48]**[Typhaphthalide 48]**

Typhaphthalide [48] was obtained as pale white crystals as described in 8.2.1 (6.8 mg)..

M.P. 75°C –77°C

Mass spec: HRMS: $[M^+]$ at m/z 240.0786, $C_{15}H_{12}O_3$ requires 240.0786

EIMS: m/z (rel. int.): 240 (53.2) $[M^+]$, 149 (100), 121 (5.4), 91 (8.1)

[Plate MS-3, Scheme M1]

1H NMR: δ [$CDCl_3$, 300MHz, 298K, plate H-11, Table A4]

^{13}C NMR: δ [$CDCl_3$, 75MHz, 298K, plate C-8, Table A4]

COSY: plate CO-1

HETCOR: plate HE-1

NOESY: plate NO-1

I.R.: plate I-2 ν_{\max} (cm^{-1}): 3544, 3437 (chelated OH, phenolic), 2922 (CH_2 , CH_3), 1714 (C = O stretching), 1624, 1607 (aromatic) 1471 (aromatic C = C stretching),

UV activity: blue (254nm) Optical Rotation: $[\alpha]_{\text{D}}^{25} = -9.191$ (conc.= 0.136)

Rf: 0.65 (H:EA 8:2 v/v)

Spray reagent: Dragendorff-[brown]

8.2.1.2 8-Hydroxy-3-[2-(phenyl)ethenyl]-3,4-dihydroisocoumarin [47]

[Typharin 47]

TLC analysis of fraction 3 (H : EA, 9 : 1, v/v) produced a single spot which appeared purple after spraying with anisaldehyde / H_2SO_4 spray reagent and developing at 120°C . The spot appeared an intense blue under UV light (366nm). Typharin [47] was isolated as a yellow solid, insufficient to yield an accurate melting point.

Mass spec.: EIMS: m/z (rel. int.): 266 (85.5) [M^+], 248 (100), 230 (63.8), 219(40.9)

[Plate MS-4]

^1H NMR: δ [CDCl_3 , 300MHz, 298K, plate H-12, Table A5]

^{13}C NMR: δ [CDCl_3 , 75Mhz, 298K, plate C-9, Table A5]

COSY: plate CO-2

HETCOR: plate HE-2

NOESY: plate NO-2

IR: plate I-3 ν_{\max} (cm^{-1}): 3440 (O – H stretching), 3063 (CH_2) 1690 (C = O stretching) 1600, 1580, 1475 (C = C stretching), 1000 (C-OO-C stretching), 980 (-CH = CH-, *trans*)

UV activity: light blue (254nm) Optical Rotation: $[\alpha]_{\text{D}}^{25} = +3.571$ (conc. = 0.07)

Rf: 0.49 (H:EA 9:1 v/v]

Spray reagent: anisaldehyde-[light purple]

8.2.1.3 24 α -Ethylcholest-5-ene-3 β -ol [49]

[β -Sitosterol 49]

The sterol [49] was obtained relatively pure as white needle-like crystals from fraction 6 (9.1 mg). Its structure was identified by comparison with an authentic specimen on an analytical TLC plate, and by comparison of the spectral characteristics of the compound obtained and the authentic sample.

M.P. 136°C-138°C [lit. 136°C-137°C]⁷⁵

¹H NMR: δ [CDCl₃, 300MHz, 298K, plate H-13, Table A7]

¹³C NMR: δ [CDCl₃, 75MHz, 298K, plate C-11]

UV activity: none

Rf: 0.72 (H:EA 8:2 v/v)

Spray reagent: anisaldehyde-[blue]

8.2.2 Acetone Extract

A portion of the solid material obtained from the acetone extract (2g) was separated by means of flash chromatography [Silica gel, Mesh 230-400]. Eluents of approximately 20 ml were collected in test tubes by eluting with B:EA:A mixtures of (6:3:2, 500ml) and (6:3:3, 1000ml).

Eluents were monitored by TLC (B:EA:A) and combinations were made according to that shown in Table 8.2.

Table 8.2 Summary of Fractions

FRACTION NUMBER	TEST TUBE
1	1-23
2	25-30
3	31-35
4	37-40
5	41-60
6	63-76

8.2.2.1 Mixture of afzelechin [10] and epiafzelechin [23]

TLC analysis of fraction 2 (B:A 8:6 v/v) produced one spot with Rf 0,43. The fraction was a mixture of afzelechin [10] and epiafzelechin [23] (18.3 mg). Acetylation of the mixture allowed a greater Rf range thus allowing the separation of the two compounds as their acetates. PLC separation of the acetylated mixture produced two bands at Rf 0.64 and 0.55.

8.2.2.2 (2R,3S)-2,3-trans-Flavan-3,4',5,7-tetraacetate [54] [Afzelechin tetraacetate 54]

The band with Rf 0.64 gave afzelechin tetraacetate [54] as a brown non-crystalline solid (3mg).

¹H NMR: δ [CDCl₃, 300MHz, 298K, plate H-16, Table A2]

Mass Spec.: [Plate MS-5, Scheme M2]

Spray reagent: anisaldehyde-[brown]

8.2.2.3 (2R,3R)-2,3-cis-Flavan-3,4',5,7-tetraacetate [55] [Epiafzelechin tetraacetate 55]

Epiafzelechin tetraacetate [55] was also obtained as a brown, amorphous solid from the band with Rf 0,55 (ca. 2mg).

¹H NMR: δ [CDCl₃, 300MHz, 298K, plate H-17, Table A2]

Mass Spec.: [Plate MS-5, Scheme M2]

were made to separate the isomers in their free phenolic form. Like the previous isomeric pair, the mixture was acetylated and subject to PLC separation producing two bands with Rf 0.49 and 0.42 (B:A 9:1 v/v).

8.2.2.5 (2R,3S)-2,3-trans-Flavan-3,3',4',5,7-pentaacetate [56]

[Catechin pentaacetate 56]

The band with Rf 0.49 yielded catechin pentaacetate [56] (15mg).

¹H NMR: δ [CDCl₃, 300MHz, 298K, plate H-18, Table A3]

¹³C NMR: δ [CDCl₃, 75MHz, 298K, plate C-8, Table A14]

spray reagent: anisaldehyde-[brown]

8.2.2.6 (2R,3R)-2,3-cis-Flavan-3,3',4',5,7-pentaacetate [46]

[Epicatechin pentaacetate 46]

The second band (Rf 0.42), produced epicatechin pentaacetate [46] as a light brown, non-crystalline solid (22mg).

¹H NMR: δ [CDCl₃, 300MHz, 298K, plate H-7, Table A3]

¹³C NMR: δ [CDCl₃, 75MHz, 298K, plate C-7, Table A11]

Spray reagent: anisaldehyde-[brown]

8.3 SPRAY REAGENTS

Two spray reagents were employed namely, anisaldehyde/H₂SO₄ and Dragendorff reagent. Reagents were prepared as described in section 6.1.5. Colours are discussed in section 5.6.

8.4 BIOLOGICAL ACTIVITY⁸⁵

A preliminary screening of the biological activity of the crude methanolic extract of *T. capensis* was carried out in an independent study. A brief description of each test is given. A more detailed explanation of experimental technique, methodology and experimental materials used is given in the appropriate reference.

8.4.1 Antibacterial activity

The disc diffusion test method in agar medium was used to test for antibacterial activity. The following microorganisms were tested:

Staphylococcus aureus

Klebsiella pneumoniae

Escherichia coli

Pseudomonas aeruginosa

Citobacter freundii

Proteus mirabilis

Salmonella typhi

Shigella flexneri

Enterobacter aerogenes

Candida albicans

8.4.2 Antifungal activity

Spores of seven day cultures of *Aspergillus niger* and *Penicillium* sp. were sprayed on tlc plates which were spotted with the crude extract and run in an appropriate solvent system. After a prescribed incubation period the plates were examined for zones of inhibition.

8.4.3 Cytotoxic activity

The brine shrimp bioassay was used to test for cytotoxic activity in the crude extract.

8.4.4 Determination of uterotonic activity

Female Dunkin Hartley guinea pigs were used in this investigation. A specimen of the uterine muscle tissue was examined for the above activity in a suitably prepared organ bath in the presence of a muscle stimulant; in this case, acetylcholine.

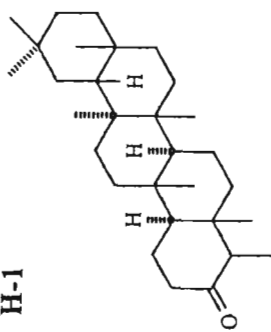
PART D

APPENDIX

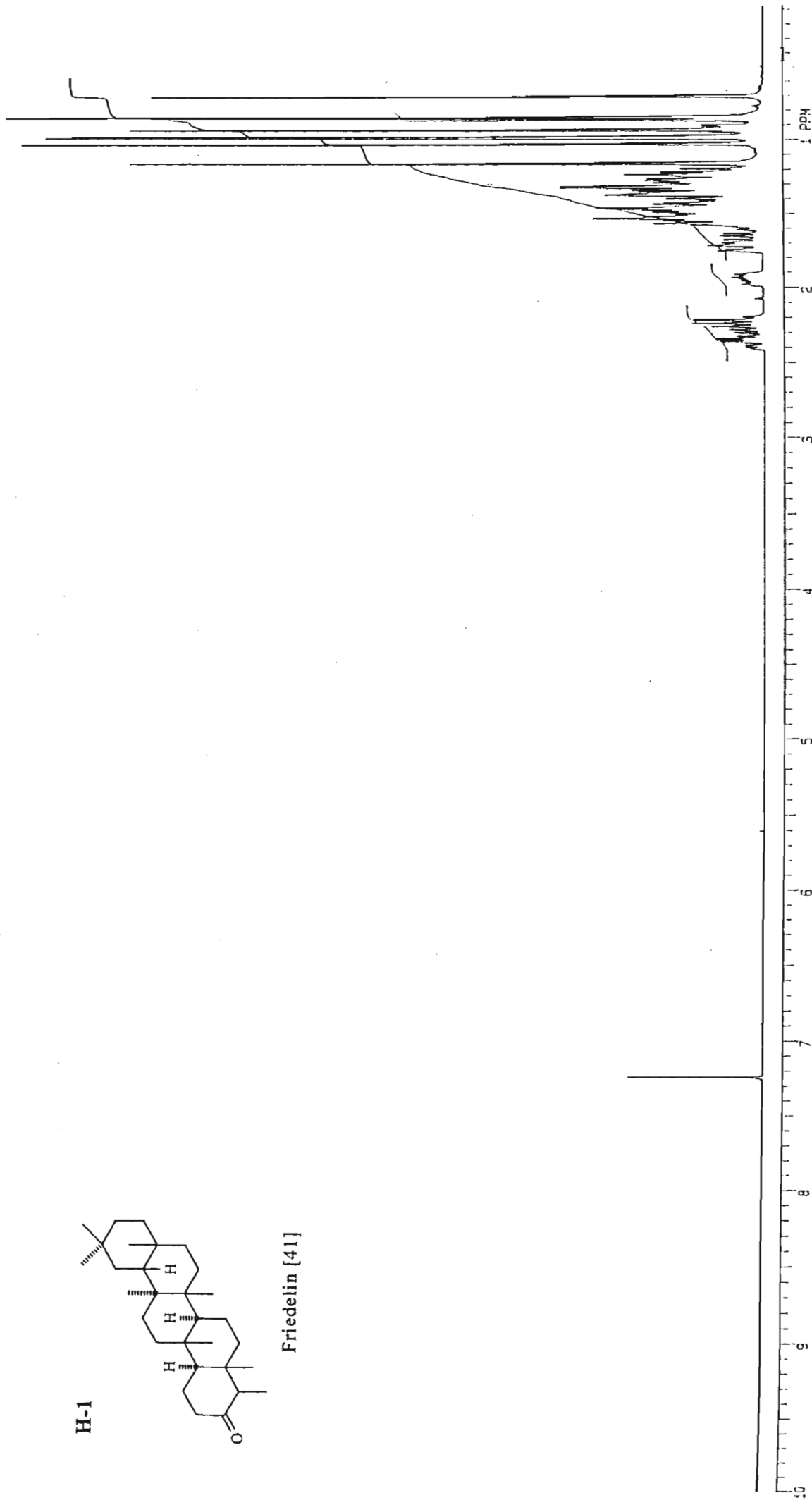
INDEX – ¹H NMR

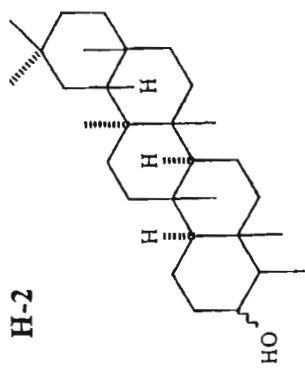
<u>PLATE</u>	<u>COMPOUND</u>	<u>PAGE</u>
H-1	Friedelin [41]	112
H-2	<i>epi</i> -Friedelinol [42]	113
H-3	Lupeol [43]	114
H-4	Oleanolic acid [44]	115
H-5	Stigmasterol [45]	116
H-6	Epicatechin [4]	117
H-7	Epicatechin pentaacetate [46]	118
H-8	Glucose [64]	119
H-9	Sucrose [65]	120
H-10	EF-1 mixture of friedelin and <i>epi</i> -friedelinol	121
H-11	Typhaphthalide [48]	122
H-12	Typharin [47]	123
H-13	β -Sitosterol [49]	124
H-14	Afzelechin [10] /Epiafzelechin [23] mixture	125
H-15	Catechin [11] / Epicatechin [4] mixture	126
H-16	Afzelechin tetraacetate [54]	127
H-17	Epiafzelechin tetraacetate [55]	128
H-18	Catechin pentaacetate [56]	129
H-19	Fatty acid	130

H-1

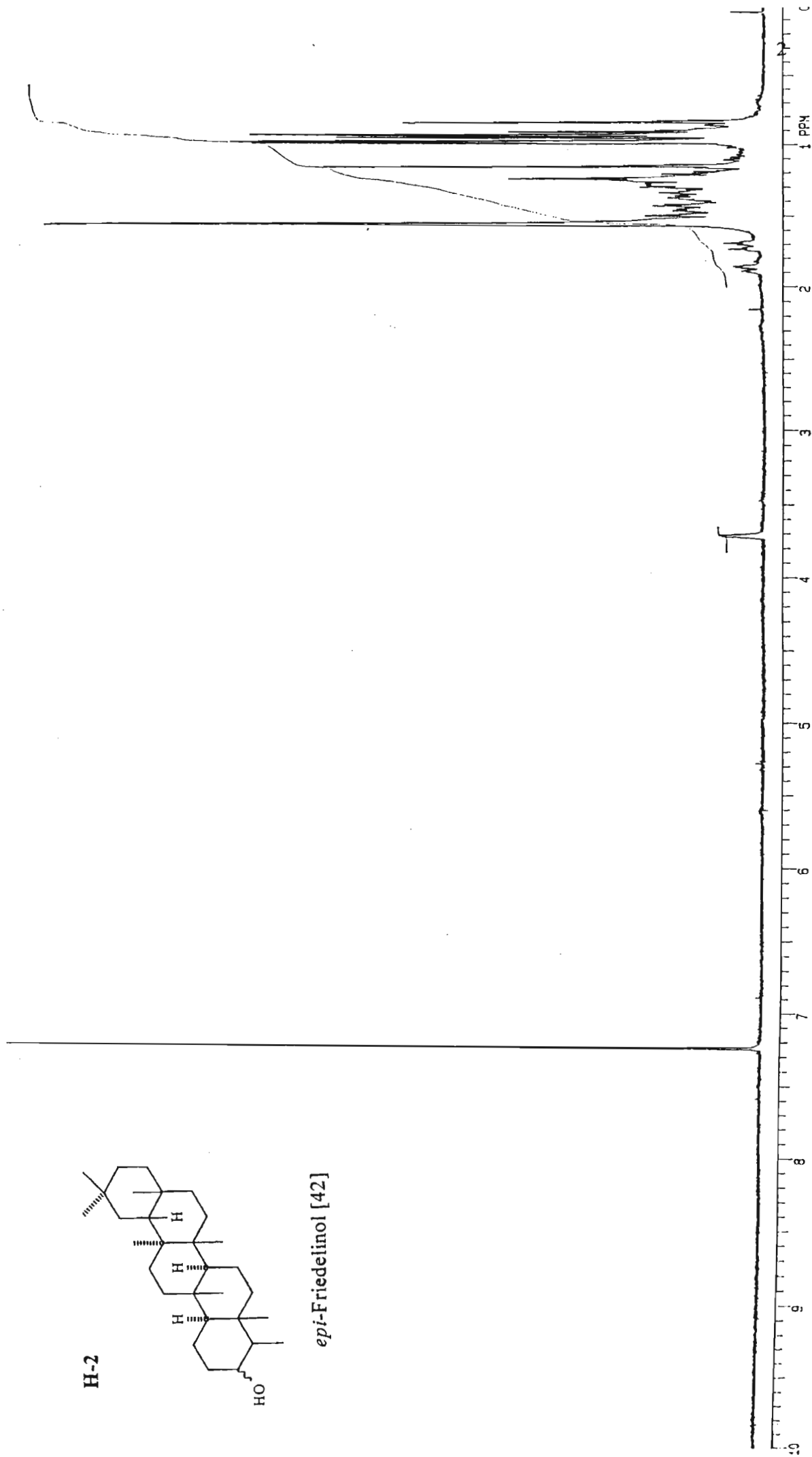


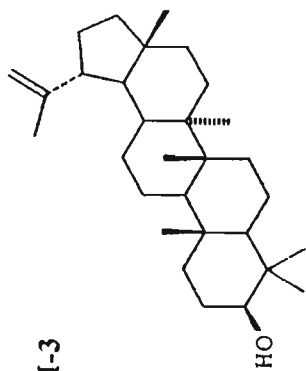
Friedelin [41]



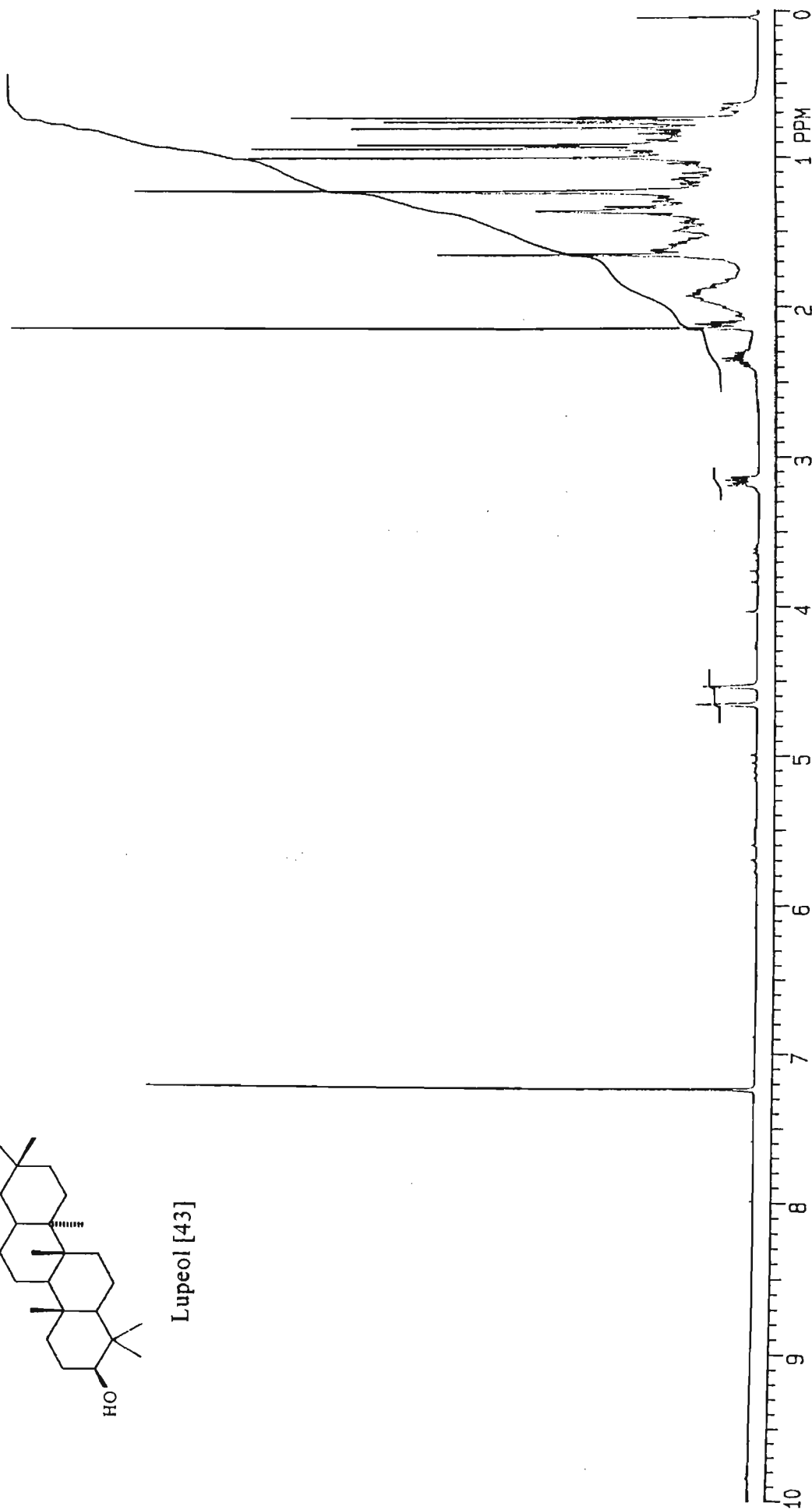


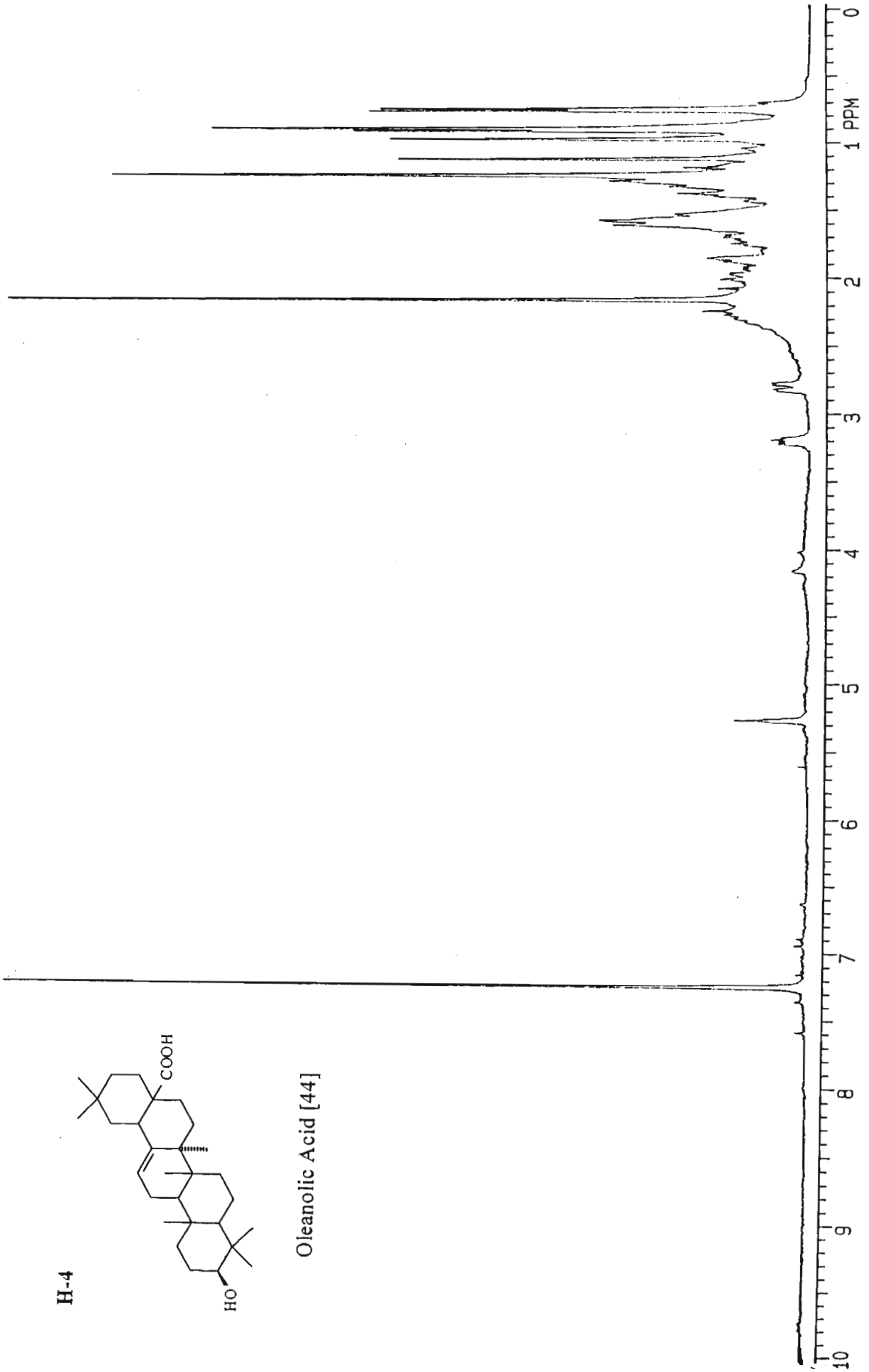
epi-Friedelinol [42]





Lupeol [43]

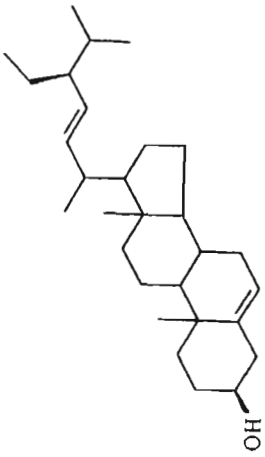




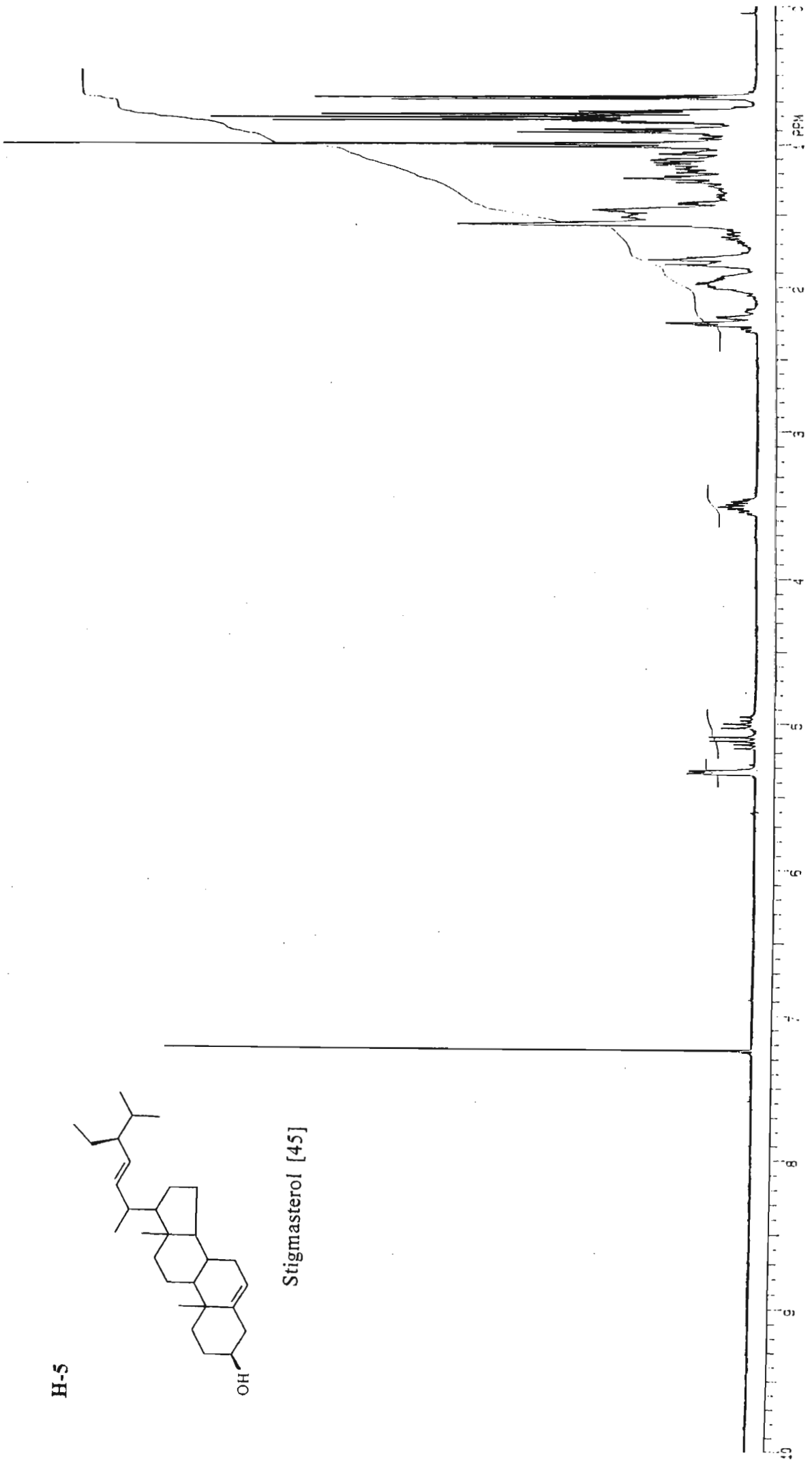
H-4

Oleanolic Acid [44]

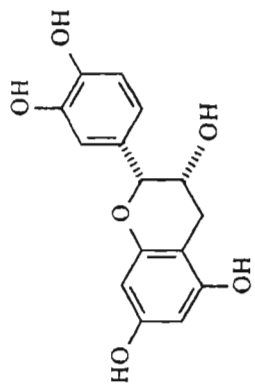
H-5



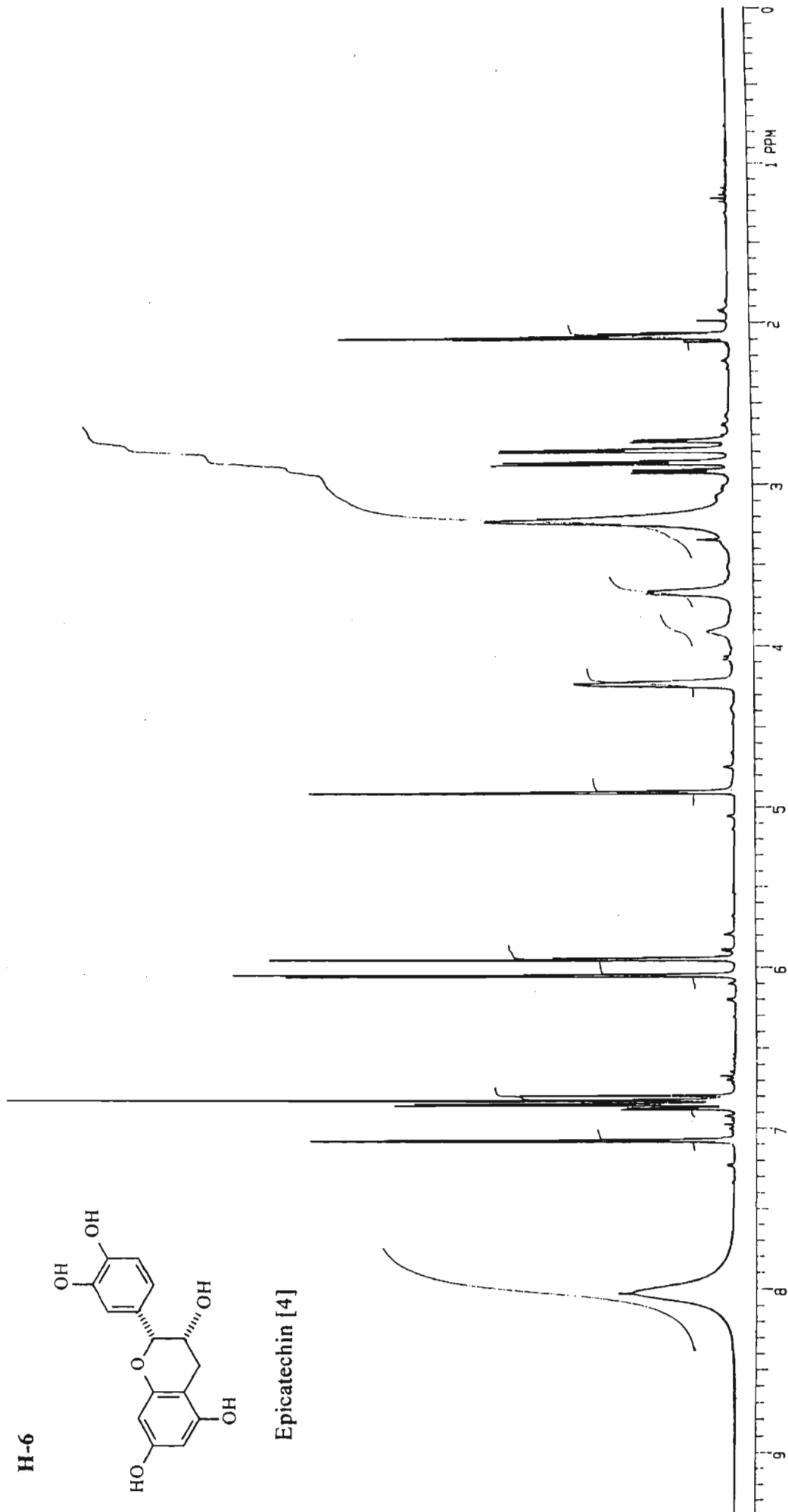
Stigmasterol [45]



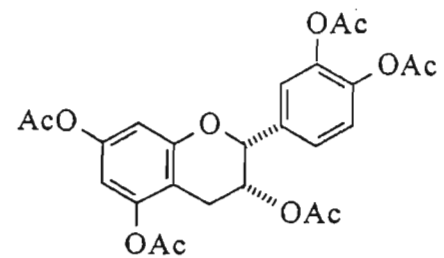
H-6



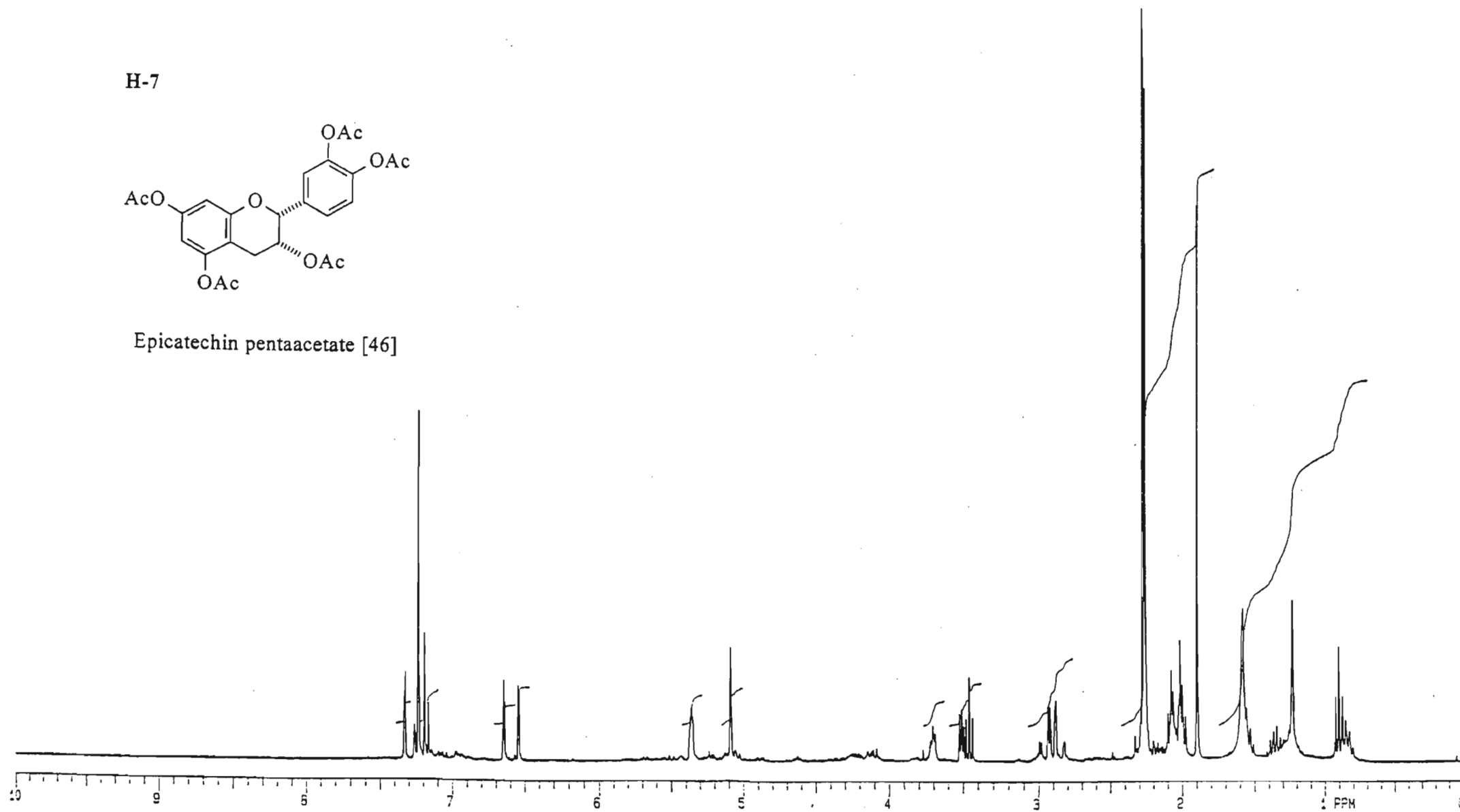
Epicatechin [4]

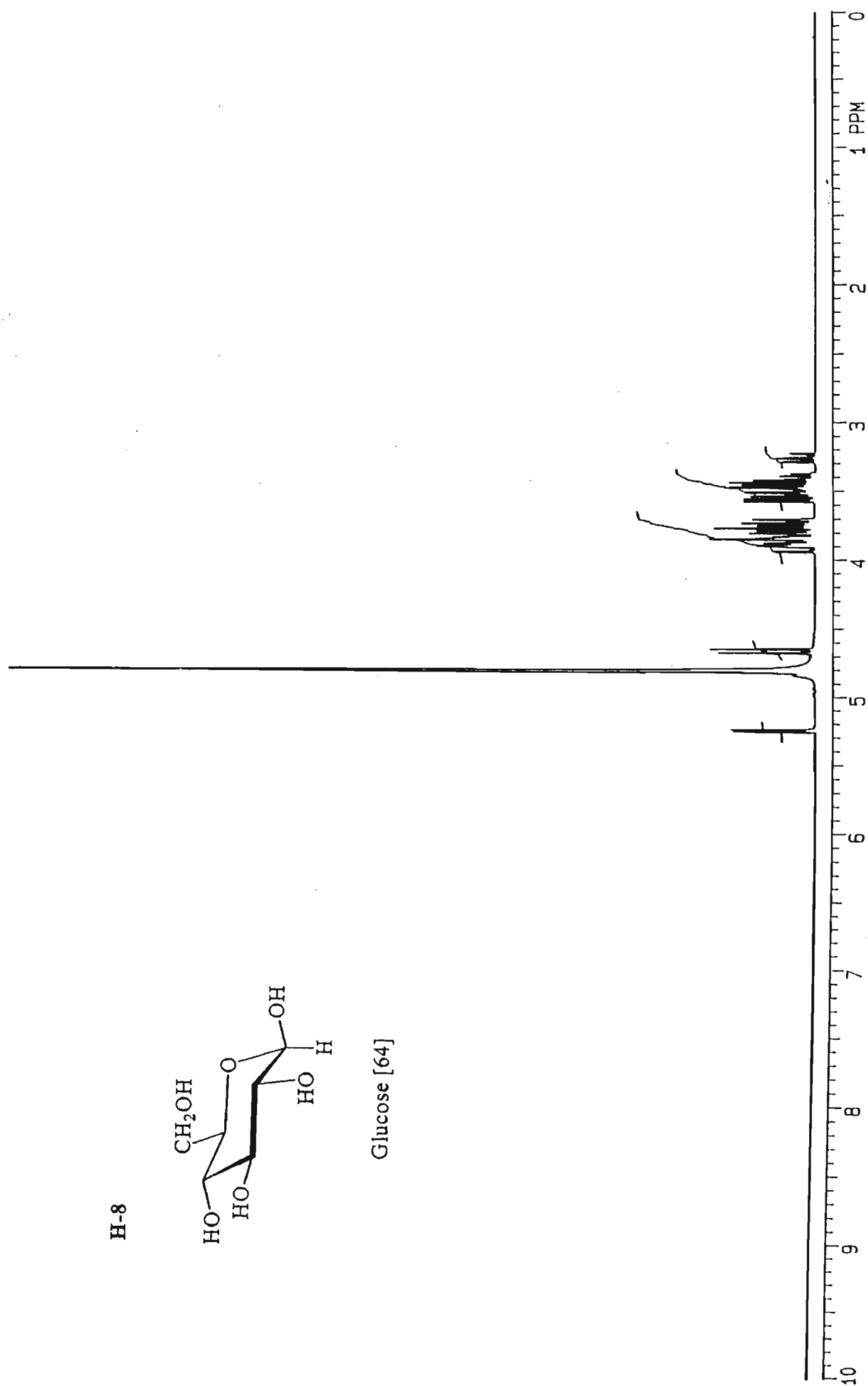


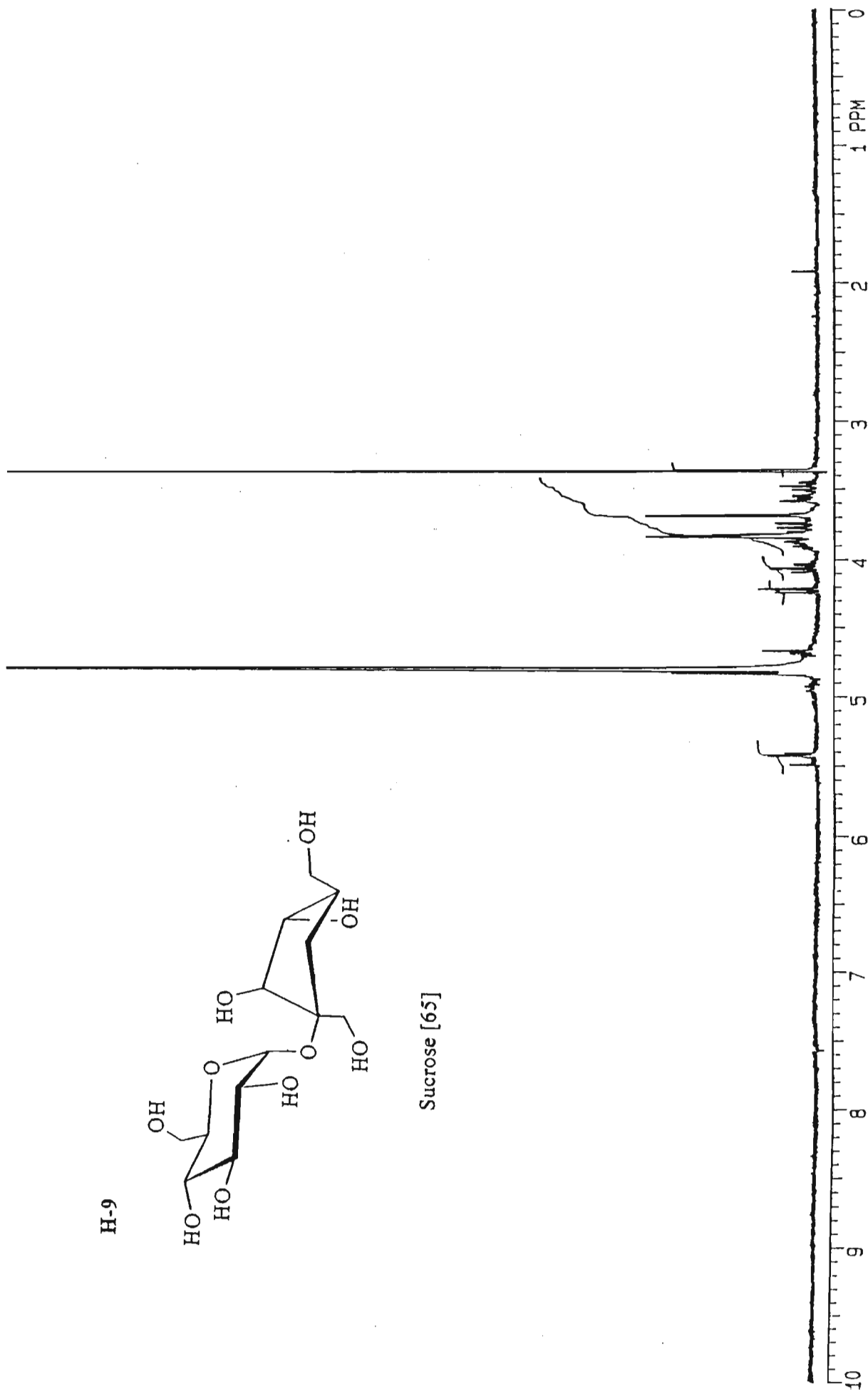
H-7



Epicatechin pentaacetate [46]

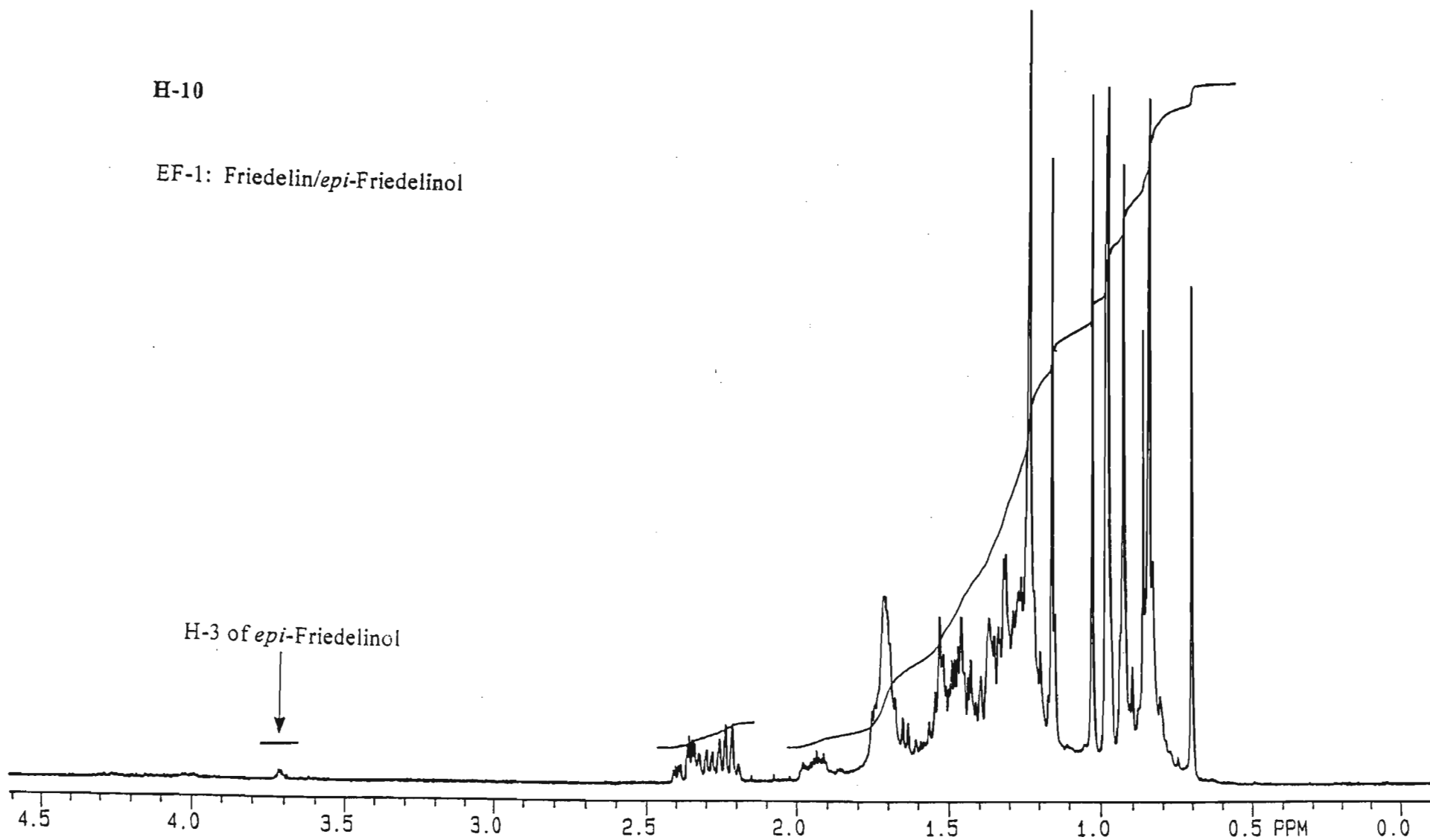




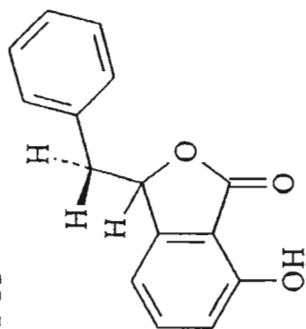


H-10

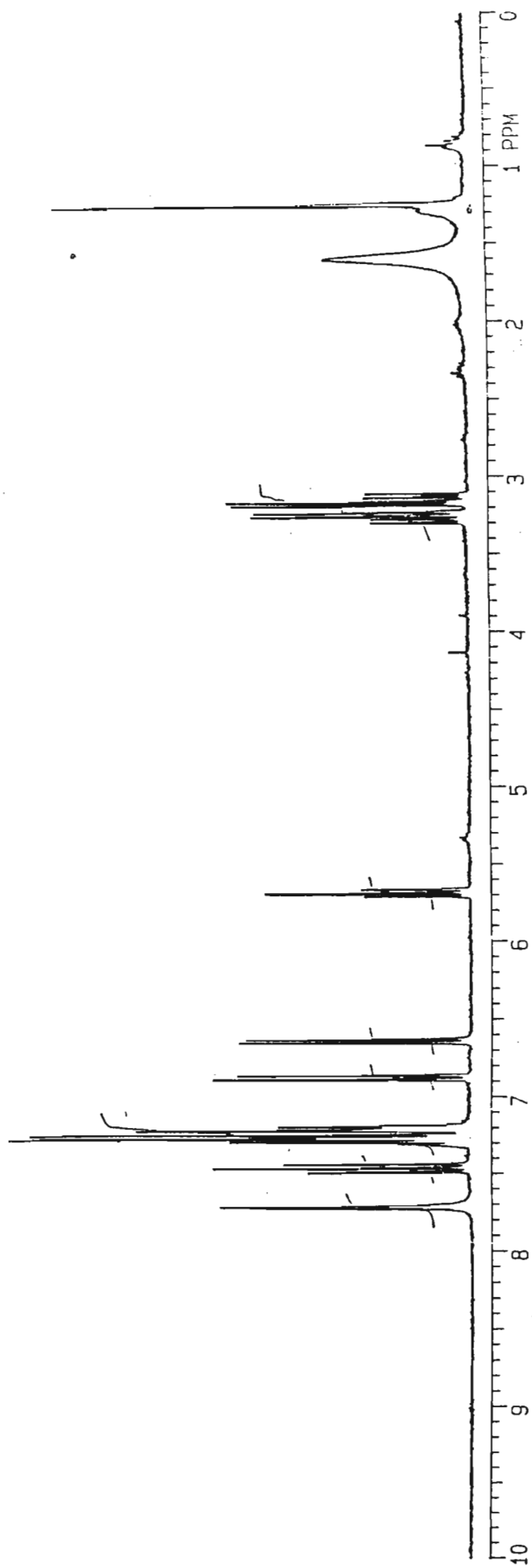
EF-1: Friedelin/*epi*-Friedelinol



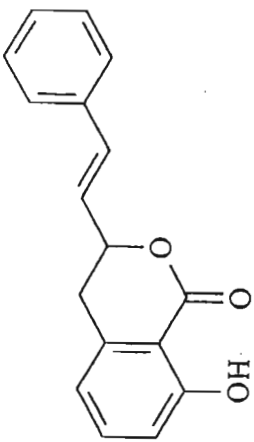
H-11



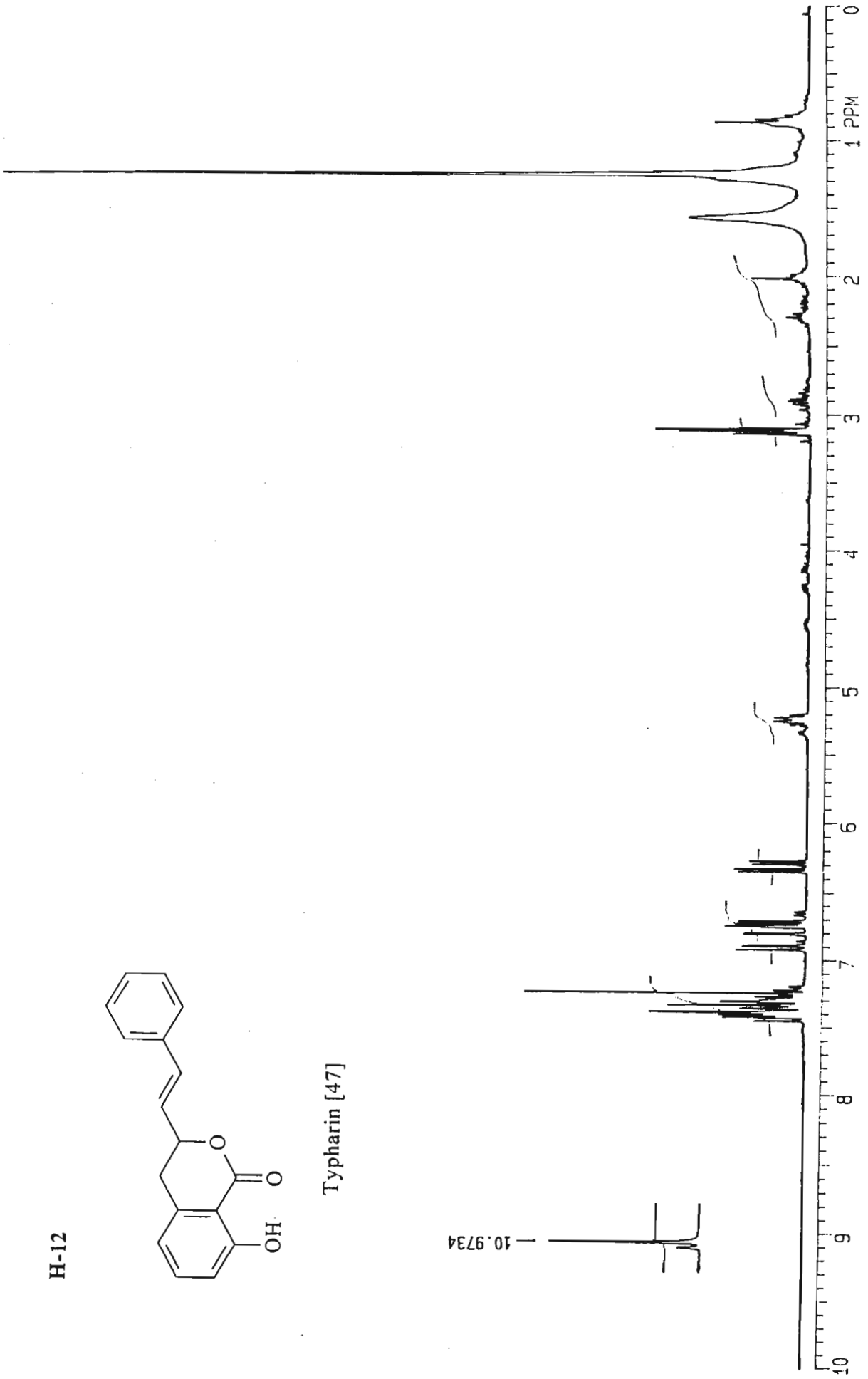
Typhaphthalide [48]



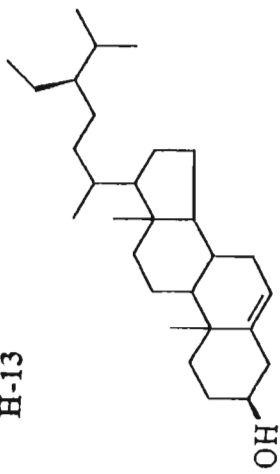
H-12



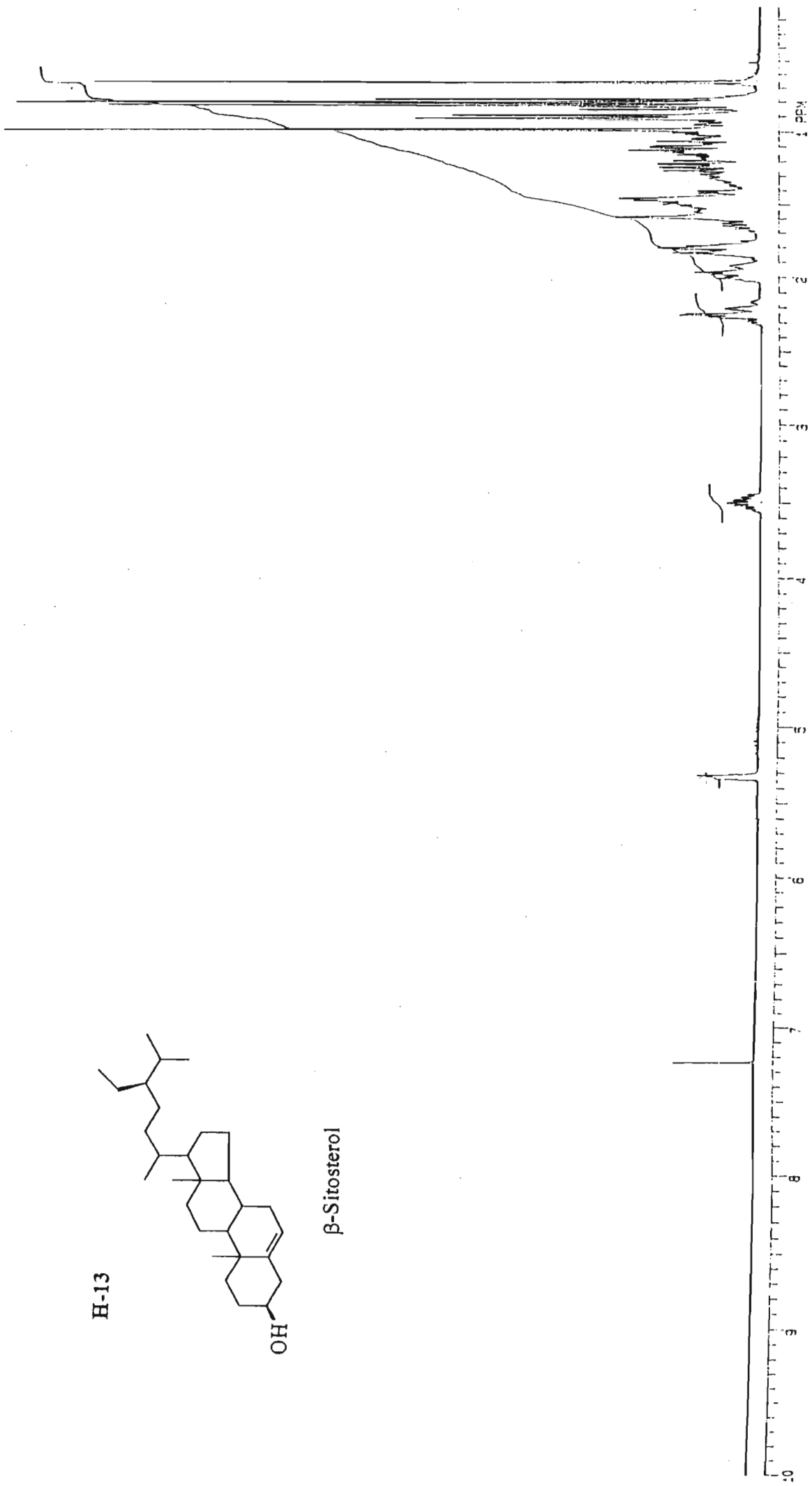
Typharin [47]



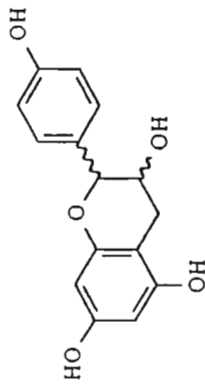
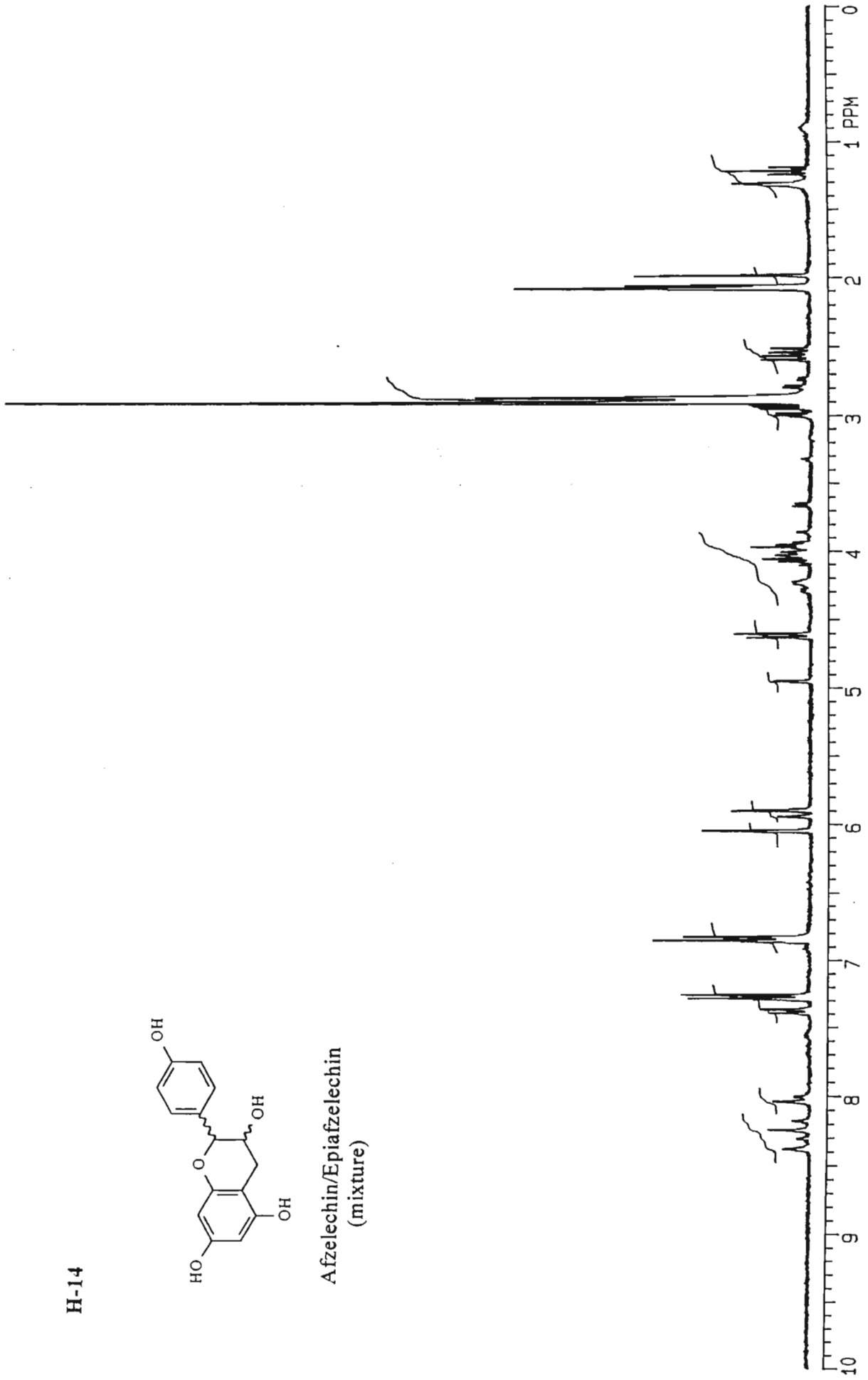
H-13



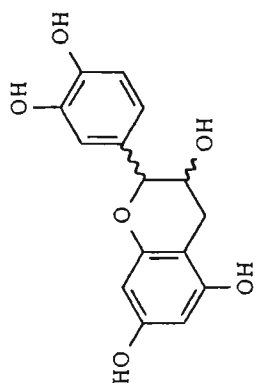
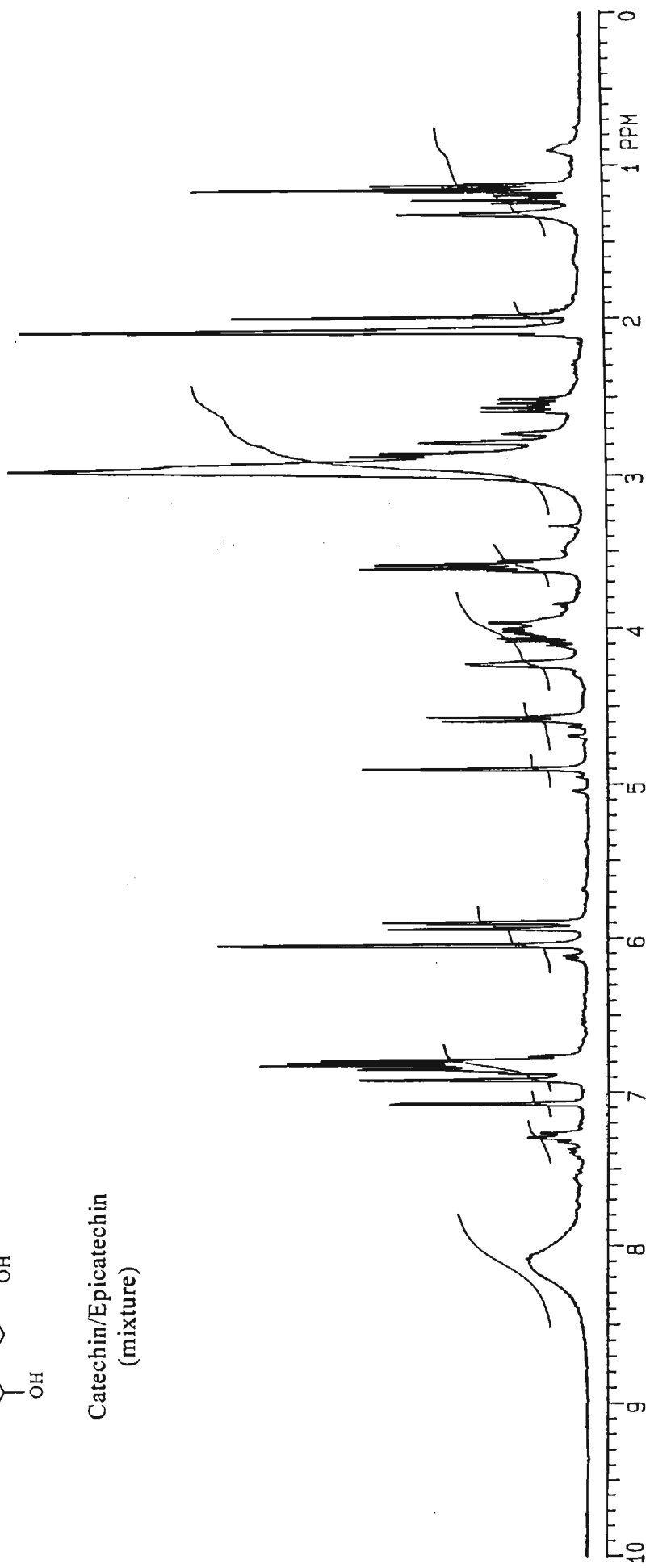
β -Sitosterol



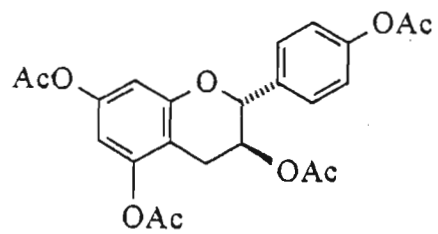
H-14

Afzelechin/Epiafzelechin
(mixture)

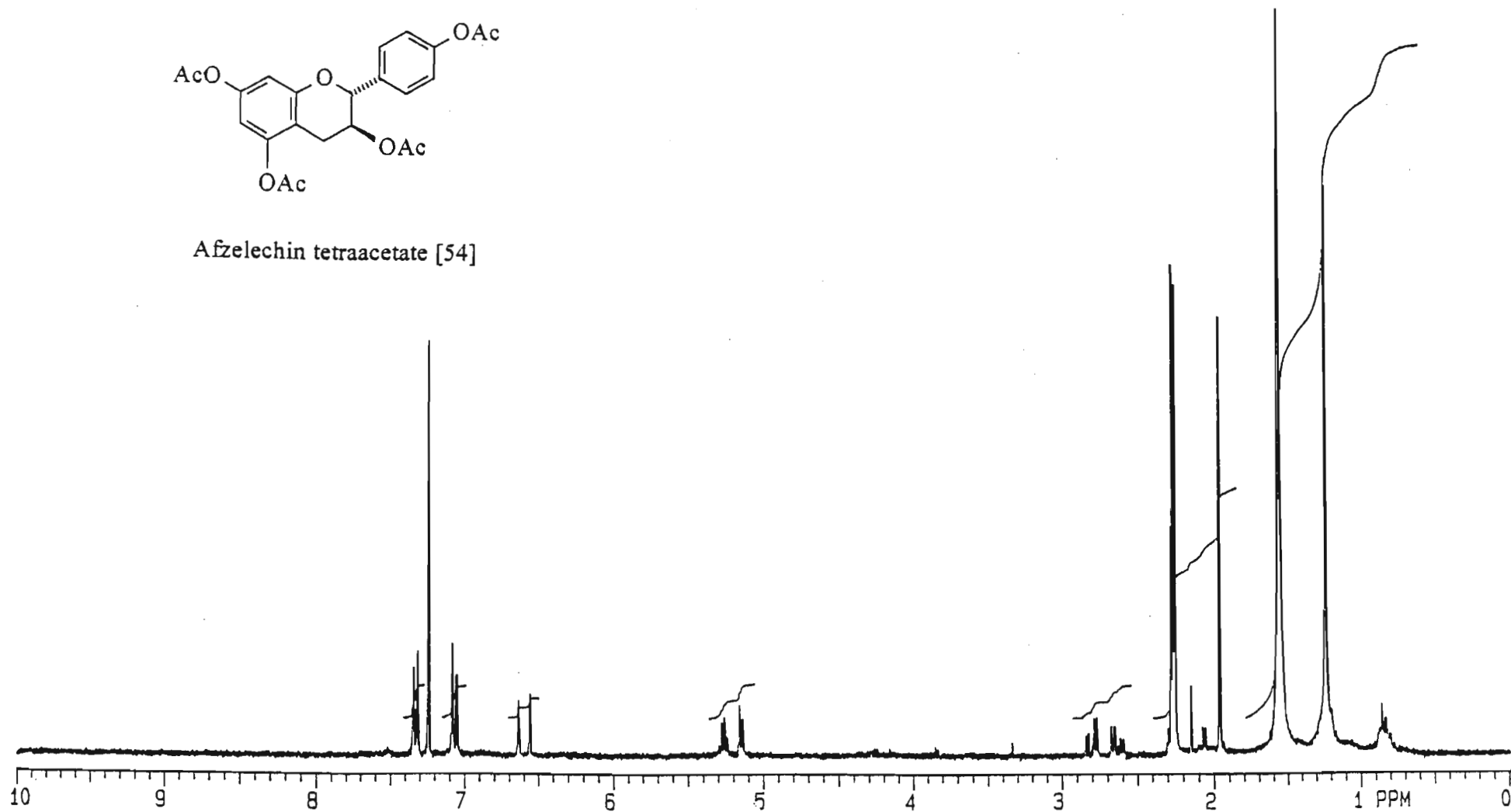
H-15

Catechin/Epicatechin
(mixture)

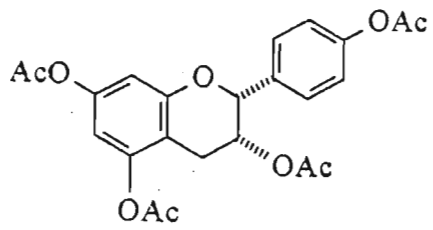
H-16



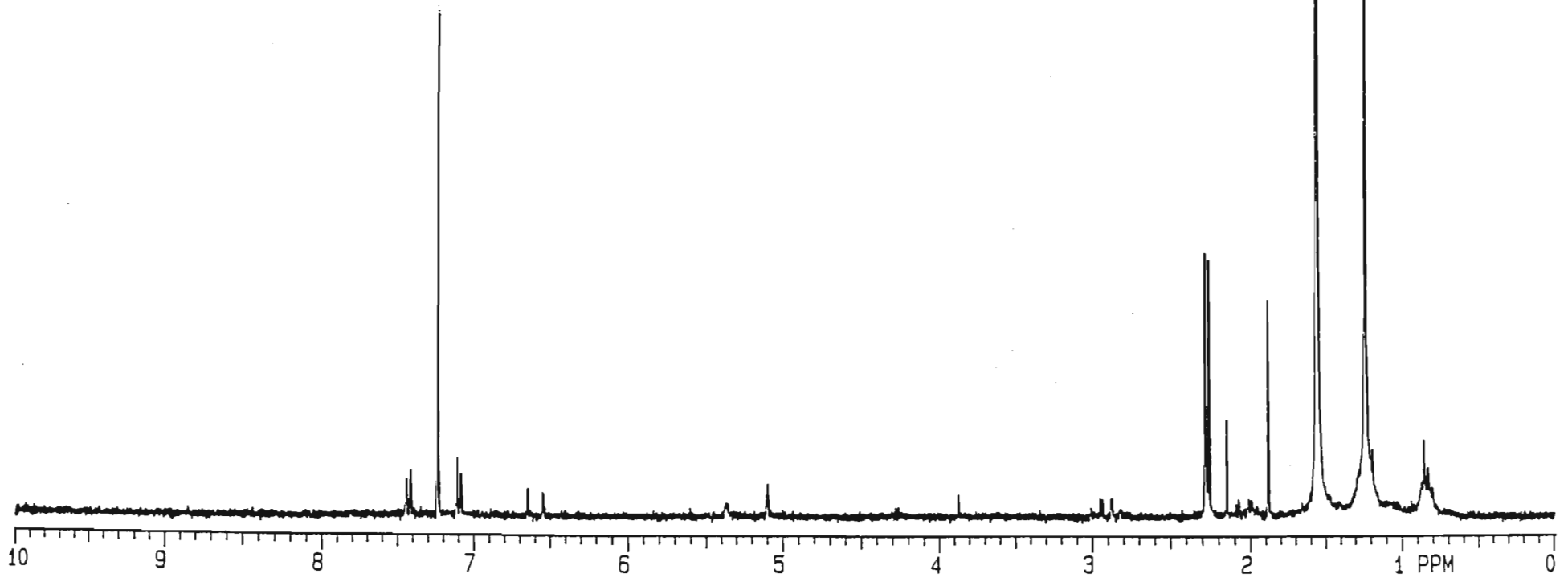
Afzelechin tetraacetate [54]



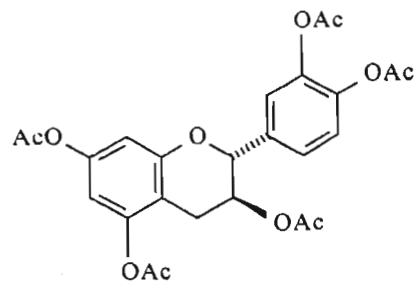
H-17



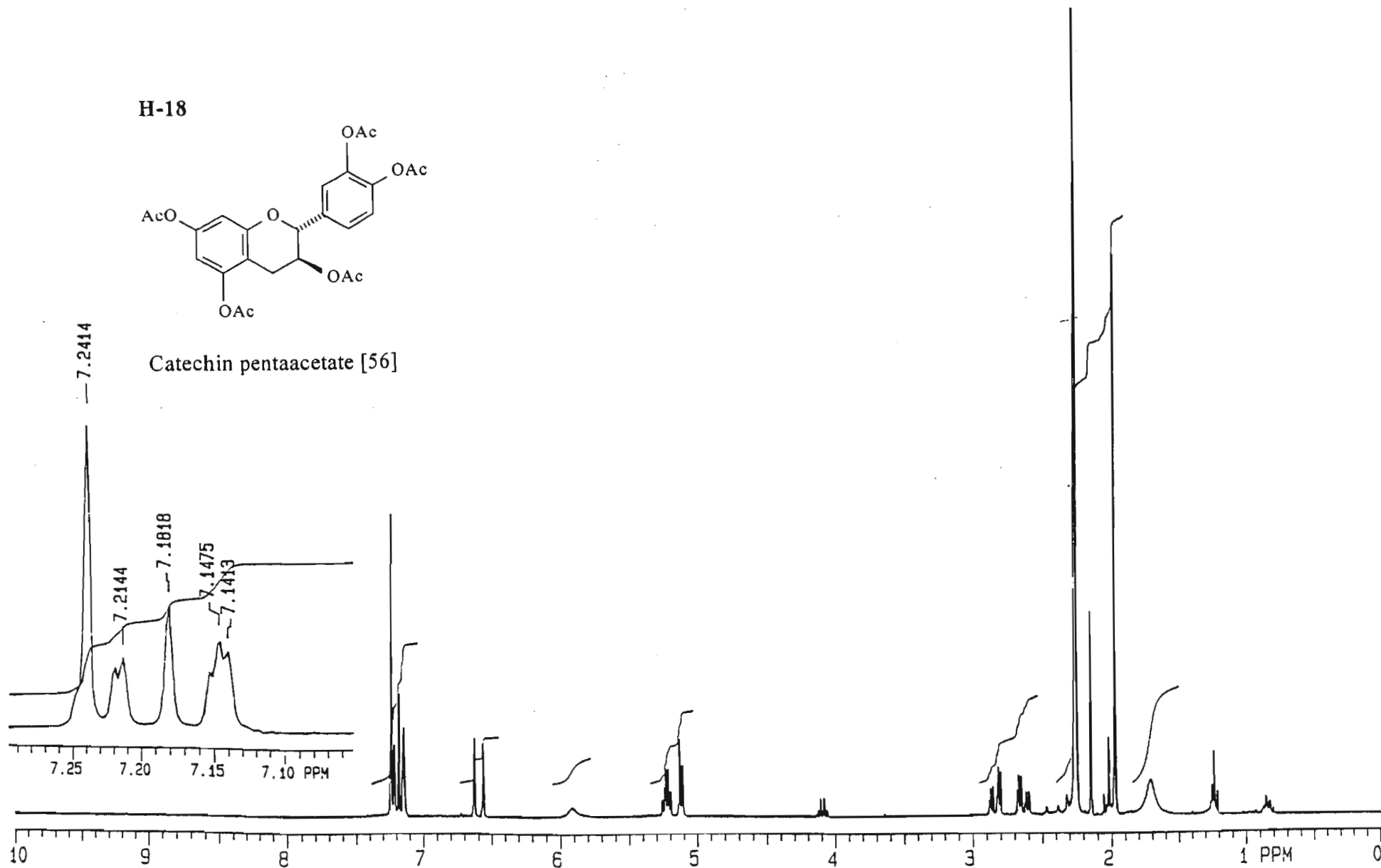
Epiafzelechin tetraacetate [55]



H-18

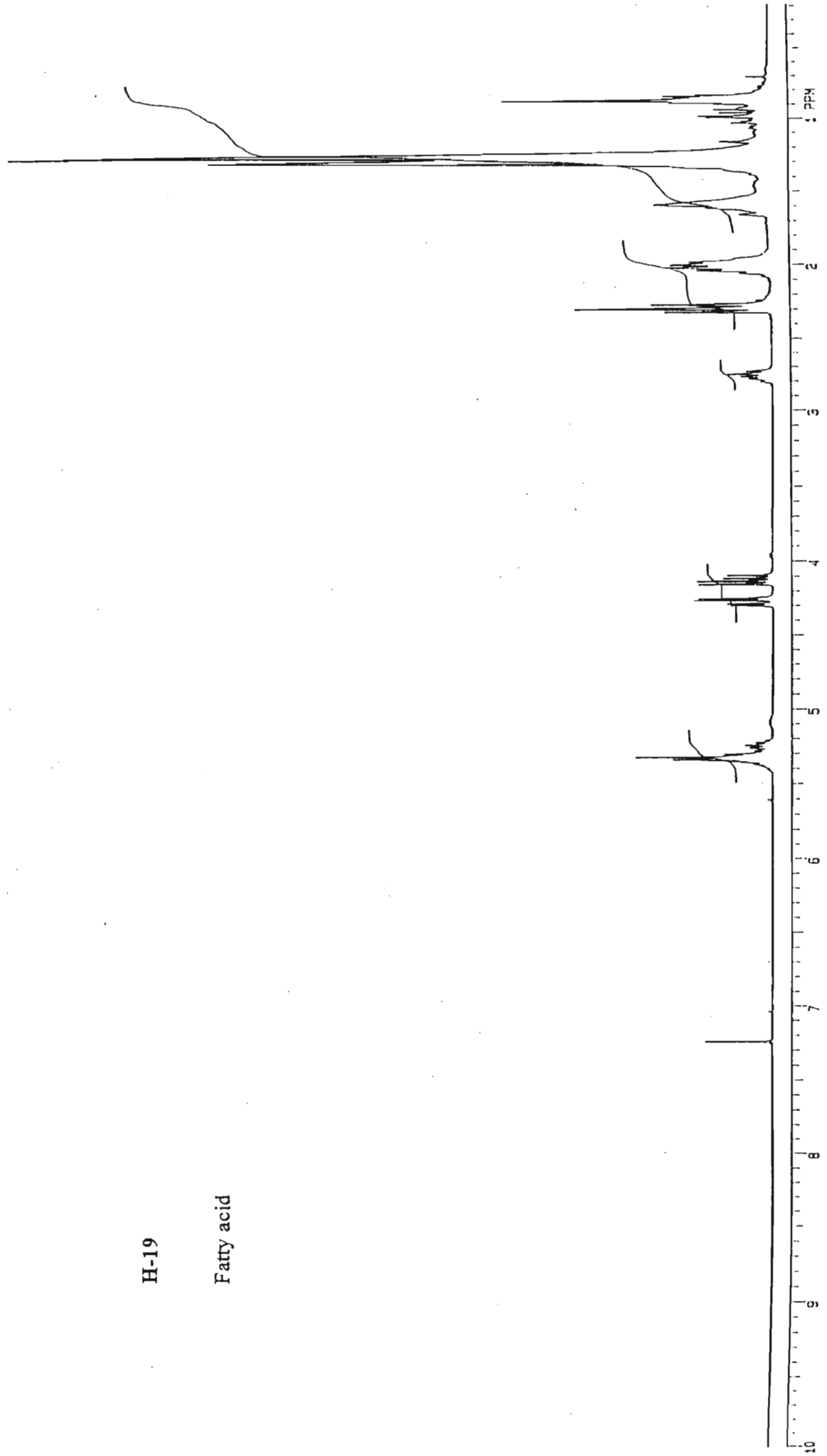


Catechin pentaacetate [56]



H-19

Fatty acid



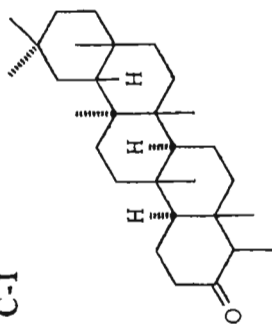
INDEX – ¹³C NMR

<u>PLATE</u>	<u>COMPOUND</u>	<u>PAGE</u>
C-1	Friedelin [41]	132
C-2	<i>epi</i> -Friedelinol [42]	133
C-3	Lupeol [43]	134
C-4	Oleanolic acid [44]	135
C-5	Stigmasterol [45]	136
C-6	Epicatechin [4]	137
C-7	Epicatechin pentaacetate [46]	138
C-8	Typhaphthalide [48]	139
C-9	Typharin [47]	140
C-10	β -Sitosterol [49]	141
C-11	Catechin pentaacetate [56]	142
C-12	Afzelechin [10] / Epiafzelechin [23] mixture	143
C-13	Catechin [11] / Epicatechin [4] mixture	144

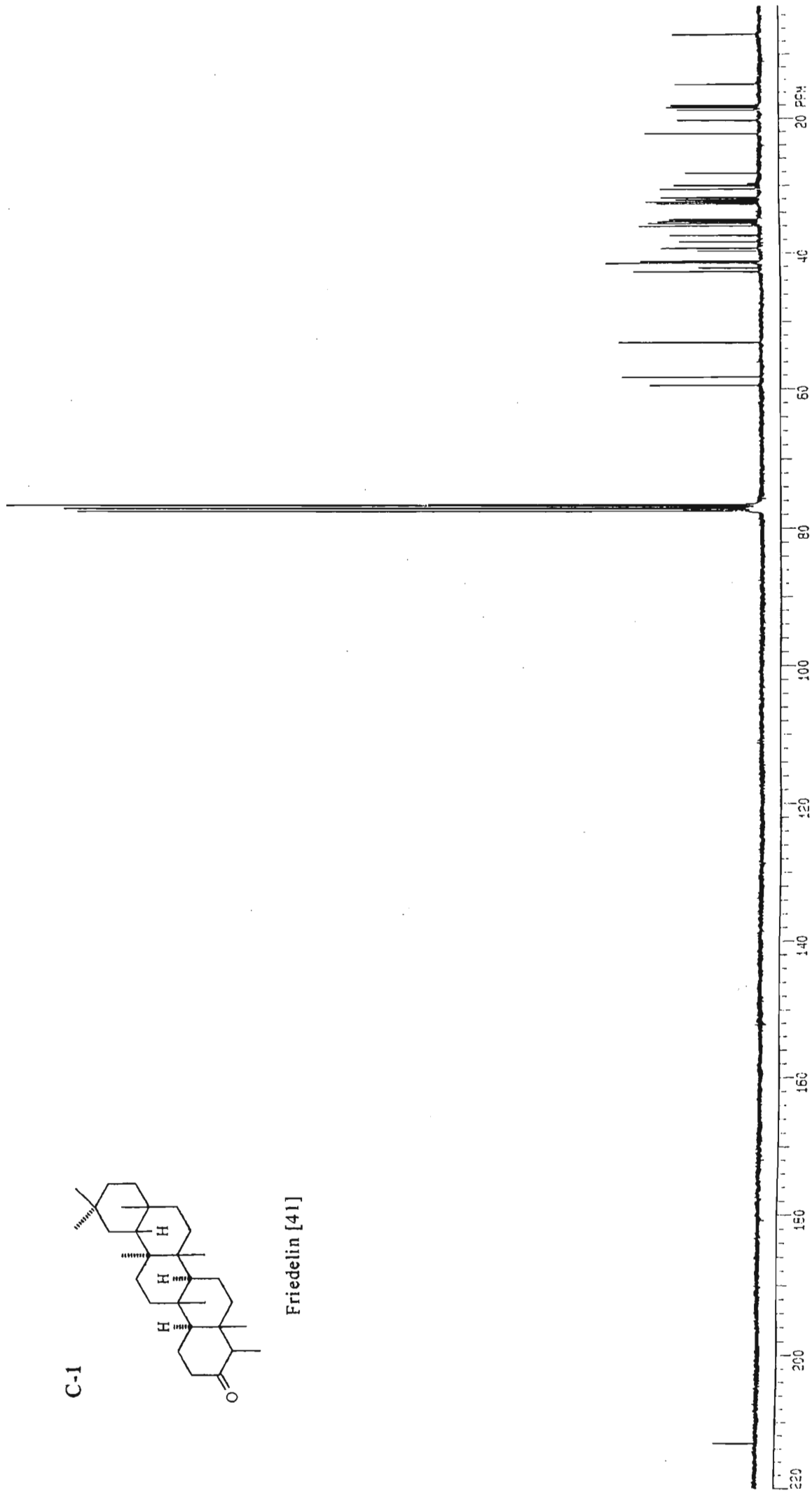
INDEX – ADEPT

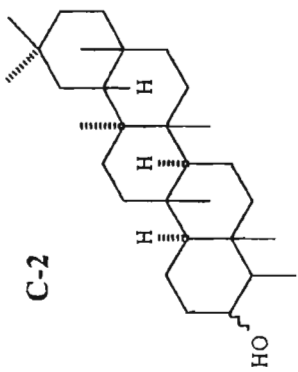
<u>PLATE</u>	<u>COMPOUND</u>	
AD-1	Typhaphthalide [48]	145
AD-2	Typharin [47]	146

C-1

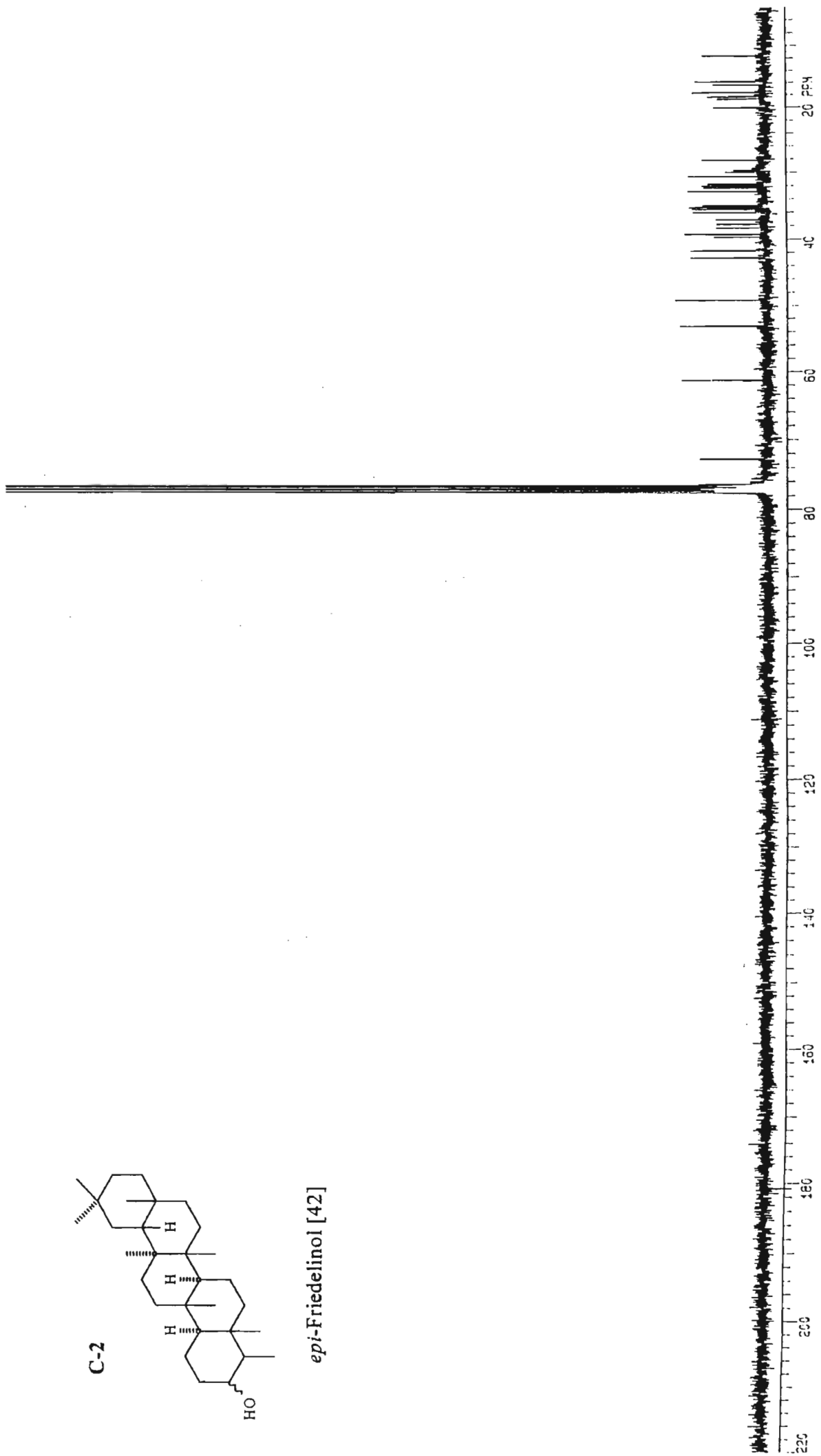


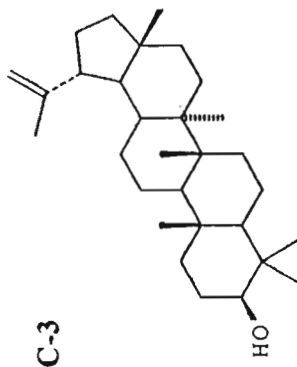
Friedelin [41]



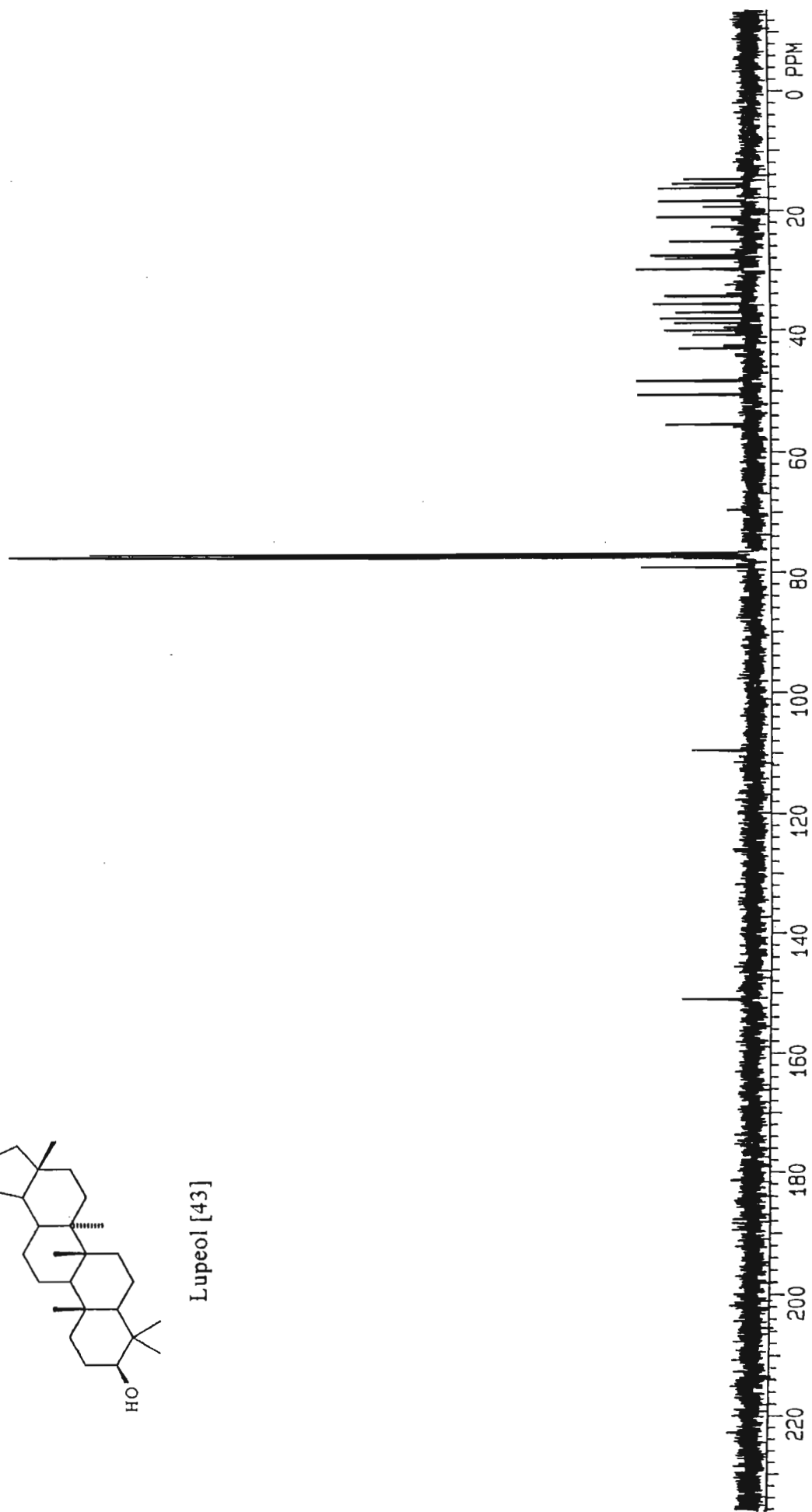


epi-Friedelinol [42]

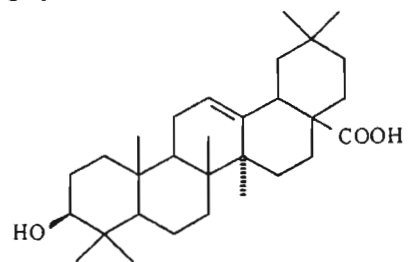




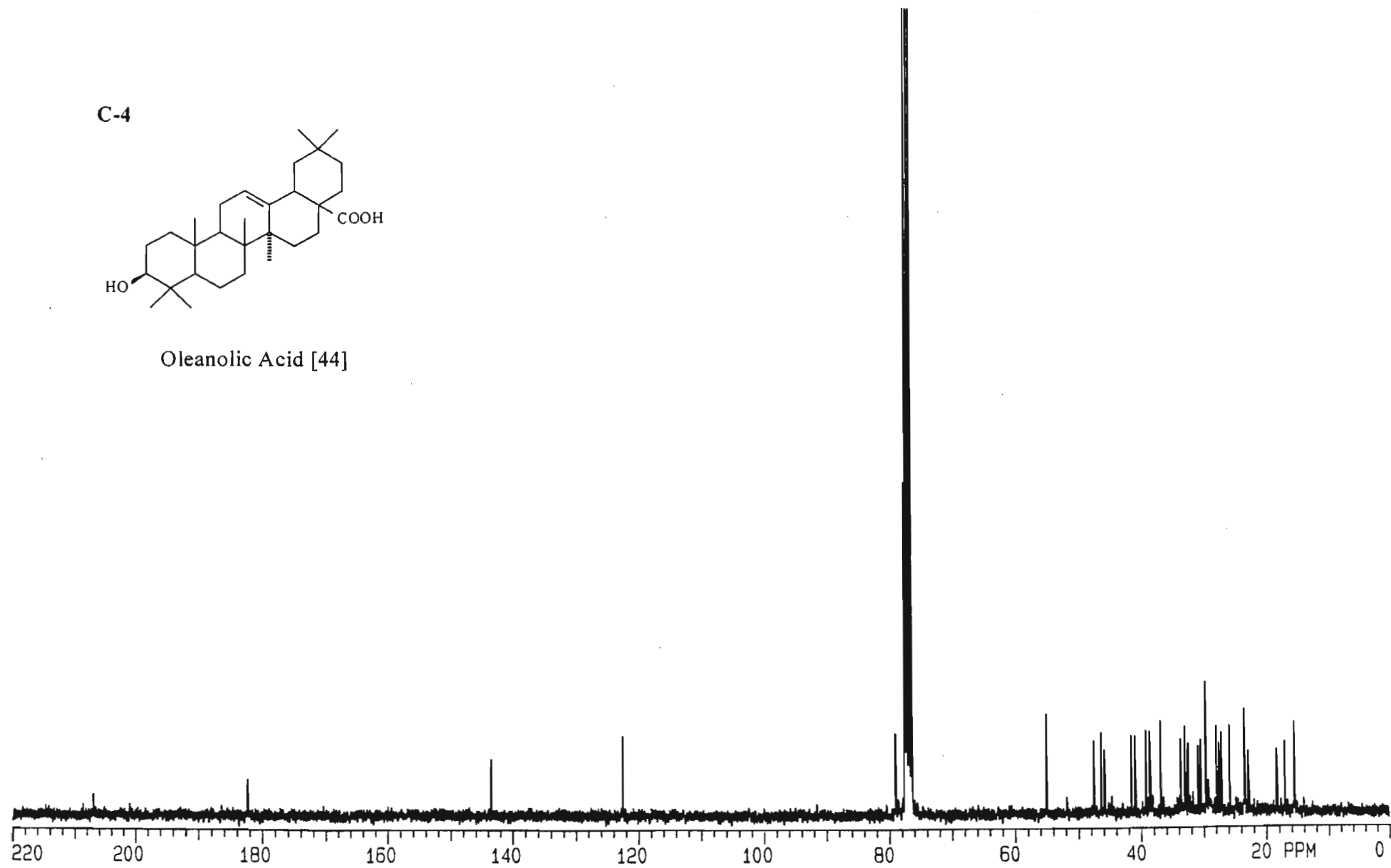
Lupeol [43]



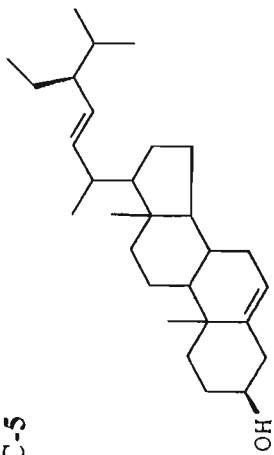
C-4



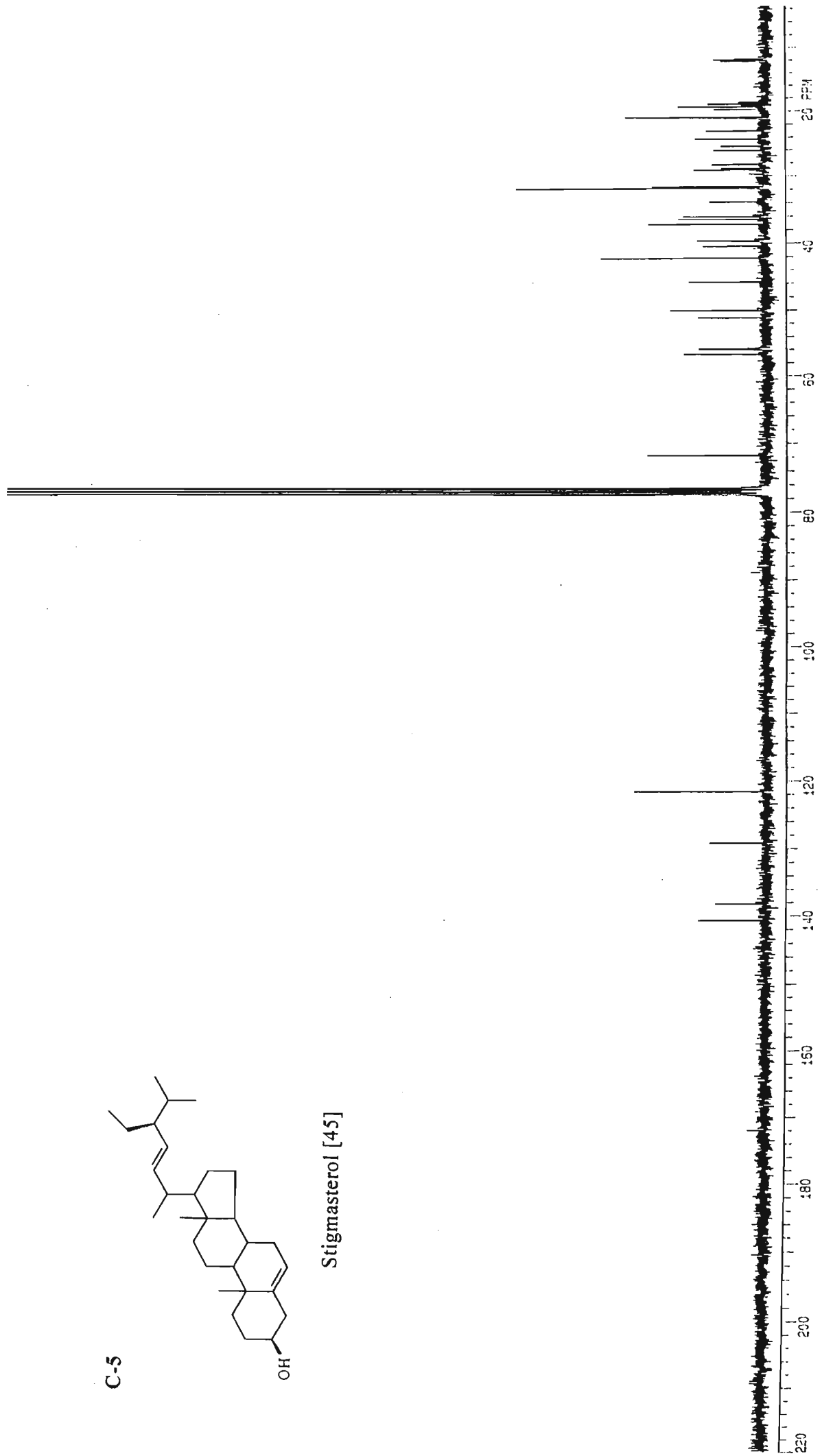
Oleanolic Acid [44]



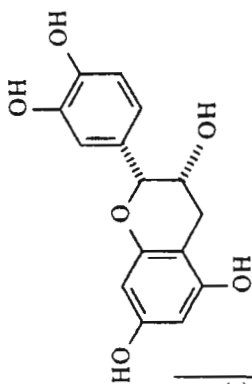
C-5



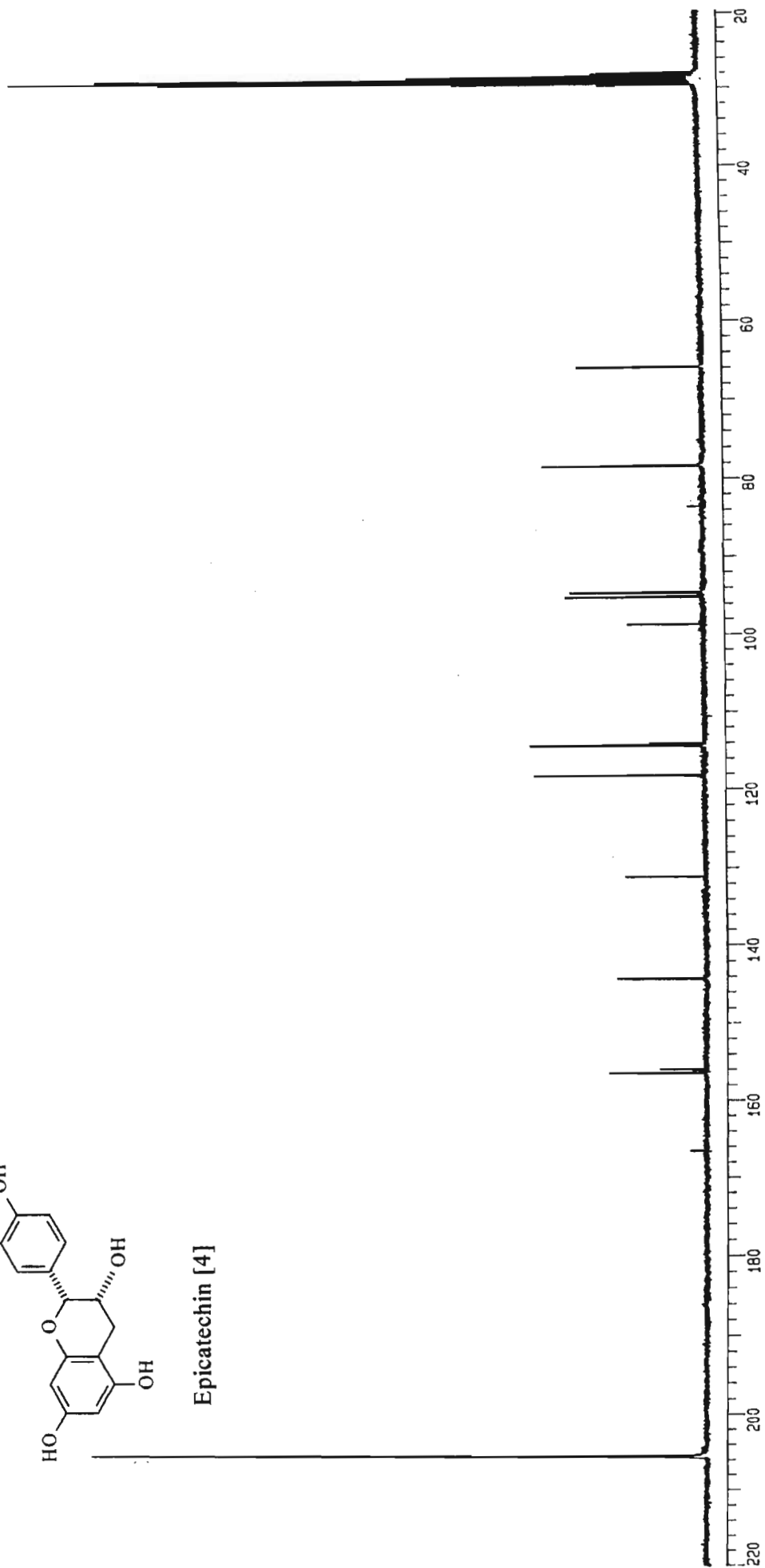
Stigmasterol [45]



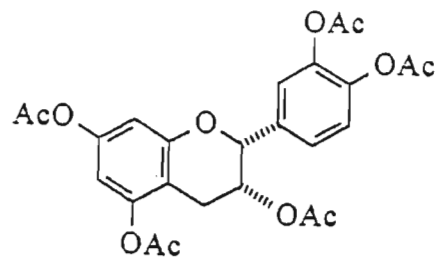
C-6



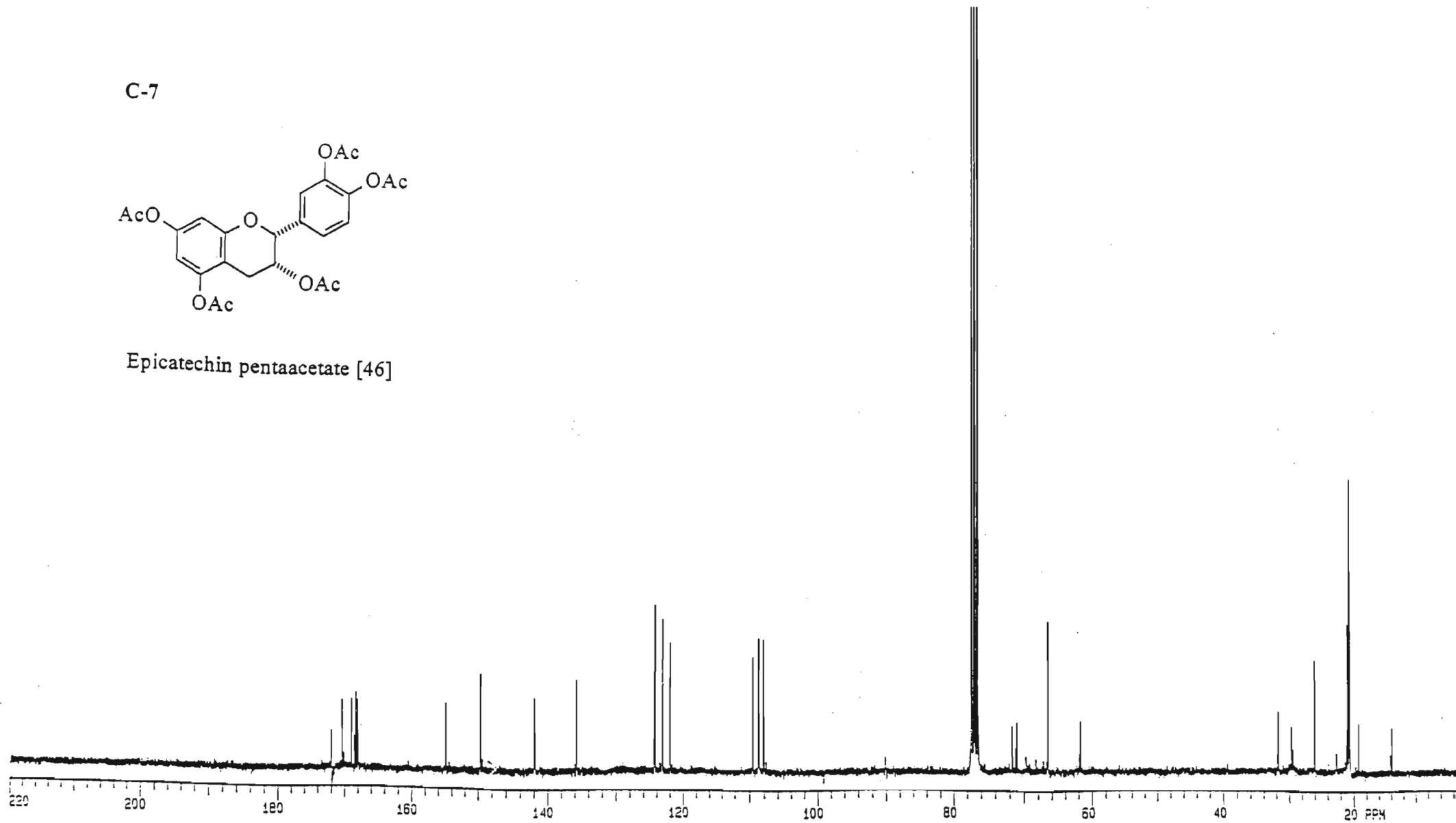
Epicatechin [4]

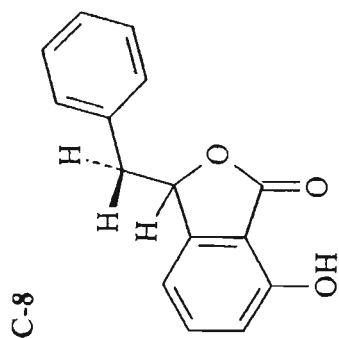


C-7

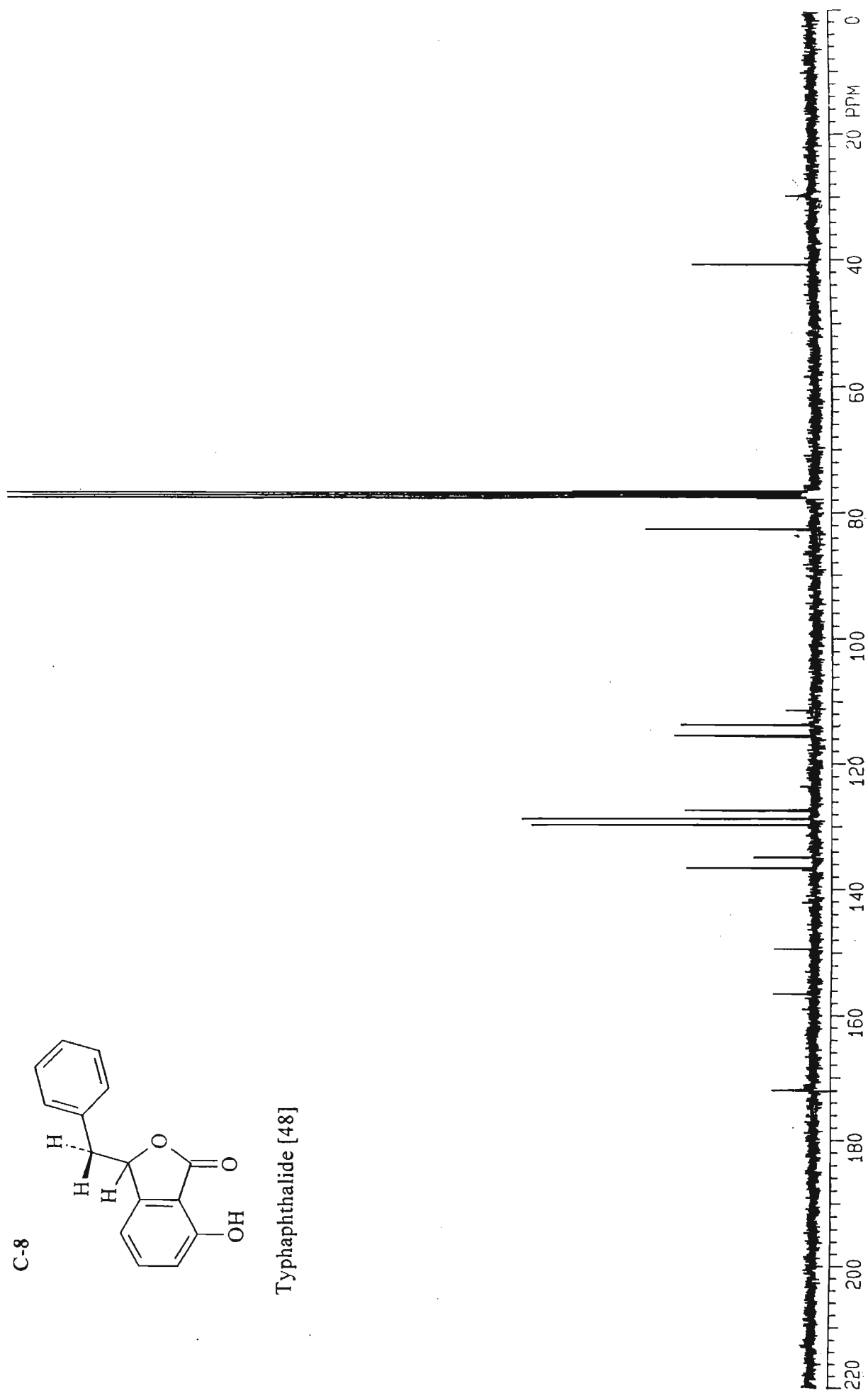


Epicatechin pentacetate [46]

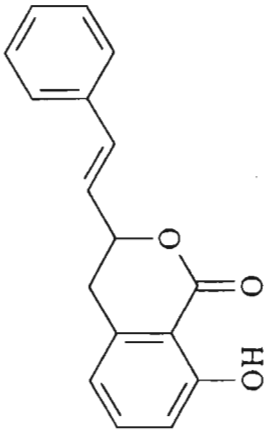




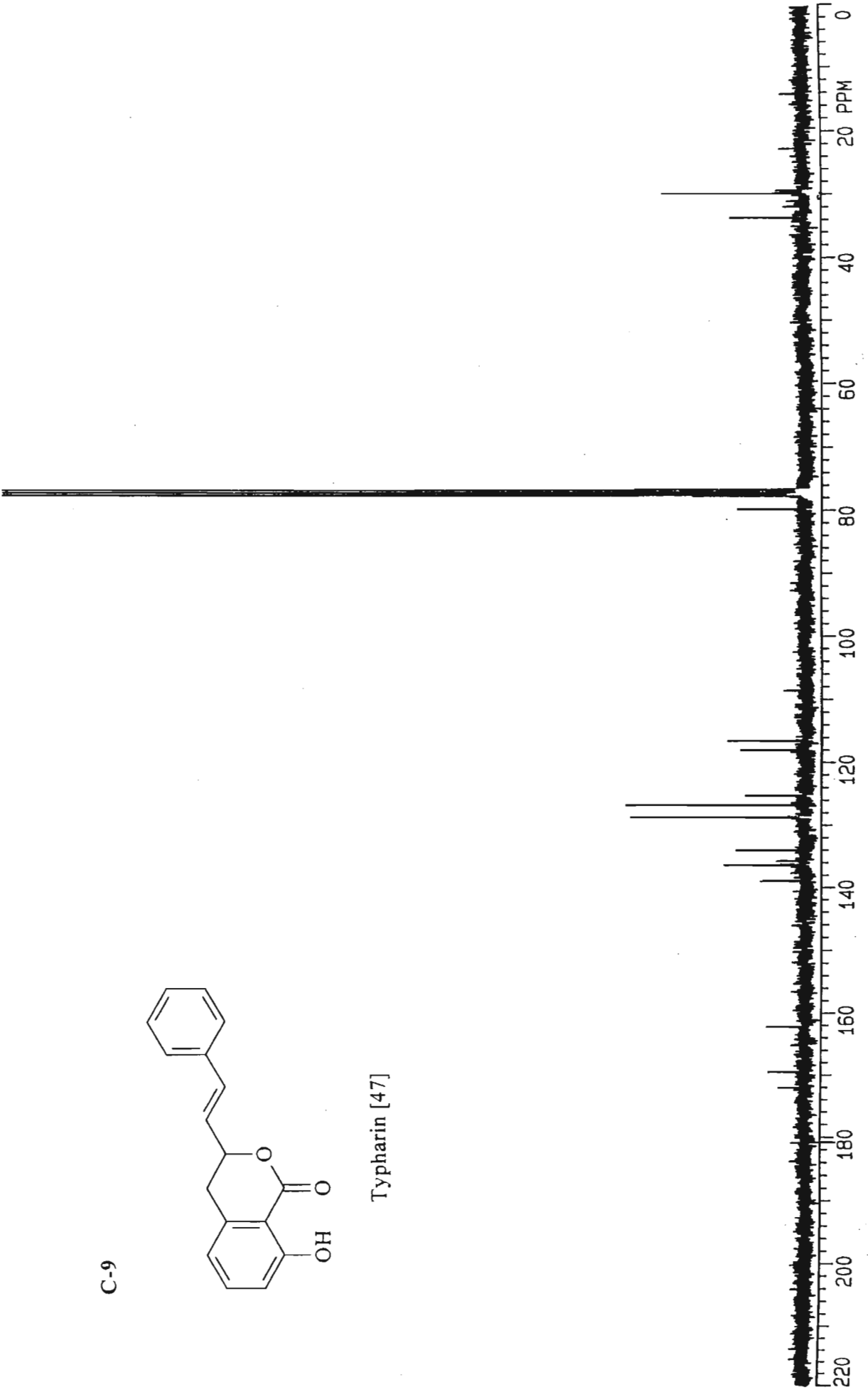
Typhaphthalide [48]



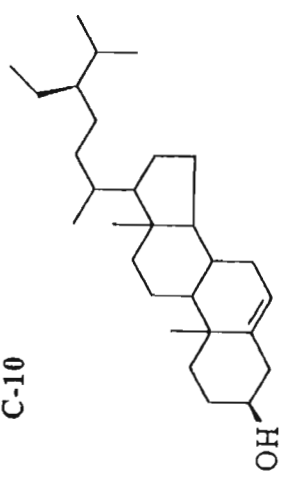
C-9



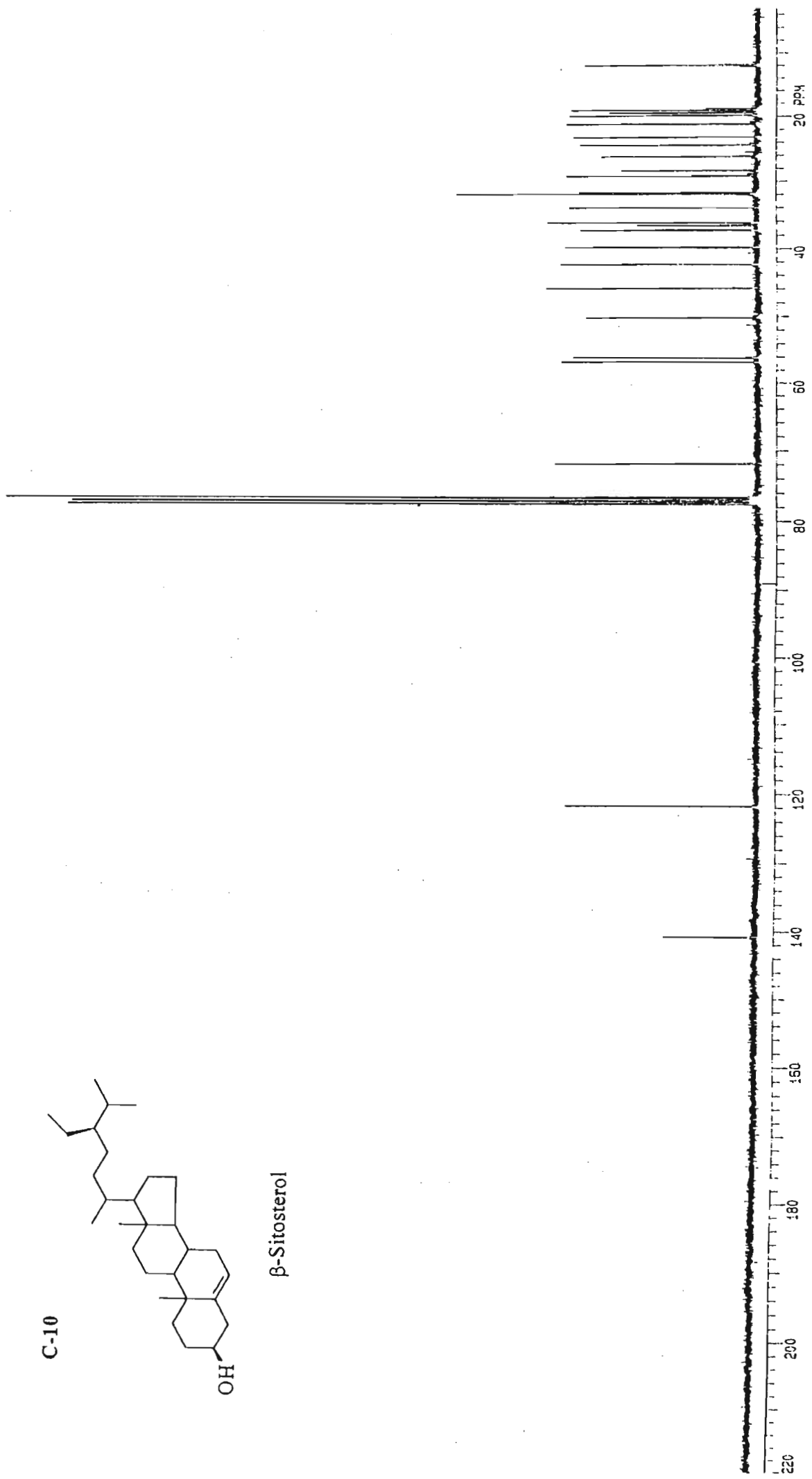
Typharin [47]



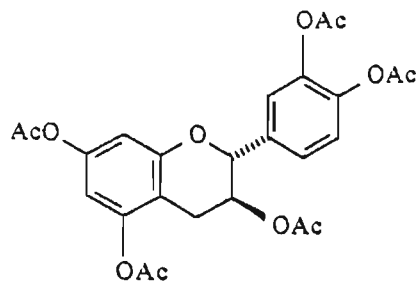
C-10



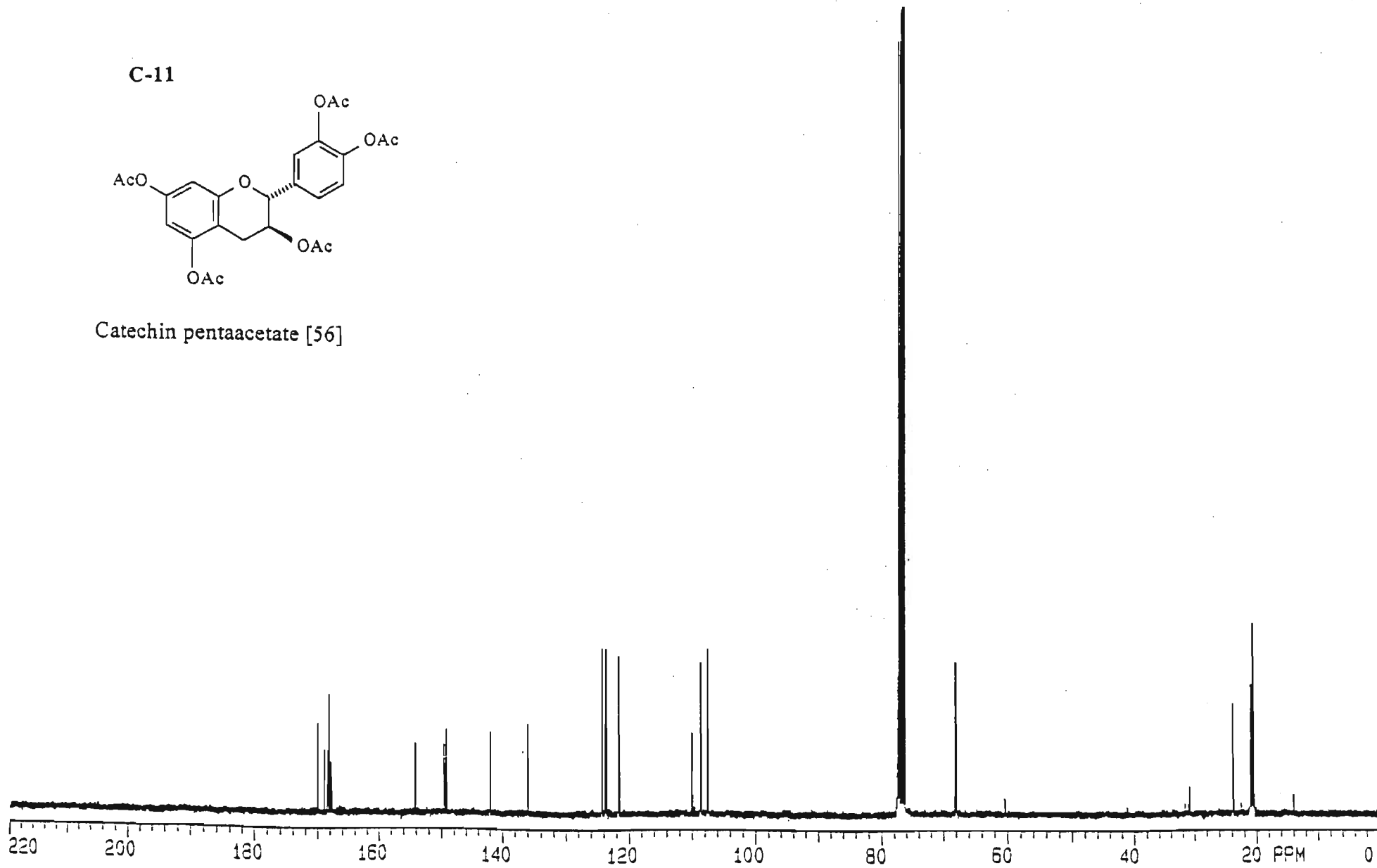
β -Sitosterol



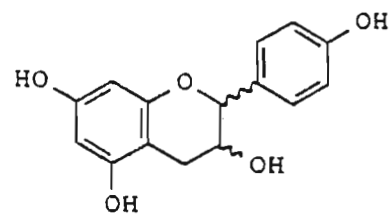
C-11



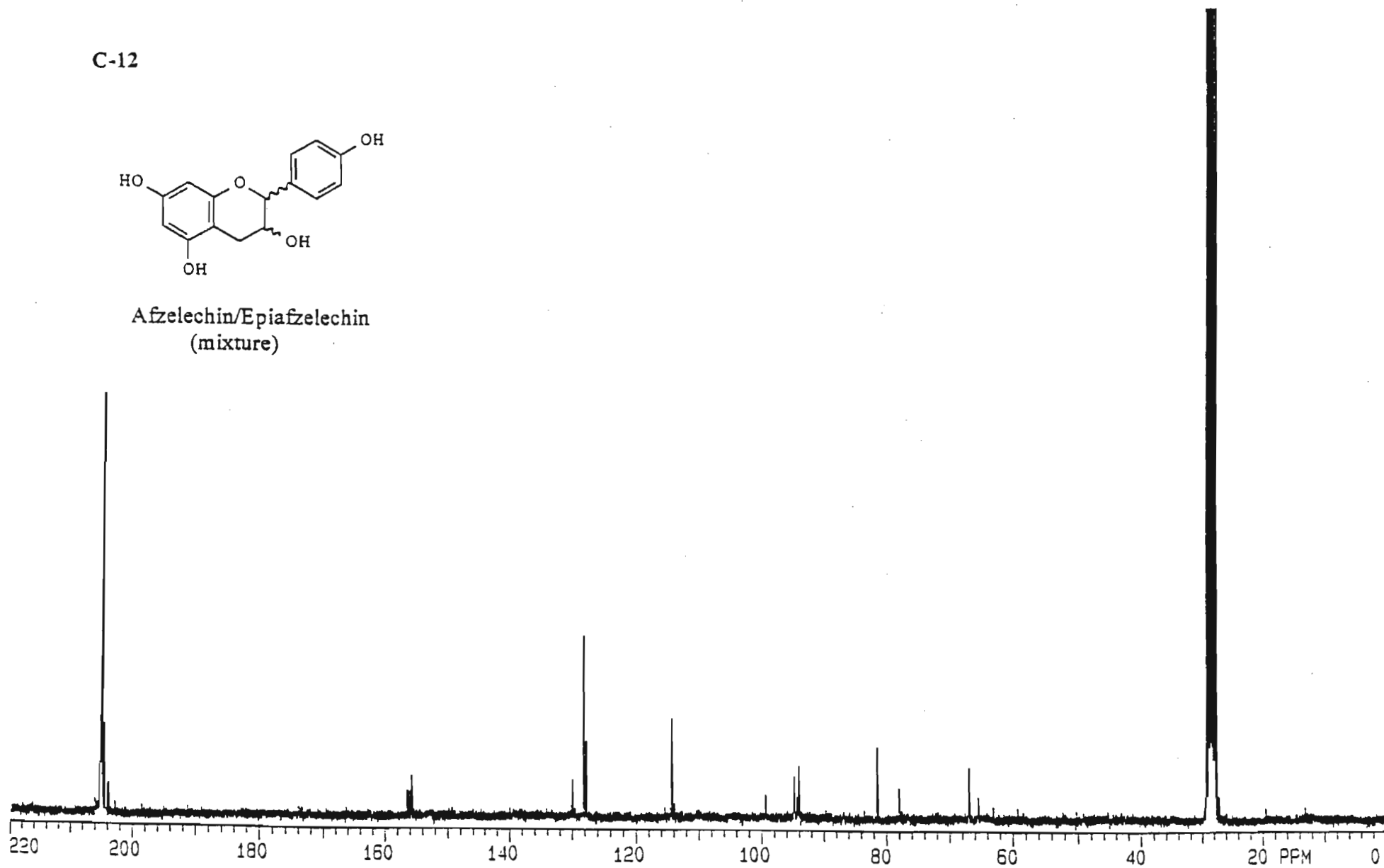
Catechin pentaacetate [56]



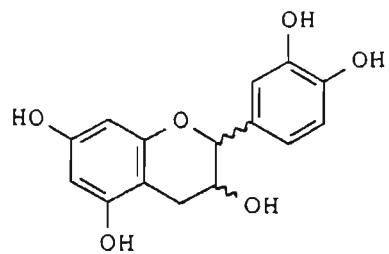
C-12



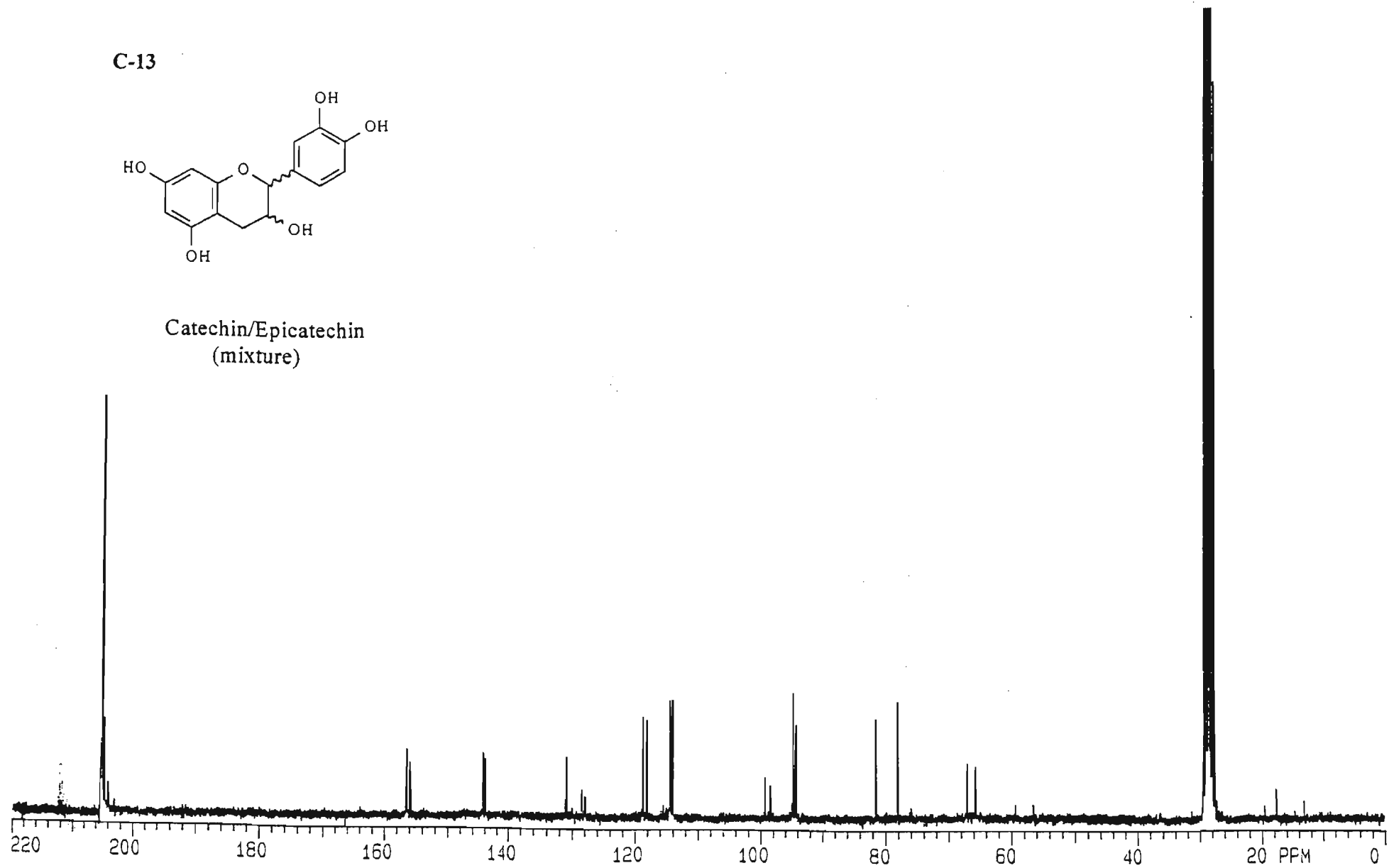
Afzelechin/Epiafzelechin
(mixture)



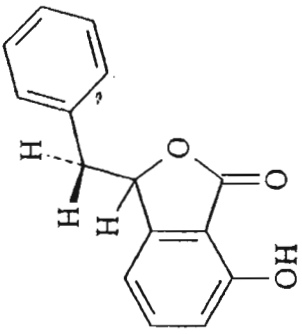
C-13



Catechin/Epicatechin
(mixture)



AD-1



Typhthalide [48]

CH 3



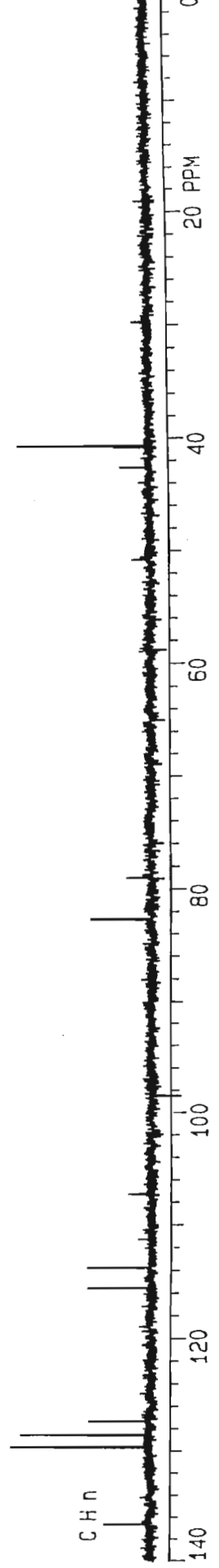
CH 2



C|H



C H n



20 PPM

140

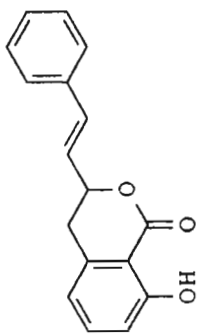
80

60

40

0

AD-2



Typharin [47]

CH 3



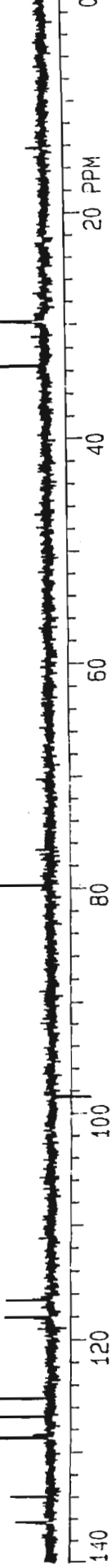
CH 2



CH

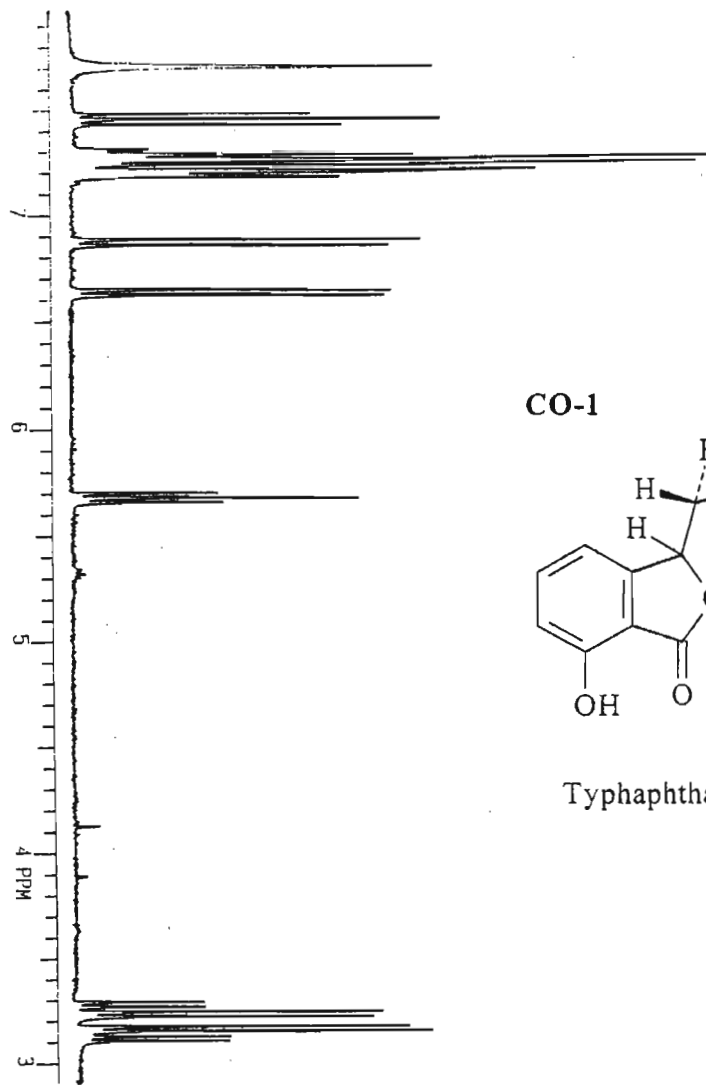
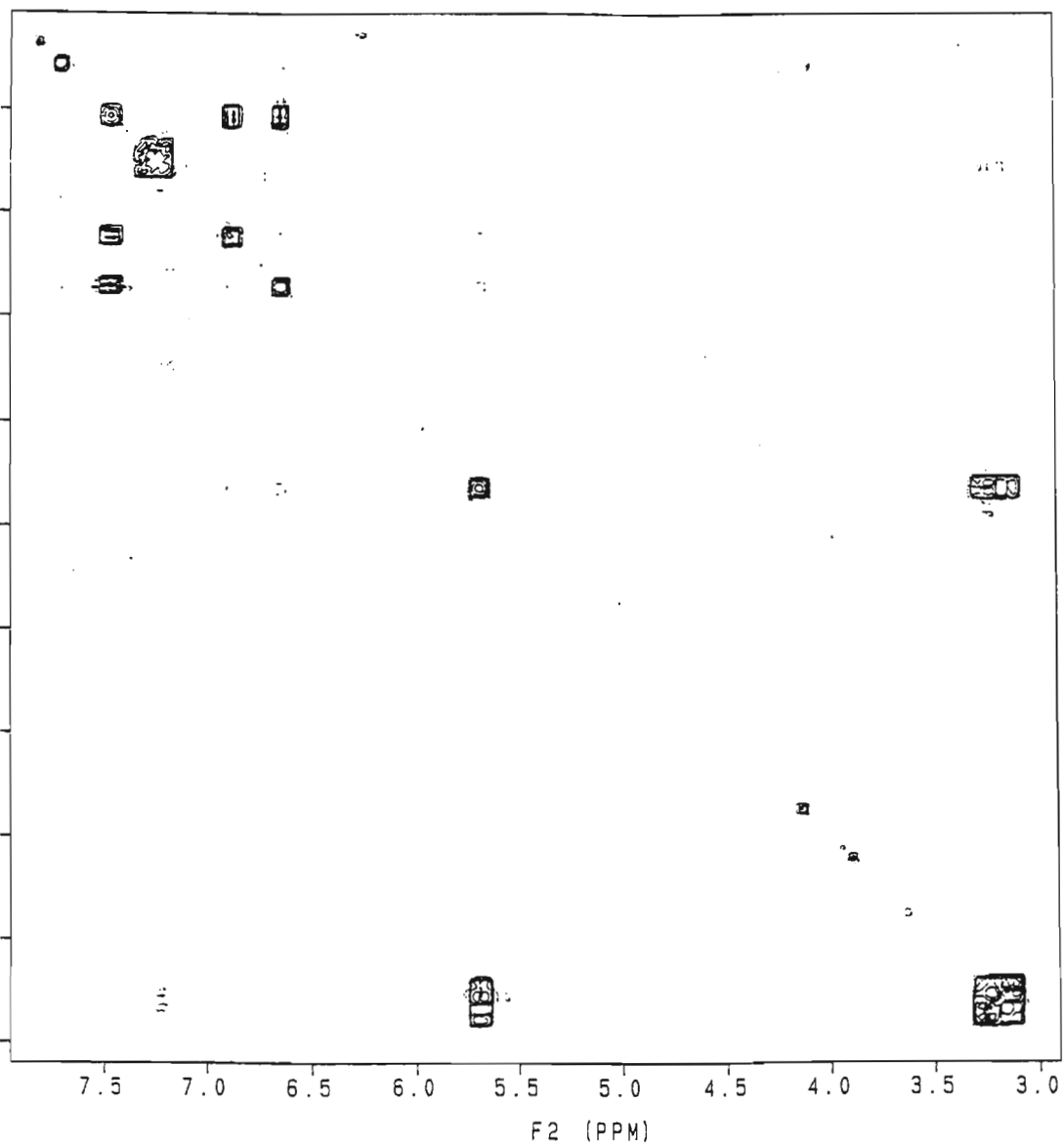


CH n

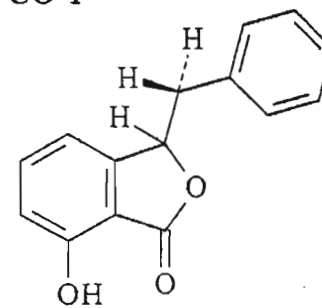


INDEX – 2D - NMR

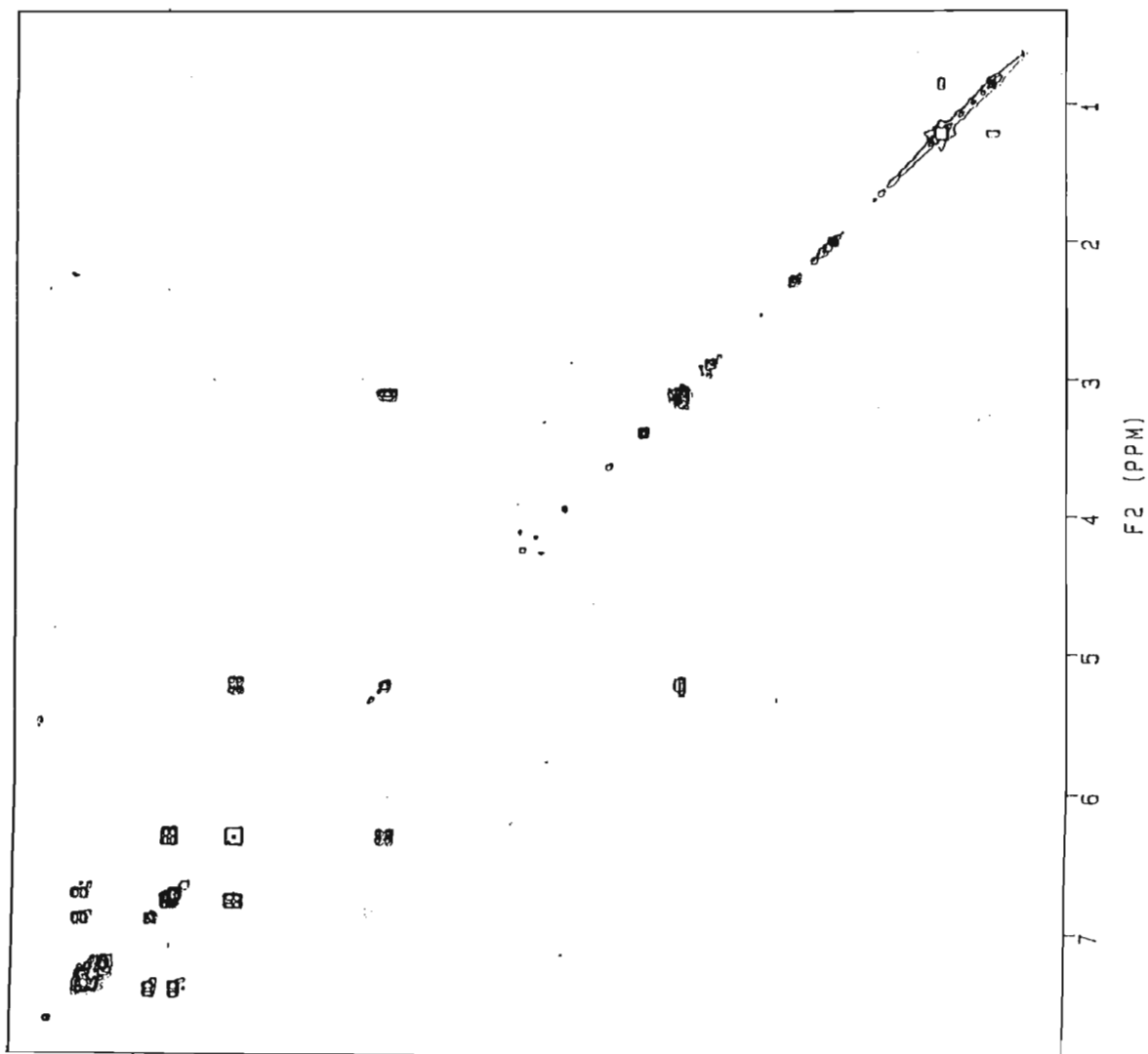
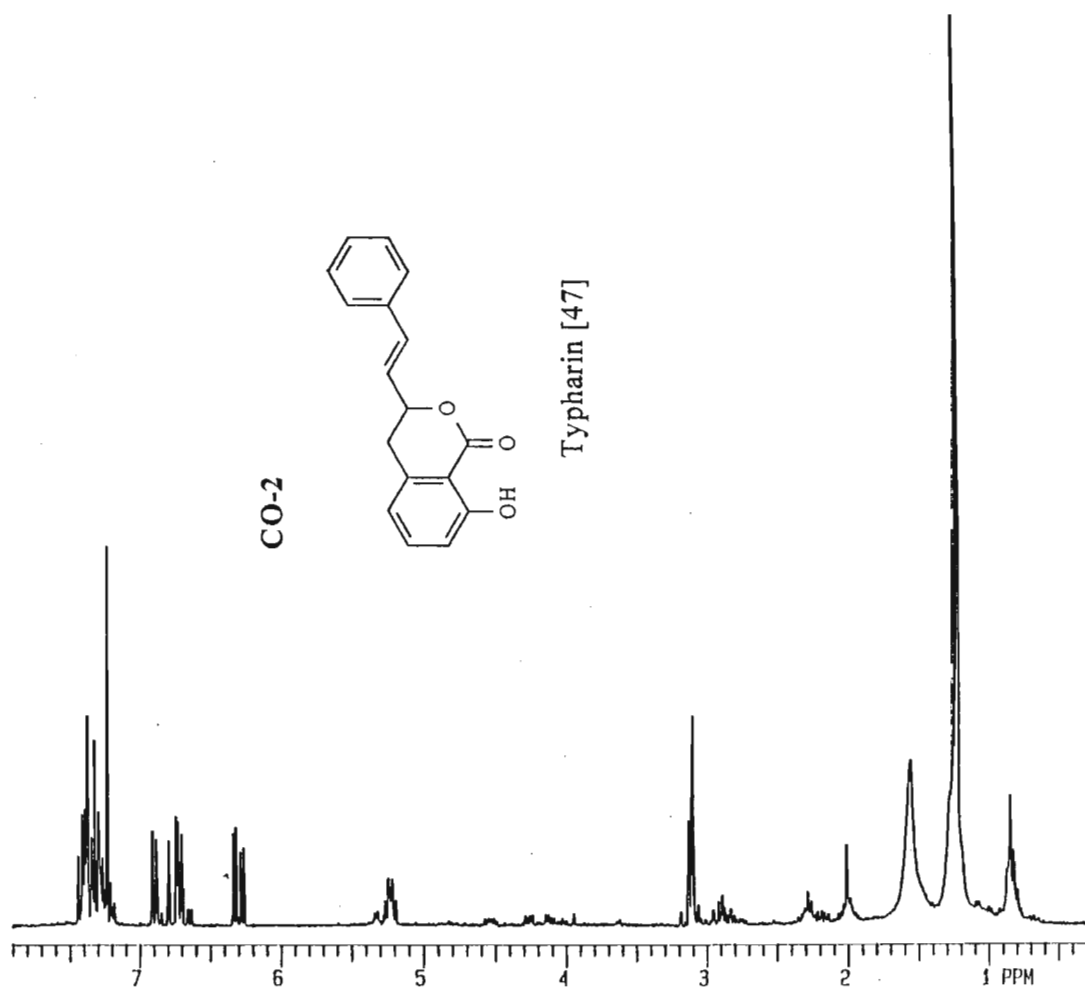
<u>PLATE</u>	<u>COMPOUND</u>	<u>PAGE</u>
<u>COSY</u>		
CO-1	Typhaphthalide	148
CO-2	Typharin	149
<u>HETCOR</u>		
HE-1	Typhaphthalide	150
HE-2	Typharin	151
<u>NOESY</u>		
NO-1	Typhaphthalide	152
NO-2	Typharin	153

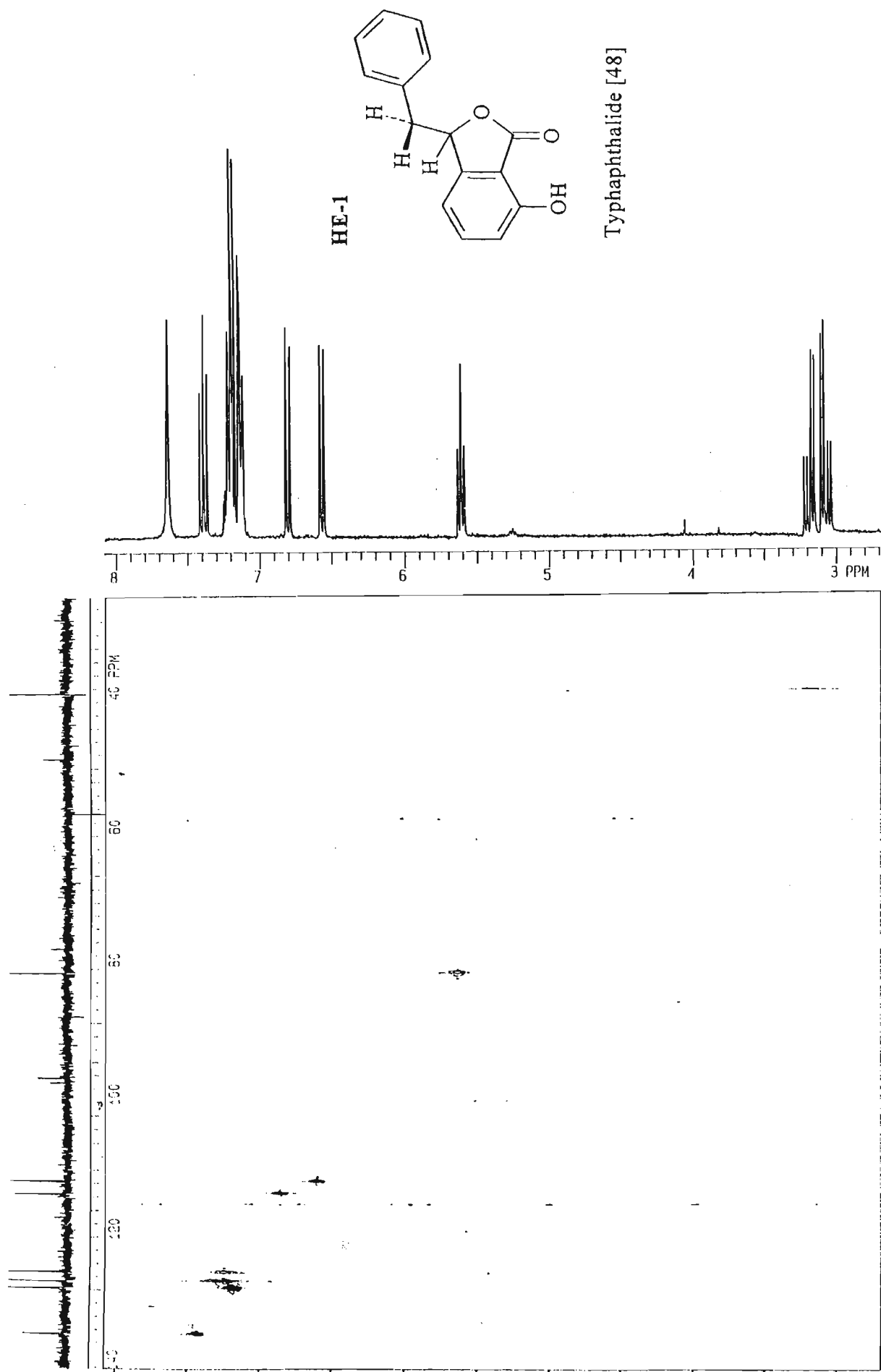


CO-1

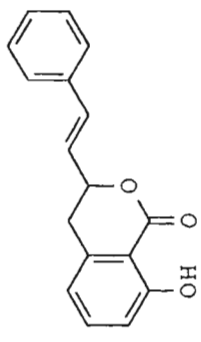


Typhaphthalide [48]

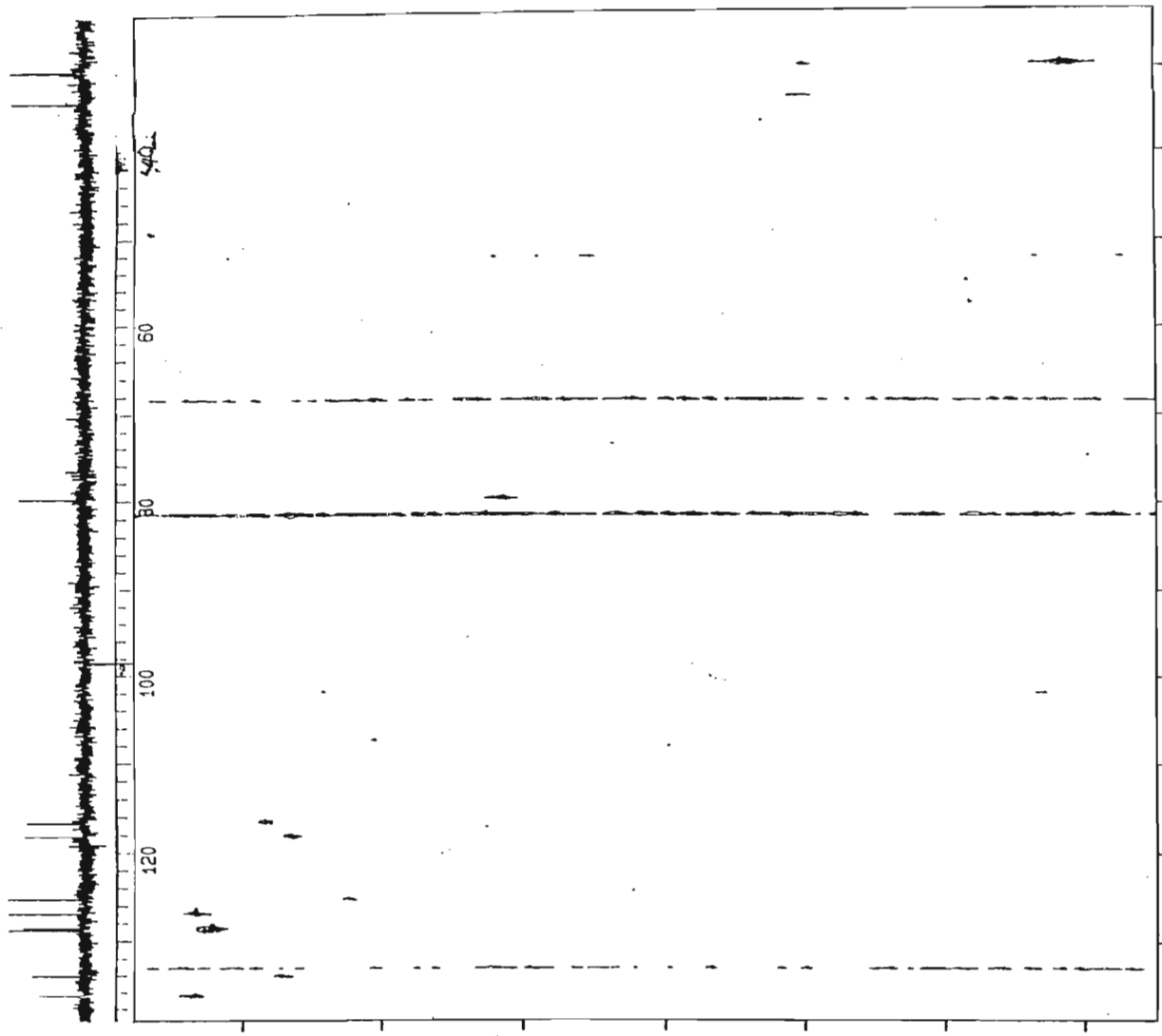
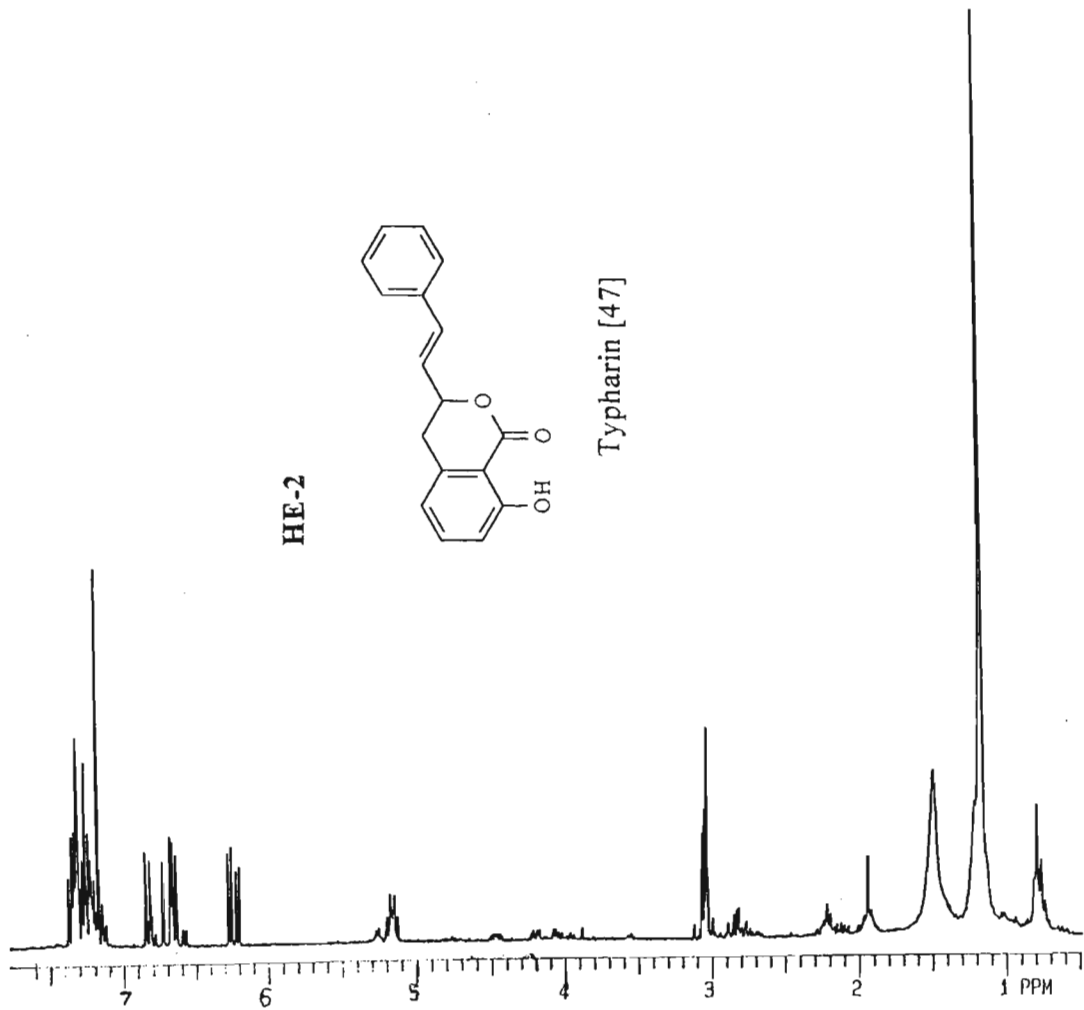




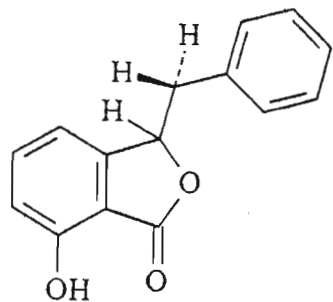
HE-2



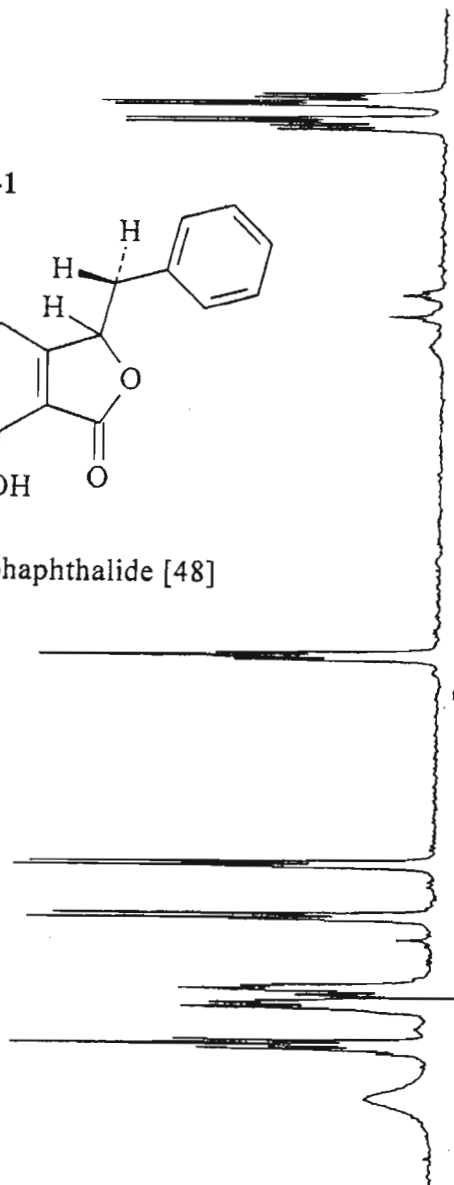
Typharin [47]



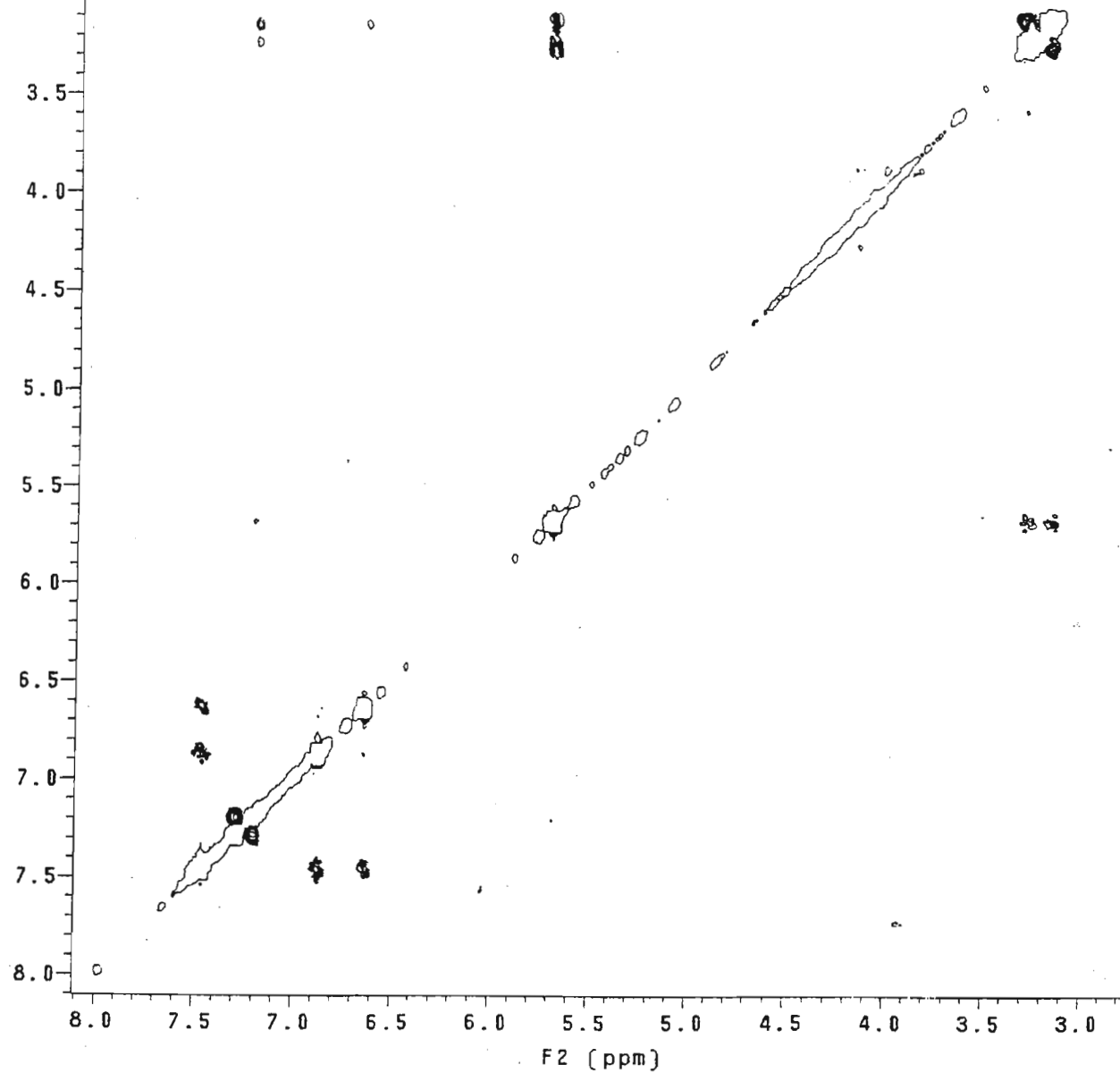
NO-1

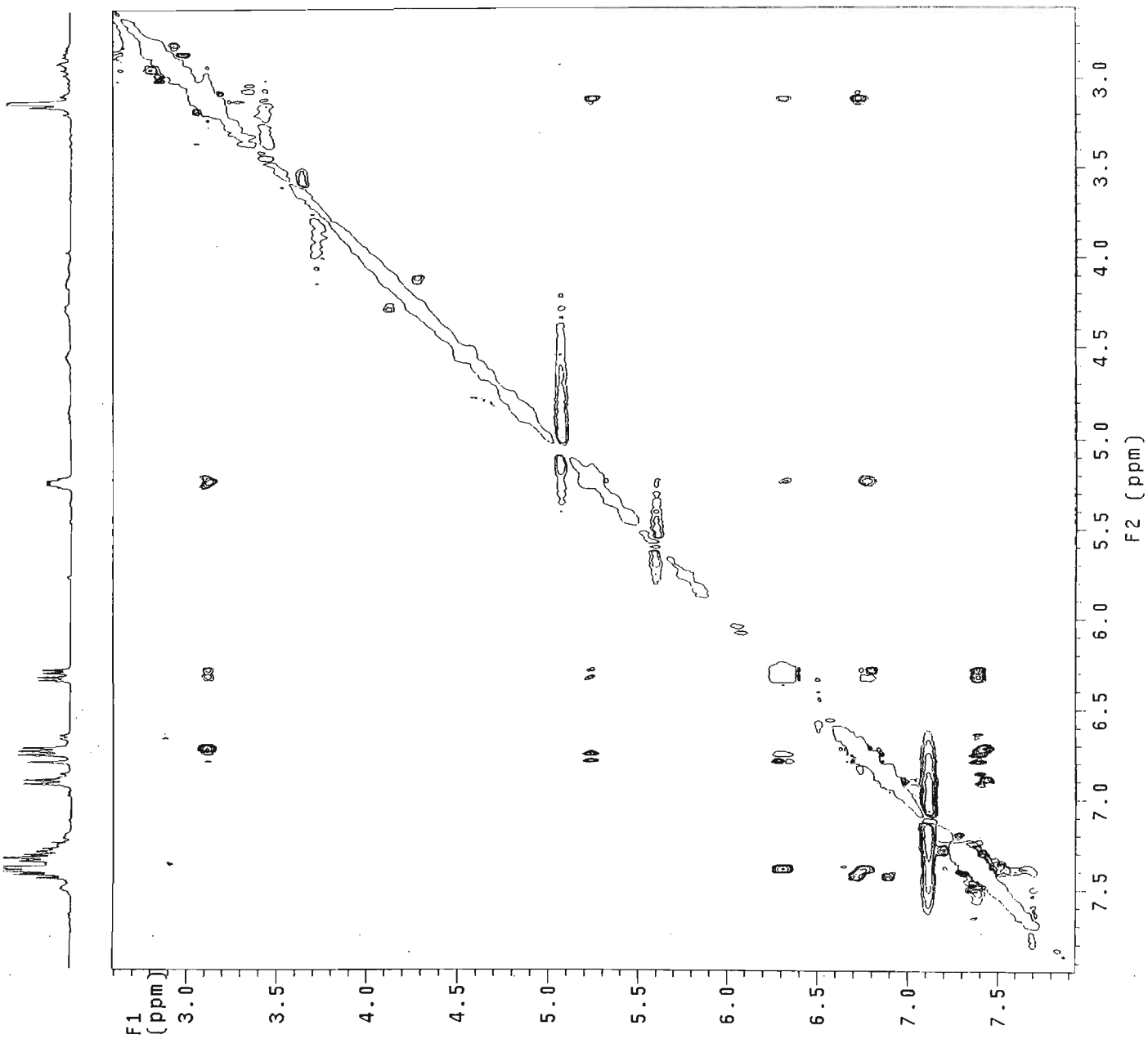


Typhaphthalide [48]

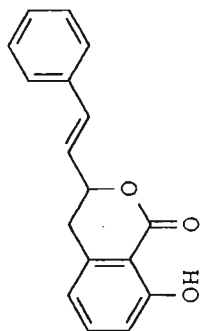


F1
(ppm)





NO-2



Typharin [47]

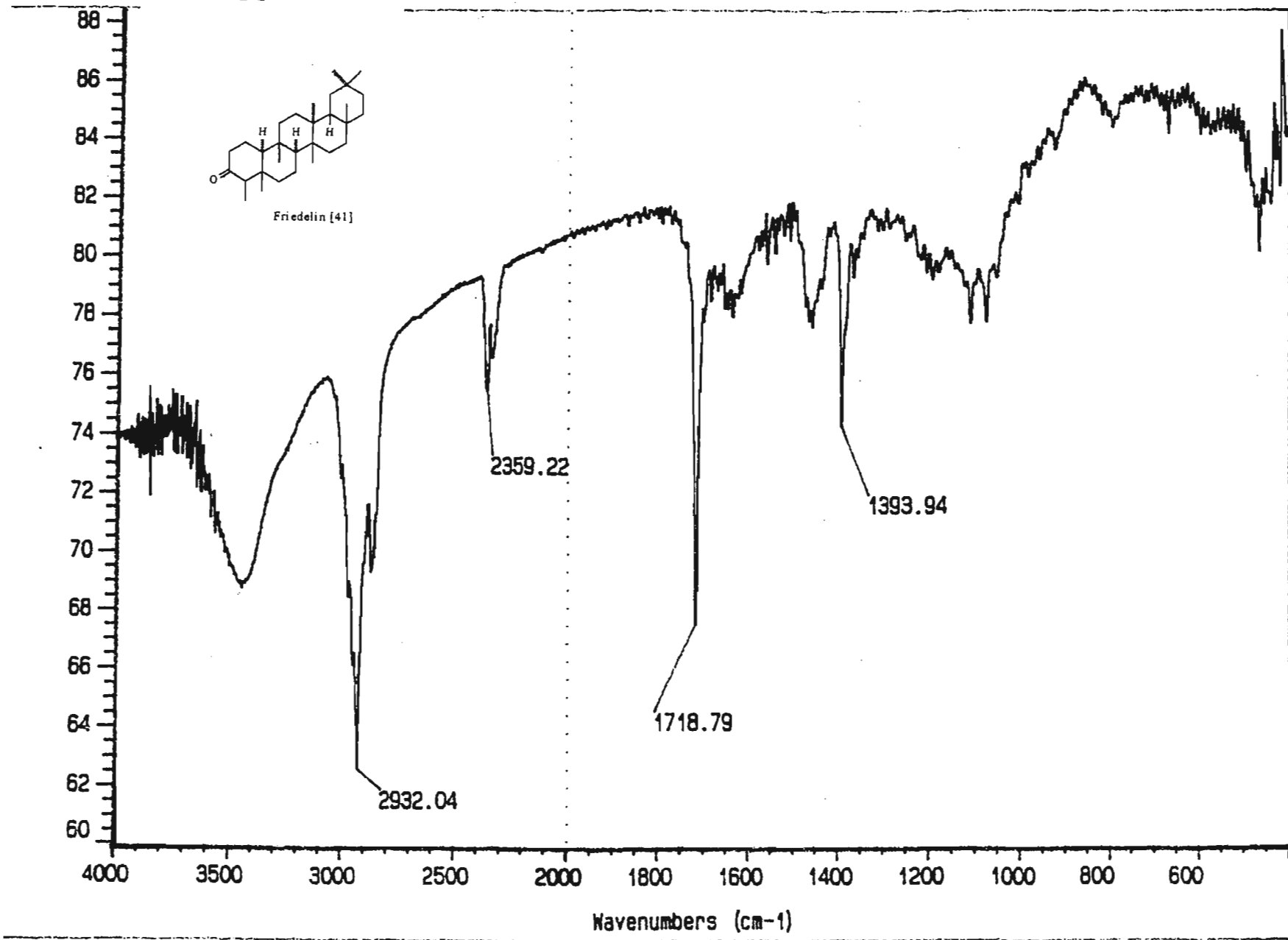
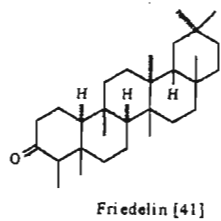
INDEX – INFRARED (IR)

<u>PLATE</u>	<u>COMPOUND</u>	<u>PAGE</u>
I-1	Friedelin [44]	155
I-2	Typhaphthalide [48]	156
I-3	Typharin [47]	157

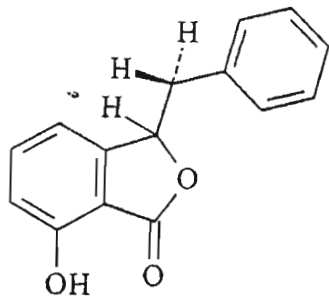
INDEX – MASS SPECTROMETRY (MS)

<u>PLATE</u>	<u>COMPOUND</u>	
MS-1	Friedelin [41]	158
MS-2	<i>epi</i> -Friedelinol [42]	159
MS-3	Typhaphthalide [48]	160
MS-4	Typharin [47]	162
MS-5	Afzelechin tetraacetate [54] / Epiafzelechin tetraacetate [55]	163

I-1

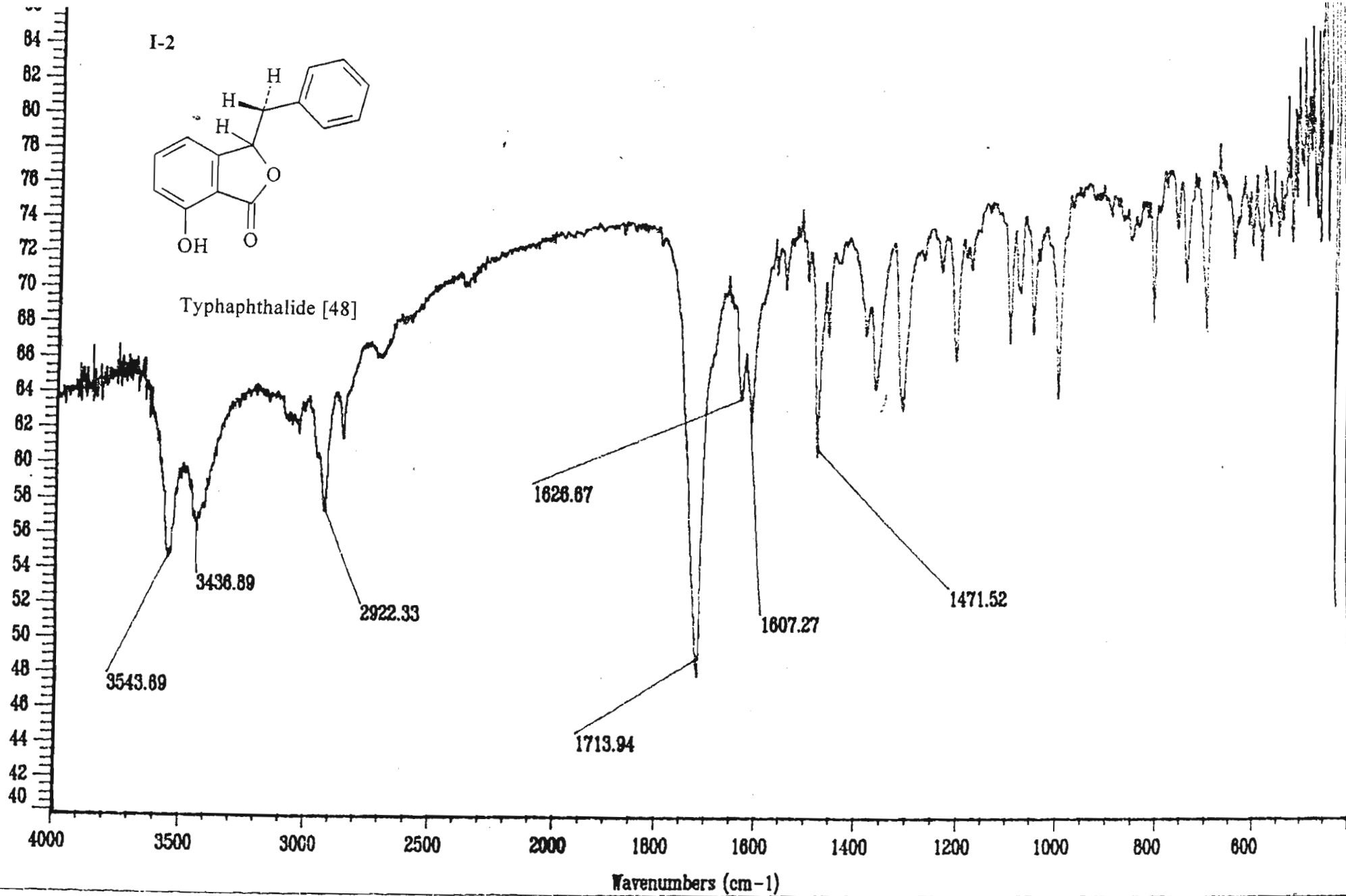


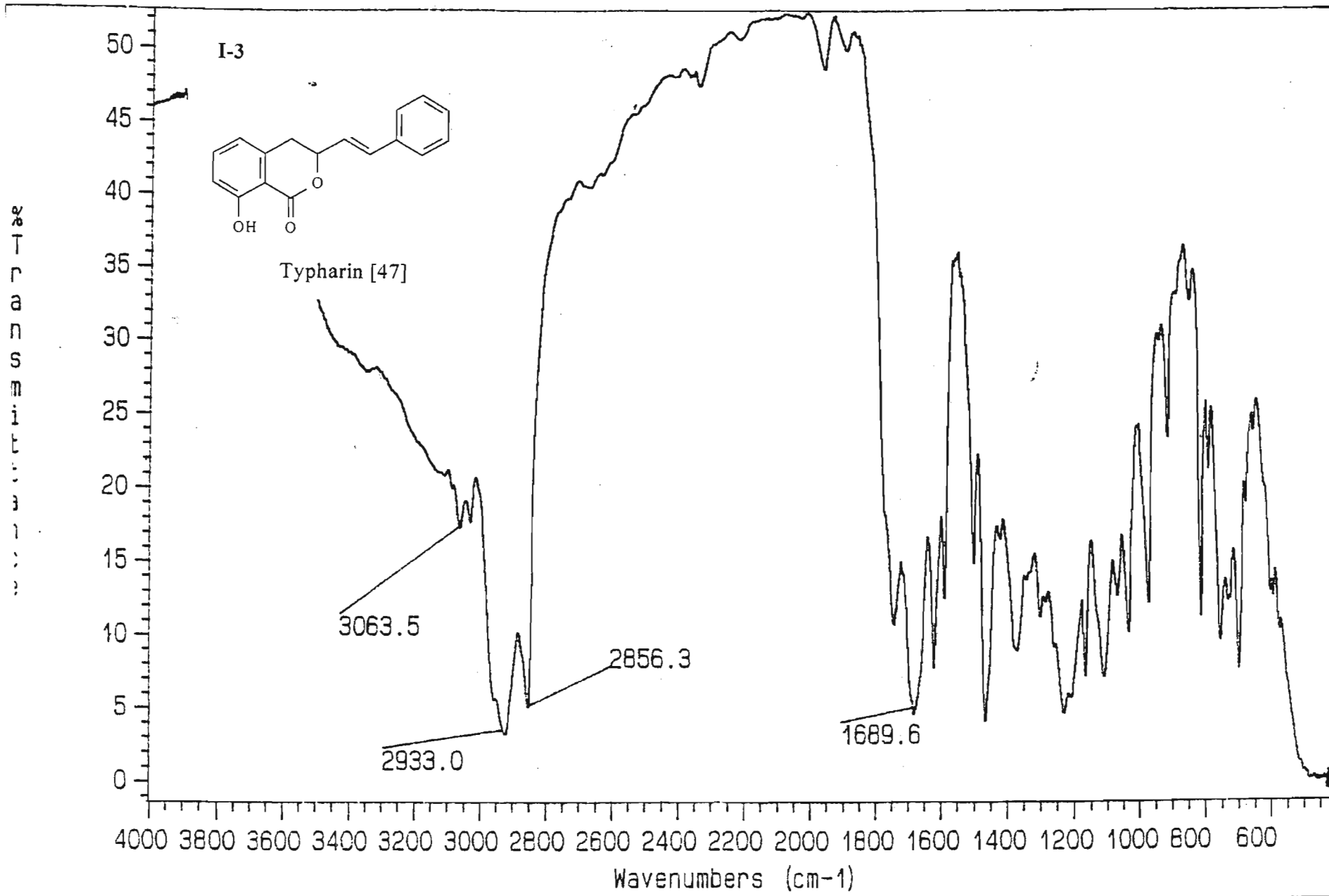
I-2



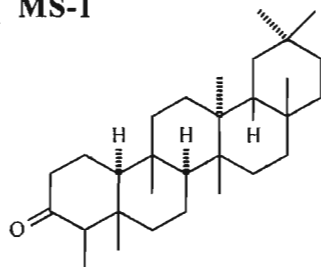
Typhaphthalide [48]

% Transmittance

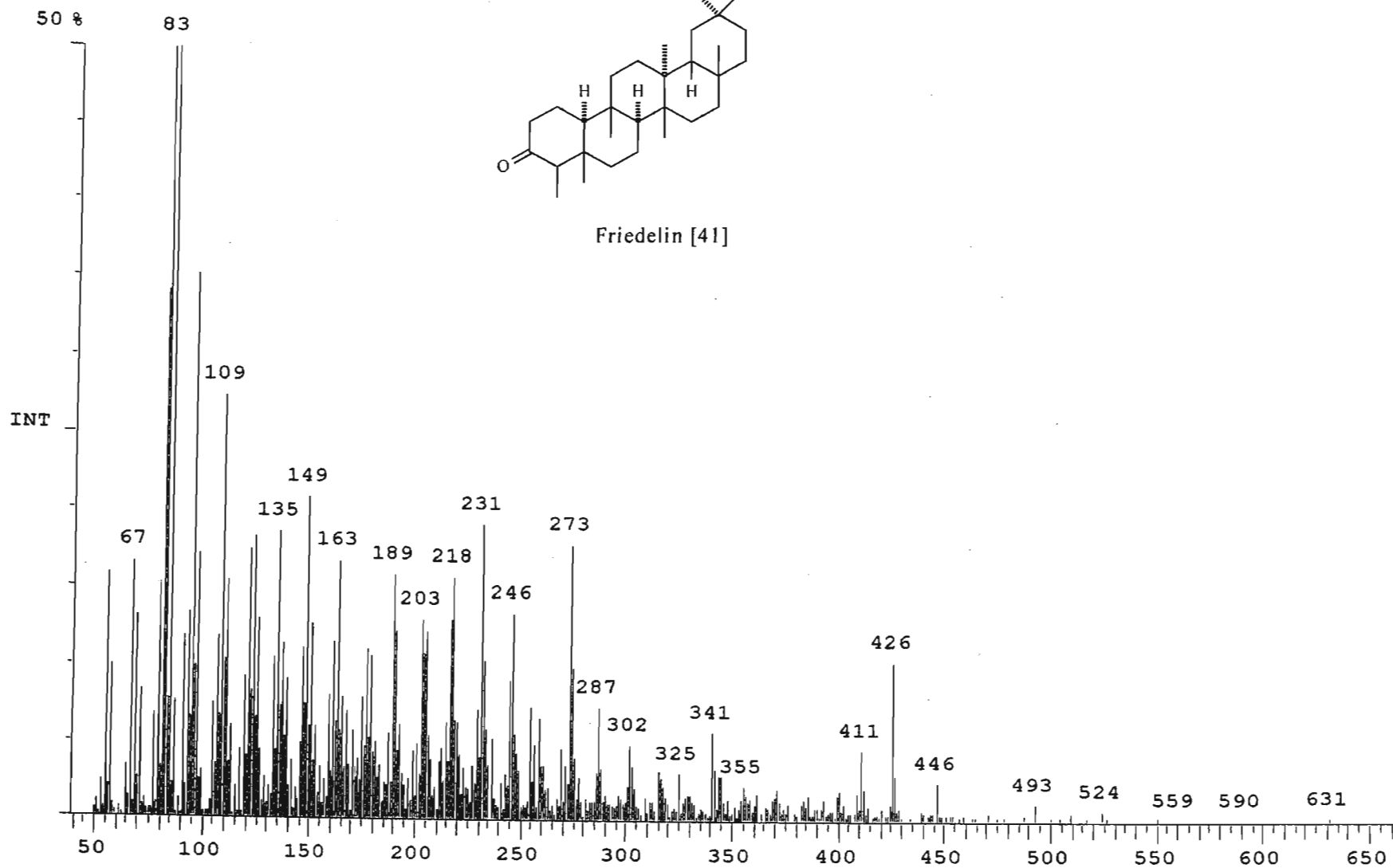




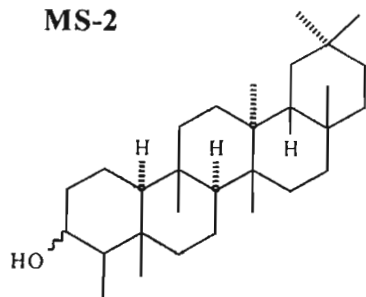
MS-1



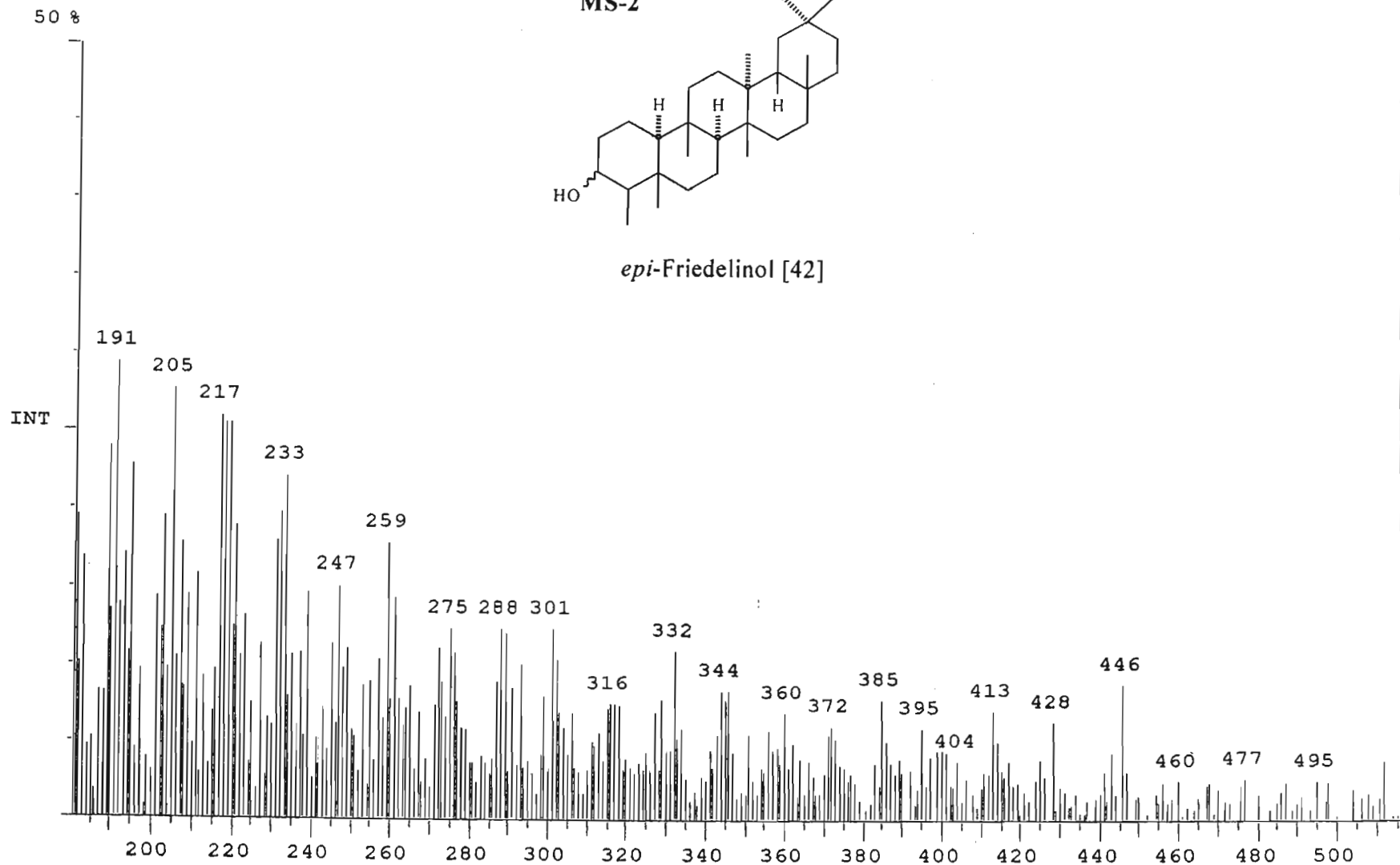
Friedelin [41]

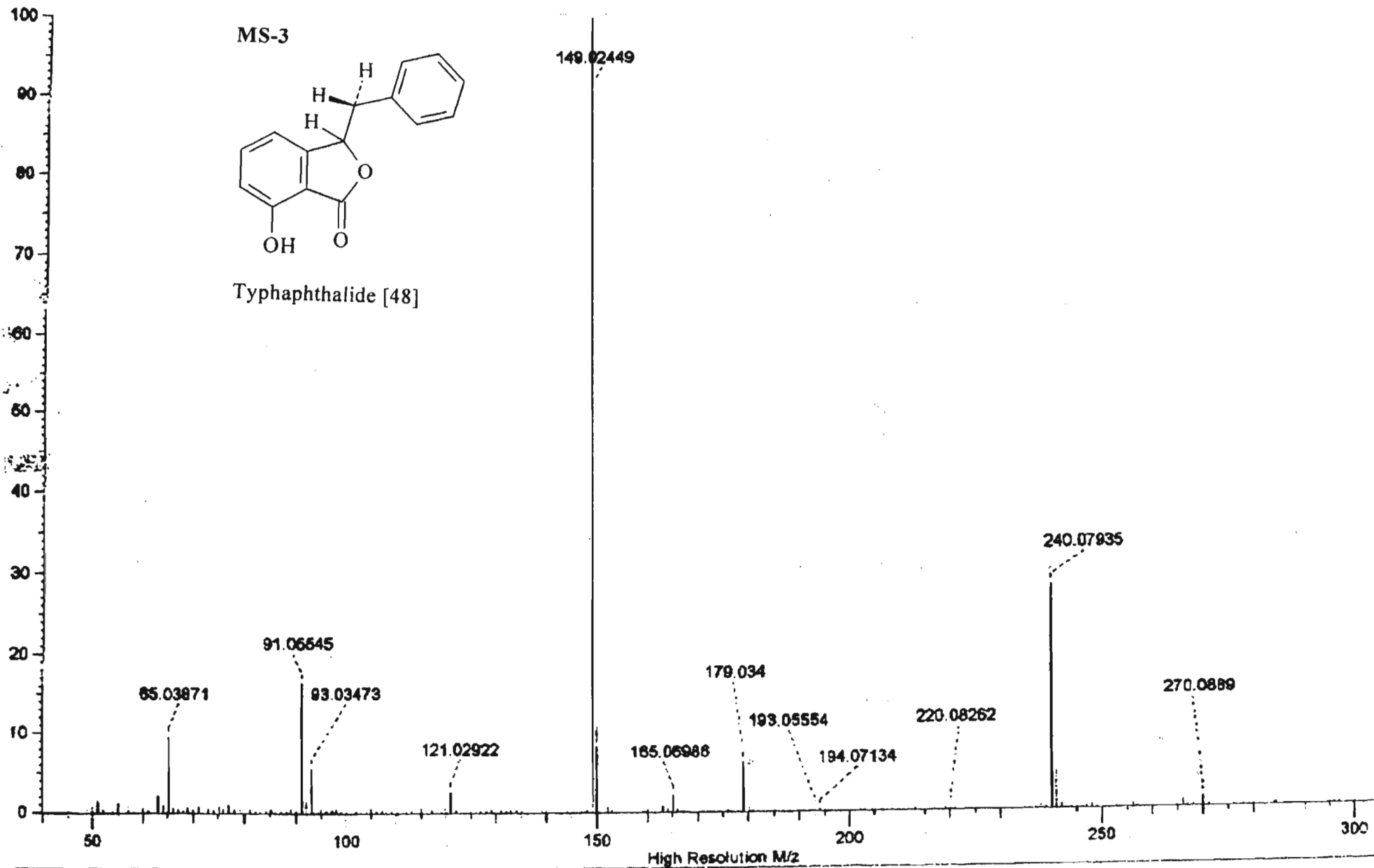


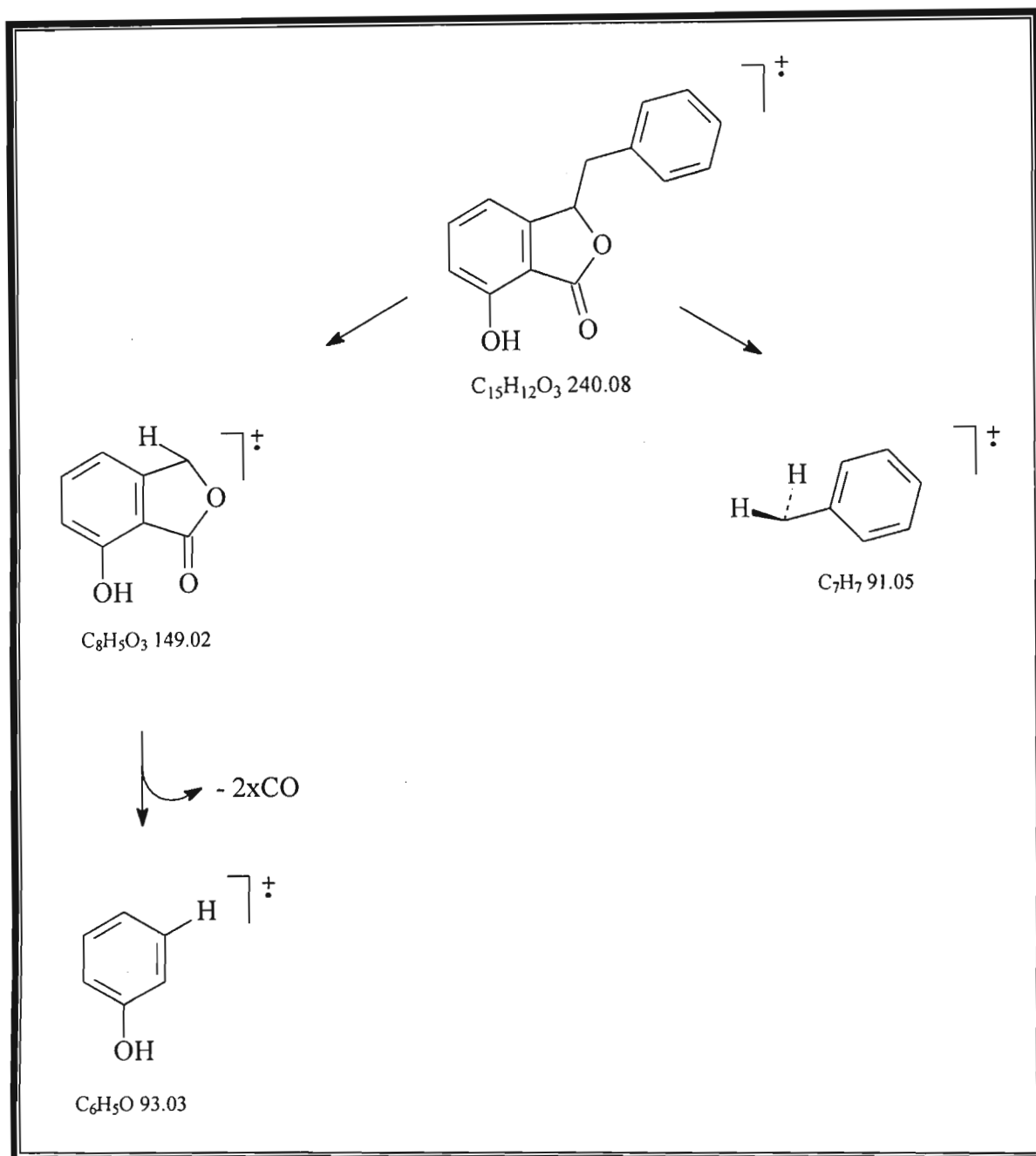
MS-2



epi-Friedelinol [42]

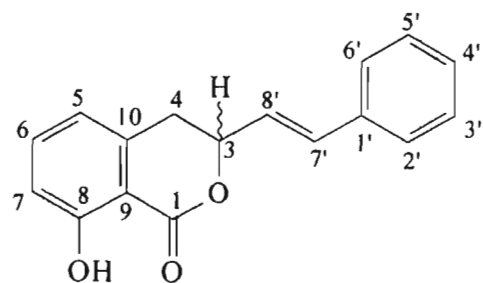




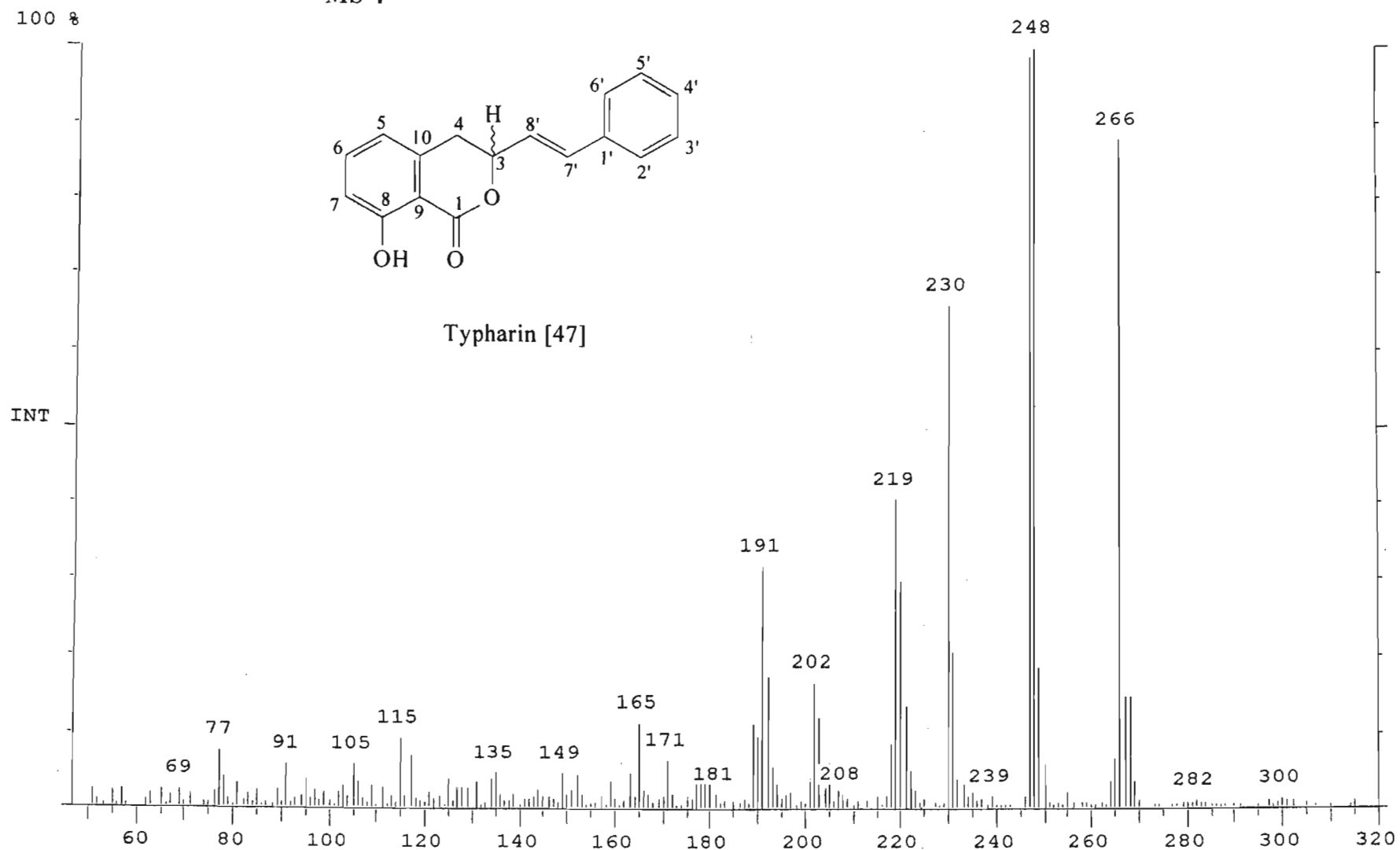


Scheme M1: Fragmentation of Typhaphthalide

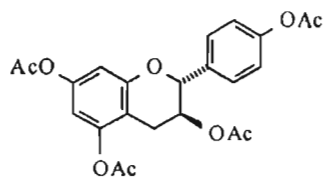
MS-4



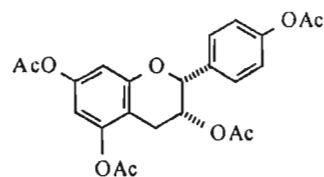
Typharin [47]



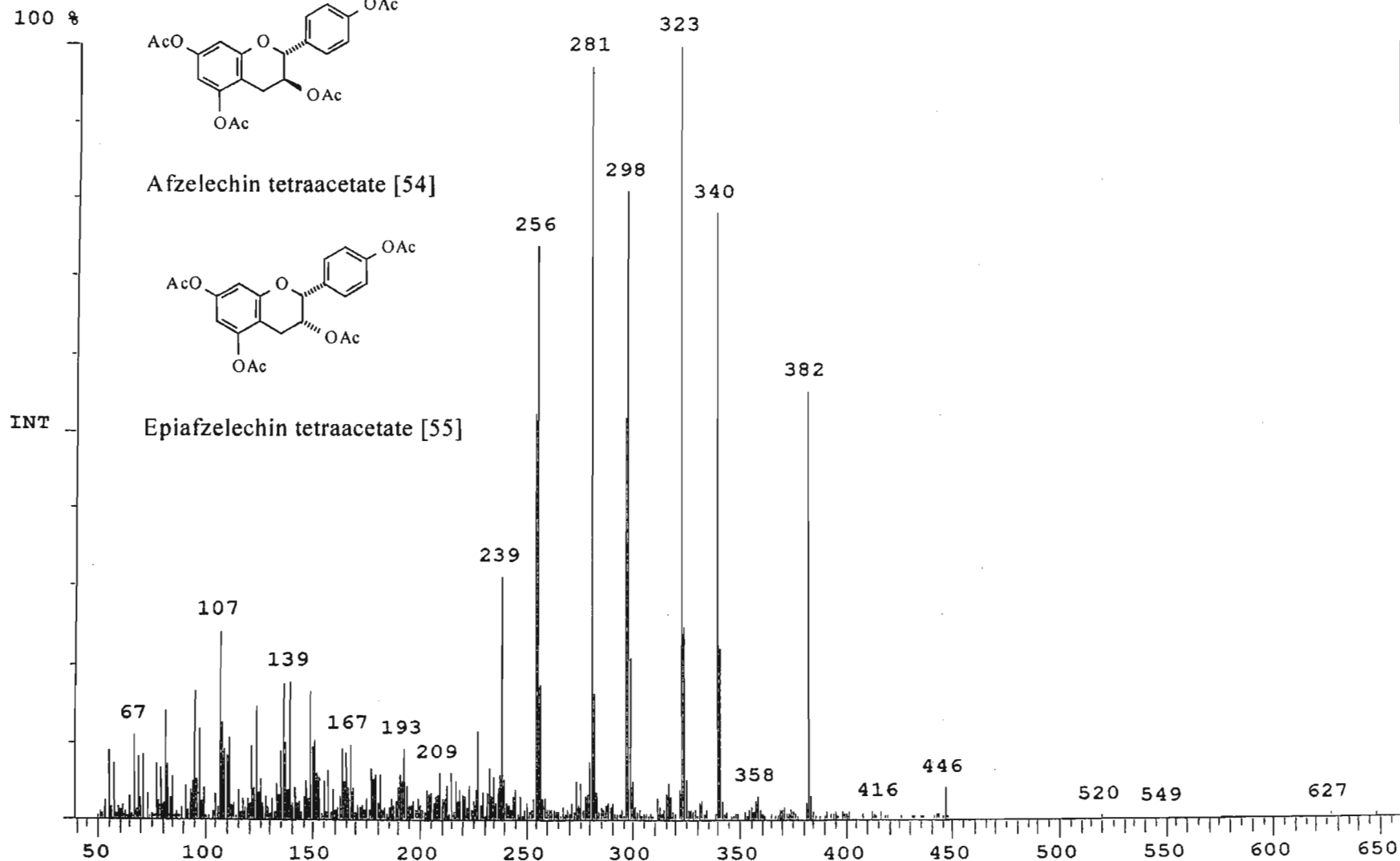
MS-5

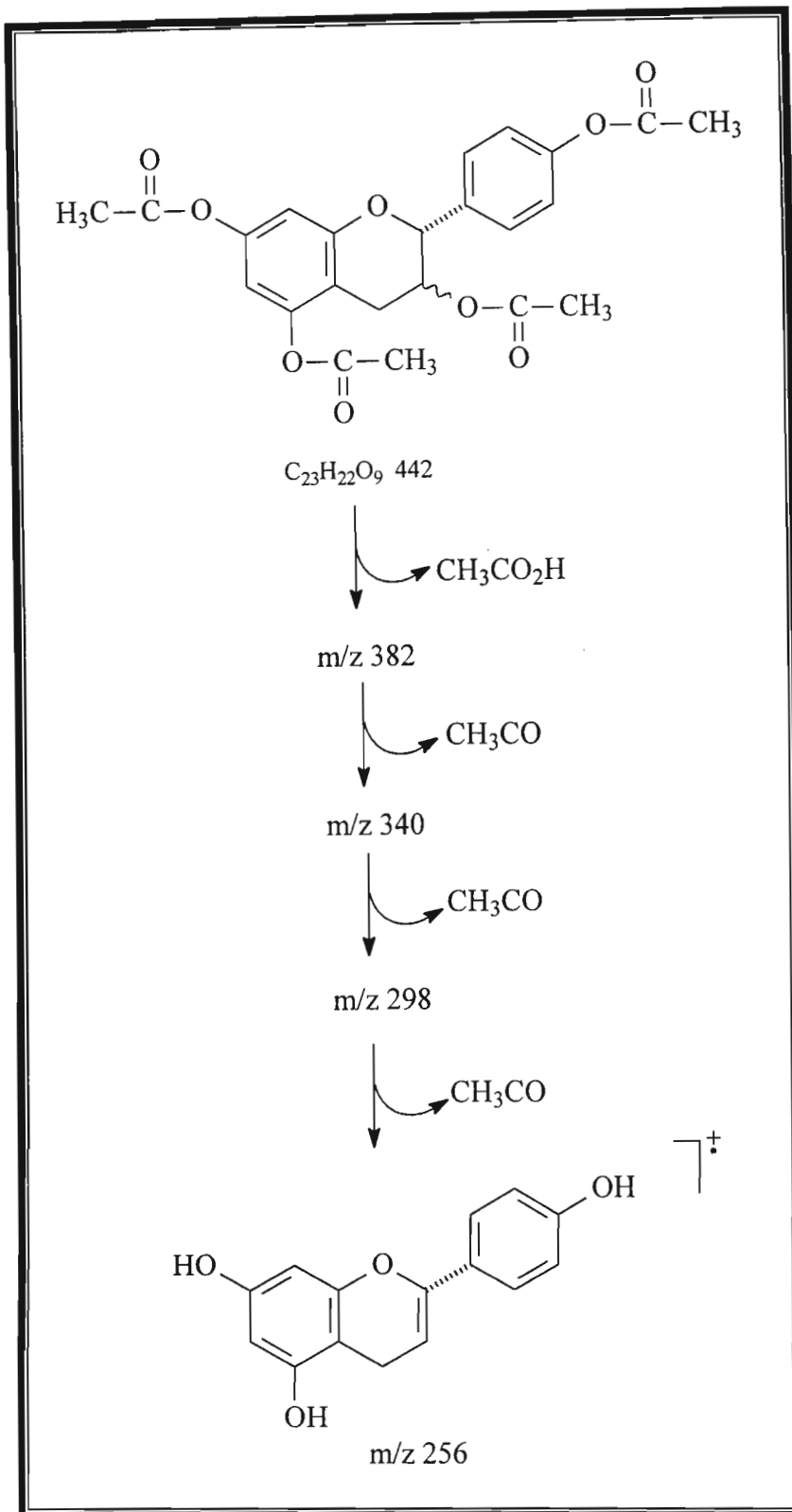


Afzelechin tetraacetate [54]



Epiafzelechin tetraacetate [55]





Scheme M2: Fragmentation pattern of afzelechin/epiafzelechin tetraacetate

INDEX – NMR DATA TABLES

<u>TABLE</u>		<u>PAGE</u>
A1	¹³ C NMR data of pentacyclic triterpenoids from <i>A. natalitius</i>	166
A2	¹ H NMR of afzelechin tetraacetate and epiafzelechin tetraacetate	167
A3	¹ H NMR of catechin pentaacetate and epicatechin pentaacetate	168
A4	¹ H NMR and ¹³ C NMR of typhaphthalide	169
A5	¹ H NMR and ¹³ C NMR of typharin	170
A6	¹ H NMR of stigmasterol	171
A7	¹ H NMR of β-sitosterol	171
A8	¹ H NMR of lupeol	172
A9	¹ H NMR of sucrose	172
A10	¹ H NMR of oleanolic acid	173
A11	¹³ C NMR of epicatechin	173
A12	¹ H NMR of epicatechin	174
A13	¹³ C NMR of epicatechin pentaacetate	174
A14	¹³ C NMR of catechin pentaacetate	175

Table A1: ^{13}C NMR data of pentacyclic triterpenoids from *A. natalitius*

CARBON	FRIEDELIN	FRIEDELINOL	LUPEOL	OLEANOLIC ACID	STIGMASTEROL
1	22.3	15.7	38.7	38.4	37.3
2	41.5	35.0	27.4	27.5	31.7
3	213.2	72.7	78.9	79.0	71.8
4	58.2	49.17	38.8	38.7	42.3
5	42.1	37.1	55.3	55.2	140.8
6	41.3	41.7	18.3	18.3	121.7
7	18.2	17.5	34.2	32.6	31.9
8	53.1	53.2	40.8	39.3	31.9
9	37.4	37.8	50.4	47.6	50.2
10	59.4	61.3	37.1	37.1	36.5
11	35.6	35.3	20.9	23.0	21.1
12	30.5	30.6	25.1	122.6	39.7
13	39.7	39.7	38.0	143.6	42.3
14	38.3	38.3	42.8	41.6	56.9
15	32.4	32.3	27.4	27.7	24.4
16	36.0	36.1	35.5	23.4	28.9
17	30.0	30.0	43.0	46.5	56.1
18	42.8	42.8	48.2	41.0	12.1
19	35.3	35.5	47.9	45.9	19.4
20	28.2	28.2	150.9	30.7	40.5
21	32.7	32.8	29.8	33.8	21.1
22	39.2	39.3	40.0	32.4	138.3
23	6.8	11.6	28.0	28.1	129.4
24	14.6	16.4	15.4	15.6	51.2
25	17.9	18.2	16.1	15.3	31.9
26	20.2	20.1	15.9	17.1	19.0
27	18.6	18.7	14.5	25.9	21.2
28	32.1	32.1	18.0	182.4	25.4
29	35.0	31.8	109.3	33.1	12.3
30	31.8	35.2	19.3	23.6	

Table A2: ^1H NMR (300 MHz, 298K, CDCl_3) signals (ppm) of:

Afzelechin tetraacetate [54]

Epiafzelechin tetraacetate [55]

[Splitting patterns and J values (Hz) in parenthesis]

RING	PROTON NO.	[54]	[55]	
A	6	6.56 (d, 2.4)	6.55 (d, 2.4)	
	8	6.64 (d, 2.4)	6.65 (d, 2.1)	
B	2', 6'	7.33 (d, 8.4)	7.43 (d, 8.4)	
	3', 5'	7.07 (d, 8.7)	7.10 (d, 8.7)	
C	2	5.15 (d, 6.0)	5.10 (br. s)	
	3	5.26 (m)	5.38 (m)	
	4ax	2.63 (dd, 6.0, 16.9)	2.85 (dd, 2.1, 20.1)	
	4eq	2.81 (dd, 5.1, 16.8)	2.98 (dd, 5.0, 18.2)	
	OAc		2.25 (s)	2.26 (s)
			2.26 (s)	2.28 (s)
		2.27 (s)	2.29 (s)	
		1.96 (s, 3-OAc)	1.89 (s, 3-OAc)	

Table A3: ^1H NMR (300 MHz, 298K, CDCl_3) signals (ppm) of:

Catechin pentaacetate [56]

Epicatechin pentaacetate [46]

[Splitting patterns and J values (Hz) in parenthesis]

RING	PROTON	[56]	[46]
A	6	6.63 (d, 2.1)	6.65 (d, 2.1)
	8	6.57 (d, 2.1)	6.55 (d, 2.1)
B	2'	7.22 (d, 2.1)	7.33
	5'	7.18 (d, 8.4)	7.17 (d, 8.1)
	6'	7.15 (dd, 2.1, 8.4)	7.26 (dd, 1.8, 9.0)
C	2	5.12 (d, 6.3)	5.09 (br. s)
	3	5.23 (m)	5.36 (m)
	4ax	2.61 (dd, 6.6, 16.8)	2.74 (dd, 1.5, 17)
	4eq	2.84 (dd, 5.1, 16.8)	2.96 (dd, 4.5, 17)
	OAc	2.26 (s)	2.28 (s)
		2.26 (s)	2.28 (s)
		2.25 (s)	2.26 (s)
	-	-	
		1.98 (s, 3-OAc)	1.90 (s, 3-OAc)

Table A4: ^1H NMR (300 Mhz, 298K, CDCl_3) and ^{13}C NMR (75 MHz) signals (ppm) of:

Typhaphthalide [48]

[Splitting patterns and J values (Hz) in parenthesis]

Proton and carbon no.	^1H NMR	^{13}C NMR
1		171.93
3	5.68 (t, 6.5, 6.3)	82.59
4	6.87 (d, 8.22)	115.51
5	7.46	136.64
6	6.63 (d, 7.4)	113.68
7	7.71 (br. s, -OH)	156.49
8	-	111.0
9	-	149.38
10a	3.26 (dd, 6.7, 14)	40.69
10b	3.14 (dd, 6.2, 14)	134.76
1'	-	
2', 6'	^	129.67*
3', 5'	^	128.57*
4'	^	127.27

* = interchangeable

^ = unassignable due to overlap of signals

Table A5: ^1H NMR (300 Mhz, 298K, CDCl_3) and ^{13}C NMR (75 MHz) signals (ppm) of :

Typharin [47]

[Splitting patterns and J values (Hz) in parenthesis]

PROTON AND CARBON NO.	^1H NMR	^{13}C NMR
1	-	169.49
3	5.23 (q, 6.2, 14.3)	79.65
4	3.12 (m)	33.47
5	6.72 (d, 8.1)	118.05
6	7.42 (dd, 8.0, 8.1)	136.32
7	6.90 (d, 8.4)	116.46
8	10.97 (s, -OH)	162.26
9	-	109.30
10	-	138.89
1'	-	135.62
2', 6'	^	128.73*
3', 5'	^	126.79*
4'	^	128.53
7'	6.78 (d, 16)	125.14
8'	6.30 (dd, 6.4, 16)	133.96

* = interchangeable

^ = unassignable due to overlap of signals

Table A6: ^1H NMR (300 MHz, 298K, CDCl_3) signals (ppm) of:

Stigmasterol [45]

[Splitting patterns and J values (Hz) in parenthesis]

PROTON	STIGMASTEROL [45]
3	3.50 (m)
6	5.35 (brs)
18	0.66 (s)
19	0.69 (s)
21	0.99 (d, 6.7)
22	5.00 (dd, 7.5 and 15.4)
23	5.15 (dd, 11.5 and 15.4)
24	2.21 (m)
26	0.90 (d, 6.5)
27	0.78 (d, 6.35)
29	0.80 (t, 6.5)

Table A7: ^1H NMR (300 MHz, 298K, CDCl_3) signals (ppm) of: β -Sitosterol [49]

[Splitting patterns and J values (Hz) in parenthesis]

PROTON	β -SITOSTEROL [49]
3	3.50 (m)
6	5.33 (d, 5.4)
18	0.66 (s)
19	0.82 (s)
21	0.98 (d, 6.7)
24	2.21 (m)
26	0.90 (d, 6.5)
27	0.78 (d, 6.35)
29	0.80 (t, 6.6)

Table A8: ^1H NMR (300 MHz, 298K, CDCl_3) signals (ppm) of:

Lupeol [43]

[Splitting patterns and J values (Hz) in parenthesis]

PROTON	LUPEOL [43]
2	2.35 (m)
3	3.17 (dd, 5.1 and 10.8)
23	0.94 (s)
24	0.73 (s)
25	0.80 (s)
26	1.00 (s)
27	0.92 (s)
28	0.76 (s)
29a	4.54 (d, 2.4)
29b	4.66 (d, 2.4)
30	1.65 (s)

Table A9: ^1H NMR (300 MHz, 298K, D_2O) signals (ppm) of:

Sucrose [65]

[Splitting patterns and J values (Hz) in parenthesis]

PROTON	SUCROSE [65]
1	5.41 (d, 3.9)
2	3.55 (m)
3	3.76 (t, 9.6)
4	3.46 (t, 9.3)
5	3.86 (m)
6	3.82 (d, 2.1)
1'	3.67 (brs)
2'	-
3'	4.21 (d, 8.7)
4'	4.05 (t, 8.4)
5'	3.90 (m)
6'	3.82 (d, 2.1)

Table A10: ^1H NMR (300 MHz, 298K, CDCl_3) signals (ppm) of:

Oleanolic Acid [44]

[Splitting patterns and J values (Hz) in parenthesis]

PROTON	OLEANOLIC ACID [44]
2a	2.35 (m)
2b	2.50 (m)
3	3.21 (m)
23	0.94 (s)
24	0.73 (s)
25	0.80 (s)
26	1.00 (s)
27	0.92 (s)

Table A11: ^{13}C NMR (75 MHz, 298K) signals (ppm) of:

Epicatechin [4]

CARBON NO.	(-)-EPICATECHIN [4]	LITERATURE
2	78.27	79.1
3	65.82	66.8
4	27.94	28.6
5	156.0	156.7
6	95.04	96.8
7	156.41	156.7
8	95.04	96.0
9	156.46	157.1
10	98.65	100.3
1'	131.09	131.8
2'	114.12	115.4
3'	144.14	145.0
4'	144.26	145.2
5'	114.35	116.4
6'	118.21	119.6

Table A12: ^1H NMR (300 MHz, 298K, CDCl_3) signals (ppm) of:

(-)-Epicatechin [4]

[Splitting patterns and J values (Hz) in parenthesis]

RING	PROTON	EPICATECHIN [4]	LITERATURE ⁴
A	6	5.94 (d, 2,1)	5.72 (d, 1,7)
	8	6.04 (d, 2,1)	5.89 (d, 1,7)
B	2'	7.07 (d, 2,1)	6,90 (d, -)
	5'	6.81 (d, 8,1)	6.66 (d, 8,7)
	6'	6.86 (dd, 2,1 and 8,1)	6.66 (dd, 8,7 and -)
C	2	4.89	4.74 (d, -)
	3	4.23 (m)	4.01 (m)
	4ax	2.75 (dd, 3 and 16,8)	2.48 (dd, 3,3 and 16,3)
	4eq	2,89 (dd, 5 and 16,7)	2.79 (dd, 4,2 and 16,3)

Table A13: ^{13}C NMR (75 MHz, 298K) signals (ppm) of

Epicatechin pentaacetate [46]

CARBON NO.	(-)-EPICATECHIN PENTACETATE [46]	LITERATURE ³
2	76.70	76.7
3	66.67	66.7
4	26.04	26.0
5	149.74*	149.8
6	108.78	108.8
7	149.69*	149.8
8	108.08	108.0
9	154.98	155.0
10	109.62	109.7
1'	135.86	135.9
2'	122.06	122.1
3'	141.91	142.0
4'	142.03	142.1
5'	123.25	123.2
6'	124.39	124.4

* = exchangeable carbons

Table A14: ^{13}C NMR (75 MHz, 298K) signals (ppm) of**(+)-Catechin pentaacetate [56]**

CARBON NO.	(+)-CATECHIN PENTAACETATE	LITERATURE ³
2	77.62	77.8
3	68.26	68.4
4	23.89	24.0
5	149.41	149.8
6	108.78	108.8
7	149.84	150.0
8	107.69	107.7
9	154.36	154.5
10	110.17	110.2
1'	136.14	136.2
2'	121.77	121.8
3'	142.07	142.2
4'	142.07	142.2
5'	123.71	123.7
6'	124.41	124.4

REFERENCES

1. Cannell, J.P. (Editor), *Natural products isolation*, Humana Press Inc., New Jersey, (1998).
2. Roux, D.G., Ferreira, D., Hundt, H.K.L. and E. Malan, *Applied Polymer Symposium No 28*, 335 – 353, (1975).
3. Agrawal, P.K. (Editor), *Carbon-13-NMR of Flavonoids*, Elsevier, Amsterdam, pp. 3 and 433, (1989).
4. Porter, L.J., *The Flavonoids: Advances in Research since 1986* (Editor, Harborne, J.B.), Chapman and Hall, London, p.23, (1994).
5. *The Flavonoids: Advances in Research* (Editors, Harborne, J.B. and Mabry T.J.), Chapman and Hall, London, (1982).
6. Haslam, E., *The Flavonoids* (Editors, Harborne, J.B., Mabry, T.J. and Mabry H.), Academic Press, New York, (1975).
7. Porter, L.J., *The Flavonoids: Advances in Research since 1980* (Editor, Harborne, J.B.), Chapman and Hall, London, pp. 21-62, (1988).
8. Marini-Bettolo, G.B., Ferrari, F., Monache, F.D. and A. Poce-Tuce, (1972), *Phytochemistry*, **11**, 2333.
9. Drewes, S.E. and D.G. Roux (1966), *J. Chem. Soc. (C)*, 1644.
10. Hillis, W.E. and A. Carle, *Aust. J. Chem.*, (1960), **13**, 390.
11. Hillis, W.E. and T. Inoue, *Phytochemistry*, (1967), **6**, 59
12. Poce-Tuce, A., Monasche, F.D. and G.B. Marini-Bettolo, *Ann. Ist Sanita*, (1969), **5**, 555.
13. Marletti, F., Monarache, F.D., Marini-Bettolo, G.B. and I.L.D' Albuquerque, *Phytochemistry*, (1976), **15**, 443.
14. Friedrich, H. and R.Engelstowe, *Planta Med.*, (1978), **33**,251.
15. Ohigashi, H., Minami, S., Fukui, H., Koshimizu, K., Mizutani, F., Sugiara, A. and T. Tomana, *Agric. Biol. Chem.*, (1982), **46**, 2555.
16. Hsu, F., Nonaka, G. and I. Nishioka, *Chem. Pharm. Bull.*, (1985), **33**, 3142.

17. Swinny, E.E., *The Structure and synthesis of natural products isolated from Cassia abbreviata, Distemonanthus benthamianis and Combretum apiculatum*, Doctotal Thesis, UDW, (1995).
18. King, F.E., Clark-Lewis, J.W. and W.F.Forbes, *J. Chem. Soc.*, (1955), 2948.
19. Waterman, P.G. and D.F. Faulkner, *Planta Med.*, (1979), **37**, 178.
20. Patil, A.D. and V.H. Deshpande, *Ind. J. Chem.*, (1962), **21B**, 626.
21. Shen, Z., Falshaw, C.P., Haslam, E. and M.J. Begley, *J. Chem. Soc. Chem. Commun.*, (1985), 1135.
22. Hikino, H., Shimoyama, N., Kasahara, Y., Takahashi, M. and C. Kono, *Heterocycles*, (1982), **19**, 1381.
23. Freudenberg, K., *Die Chemie der Naturlichen Gerbstoffe*, Springer-Verlag, Berlin, (1920).
24. Runge, F.F., *Wiss. Phytochem.*, (1821), 245.
25. Swinny, E.E., *The Structure and Synthesis of Metabolites from Virgilia oroboides and Chlorophora excelsa*, Masters Dissertation, UDW, (1989).
26. Mabry, T.J., Markham, K.R. and M.B.Thomas, *The Systematic Identification of Flavonoids*, Springer-Verlag, New York, p. 260, (1970).
27. Seikel, M.K. and T.J. Mabry, *Tetrahedron Letters*, (1965), **16**, 1105.
28. Seshadri, T.R., *Phytochemistry*, (1964), **11**, 881.
29. Clark-Lewis, J.W., Jackman, L.M. and T. MeL. Spotswood, *Aust. J. Chem.*, (1964), **17**, 632.
30. Clark-Lewis, J.W., Jemison, R.W. and V. Nair, *Aust. J. Chem.*, (1968), **21**, 3015.
31. Schneider, H.J. and V. Hoppen, *J. Org. Chem.*, **43**, 3866.
32. Koukal, J. and E. Conn, *J. Biol. Chem.*, (1961), **236**, 2692.
33. Russell, D.W., *J. Biol. Chem.*, (1971), **246**, 3870.
34. Rhodes, M.J.C. and L.S.C. Woollorton, *Phytochemistry*, (1973), **12**, 2381.
35. Stafford, H.A. and H.H Lester. (1985), *Plant Physiol.*, **78**, 791.
36. Kristiansen, K.N. (1986), *Carlsberg Res. Commun.*, **51**, 51.
37. Newman A.A., *Chemistry of Terpenes and Terpenoids*, Academic Press, London, (1972).

38. de Mayo, P., *The Chemistry of Natural Products-The higher terpenoids*, Interscience Publishers, N. York, (1959).
39. Mahato, S.B. and A.P. Kundu, *Phytochemistry*, (1994), **37**, 1517.
40. Mahato, S.B., Nandy A.K. and G. Roy, *Phytochemistry*, (1992), **31**, 2199.
41. Rogers, C.B., *Phytochem.*, (1988), **27**, 3217
42. Ling, H.C., King M.L., Chen C.F., Hsu K.P., Su M.H. and M.H. Lin, *Chung-hua I Hsueh Tsa Chih*, (1982), **29**, 308, *Chem. Abs.*, (1982), **97**, 120120p.
43. Armanini, D., Karbowiak I., Krozowski Z., Finder J.W. and W.R. Adam, *Endocrinology*, (1982), **111**, 1683.
44. Rask-Maden, J., Bukhave K. Madsen P.E.R. and C. Bekker, *Eur. J. Clin. Invest.*, (1983), **13**, 351.
45. Suetina, I.V., *Biol. Nauki.*, (1982), 47.
46. Inoue, H., Mori T., Suibata S. and Y. Koshihara, *J. Pharm. Pharmacol.*, (1988), **40**, 272.
47. Ganes, A., Sharma R.M. and B.J. RayGhatak, *Indian J. Exp. Biol.*, (1987), **25**, 826.
48. Ma, X., Zhao Y., Yin L, Han D. and C. Ji, *Yaoxue Xuebao*, (1982), **17**, 93.
49. Mooreville, M., Fritz R. W. and S.G. Mulholland, *J. Urol.*, (1983), **130**, 607.
50. Bian, R., Xie Q. and H. Guo, *Zhejiang Yike Daxue Xuebao*, (1982), **11**, 273.
51. Phoeland, B.L., Carte B.K., Francis T.A., Hayland I.J., Allaudeen H.S. and N. Troupe, *J. Nat. Prod.*, (1987), **50**, 706.
52. Filczewski, M., Kosmala M. and K. Oledska, *Pol. J. Pharmacol.*, (1988), **40**, 233.
53. Wehrli, F.W. and T. Nishid, *Progress in the Chemistry of Organic Natural Products*, Vol. **36**, p.1, Springer, N. York, (1979).
54. Agrawal, P.K. and D.C. Jain, *Progress in NMR Spectroscopy*, (1992), **24**, 1.
55. Akisha, T., Yamamoto, K., Tammura, T., Kamura, Y., Iida, T., Nambara, T. and F.C. Chang, *Chem. Pharm. Bull.*, (1992), **40**, 789.
56. Patra, A., and S.K. Chaudhuri, *Magn. Reson. Chem.*, (1987), **25**, 95.
57. Patra, A., Mukhopadhyay, A.K. and A.K. Mitra, *Org. Magn. Reson.*, (1981), **17**, 166.

58. Breitmaier, E. and W. Voelter, *Carbon-13 NMR Spectroscopy*, (3rd ed.), VCH, Germany, (1990)
59. Gershenzon, J., *Joint Meeting-Book of Abstracts*, **L04**, Amsterdam, (1999).
60. Knoss, W., *Joint Meeting-Book of Abstracts*, **L32**, Amsterdam, (1999).
61. Knoss, W., Reuter B. and J. Zapp, *Biochem J.*, (1997), **326**, 449.
62. Dewick, P.M., *Medicinal Natural Products-A biosynthetic Approach*, J. Wiley and Sons, Chichester, (1997).
63. Pooley, E., *The Complete Field Guide to Trees of Natal*, Natal Flora Publications Trust, Durban, (1993).
64. Ferraira, F.H., *The Trees and Shrubs of South Africa*, Pretoria, (1952).
65. Glasby, J. S., *Encyclopaedia of the Terpenoids*, Wiley-Interscience, Chichester, (1982).
66. Hardwood, L.M. and C.J. Moody, *Experimental Organic Chemistry-Principles and Practice*, Blackwell Scientific Publications, London, (1989).
67. Naidoo, N., *Extractives from the Meliaceae and the Annonaceae*, Masters Dissertation, University of Natal-Durban, (1997).
68. Cherest, M. and H. Felkin, *Tetrahedron Letters*, (1968), 2205.
69. Cherest, M., Felkin, H. and C. Frajerman, *Tetrahedron Letters*, (1971), 379.
70. Cherest, M. and H. Felkin, *Tetrahedron Letters*, (1971), 383.
71. van Wyk, B.E., van Oudtshoorn B. and N. Gericke, *Medicinal Plants of S. Africa*, Briza Publications, Pretoria, (1997).
72. Watt, J.M. and M.G. Breyer-Brandwijk, *The Medicinal and Poisonous Plants of Southern and Eastern Africa*, (2nd edition), Livingstone, London, (1962).
73. Hutchings, A., *Zulu Medicinal Plants*, Natal University Press, Pietermaritzburg, (1996).
74. Pujol, J., *Naturafrika-The Herbalist Handbook*, Jean Pujol Natural Healers' Foundation, Durban, (1990).
75. Dictionary of Natural Products on CD-ROM, release 9:1, Chapman and Hall, London, (2000).
76. Dictionary of Natural Products on CD-ROM, release 4:2, Chapman and Hall, London, (1996).

77. Breitmaier, E., *Structure Elucidation by NMR in Organic Chemistry-A Practical Guide*, Wiley and Sons, England, (1993).
78. Mizuno, M., Yoshida S., Iinuma M., Tanaka T., Lang F.A. and K. Goto, *Chem. Pharm. Bull.*, (1990), **38**, 2075.
79. Yoshikawa, M., Uchida E., Chatani N., Kobayashi H., Naitoh Y., Okuno Y., Matsuda H., Yamahara J. and N. Murakami, *Chem. Pharm. Bull.*, (1992), **40**, 3352.
80. Takeuchi, N., Ochi K., Murase M. and S. Tobinaga., *Chem. Pharm. Bull.*, (1983), **31**, 4360.
81. Asakawa, Y. Takikawa K., Toyota M. and T. Takemoto, *Phytochem.*, (1982), **21**, 2481.
82. Asakawa, Y., Takikawa K. and M. Tori, *Phytochem.*, (1987), **26**, 1023.
83. Asakawa, Y., Takikawa K., Tori M. and E.O. Campbell, *Phytochem.*, (1986), **25**, 2543.
84. Yoshikawa, M., Harada E., Yagi N., Okuno Y., Muraoka O., Aoyama H. and N. Murakami, *Chem. Pharm. Bull.*, (1994), **42**, 721.
85. Krishinchand, N. and D. Naidoo, *The preliminary screening of the biological activities of Typha capensis*, Dissertation-BSc. Pharm., UDW, (1999).
86. Walton, N.J. and D.E. Brown, *Chemicals from Plants-Perspectives on Plant Secondary Products*, Imperial College Press, London, (1999).
87. King, F.E. and W. Bottomley, *Chem. And Ind.*, (1953), 1368.